ROLE OF G PROTEIN-COUPLED RECEPTOR KINASE 5 IN DESENSITISATION OF THE V1B VASOPRESSIN RECEPTOR IN RESPONSE TO ARGININE VASOPRESSIN

Katherine van Bysterveldt

A thesis
submitted in partial fulfilment
of the requirements for the Degree
of
Master of Science in Biochemistry

University of Canterbury
2011

TABLE OF CONTENTS

ABSTRACT

Arginine vasopressin (AVP) is a hypothalamic nonapeptide which regulates the hypothalamic-pituitary-adrenal axis response to stress by stimulating the secretion of adrenocorticotropin (ACTH) from corticotroph cells of the anterior pituitary. This effect is mediated by binding of AVP to the pituitary vasopressin receptor (V1bR). The V1bR belongs to the G protein-coupled receptor (GPCR) super family. Repeated stimulation of anterior pituitary cells with AVP has been shown to produce a loss of responsiveness to subsequent AVP stimulation. This phenomenon appears to be mediated by desensitisation of the V1bR, and may be due to phosphorylation of the receptor by G protein-coupled receptor kinase 5 (GRK5). The aim of this research was to establish and validate methods that would allow the role of GRK5 in the desensitisation of V1bR to AVP stimulation to be investigated. As no isoform specific inhibitors for GRK5 were available, HEK293 cells transiently transfected with the rat V1bR were used as a model system for this research. This allowed RNA interference (RNAi) to be used to knockdown GRK5 expression. The protocol for RNAi-mediated knockdown of GRK5 was established as part of this research. Protocols for Western blotting and qRT-PCR were also established to allow the RNAi-mediated knockdown of GRK5 protein and mRNA to be measured. Transfection of HEK293 cells with 10nM GRK5-targeting small interfering RNAs (siRNAs) reduced the expression of GRK5 protein to 53.4% ± 3.4% (mean ± SEM) of that seen in untreated control cells at 84 hours after transfection, while GRK5 mRNA levels were reduced to 28.7% ± 1.9% (mean ± SEM) of that of control cells 48 hours after transfection.

An experimental protocol was designed in this research that would coordinate the RNAi-mediated knockdown of GRK5 with transient transfection of the HEK293 cells with the rV1bR. Since, activated V1bRs couple to $G_{q/11}$ and stimulate the production of inositol phosphates (IPs), the responsiveness of the V1bR can be determined by measuring the accumulation of [H^3]-IPs in cells labelled with [H^3]-*myo*-inositol. In the protocol designed, the effect of GRK5 knockdown on V1bR desensitisation is determined by stimulating HEK293 cells expressing the rV1bR (and previously transfected with GRK5-targeting siRNA) with

0nM or 100nM AVP for 0, 5, 15, 30 or 60 minutes, and comparing the accumulation if IPs over time with that of cells that are not transfected with GRK5-targeting siRNA. This protocol can be used in future to investigate the role of GRK5 in V1bR desensitisation, and may be adapted to determine if other GRK isoforms are involved in V1bR desensitisation.

ABBREVIATIONS

ACTH	adrenocorticotropin hormone
AP-2	adaptor protein 2
AVP	arginine vasopressin
AVPR1B	human gene for V1bR
β_2-AR	β_2-adrenergic receptor
BCA	bicinchoninic Acid
BCP	bromochloropropane
bp	base pairs
BSA	bovine serum albumin
Ca^{2+}	calcium ion
CCD	Charged-Coupled Device
cDNA	complementary DNA
CHO cells	Chinese hamster ovary cells
CK1α	caesin kinase 1α
CRH	corticotrophin-releasing hormone
CRHR1	CRH receptor type 1
DAG	diacylglycerol
DMSO	dimethyl sulfoxide
DNA	deoxyribose nucleic acid
dsRNA	double stranded RNA
EGFP	green fluorescent protein isoform
GADPH	glyceraldehyde-3-phosphate dehydrogenase
GNB2L1	guanine nucleotide-binding protein subunit beta-1-like-1
GPCR	G protein-coupled receptor
G protein	heterotrimeric guanine nucleotide-binding protein
$G_{q/11}$	G protein subtype q/11
G_i	G protein subtype i
G_s	G protein subtype s
G_{12}	G protein subtype 12
GRKs	G protein-coupled receptor kinases
GRK4	G protein-coupled receptor kinase 4
GRK5	G protein-coupled receptor kinase 5
GRK6	G protein-coupled receptor kinase 6
HEK293	human embryonic kidney 293 cells
HIV	Human Immunodeficiency Virus
HMBS	Hydroxymethylbilane synthase
HPA axis	Hypothalamic-pituitary-adrenal axis
HRP	Horse radish peroxidase

HPRT1	Hypoxanthine-guanine phosphoribosyl transferase
Ig	Immunoglobin
IgG	Immunoglobin type G
IP	inositol phosphate
IP_3	Inositol-1,4,5-trisphosphate
LiCl	lithium chloride
MEM	Eagle's Minimum Essential Medium
mGluR1a	Metabotropic glutamate receptor 1A
NPH_2O	nanopure H_2O
ORFs	Open reading frames
Oxt	Oxytocin
PBST	Phosphate buffered saline
PBSTM	PBST with milk
PCR	Polymerase chain reaction
PKC	Protein kinase C
PLCβ	Phospholipase Cβ
PPIB	Peptidyl isomerase B
PIP_2	Phosphatidylinositol-4,5-bisphosphate
PVN	Paraventricular Nucleus
qPCR	Quantitative PCR
qRT-PCR	quantitative reverse transcriptase PCR
RISC	RNA-interference silencing complex
RNA	Ribose nucleic acid
RNAi	RNA interference
RPLI3A	60S ribosomal protein LI3a
RT	Reverse transcriptase
SDHA	Succinate dehydrogenase complex subunit A
SDS	Sodium dodecyl sulfate
SDS-PAGE	SDS-polyacrylamide electrophoresis
siRNA	Small interfering RNA
TBP	Tata-box binding protein
UBC	Ubiquitin C
V2R	Vasopressin V2 receptor
V1bR	Vasopressin V1b receptor
YWHAZ	Tyrosine-3-monooxygenase/tryptophan-5-monooxygenase activation protein, zeta polypeptide

1

INTRODUCTION

1.1 THE HYPOTHALAMIC-PITUITARY-ADRENAL AXIS

1.1.1 The Hypothalamic-Pituitary-Adrenal axis

Homeostasis is the process by which an organism maintains a desired and constant internal state by responding appropriately to challenges and fluctuations which disturb this state (Roper *et al.*, 2011; Sherwood *et al.*, 2005). Maintenance of homeostasis is crucial for the survival of the organism, and is regulated by a number of pathways. In mammals the endocrine response to 'noxious' stimuli or 'stressors' (Buckingham *et al.*, 1997) is coordinated principally by the hypothalamic-pituitary-adrenal (HPA) axis, a neuroendocrine system which results in the instigation of mechanisms which allow the organism to restore homeostatic balance (Roper *et al.*, 2011). Stressors may be cognitive, such as emotional disturbances, or non-cognitive, such as physical trauma (Buckingham *et al.*, 1997).

Stressful stimuli activate the HPA axis (see Figure 1.1), resulting in the rapid release of adrenocorticotropin (ACTH) from corticotroph cells of the anterior pituitary (Aguilera, 1994). Regulation of ACTH secretion is complexly and tightly regulated. The peptide hormones arginine vasopressin (AVP) and corticotrophin releasing hormone (CRH) are the most potent activators of pituitary ACTH secretion (Antoni, 1993). Both are released from the hypothalamus into the hypophysial portal system in response to stress, and are transported to the anterior pituitary where they interact specifically with receptors found in the plasma membranes of corticotroph cells (Jard *et al.*, 1986; Perrin & Vale, 1999). These interactions stimulate the secretion of ACTH into the systemic blood, through which it is transported to the adrenal gland (Bilezikjian & Vale, 1987). In some cases, binding of CRH and AVP at the

anterior pituitary stimulates the biosynthesis of ACTH from its precursor proopiomelanocortin (POMC) (Liu *et al.*, 1990). Secreted ACTH induces the secretion of glucocorticoid hormones from the adrenal cortex. Glucocorticoids regulate the peripheral stress responses, mediating the return to homeostasis. They do this via a number of widespread mechanisms such as energy mobilisation and immunomodulation (Ashwell *et al.*, 2000; Buckingham *et al.*, 1997; Elemkov & Chrousos, 1999). The secretion of ACTH from the anterior pituitary is also regulated by inhibitory forces, by which glucocorticoids regulate their own secretion. They do so by providing negative feedback to upstream components of the HPA axis (Labrie *et al.*, 1984), inhibiting secretion of AVP and CRH from the hypothalamus and at the anterior pituitary; inhibiting the cleavage of POMC into ACTH (and other products)(Drouin *et al.*, 1989).

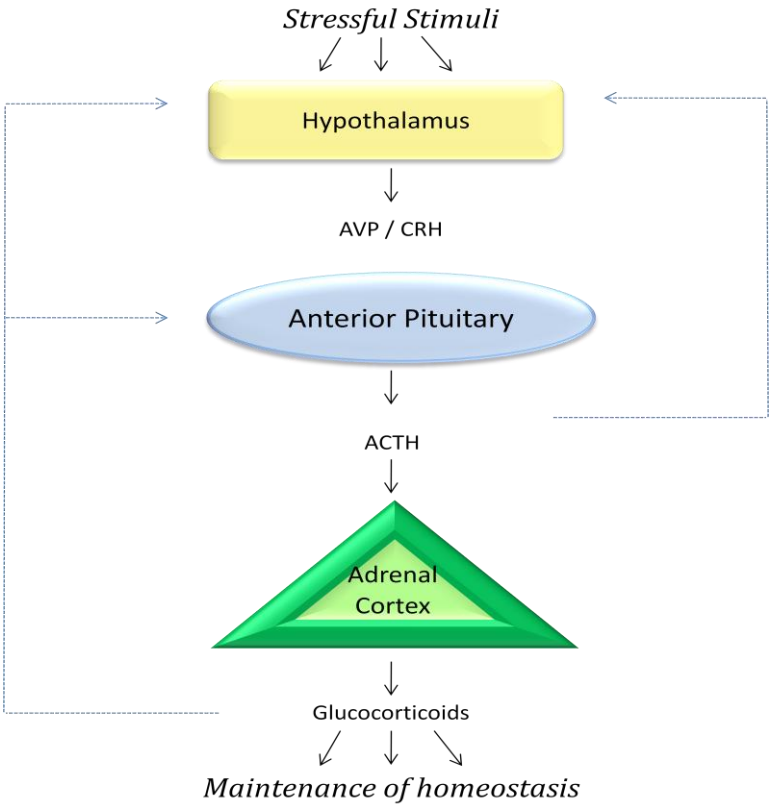

Figure 1.1 The HPA axis. Schematic representation of activation of the HPA axis in response to stress. Solid lines represent positive stimulation, while dashed arrows represent negative feedback. Figure adapted from Buckingham, Gillies, and Cowell (1997)

Dysregulation of the HPA axis has been implicated in a number of pathological disorders (Buckingham *et al.*, 1997), such as hypertension (Wirtz *et al.*, 2007), cardiovascular disease

(Rosmond & Björntorp, 2000), irritable bowel syndrome (Chang *et al.*, 2009), and many inflammatory diseases (Gold *et al.*, 2005; Morand & Leech, 2001; Sternberg, 2001). Furthermore, recent studies have provided evidence that chronic psychological stress can induce DNA/RNA damage (Flint *et al.*, 2007; Joergensen *et al.*, 2011).

The role of stress-induced dysregulation of the HPA-axis in the instigation of serious psychiatric conditions such as depression, anxiety, and bipolar disorder has been the subject of numerous studies, resulting in strong evidence for a causative relationship (Hammen, 2005).

1.1.2 Vasopressinergic control of ACTH secretion

AVP is a nonapeptide hormone (Cys-Tyr-Phe-Gln-Asn-Cys-Pro-Arg-Gly-NH_2) synthesised and secreted from two distinct types of hypothalamic neurons. The first type of hypothalamic AVP-secreting neurons are magnocellular neurons of the supraoptic (SON) and paraventricular nuclei (PVN), while the second class are parvicellular neurons of the PVN (reviewed in Antoni, 1993). There are two subdivisions of parvicellular PVN neurons; one that releases CRH alone, and a second that secretes both CRH and AVP packaged into the same vesicles (Antoni, 1993). It appears that while AVP from both groups of neurons is involved in regulating ACTH secretion, the origin of AVP secretion may differ between different stress paradigms (Antoni, 1993). Most evidence suggests that parvocelluar AVP is involved in regulating the HPA axis during chronic stress (Aguilera, 1994), though some acute stressors (such as osmotic stress) have been shown to induce AVP secretion from magnocellular neurons (Jackson *et al.*, 2003).

That AVP is capable of stimulating ACTH secretion has been known since the mid 1950's (Martini & Morpurgo, 1955). However, investigation into vasopressinergic regulation of ACTH secretion has been relatively neglected in favour of CRH. The importance of AVP in regulating ACTH secretion is becoming increasingly evident (Antoni, 1993). A good correlation has been observed between the number of pituitary AVP receptors and the ACTH responsiveness of corticotroph cells (Aguilera, 1994). Furthermore, the physiological consequences of preventing AVP signalling via the pituitary AVP receptor have been examined using a number of animal models in which the pituitary AVP receptor has been

knocked out. The results of these studies suggest that AVP signalling via this receptor plays an important role in regulation of the HPA axis (Itoh *et al.*, 2006; Lolait *et al.*, 2007a; Tanoue *et al.*, 2004), in central processes such as learning, behaviour (Egashira *et al.*, 2005; Wersinger *et al.*, 2007; Wersinger *et al.*, 2002) and social memory (Wersinger *et al.*, 2007; Wersinger *et al.*, 2008), as well as peripheral responses (Daikoku *et al.*, 2007; Fujiwara *et al.*, 2007a; Fujiwara *et al.*, 2007b; Lolait *et al.*, 2007b). The aim of this thesis was to build on previous work from this laboratory (Hassan *et al.*, 2003; Hassan & Mason, 2005), elucidating the molecular mechanism of AVP-stimulated secretion of ACTH from the anterior pituitary.

Secretion of AVP into the hypophysial portal occurs in a pulsatile fashion (Antoni, 1993), the amplitude of which tends to be increased following stress rather than the frequency (reviewed in Mason *et al.*, 2002). The concentration of AVP in the hypophysial portal has been shown to increase following numerous types of stress (Antoni, 1993). For example, in sheep, the hypophysial AVP concentration produced by basal AVP secretion ranges from 5 to 83pM (Caraty *et al.*, 1988). Application of a stressor stimulates AVP pulses that are less than 30 minutes long, and range in concentration from ~1nM for acute haemorrhage (Caraty *et al.*, 1988) to ~6nM for high-dose insulin-induced hypoglycaemia (2IU/kg) (Caraty *et al.*, 1990). Both physical and emotional stressors have been shown to induce AVP secretion (Antoni, 1993).

The synergistic stimulation of ACTH secretion by concurrent stimulation of anterior pituitary cells with AVP and CRH is well documented both *in vivo* (McFarlane *et al.*, 1995; Rivier & Vale, 1983) and *in vitro* (Evans *et al.*, 1996; Gilllies *et al.*, 1982), and occurs in all mammalian models tested. Synergism between the two hormones appears to be caused by AVP enhancing CRH-mediated production of cyclic adenosine monophosphate (cAMP) (potentially by increasing the activity of protein kinase C (PKC) (Abou-Samra *et al.*, 1987)), and results in ACTH secretion that is greater than the sum of ACTH release stimulated when AVP or CRH are used independently (Bilezikjian & Vale, 1987). However, the relative potency of AVP and CRH appears to be species-dependant (Evans *et al.*, 1993; McFarlane *et al.*, 1995; Vale *et al.*, 1983). It has been proposed that synergism between CRH and AVP allows CRH to act as a permissive signal, regulating the overall responsiveness of the corticotroph by setting the basal level of ACTH secretion and determining the amplitude of ACTH pulses (Antoni, 1993; Evans

et al., 1996). In this scenario, AVP acts as the dynamic regulator of ACTH section (Antoni, 1993; Evans *et al.*, 1996).

1.2 MECHANISMS OF AVP-STIMULATED ACTH RELEASE BY THE ANTERIOR PITUITARY

AVP and CRH stimulate ACTH secretion by binding specifically to receptors belonging to the G protein-coupled receptor (GPCR) super family (Perrin & Vale, 1999; Sugimoto *et al.*, 1994) GPCRs are integral membrane proteins which transmit the incoming signal (reviewed in Kobilka, 2006) into intracellular signalling molecules by interacting or 'coupling' with a heterotrimeric guanine nucleotide binding protein (G protein). G proteins are comprised of 3 different subunits; α, β and γ (Strader *et al.*, 1994), and are grouped into four subclasses: G_s, G_i, G_q and G_{12} (Ulloa-Aguirre *et al.*, 1999). Functional diversity amongst the G protein subunits allows the activation of a range of signalling pathways, as interaction of a G protein with an agonist-bound GPCR stimulates the production of second messenger signalling molecules by an effector enzyme or channel (Ferguson, 2001). Binding of CRH to its CRH type 1 receptor (CRHR1)—located at the membrane of corticotroph cells—activates the cAMP-mediated signalling pathway via a G_s type G protein, by stimulating adenylyl cyclase-mediated synthesis of cAMP from adenosine triphosphate (ATP) (Aguilera, 1994). AVP signalling via AVP receptors is described below.

1.2.1 AVP Receptors

In addition to its role in stimulating ACTH secretion, AVP is known to exert other diverse biological effects. To date, three functionally distinct mammalian AVP receptors have been cloned. They are the V1aR, the V1bR (also known as V3R), and the V2R (Frank & Landgraf, 2008). The three receptors share a structure typical of GPCRs; consisting of seven hydrophobic-transmembrane α-helices, which are linked by intracellular and extracellular loops (Strader *et al.*, 1994). Despite their high level of structural homology and common ligand, each receptor subtype has different pharmacological properties (Jard *et al.*, 1986).

These differences allow AVP to exert a range of tissue-dependant effects (Frank & Landgraf, 2008). AVP has also been shown to bind with high affinity to receptors for oxytocin—a nonapeptide hormone with high structural similarity to AVP—which plays a role in lactation, parturition, and sexual behaviour (Holmes *et al.*, 2003; Maybauer *et al.*, 2008).

Since its characterisation, the V1bR sequence has been cloned from the rat (Lolait *et al.*, 1995), mouse (Ventura *et al.*, 1999) and human genomes (de Keyzer *et al.*, 1994 ; Sugimoto *et al.*, 1994). The human gene for V1bR (AVPR1B) is located at region q32 of chromosome 1 and codes for a protein 424 amino acid residues long (Rousseau-Merck *et al.*, 1995; Sugimoto *et al.*, 1994). This polypeptide has considerable homology with the human V1a, V2 and oxytocin receptors (45, 39, and 45% respectively), as well as with V1bR from other species (Ventura *et al.*, 1999). Despite these similarities, studies directly comparing the relative binding affinities of the mouse and human V1bRs for AVP, vasotocin (a non-mammalian hybrid of vasopressin and oxytocin) and oxytocin demonstrated that significant intra-species pharmacological differences exist (Ventura *et al.*, 1999).

The V2R, expressed predominately in the kidneys, is involved in water reabsorption (Holmes *et al.*, 2003). Like the CRHR1, the V2R is coupled to G_s an activates adenylyl cyclase-mediated synthesis of cAMP from ATP (Birnbaumer, 2000). In contrast, the V1a, V1b and oxytocin receptor are $G_{q/11}$-coupled, recruiting phospholipase Cβ (PLCβ) to produce second messenger signalling molecules (Raggenbass, 2008; Roper *et al.*, 2011; Thibonnier *et al.*, 1997). The V1aR is primarily expressed in vascular smooth muscle, enhancing prostaglandin release (Maybauer *et al.*, 2008), and regulating blood pressure (Frank & Landgraf, 2008). It is this classical 'pressor' action for which its ligand is named. The V1bR is predominately expressed in corticotroph cells of the anterior pituitary (Holmes *et al.*, 2003) where it facilitates the release of ACTH as part of the HPA axis-response to stress. It has also been detected in peripheral tissues (Regard *et al.*, 2008; Roper *et al.*, 2011), of note, in the pancreatic islets where it is involved in the regulation of insulin secretion (Maybauer *et al.*, 2008; Regard *et al.*, 2008).

1.2.2 V1bR-mediated activation of the phosphoinositol signalling pathway by AVP

1.2.2.1 Mechanisms of GPCR signalling via $G_{q/11}$

AVP-bound V1bR is known to activate PLCβ by coupling to the G protein $G_{q/11}$ (Sugimoto *et al.*, 1994), thus transducing its signal via the phosphatidyl-inositol signalling pathway. The general mechanism of signal transduction common to $G_{q/11}$-coupled GPCRs is described below, and depicted schematically for AVP in Figure 1.2.

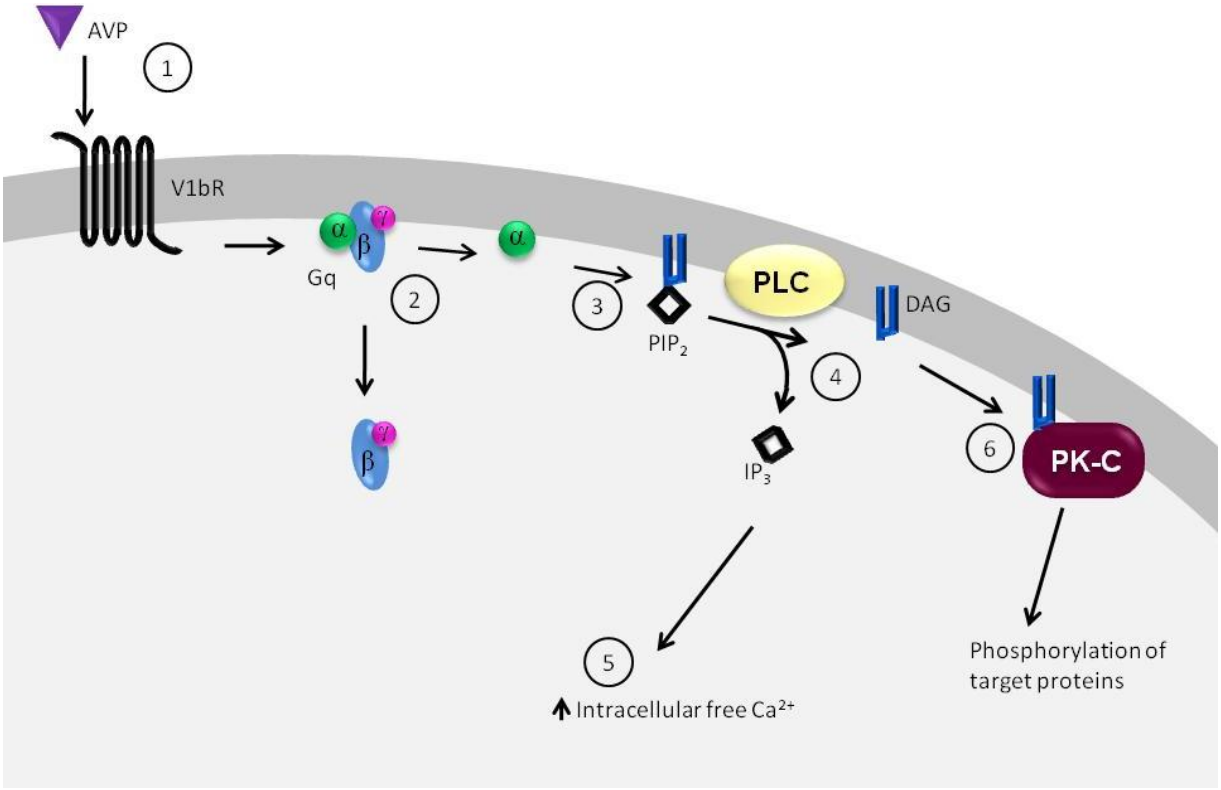

Figure 1. 2 Activation of the phosphoinositide signalling pathway by AVP. (1) AVP binds to the V1bR at the membrane of corticotroph cells, inducing a conformational change in the receptor – allowing it to couple with the Gq G protein. (2) Interaction of Gq and ligand-bound V1bR triggers the dissociation of the Gq α subunit from the β & γ complex, allowing it to travel through the membrane and (3) activate PLCβ, (4) which hydrolyses PIP_2 into second messenger molecules: IP_3 and DAG. (5) IP_3 is released into the cytosol where is acts to increase intracellular free $Ca2^+$, while (6) DAG remains associated with the membrane, where it activates PKC which also results in an increase in the intracellular Ca^{2+} concentration.

Activation of a GPCR, such as the V1bR, by binding of its ligand induces a conformational change in the receptor structure. This allows it to interact with its G-protein ($G_{q/11}$). The resulting G protein-GPCR interaction catalyses the exchange of G protein-bound guanosine diphosphate (GDP) for guanosine triphosphate (GTP) (Oldham *et al.*, 2006), triggering the dissociation of the GTP-bound $G_q\alpha$-subunit from the $G_q\beta\gamma$-subunits (Milligan & Kostenis, 2006). The α-subunit then activates the effector enzyme, PLCβ (Taylor *et al.*, 1990). PLCβ enables transmission of the incoming signal by catalysing the hydrolysis of the membrane constituent phosphatidylinositol-4,5-bisphosphate (PIP_2) into two second messenger molecules; inositol-1,4,5-trisphosphate (IP_3), which is released into the cytosol, and diacylglycerol (DAG) which remains associated with the membrane (Berridge & Irvine, 1984). Both act to increase the cytoplasmic concentration of calcium ions (Ca^{2+}). IP_3 does so by interacting with IP_3 receptors at the endoplasmic reticulum, triggering the release of Ca^{2+} into the cytosol from intracellular stores (Berridge & Irvine, 1984), while DAG activates the second messenger-dependant kinase, PKC, which phosphorylates cell membrane-localised ion channels, resulting in an influx of extracellular Ca^{2+} (Berridge, 1985). In anterior pituitary cells, the V1bR-mediated increase in intracellular Ca^{2+} concentration triggers the fusion of ACTH-containing vesicles with the cell membrane, resulting in secretion of ACTH into the systemic blood.

1.2.2.2 Mechanisms of V1bR signalling

While the V1bR is known to couple to PLCβ in anterior pituitary cells, the mechanism of receptor activation has not yet been fully elucidated. However, it is likely to be similar to that of its fellow PLCβ-coupled GPCRs; V1aR and the oxytocin receptor with which it has considerable homology.

1.2.2.2.1 V1bR activation

AVP is thought to interact with its receptors by binding in a pocket created by the seven transmembrane domains, which are arranged in a ring shape. This interaction appears to be mediated by a large number of weak electrostatic interactions involving many amino acid residues, rather than via a few discrete binding regions (Barberis *et al.*, 1998). However,

alanine-scanning mutagenesis studies of the V1aR N-terminal region have demonstrated that the residues Glu^{54} and Arg^{46} (both part of a $-R(X_3)L/V(X_3)E(X_3)L-$ motif conserved within the vasopressin/oxytocin receptor subfamily) play crucial roles in the binding of AVP to the V1aR (Hawtin *et al.*, 2005) For most GPCRs, activation is caused by a conformational change triggered by association of their ligand (reviewed in Kobilka, 2007). Biochemical and biophysical studies have suggested that common structural changes occur within GPCRs, particularly within their transmembrane and intracellular domains (Kobilka, 2007). These regions are also the most conserved between receptors, which may allow receptors for very different ligands to couple to the same G protein (Kobilka, 2007). While the site of V1bR interaction with $G_{q/11}$ has not been confirmed, the ability of the V1aR to couple to the same G protein appears to involve residues located within its second intracellular loop (Barberis *et al.*, 1998).

There is growing evidence that GPCR signalling may be more complex than depicted in the linear mechanism described in Section 1.2.2.1 (Albizu *et al.*, 2010; Chini & Manning, 2007), with some GPCRs having been shown to form homo- or hetero-dimers under physiological conditions, with dimerisation potentially playing a role in their maturation (Park & Palczewski, 2005), signalling and regulation (Albizu *et al.*, 2010) (reviewed in Terrillon & Bouvier, 2004). A number of recent studies have suggested that the members of the vasopressin/oxytocin receptor family can form functional hetero- and homo-dimers *in vivo* (reviewed in Cottet *et al.*, 2010). Hetero-dimerisation of V1bR and CRHR1 has also been reported (Young *et al.*, 2007). However formation of this dimer was constitutive not ligand dependant, and as such it is unlikely that heterodimerisation of the CRHR1 and V1bR alters their binding properties.

Adding another layer of complexity is the recent demonstrations that some GPCRs —including the V1bR— can differentially couple to more than one subtype of G protein, enabling the activation of multiple second messenger pathways by a single receptor (Chini & Manning, 2007). Data obtained by Orcel et al.(2009) using Chinese hamster ovary (CHO) cells, COS-7 cells, and human embryonic kidney 293 (HEK293) cells transfected with the rat V1bR, showed that the V1bR was capable of simultaneously activating both the PLCβ (described above) and adenylyl cyclase-mediated signal transduction pathways by differentially coupling to $G_{q/11}$ and G_s, though not to G_i (Orcel *et al.*, 2009). AVP was a more potent stimulator of the $G_{q/11}$-PLCβ

pathway, with higher concentrations of ligand required to induce G_s-mediated cAMP production by adenylyl cyclase (EC_{50} 18.6 to 32.7nM depending on cell type) than $G_{q/11}$ mediated inositol phosphate (IP) production (EC_{50} 3.84 to 7.28nM depending on cell type). Though signalling was detected in all three cell types tested and at endogenous levels of receptor expression, it is unclear if significant activation of the cAMP pathway occurred at physiologically relevant concentrations of AVP.

1.3 ATTENUATION OF THE RESPONSE TO AVP: DESENSITISATION

Most signalling systems contain autoregulatory loops, which allow stimulated target-cells to modify their response to future stimuli (Lohse, 1993). In many hormonal pathways, such as the HPA axis, repeated or chronic stimulation leads to a reduction in system responsiveness (Aguilera, 1994). Aspects of this attenuation were described earlier, in the form of negative feedback by glucocorticoids. Similar mechanisms are also seen in GPCR-mediated intracellular signalling pathways, in which the activation of a receptor by binding of its ligand not only results in signal transduction, but also initiates desensitisation (Lohse, 1993). This loss of responsiveness can be due to regulation of many aspects of the signalling pathway, though receptor desensitisation is the predominant cause (Krupnick & Benovic, 1998). Studies using primary cultures of ovine anterior pituitary cells have shown that the responsiveness of ACTH release to AVP stimulation undergoes rapid desensitisation (Hassan *et al.*, 2003). Furthermore, desensitisation was measured following AVP treatments which closely resembled—both in pulse duration and concentration—endogenous AVP pulses (Hassan *et al.*, 2003). This indicates that the V1bR undergoes desensitisation, and that it is likely a physiologically relevant phenomenon.

1.3.1 Mechanisms of desensitisation in GPCRs

The characteristics of β_2-adrenergic receptor (β_2-AR)-mediated signalling have been extensively studied, and have been used to generate a model for understanding general GPCR signalling and regulation (Ferguson, 2001). While receptor-specific differences limit the ability

to extrapolate, components of the mechanisms are thought to be generally relevant for all GPCRs and are described below. Some aspects of these mechanisms are shown in Figure 1.3.

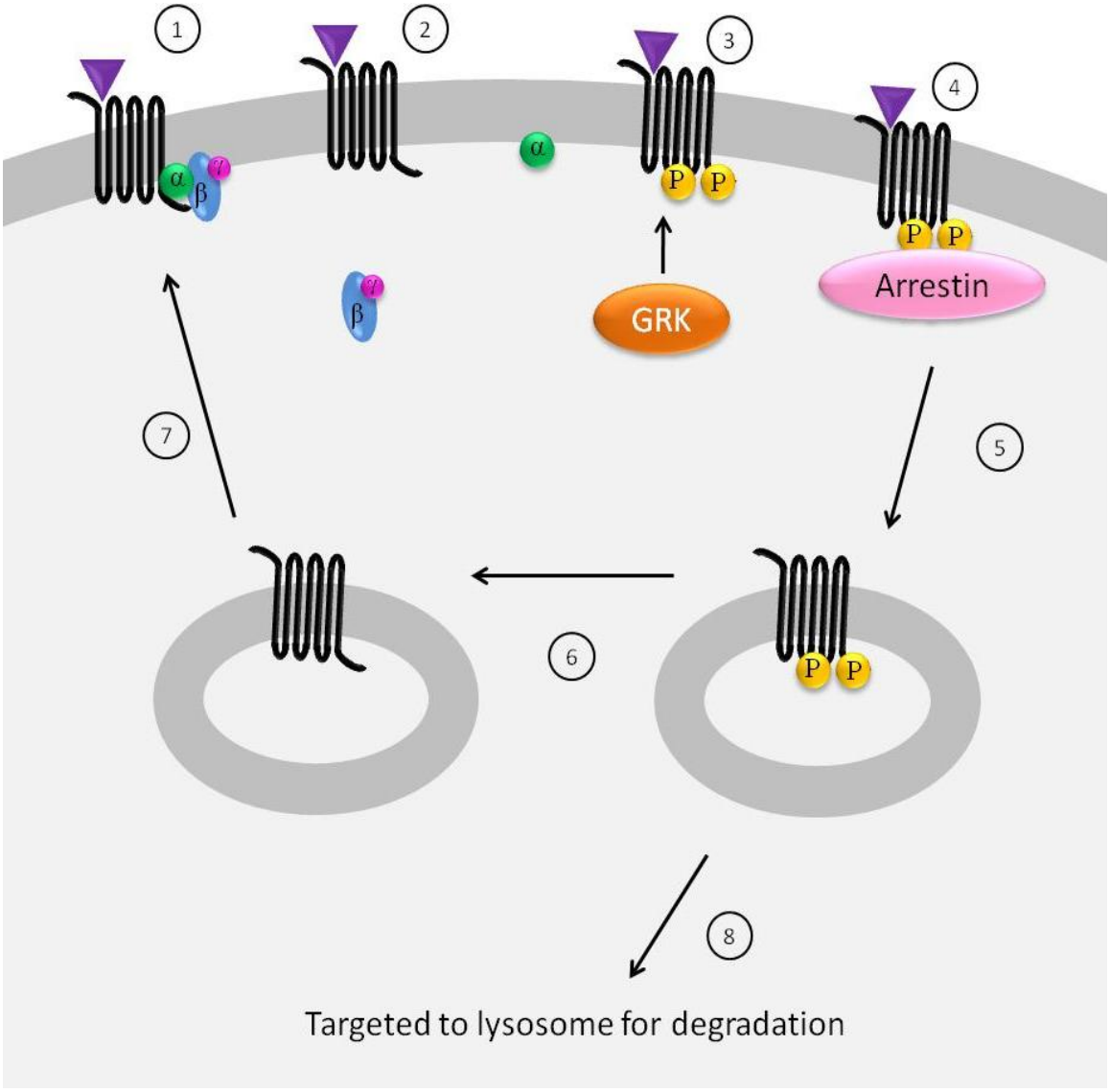

Figure 1.3 the 'classical' model of GPCR desensitisation. (1) The ligand-bound receptor couples to its G protein, (2) resulting in signal transduction. (3) The activated receptor is phosphorylated by a GRK, (4) recruiting arrestin from the cytoplasm, which binds to the receptor, preventing it from coupling to its G protein. (5) The desensitised receptor is internalised, where it is either (6) resensitised and (7) returned to the membrane, or (8) targeted to the lysosomes for degradation resulting in receptor down-regulation. Figure adapted from (Kelly *et al.*, 2008)

The phenomenon of GPCR desensitisation can involve three complementary mechanisms. The first is mediated by the 'uncoupling' of the receptor from its signalling pathway, resulting in a loss of signal transduction. The second, 'internalisation' isolates the receptor from downstream components of the signalling pathway in endocytotic vesicles, while the third, 'down regulation', is mediated by a reduction in receptor numbers via receptor degradation or decreased synthesis (Lohse, 1993).

1.3.1.1 Receptor uncoupling

Phosphorylation of serine and threonine residues located in the intracellular domains of GPCRs results in uncoupling of the receptor from its G protein, thus preventing it from activating its signalling pathway (Ferguson, 2001). This form of desensitisation is rapid, occurring within seconds of ligand binding (Lohse, 1993). It is also readily reversed by dephosphorylation of the receptor (Krupnick & Benovic, 1998). GPCRs are commonly phosphorylated by two classes of protein kinase; second messenger-dependent kinases and G protein-coupled receptor kinases (GRKs).

1.3.1.1.1. Second messenger-dependent kinases and others

The activity of the aptly named 'second messenger-dependant kinases' is stimulated by increases in the intracellular concentration of second messenger signalling molecules such as cAMP, Ca^{2+} and DAG. As well as mediating down-stream signalling events (for example see Figure 1.2, [6]), the activated kinases can negatively regulate receptor function by feedback phosphorylation of GPCRs (reviewed in Lohse, 1993). Phosphorylation of a receptor by second messenger-dependent kinases occurs at consensus motifs within the intracellular loops and C-terminal tail, and appears to directly prevent the interaction of the receptor with its G protein as it is sufficient to induce desensitisation. Second messenger-dependent kinases are capable of simultaneously inducing both 'homologous' desensitisation, by phosphorylation the ligand-bound receptors which stimulated their activation, and 'heterologous' desensitisation, by phosphorylating inactivate receptors, which may also be of a different type (Ferguson, 2001). There is also evidence that other kinases, such as casein kinase 1α (CK1α) (Budd *et al.*,

2000) and tyrosine kinases (reviewed in Ferguson, 2001), may play a more limited role in GPCR regulation.

1.3.1.1.2 G protein-coupled receptor kinases (GRKs)

G protein-coupled receptor kinase (GRK)-mediated phosphorylation of GPCRs (depicted in Figure 1.3) differs from that induced by second messenger-dependant kinases in that is not sufficient, in and of itself, to prevent receptor-G protein interactions. Instead, GRK-mediated phosphorylation of the receptor recruits an additional protein from the arrestin family (such as β-arrestin-1 or -2) from the cytosol to the plasma membrane. β-arrestin binds to the phosphorylated receptor, thus sterically inhibiting further interaction with its associated G-protein (Lohse *et al.*, 1990). This results in decreased receptor responsiveness (Han *et al.*, 2001). GRK-mediated desensitisation is classed as 'homologous', as GRKs preferentially phosphorylate ligand-bound receptors (Penn *et al.*, 2000). This homologous desensitisation is often referred to as 'classical' desensitisation (depicted in Figure 1.3), and is a common mechanism of regulation among GPCRs (Kelly *et al.*, 2008).

To date, seven GRK isoforms have been identified, which can be divided into three groups based on structural and functional homology (alternative names are given in parentheses): 1) GRK1 (rhodopsin kinase) and GRK7 (cone opsin kinase); 2) GRK2 and GRK3 (β-AR kinases 1 and 2 respectively); and 3) GRK4, 5 and 6 (known collectively as the GRK4 subfamily). GRK2, 3, 5 and 6 are ubiquitously expressed, while expression of GRK4 is limited to the testis, and GRK1 and 7 to the retina (Ferguson, 2001). The general structure of GRKs is conserved, consisting of a central catalytic region flanked by an N-terminal regulators of G protein signalling (RGS) domain, and a C-terminus of variable length (Penn *et al.*, 2000). The C-terminal domain is thought to determine the cellular location of the GRK, and/or its recruitment to plasma membrane, either through internal regulatory domains (GRK2, 3 and 5) or post-translational modifications (GRK1, 7, 4 and 6) (reviewed in Penela *et al.*, 2003). The N-terminal domain is thought to be involved in recognition of the receptor (reviewed in Penn *et al.*, 2000). Regulation of GRK activity may occur via a number of mechanism, such as autophosphorylation, and is reviewed in Pitcher et al. (1998) and Penela, Ribas, and Mayor (2003).

The rules governing specificity of GRK-GPCR interactions are unclear, with an apparently high level of functional redundancy between isoforms and with each isoform interacting with a diverse range of GPCRs (Ren *et al.*, 2005). However, case-by-case analysis of GPCR desensitisation does suggest that preferential relationships exist between GRK isoforms and members of the GPCR family. For example, Ren et al. (2005) recently demonstrated *in vitro* using knockdown studies, that phosphorylation of the V2R by GRK2 or 3 promoted much stronger β-arrestin recruitment than that of GRK5 or 6. Furthermore, the rate of evolution had differed dramatically between GRK isoforms, suggesting that at least some of the GRK isoforms have specialised functions (Premont *et al.*, 1999).

1.3.1.2 Receptor internalisation

Receptor internalisation isolates the receptor from its down-stream G protein dependent signalling pathway, and can be involved in both the desensitisation and/or resensitisation of GPCRs. Investigation into β_2-AR signalling has shown that the β-arrestin isoform 1 (β-arrestin-1) plays an important role in coordinating receptor internalisation following agonist-induced desensitisation (Han *et al.*, 2001). β-arrestin-1 regulates receptor internalisation via a series of protein-protein interactions. One such interaction is with adaptor protein-2 (AP-2), a membrane bound protein which acts as a major binding hub, recruiting accessory proteins from the cytosol to clathrin-coated pits, specialised sites in the membrane at which coat proteins assemble for endocytosis. Association of the receptor-arrestin complex with AP-2 targets the complex to clathrin-coated pits. From here, it is sequestered into endocytotic vesicles and internalised (Barki-Harrington & Rockman, 2008; Milano *et al.*, 2002). Clathrin interacts with AP-2 at a site which signficantly overlaps with the β-arrestin-1 binding site, causing β-arrestin-1 displacement once the receptor-arrestin complex has reached a clathrin coated pit. This frees β-arrestin-1 to interact directly with clathrin, leading to arrestin-receptor complex internalisation (Laporte et al., 2002; Schmid et al., 2006). The β-arrestin-1-dependent recruitment of c-src (a tyrosine kinase) to the activated receptor is also important for endocytosis as c-src-dependant phosphorylation of dynamin is essential for the final pinching off of vesicles from clathrin coated pits (Ahn *et al.*, 1999; Milano *et al.*, 2002). Without functional dynamin, internalisation of agonist-activated receptors cannot be completed leaving

the accumulated receptor-arrestin complexes in limbo at the plasma membrane. The internalised receptors can be recycled back to the plasma membrane following resensitisation, or targeted to lysosomes for degradation, depending of the stability of their interaction with the β-arrestin. For some receptors, internalisation has been shown to play a key role in their resensitisation (reviewed in Krupnick & Benovic, 1998). Resensitisation appears to involve acidification of the endosomes, which induces ligand dissociation, and enables receptor dephosphorylation by activating protein phosphatases 2A and 2B (PP2A and PP2B) (Böhm *et al.*, 1997).

1.3.1.3 Receptor down-regulation

Down-regulation of the receptor also results in an attenuated response, by decreasing the number of receptors expressed by the cell (Lohse, 1993). Down-regulation is caused by the degradation of internalised receptors, and/or by decreasing the rate of transcription and/or translation of new receptors (Bouvier *et al.*, 1989; Hadcock & Malbon, 1993). Compared with uncoupling and internalisation, down-regulation is a slow process, taking hours for degradation-mediated down-regulation, and up to several days for transcriptionally-regulated down-regulation (depending on the turnover rate of the receptor) (Lohse, 1993). Resensitisation following down-regulation is also slow, as it requires new receptors to be synthesised (Böhm *et al.*, 1997).

1.3.2 Desensitisation of V1bR

1.3.2.1 Current knowledge

Various stressful stimuli, such as osmotic stress, have been shown to produce regulatory changes to V1bR signalling *in vivo* (reviewed in Mason *et al.*, 2002), resulting in a decrease in ACTH responsiveness. Numerous *in vitro* studies have also induced desensitisation of the ACTH response to AVP, by exposing the V1bR to repeated or prolonged stimulation with AVP (Mason *et al.*, 2002). Furthermore, V1bR desensitisation has been induced in primary cultures of anterior pituitary cells by AVP treatments that approximated endogenous AVP

secretion (Hassan *et al.*, 2003). Pre-treatment with as little as 2nM AVP was seen to be capable of significantly reducing the responsiveness of the cells to further AVP stimulation. This desensitisation was rapid (reaching completion within 10 minutes) and readily reversible. While the mechanisms of V1bR desensitisation have not been fully elucidated, some inferences can be made based on what is known.

Primarily, rapid and reversible desensitisation of a GPCR (such as that observed for the V1bR) is commonly caused by uncoupling of the receptor from its G protein. This process is typically mediated by phosphorylation of the receptor by GRKs or second messenger-dependent kinases, such as PKC (see Section 1.3.1.1). An immunoprecipitation/immunoblotting study by Berrada et al. (2000) investigating the interaction of GRK and PKC isoforms with green fluorescent protein-tagged AVP receptors reported a direct physical interaction between GRK5 and the V1bR (Berrada *et al.*, 2000). This interaction was induced only in response to AVP-stimulation and was rapid: occurring after ~30 seconds of agonist stimulation. The interaction was also transitory, with no physical association detected at later time-points. There was no evidence of an association between the V1bR and other GRK isoforms. A physical interaction was detected between the PKC isoform PKCα and the V1bR. Like that seen with GRK5, this interaction was induced by agonist stimulation of the receptor and was not seen with inactivate receptors. PKCα-V1bR association was less sensitive to receptor activation than that involving GRK5, occurring only after 2 minutes of agonist stimulation. Collectively, these data indicated a possible involvement of both GRK5 and PKCα in the regulation of V1bR signalling. Around the same time, a second study by Budd et al. (2000) demonstrated the involvement of CK1α-mediated phosphorylation in regulating the magnitude of the agonist-dependent response elicited in a different $G_{q/11}$-coupled GPCR, the m3-muscarinic receptor. This phosphorylation did not, however, cause desensitisation. This suggested CK1α as an additional candidate kinase for phosphorylation of the V1bR.

Previous studies from the Mason laboratory examined the desensitisation of the ACTH-response to AVP in primary cultures of ovine anterior pituitary cells, using perifusion of the cells with various pharmacological agents to elucidate the roles of the kinases PKC and CK1α, the protein phosphatases type 1A (PP1A), PP2A and PP2B, and receptor internalisation in V1bR desensitisation and resensitisation (Hassan *et al.*, 2003; Hassan & Mason, 2005).

Inhibition of PP1A and PP2A activity did not affect the rate of receptor desensitisation or resensitisation. However, inhibition of PP2B-mediated dephosphorylation produced a marked decrease in the rate of receptor resensitisation, indicating that phosphorylation was likely involved in receptor desensitisation. However, as numerous other protein components of the AVP signalling pathway may also subject to phosphorylation-mediated regulation, it is possible that phosphorylation of the receptor itself was not responsible for this effect. Inhibition of CK1α activity had no effect on the extent of desensitisation measured. The role of PKC in desensitisation was also examined. Perifusion of the ovine anterior pituitary cells with the PKC-inhibitor Ro 31-8220 did not reduce the extent of desensitisation measured, nor did use of the PKC-activator 1,2-dioctanoyl-*sn*-glycerol increase the extent of desensitisation. This indicated that while phosphorylation was likely to be involved in V1bR desensitisation, it is not mediated by PKC and CK1α (Hassan & Mason, 2005).

In some receptors, endocytosis of the activated receptors is a critical part of their desensitisation and/or resensitisation (see Section 1.3.1.2). Hassan and Mason (2005) examined the role of receptor internalisation in the desensitisation and resensitisation of ACTH responsiveness to AVP by blocking endocytosis. Blockade resulted in a decrease in the extent of desensitisation, though this effect was partial. It was unclear whether the concentration of endocytosis-inhibitor used was sufficient to induce full blockade of internalisation. If full inhibition was obtained, these results would indicate that the remaining desensitisation measured was mediated by non-internalisation based mechanism. However, partial inhibition of internalisation would also account for the partial inhibition of desensitisation measured (Hassan & Mason, 2005). Blockade of endocytosis did not appear to have any effect on the rate of resensitisation.

From this study, it appears that both phosphorylation (by an unidentified kinase) and internalisation of the V1bR are involved in desensitisation of the ACTH-response to AVP in anterior pituitary cells. The interaction between these two aspects is unclear, however it is possible that internalisation is the actual desensitising mechanism, and phosphorylation of the V1bR acts as a signal to promote internalisation.

1.3.2.2 Aims of this study

Current information from the Mason laboratory indicates that phosphorylation is involved in the desensitisation of the V1bR (Hassan & Mason, 2005). However, inhibition of two kinases responsible for GPCR phosphorylation (PKC and CK1α), has been shown to have no effect on the rate or extent of V1bR desensitisation (Hassan & Mason, 2005). As described in Section 1.3.1.1.2, GPCR desensitisation can also be produced by GRK-mediated receptor phosphorylation. In particular, there is evidence that the GRK5 isoform may be able to physically interact with the V1bR (Berrada *et al.*, 2000).

One aim of the research reported in this thesis was to establish and validate the methods required to determine if GRK5-mediated phosphorylation of the V1bR is involved in desensitisation of the receptor to AVP stimulation. As described above, the mechanisms of V1bR desensitisation have previously been examined in the Mason laboratory by using pharmacological agents to alter the activity of key enzymes or cellular processes. Primary cultures of ovine anterior pituitary cells were used for those experiments and the level of AVP-induced ACTH secretion was used as a measure of V1bR responsiveness. As there are currently no GRK5 isoform-specific pharmacological inhibitors available, an alternative approach was required to investigate possible involvement of GRK5 in V1bR desensitisation.

The approach was to use RNA interference (RNAi) techniques to specifically reduce the expression of GRK5. RNAi exploits a homology-dependant silencing system found in all eukaryotes (Agrawal *et al.*, 2003) to induce post-transcriptional silencing of specific genes (Fire *et al.*, 1998). RNAi is not practical for use in primary cell cultures, as they are difficult to obtain, culture and transfect. As such, the use of RNAi to knockdown GRK5 expression necessitated the use of a model cell system in place of primary cultures of anterior pituitary cells. Sequences for specific short interfering RNAs (siRNAs) targeted against human GRK5 have previously been published by others (Chen *et al.*, 2009; Kim *et al.*, 2005; Ren *et al.*, 2005) and commercial antibodies for human GRKs are available. These factors made the use of a cell line originating from human tissue a prudent choice. HEK293 cells transiently transfected to express the rat V1bR were used as a model cell line in which the V1bR could be

expressed. Its activity could be monitored by labelling with [^{3}H]*myo*-inositol and measuring [^{3}H]-inositol phosphate production following AVP stimulation .

This research consisted of the optimisation and validation of protocols needed to:

1. Induce RNAi-mediated knock down of GRK5 expression (Chapter 5)
2. Demonstrate the knockdown of GRK5 mRNA using quantitative reverse-transcriptase polymerase chain reaction (Chapter 4), and
3. Demonstrate the knockdown of GRK5 protein using Western blotting (Chapter 3)

2

METHODS FOR USE OF HEK293 CELLS AS A MODEL CELL SYSTEM FOR ANTERIOR PITUITARY CELLS: CELL CULTURE, TRANSFECTION WITH rV1bR AND IP ASSAY

2.1 INTRODUCTION

In this research, HEK293 cells transiently transfected to express the rat V1bR (rV1bR) were used as a model cell line for human anterior pituitary cells.

2.1.1 HEK293 cells

The HEK293 cell line was developed by Graham et al (1977) by transfecting a primary culture of HEK (human embryonic kidney) cells with fragments of human adenovirus 5 DNA. HEK293 cells are an immortal adherent cell line, which divide to produce a monolayer on the plating surface (Figure 2.1). They were initially assumed to have descended from an embryonic kidney epithelial cell, however, since the mid 1990's multiple groups have observed and reported the presence of neuronal phenotypes in HEK293 cells (Anderson *et al.*, 1995; Daaka *et al.*, 1997; Dautzenberg *et al.*, 2000; He & Soderlund, 2010; Schachter *et al.*, 1997; van Koppen *et al.*, 1996; Zhu *et al.*, 1998). In 2002, Graham and colleagues published an in-depth investigation into the expression profile of HEK293 cells (Shaw *et al.*, 2002a; b), http://www.mbi.ufl.edu/~shaw/293.html). This study confirmed the expression of neuron-specific proteins by HEK293 cells and demonstrated that the pattern of their expression of vimentin, and keratins 8 and 18 was characteristic of that seen in early differentiating cells. These findings, coupled with evidence that neuronal cells are preferentially transformed by adenovirus 5 (Shaw *et al.*, 2002b), suggested that a neuronal stem cell within the original HEK

cell primary culture was the most likely parent cell of the HEK293 cell line. This heritage makes HEK293 cells particularly suitable for use as a model of neuronal cells.

2.1.2 Expression of the rV1bR

HEK293 cells do not appear to express the V1bR (Atwood *et al.*, 2011). As such, its expression was induced for this research by transfecting the cells with a plasmid containing the rat V1bR gene (Cummings, 2011). No selection pressure for maintenance of the plasmid was applied, making this expression transient (<7 days). Transient transfection is a common method for inducing the expression of a protein of interest, and has previously been used by others to study mechanisms of GPCR signalling and regulation. For example, transiently transfected HEK293 cells have been used to look at the involvement of GRKs in signalling by the H1 histamine receptor (Iwata *et al.*, 2005); the angiotensin II receptor (Kim *et al.*, 2005); and the V2 vasopressin receptor (Ren *et al.*, 2005).

2.1.3 Measurement of V1bR activity

As described in Chapter 1, AVP-induced activation of the V1bR results in the production of the second messenger signalling molecules DAG and IP_3 by PLCβ (Antoni, 1993; Maybauer *et al.*, 2008). The production of IP_3 can be measured using an inositol phosphate assay (IP assay) (Tobin *et al.*, 1997). For this analysis, the cells are labelled with [^{3}H]*myo*-inositol prior to receptor stimulation. The [^{3}H]*myo*-inositol is incorporated into the IP metabolic pathway, and allows the inositol phosphates (IPs) produced in response to receptor activation to be measured based on the radioactivity of the isolated IPs. IP assays have previously been used in this laboratory to measure the desensitisation of both transiently and stably expressed rV1bR, in HEK293 cells (Cummings, 2011; Gatehouse, 2008). IP assays have also been used by others to assess the desensitisation of numerous PLCβ-coupled receptors, including investigating the role of various GRKs (Dale *et al.*, 2000; Price *et al.*, 2002).

Crucially for this research, HEK293 cells do not appear to express the V1a or oxytocin receptors which also interact with PLCβ via $G_{q/11}$ in response to AVP stimulation, activating

the inositol phosphate second messenger signalling pathway (Atwood *et al.*, 2011; Shaw *et al.*, 2002b). This means that any AVP-stimulated IP response detected is solely due to stimulation of the transiently expressed rV1bR.

2.2 MATERIALS

For the source of all materials referred to in this chapter, see Appendix A

2.3 SOLUTIONS AND MEDIA

For details of all solutions and media referred to in this chapter, see Appendix B

2.4 METHODS

2.4.1 Maintenance of HEK293 cells in culture

Sterile glassware and plastic ware, and aseptic working technique were used for cell culture. American Type Culture Collection (ATCC) recommendations for culture were followed whenever possible. HEK293 cells were cultured in 75cm^2 culture flasks with vented seal caps in Eagle's Minimum Essential Medium containing sodium pyruvate, sodium bicarbonate and GlutaMAX, (pH 7.1) supplemented with 10% foetal bovine serum (FBS) (MEM+). Cells were incubated at 37^{o}C in a humidified 95% air, 5% CO_2 environment (NuAIRE™ IR autoflow CO_2 water jacketed incubator) and sub-cultured (passaged) to maintain the cell density between 15 and 80% confluent. Cell cultures underwent between eight and ten passages before being discarded and a new cryopreserved cell aliquot thawed.

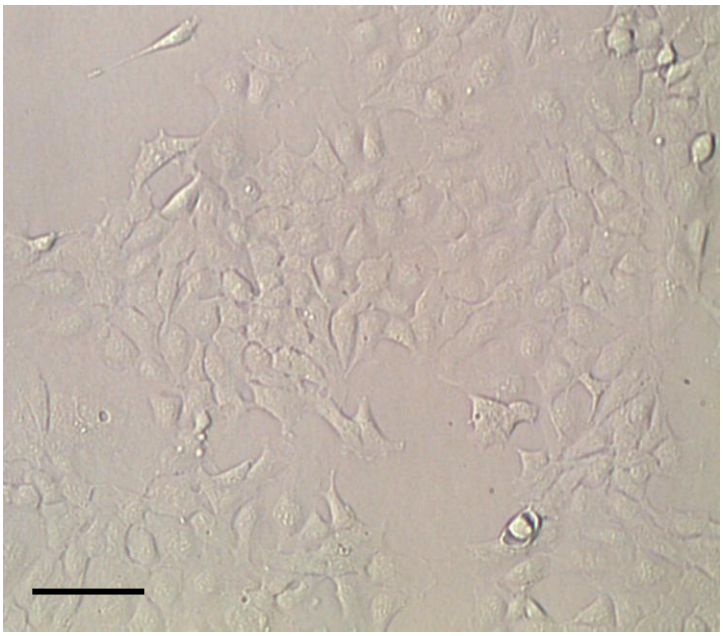

Figure 2.1 HEK293 cells showing typical adherent monolayer conformation. Scale bar is 20μm.

2.4.1.1 Thawing

An aliquot of HEK293 cells was removed from liquid nitrogen storage and thawed by shaking the tube gently in a 37^{o}C water bath. Once thawed, the aliquot was transferred into a 75cm^{2} flask containing 19mL MEM+ which had been equilibrated in a humidified 95% air, 5% CO_2 environment and pre-warmed to 37^{o}C. The cells were then cultured as described above.

2.4.1.2 Sub-culturing

Flasks were passaged (or sub-cultured) when the cell monolayer reached 50-80% confluence. For a 75cm^{2} flask, 3mL of pre-warmed 0.25% Trypsin/ 0.39g/L EDTA.4Na (T/E) solution was added, and the flask was tilted to cover the cells with solution. The flask was then righted, and the excess T/E vacuum aspirated. The flask was incubated at room temperature for approximately 8 minutes lying flat on the microscope stage until the cells were seen to dissociate from each other and the flask surface. The flask was tapped firmly once on each side, and the cells were washed from the base of the flask with 4mL of MEM+. The cell

suspension was repipetted three times with a sterile plastic pipette to dissociate clumps, and transferred to a 50mL screw top centrifuge tube. A 50µL aliquot was mixed 1:1 with Trypan blue working solution and incubated at room temperature for 2 minutes to stain dead cells, before being loaded onto a haemocytometer slide for counting. Viability ranged from 96-100%. A volume of cells containing 0.4 x 10^6 to 0.7 x 10^6 cells was added to a 75cm^2 flask containing in total a volume of 15mL. After 24 hours, the medium was aspirated and replaced with fresh MEM+.

2.4.1.3 Freezing

The following volumes were used for cryopreservation of cells harvested from one 75cm2 flask passaged at 80% confluence. Following passaging, the cell suspension was spun at 140 x g for 8 minutes at room temperature (Jouan CR412 Centrifuge) to pellet the cells. During the spin, freezing medium was prepared by combining 1.2mL of MEM without FBS (MEM-), 0.4mL FBS, and 0.4mL dimethyl sulfoxide (DMSO) in a sterile beaker. The supernatant was removed from the cells via vacuum aspiration, and the bottom of the tube tapped to loosen the cell pellet. The pellet was resuspended in 2mL of MEM-, and 2mL of the freezing medium added in a drop wise fashion, swirling thoroughly between additions. One millilitre aliquots of the cell suspension were transferred to Nunc cryo-tubes, which were then placed in a Nalgene cell freezer and incubated at -80^oC overnight. The following day, the cryo-tubes were transferred to a liquid nitrogen canister for long term storage and their details entered in the cell line inventory.

2.4.2 Transient transfection of HEK293 cells to express the rV1bR

HEK293 cells were transiently transfected to express the rat V1bR (rV1bR) (Lolait *et al.*, 1995), using the pN1-rV1bR plasmid (Section 2.4.2.1) and the transfection reagent FuGENE® 6 as described previously (Cummings, 2011). FuGENE® 6 is a non-liposomal carrier molecule which interacts with the DNA, increasing its uptake by the cell and so increases the efficiency of the transfection. FuGENE® has been shown to have low cytotoxicity, making it suitable for transfection of cells at a lower confluence (Nagy & Watzele, 2006).

2.4.2.1 Plasmid details

The pN1-rV1bR plasmid (Figure 2.2, D) was previously generated in this lab by Siobhan Cummings (Cummings, 2011) by combining elements of the plasmids pEGFP-N1 (Figure 2.2, C) which contains a neomycin/kanamycin resistance gene, and pALTER-rV1bR, (Figure 2.2, B) (Young *et al.*, 2007) which contains the rat V1bR sequence (Lolait *et al.*, 1995).

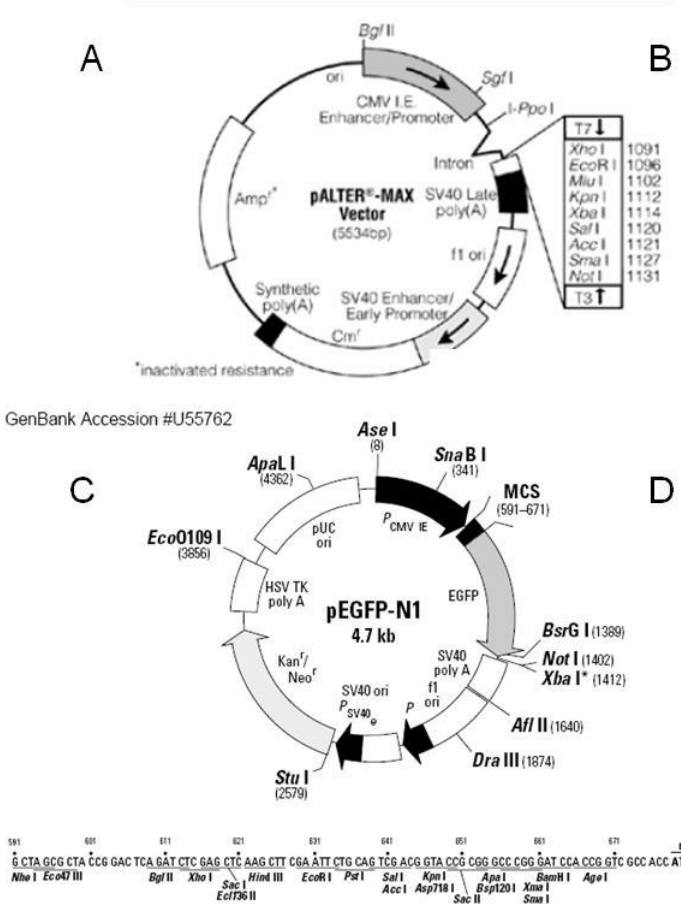

pALTER-rV1bR (Young et al., 2007)	
Vector:	pALTER-MAX (Promega)
Construct size:	8.2 kb
Insert:	rV1bR (Lolait et al.,1995)
Insert size:	2.7 kb

pN1-rV1bR (Cummings, 2011)	
Vector:	pEGFP-N1 (Clone Tech)
Construct size:	6.9 kb
Insert:	rV1bR (Lolait et al.,1995)
Insert size:	2.5 kb

Figure 2.2 Plasmid details. *A*) Schematic representation of the pALTER-MAX vector, used as the vector for pALTER-rV1bR *B*) pALTER-rV1bR details, *C*) schematic representation of pEGFP-N1 plasmid details structure, showing the *Not*1 restriction site and the multiple cloning site (MCS) containing the *Sal*1 restriction site. *D*) pN1-rV1bR details.

Briefly, the section of pEGFP-N1 encoding EGFP was excised via restriction enzyme cleavage with *Sal*1 and *Not*1, and replaced with the rat V1bR sequence from pALTER-rV1bR. The resulting plasmid, pN1-V1bR, containing both the gene of interest and antibiotic resistance

genes, was ~6.9kb. Generation of the plasmid was confirmed via gel electrophoresis of the products of its digestion with *Sal*1 and *Not*1. Banding was seen as expected at ~4.4kb, representing the destination vector, and ~2.5kb, representing the V1bR insert. pN1-rV1bR was stored at -20^{o}C and diluted to 0.1µg/µL for use.

2.4.2.2 Transient Transfection protocol

To induce the expression of the rV1bR, HEK293 cells were transiently transfected with the pN1-rV1bR plasmid using FuGENE® 6 36 hours after plating, and, if applicable, reverse transfection with siRNA (see Chapter 5). Typically, the cells were between 45% and 80% confluent when transfected with the pN1-rV1bR.

At the time of transfection, the volume of medium in each culture vessel was 600µL for wells of a 24-well plate, and 3mL for a 35mm-diameter dish. The cells were transfected with the FuGENE® 6/DNA transfection complex as described below. An appropriate volume of master mix was prepared, depending on the number of wells/plates used in the experiment. For clarity, the relative volumes of the transfection complex components are shown in Table 2.1.

Reagent	**Volume per well of 24-well plate**	**Volume per 35mm-diameter dish**
MEM -	19.4µL	97µL
FuGENE® 6	0.6µL	3µL
pN1-V1bR (0.1µg/µL)	2µL (0.2µg)	10µL (1µg)
Total volume	22µL	110µL

Table 2.1 Relative volumes of transfection complex components.

The FuGENE® 6 was warmed to room temperature, and diluted in MEM without FBS (MEM-) in a 1.7mL microtube. Care was taken to ensure that the undiluted FuGENE® 6 did not come into contact with the plastic tube as it can bind to the plastic — limiting transfection efficiency (Roche, 2006). The solution was vortexed for 1 second to mix and incubated at room temperature for 5 minutes after which the pN1-V1bR plasmid DNA was added. The solutions

were mixed by tapping the tube vigorously, and the tube was spun briefly to collect the liquid in the bottom. The transfection solution was incubated at room temperature for 30 minutes. Immediately following this incubation, the transfection complex was added to the cells in a drop-wise fashion. The volume of transfection complex added was 22µL for each well of the 24 well cell culture plates, and 110µL for a 35mm-diameter plate. The plates were then swirled gently in both a clockwise and anti-clockwise direction to ensure thorough mixing. The time at which the cells were returned to the incubator was noted.

2.4.3 Measurement of V1bR responsiveness via inositol phosphate assay

The IP assay described below is based on assays previously performed in this lab (Cummings, 2011; Gatehouse, 2008). A flow diagram of the relative timing of each step is shown in Figure 2.3

2.4.3.1 Labelling of cells with [^{3}H]*myo*-inositol

HEK293 cells were grown in inositol-free medium spiked with [^{3}H]*myo*-inositol for 20 hours prior to the IP assay.

Twenty eight hours after transfection with the pN1-rV1bR plasmid, the standard culture medium was removed from the cells via vacuum aspiration, and each well washed once with 0.8mL inositol-free DMEM. This was followed by the addition of 0.5mL pre-warmed inositol-free DMEM plus 0.1% BSA, 2mM GlutaMAX (DMEM+) containing [^{3}H]*myo*-inositol/mL (2.5µL/10mL medium) to each well. The cells were then incubated at 37^{o}C for 20 hours before the functional assay was performed.

2.4.3.2 rV1bR functional assay

Stimulation with 100nM AVP was used as the rV1bR functional assay. The duration of stimulation differed between experiments and is indicated in the text (Sections 6.3.2.6, 6.4.2, and 6.6). The functional assay was performed as close to 20 hours after labelling as possible (Gatehouse, 2008). Lithium chloride (LiCl) was included in the wash and treatment media to

inhibit the degradation of IP_1 to free inositol by inositol monophosphatase. This resulted in the accumulation of [^{3}H]-labelled IP metabolites for counting (Berridge, 1985).

Immediately prior to the assay, the labelling medium was removed from the wells via vacuum aspiration. Each well was then washed once with 0.8 mL MEM (+0.1% BSA and 10nM LiCl) to remove unincorporated label from the wells. The cells were treated with MEM (+0.1% BSA and 10nM LiCl) or MEM (+0.1% BSA and 10nM LiCl) ± 100µM AVP as required.

At the end of the assay, 0.5mL of ice cold stop solution was added to each well, and the plates incubated at room temperature for at least 1 minute. If necessary, the cells could then be stored at 4^{o}C for a number of hours before isolation of the [^{3}H]-labelled inositol phosphates.

2.4.3.3. Isolation of [^{3}H]-labelled inositol phosphates

The [^{3}H]-labelled inositol phosphates were isolated from the cell lysates using a column-based anion-exchange system.

2.4.3.3.1 Preparation of the columns

Bio-Rad AG1-X8-resin (formate form) columns (one column per well) with a bed depth of approximately 2cm were prepared by pipetting 2mL of resin slurry (prepared by mixing the resin 1:1 with NPH_2O) into Polyprep® chromatography columns (Bio-Rad), and allowing the water to drip through before use.

2.4.3.3.2 Preparation of the cell lysates

To return the cell lysates to ~pH 7.0, 0.5mL of ice-cold neutralisation solution was added to each well immediately before they were loaded onto the columns. Neutralization of the samples was required for effective functioning of the basic anion-exchange resin (Bio-Rad AG1-X8) (Bio-Rad, 2000) used to isolate IPs. Due to the presence of phenol red in the MEM, the pH of the medium in each well could be estimated by its colour. At pH 7.0 MEM is a light salmon pink. However very small variations from pH 7.0 cause quite distinct colour changes,

ranging from an orange/yellow (slightly acidic), to a bright pink (slightly alkali). It has been reported that this variation in pH does not have a noticeable effect on the IP assay results (Gatehouse, 2008). The cells in each well were then thoroughly scraped and the lysates were homogenised by repipetting vigorously six times with a Gilson P1000 pipette.

2.4.3.3.3 Isolation of the inositol phosphates from the cell lysates

The contents of each well were loaded onto a column with a P1000 Gilson pipette (one column per well) as follows: the end of the P1000 Gilson pipette tip was placed on the side of the column just above the resin and the solution released slowly and evenly in order to minimise disruption of the resin bed. The columns were washed with 10mL of NPH_2O, and 8mL of elution buffer II to elute free inositol and glycerophosphoinositides, respectively. Both elutions were discarded. Finally, 3mL of elution buffer VI was loaded onto each column to elute the total inositol phosphates, which were collected in 35mL polypropylene vials.

2.4.3.3.4 Regeneration of columns

If necessary, packed columns could be regenerated and reused the same day. Columns to be reused were washed with 10mL of regeneration solution, followed by 30mL of NPH_2O. It has been reported that the use of regenerated columns does not significantly affect the results of the IP assay (Gatehouse, 2008).

2.4.3.4 Detection and measurement of [^{3}H]*myo*-inositol-labelled IP's

The level of [^{3}H]*myo*-inositol-labelled IPs in each sample was measured via liquid scintillation counting

2.4.3.4.1 Preparation of the samples and scintillation counting

The eluted inositol phosphates from each sample were diluted 1:10 with OPTIPHASE 'HISAFE' 3 scintillation cocktail (Perkin-Elmer) in labelled 20mL scintillation vials as described below. Care was taken not to touch the sides of the vials during set up, as the counter

reads from this area. One millilitre of each sample was transferred to the appropriately labelled vial using a P1000 Gilson pipette. Ten millilitres of scintillation cocktail was then added to each vial using a pump dispenser. The vials were capped and shaken thoroughly to mix. An initial burst of chemiluminescence is produced by mixing the reagents and can interfere with the accuracy of the counts. To avoid this, the vials were kept in the dark overnight before counting, allowing the chemiluminescence to clear. Samples were counted using the CPM function of a Packard 1900 CA Tri-Carb Liquid Scintillation Analyser for 10 minutes each.

2.4.3.5 Analysis of the IP Assay

Certain components of the elution solution or scintillation cocktail can reduce the CPM detected by absorbing either the β energy itself, or the photons it produces. This is phenomenon is called quenching. The spectral quench parameter (SQPI) for H^3, which indicates the level of quenching occurring in each sample, was calculated by and corrected for automatically by the counter. Prior to data analysis, the SQPI was checked for consistency across all samples. Variation in SQPI of ± 0.5 between samples was typical.

For each treatment, the CPM for all replicates was analysed and graphed, using GraphPad Prism 4.0 to determine the mean and SEM. Mean CPM from wells stimulated with 100nM AVP were then expressed as a fold increase of the CPM for control cells (0nM AVP).

2.4.3.6 Disposal of IP assay waste

Several types of waste which required special disposal were generated during the IP assay. The treatment of each type is described below.

Diluted tracer left over from labelling the cells was disposed of down the sink with cold running water. The sink and pipes were then flushed with cold water for at least 30 minutes. Plastic ware that came into contact with radioactivity only was placed in a dedicated radioactive waste bin. Glassware that came into contact with radioactivity only was rinsed under cold running water for at least 10 minutes, then rinsed with distilled H_2O and washed as usual. The radioactive resin was rinsed from the columns with NPH_2O and collected. Plastic

ware, such as pipette tips, that came into contact with both radioactivity and biohazardous material (i.e. HEK293 cells) were collected and soaked overnight in 1% Virkon and then placed in a dedicated radioactive waste bin. Liquid waste containing both cells and radioactivity was treated with 1% Virkon overnight, and disposed of down the sink. The sink and pipes were flushed with water for at least 30 minutes after disposal of waste.

3

WESTERN BLOTTING PROTOCOLS FOR THE DETECTION OF GRK5 AND ACTIN EXPRESSION

3.1 INTRODUCTION

To validate the results from RNAi experiments (described in Chapters 5 & 6), it was necessary to measure the reduction in the level of GRK5 protein expression in cells treated with GRK5-targeted siRNA compared to that of control cells.

Western blotting is a technique by which proteins separated based on their molecular weight/length are identified via immunoblotting (Burnette, 1981; Renart *et al.*, 1979; Towbin *et al.*, 1979). It is commonly used in medicine in the diagnosis of diseases such as HIV (Schneppenheim & Rautenberg, 1987), Lyme disease (Dressler *et al.*, 1993) and bovine spongiform encephalopathy (Schaller *et al.*, 1999), and in research to monitor induced changes in protein expression, for example, by RNA interference (Agrawal *et al.*, 2003).

Immunoblotting utilises members of the immunoglobin (Ig) family of blood-plasma proteins called antibodies, which are produced by vertebrates as part of the immune response geared against infection by foreign substances (Garrett & Grisham, 2005). Introduction of a foreign, or 'antigenic', molecule into the blood stream stimulates the production of antibodies that specifically recognise that molecule. The majority of antibodies produced during an immune response are G-class Igs (IgG) (Garrett & Grisham, 2005). Western blotting is an indirect method of immunoblotting, as it is dependent on the use of two different antibodies (Figure 3.1) to detect the protein of interest. The first, the primary antibody, is raised against a part or the whole of the protein of interest and is used to locate it. The second, the secondary antibody,

is raised against a single class of immunoglobin from the species used to produce the primary antibody, for example, against rabbit IgG. The secondary antibody is coupled to a detection system and allows visualisation of the target protein by binding specifically to its antigen, i.e. the primary antibody. The detection system can be direct, e.g. a flurophore or radiolabel, or indirect e.g. an enzyme-conjugate (such as alkaline phosphatase or horseradish peroxidase (HRP)), that converts an added substrate to a visible product (Figure 3.1) (Sambrook *et al.*, 1989). Due to the antigenic-specificity of the primary and secondary antibodies, Western blotting can be used to detect the expression of the protein of interest in a sample containing the full component of cellular proteins (Sambrook *et al.*, 1989). Western blots are primarily qualitative, not quantitative. However, they can be used to identify relative changes in the target protein across samples. Important parameters to consider when optimising Western blotting protocols are discussed in Section 3.3.1.

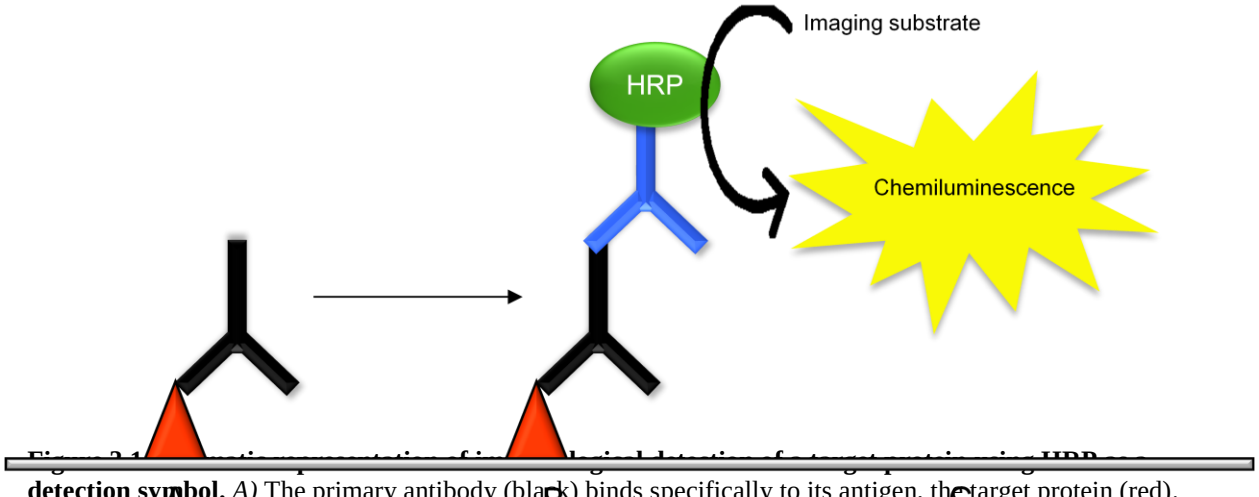

detection symbol. *A)* The primary antibody (black) binds specifically to its antigen, the target protein (red). *B)* The HRP-conjugated secondary antibody (blue) then interacts specifically with its antigen, the primary antibody. *C)* The antigen-antibody complex is visualised via processing of an imaging substrate to a chemiluminescent product by the HRP enzyme.

In this research, a Western blotting protocol was used to measure the effect of transfecting HEK293 cells with GRK5-targeting siRNA (see Chapters 5 & 6) on cellular GRK5 protein levels. The Western blotting protocol used for the detection of GRK5 is described in Section 3.2. Detection of actin, a structural protein whose expression should not be altered by the presence of GRK5-directed siRNA, was included in the protocol to control for loading errors

and uneven transfer. The optimisation and validation of the Western blotting protocols used in this research are described in Section 3.3.

3.2 WESTERN BLOTTING METHODS

3.2.1 Materials

For the source of all materials referred to in this chapter, see Appendix A

3.2.2 Solutions and Media

For details of all solutions and media referred to in this chapter, see Appendix B

3.2.3 Cell Lysis

Cell lysis allows the extraction of whole cell protein for analysis by dissolution of the cellular membranes. This process also releases proteolytic enzymes from the liposomes which can degrade proteins, thereby affecting sample quality. To limit protein degradation, all protein work was done on ice, and a protease inhibitor was added to the lysis buffer.

HEK293 cells cultured in 35mm-diameter dishes as described in Sections 2.4.1, 3.3.3, 5.2.6, and 6.3.2 were lysed as follows. The culture medium was removed by vacuum aspiration. Each dish was washed twice with 1mL of pre-warmed PBS to remove traces of medium. Fifty microlitres of 1 X SDS lysis buffer was added to each dish, and the dish tilted to ensure even coverage of the cells with lysis buffer. The cells were then incubated for ten minutes at 37^{o}C. Following the lysis incubation each dish was scraped thoroughly with a plastic cell scraper (Greiner Bio-One). The cell lysates were transferred by scraping into labelled 15mL centrifuge tubes and stored on ice or at -20^{o}C until sonication. Each sample was sonicated at 21V for 30 seconds using a Sonics Vibra-Cell™ sonicator. Sonication was performed in a pulsatile fashion with alternating 9 second pulses of on and off (sonication took 57 seconds in total, comprising

of a cumulative 30 seconds on and 27 seconds off). The tube was tilted after sonication to confirm sample fluidity. This shearing step was necessary to reduce sample viscosity caused by aggregation of chromosomal DNA released from the nucleus during cell lysis. The samples were then transferred using a P1000 Gilson pipette to labelled 1.7mL micotubes and stored at -80^{o}C until use. The protein concentration of each sample was determined via bicinchoninic acid (BCA) assay (Section 3.2.4).

3.2.4 Protein quantification via BCA assay

To compare the expression of the target protein between samples using Western blotting it is necessary to accurately determine the concentration of total protein in each sample so equal quantities can be analysed. The BCA assay (Smith *et al.*, 1985) is a colourimetric test which uses bicinchoninic acid to detect Cu^{1+}. Under alkaline conditions peptide bonds reduce Cu^{2+} to Cu^{1+}, which is then chelated by BCA molecules (at a ratio of two BCA molecules per cuprous ion) to form a bright purple solid with a maximum absorption at 562nm (Figure 3.2, *A*). This reaction has been exploited to produce commercially available kits which, when coupled with a standard curve, can be used to determine the concentration of total protein in a solution.

Traditionally, BCA assays are performed using optical cuvettes and a UV spectrophotometer. Cuvette-based protocols require large amounts of sample for protein quantification (Walker, 1996), so they are incompatible with analysis of samples of limited volume (50-100µL) such as those obtained in this study. For this reason, a microplate-adapted protocol for determination of protein concentration via BCA assay was used.

The microplate-adapted BSA assay used in this research was performed using standard NUNC™ 96-well plates (Thermo Fisher Scientific) and a BCA™ Protein Assay Kit (Thermo Fisher Scientific). A standard curve showing absorbance levels at known protein concentrations (Figure 3.2, *B*) was generated in duplicate for each assay by diluting 2mg/mL bovine serum albumin (BSA) with NPH_2O to 0, 0.2, 0.4, 0.6, 0.8, 1.0 and 1.2µg/µL BSA in a total volume of 20µL. Four microlitres of each sample was diluted 1/5 to a final volume of 20µL with NPH_2O (also in duplicate). BCA working reagent was prepared by mixing BCA

Reagents A and B at a ratio of 50:1, and 200µL of the working reagent was added to each well. The plate was then covered using a BarSeal™ adhesive cover and incubated at 37°C for 30 minutes. Absorbance was read at 560nm using a FLUOstar OPTIMA plate reader. The data were analysed using Microsoft Office Excel software to determine the protein concentration of each sample from the standard curve (Equation 3.1).

Equation 3.1 µg/µl sample = ((mean absorbance - intercept) / slope) x dilution factor

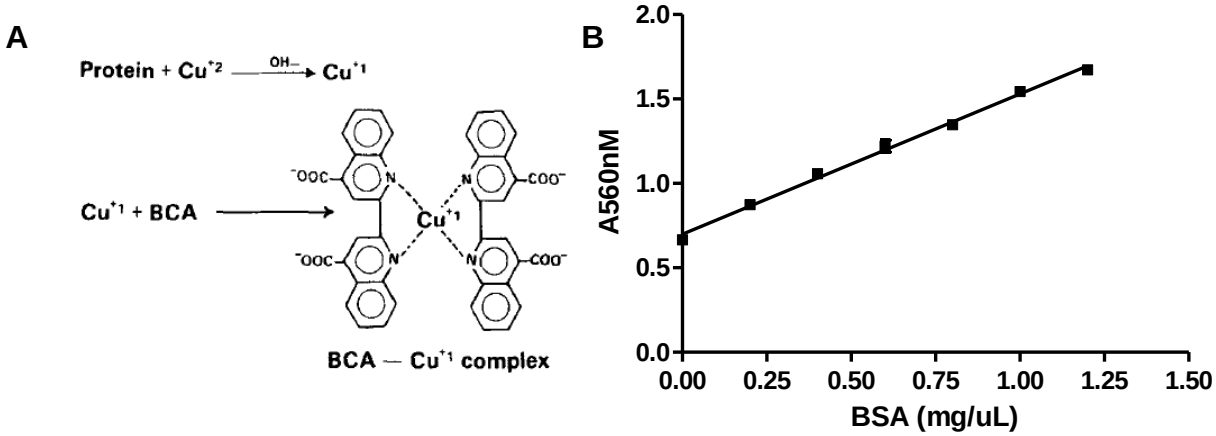

Figure 3.2 BCA assay for determining the protein concentration. *A*) Formation of the coloured compound during BCA assay (from Smith et al., 1985). *B*) Example of a typical standard curve.

3.2.5 SDS-Polyacrylamide gel electrophoresis

SDS-polyacrylamide gel electrophoresis (SDS-PAGE) is a method by which linearised proteins are electrophoretically separated in a size dependent manner (Laemmli, 1970).

Protein samples are treated with an anionic surfactant called sodium dodecylsulfate (SDS), which disrupts protein folding by forming strong interactions with polypeptide chains via its hydrophobic tail. Addition of reducing reagents such as beta-mercaptoethanol acts to eliminate stronger disulfide bonds, resulting in linearised polypeptide chains (Laemmli, 1970). As the extent of SDS binding is directly proportional to the length of the polypeptide, the resulting

charge-to-mass ratio is constant (Steele & Nielsen, 1978). Any intrinsic charge associated with the polypeptide itself is overwhelmed by the accumulated negative charge resulting from SDS-binding. The electrophoretic mobility of each protein is therefore determined by its molecular weight or length. Smaller proteins will migrate through the porous gel faster than large proteins (Garrett & Grisham, 2005; Steele & Nielsen, 1978) as their movement is less retarded by the matrix of polyacrylamide fibres. Ladders containing proteins of known molecular weights can be used to estimate the molecular weight of a particular protein band (Webb *et al.*, 1977).

3.2.5.1 Sample Preparation

Though 40µg of protein per lane was used during the majority of the protocol set up, 25µg of protein per lane was determined to be sufficient for detection of GRK5 and actin by Western blotting during knockdown experiments. Lowering the minimum amount of protein loaded allowed the use of a low loading volume (20µL), which decreased the probability of overflow between lanes, thus improving the reliability of the Western blot analysis. The amount loaded was consistent across wells within the same gel, but ranged from 25-40µg of protein per well between gels, depending on the concentration of the samples. As each lane was quantified relative to the control lane on the same gel (see Section 3.2.8.3.2), the differences in protein loaded between gels did not compromise the ability to compare results between gels. The volume of each sample required for loading the designated amount of protein was combined with 1µL each of bromophenol blue (0.1%) and beta-mercaptoethanol in 1.7mL microtubes, and the volume made up to 20µL with 1XSDS buffer (see Appendix B; final concentrations: bromophenol blue 0.005%, β-mercaptoethanol 5%). The tubes were sealed with parafilm to prevent sample evaporation and contain beta-mercaptoethanol fumes. The tubes were spun briefly in a bench top centrifuge to deposit the solution components, vortexed to mix, and spun again to collect the mixed solution at the bottom of the tube. The samples were then denatured by heating at 95^{o}C for 10 minutes, and placed on ice prior to loading.

3.2.5.2 Gel Electrophoresis

A Mini-PROTEAN 3 casting frame (Bio-Rad) was used to cast 1mm Tris-glycine gels, consisting of a 5% stacking gel and an 8% resolving gel (see Appendix A). A ten well comb was inserted into the stacking gel immediately after pouring to produce wells (see Appendix B for further casting details). Immediately prior to loading, the samples were collected by brief centrifugation, vortexed to mix, and spun again. The samples were loaded into the allocated wells with a P20 Gilson pipette. Multiple loadings were allowed to ensure the entirety of the samples were loaded. Six microlitres of PageRuler™ Prestained Protein Ladder (Fermentes) was loaded into an adjacent well to allow identification of bands by molecular weight. The gels were run at 100V in a Bio-Rad Mini PROTEAN® 3 Cell electrophoresis unit containing running buffer for 1.5-2 hours, until the 17kDa band of the ladder had run off the bottom of the gel.

3.2.6 Electrophoretic transfer of protein bands to a nitrocellulose membrane

Transfer of proteins to a membrane is advantageous as it exposes the bands, allowing for more efficient immunological probing (Towbin *et al.*, 1979). The membrane is also more durable than the gel, improving ease of handling. In electrophoretic transfer, the gel is sandwiched against a membrane which non-specifically binds proteins, and fully submerged in buffer. An electric current is used to mobilize the protein bands, moving them out of the gel and onto the membrane.

3.2.6.1 Set-up and Transfer

The transfer buffer was chilled at -20^{o}C for approximately 1 hour prior to use. The components of the transfer cassette (one piece of nitrocellulose membrane, six pieces of filter paper and two fibre pads per gel) were equilibrated in transfer buffer at 4^{o}C for at least 40 minutes before transfer. Following SDS-PAGE, the gel was removed from its glass casing and equilibrated in cold transfer buffer for 5-10 minutes before transfer. The cassette was assembled for transfer as shown in Figure 3.3, with air bubbles removed by rolling each new layer flat onto the stack with a smooth glass tube. The cassette was inserted in the buffer tank so that it was submerged in transfer buffer. The proteins were then electrophoretically transferred (Bio-Rad Mini-

PROTEAN® II Cell) to the HYBOND-C-Extra nitrocellulose membrane (Amersham Biosciences) for 2 hours at 100V.

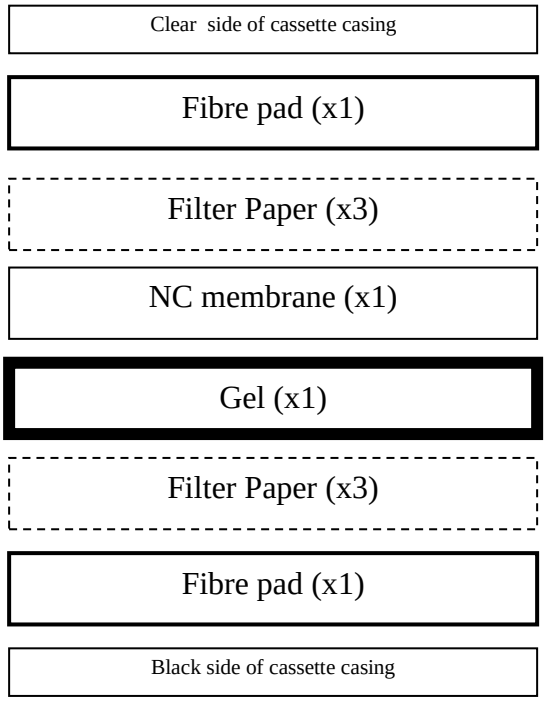

Figure 3.3 Arrangement of components in the transfer cassette. The gel is placed face down to maintain lane orientation on the membrane. The concave side of the membrane is placed against the gel.

3.2.6.2 Evaluation of Transfer efficiency

To evaluate transfer efficiency, the membrane-bound protein was stained by incubating the membrane in 0.01% Ponceau S for 1 minute. The membrane was rinsed with NPH_2O to remove excess stain, and checked for variation in protein transfer between lanes. A soft pencil was used to outline and number the lanes and excess membrane was trimmed off. The Ponceau S stain was removed via washing in PBS with 0.1% Tween-20 (PBST) for 5 minutes. The gel was stained with 1% Coomassie Brilliant Blue G for 1 hour to show untransferred protein, and was destained overnight at 4^oC in Coomassie Brilliant Blue G destain solution. The gel was imaged using a Syngene Chemigenius 2 Charged-Coupled Device (CCD) camera set to 'High Resolution', 'No Filter', with the light source set as 'Lower White'.

3.2.7 Immunoblotting

3.2.7.1 Blocking

As antibodies are themselves proteins, a blocking step is required to prevent non-specific binding of the antibodies to the nitrocellulose membrane during immunoblotting. The membrane was incubated in 20mL of PBST with 2% milk powder (PBSTM 2%) for 2 hours at room temperature with agitation. The milk protein 'blocks' the membrane by binding non-specifically to all unoccupied binding sites. Following blocking, the membrane was rinsed with PBS and the excess fluid was removed by gently shaking the membrane. This was done to prevent carryover of milk proteins into the primary antibody solution. The membrane was then cut horizontally at approximately 34, 50, and 95kDa (as guided by the molecular weight ladder) in preparation for immunoblotting (see Figure 3.4)

3.2.7.2 Primary antibody incubation.

For detection of GRK5, membrane segment *A* (see Figure 3.4) (spanning 50-95kDa) was placed in rabbit α-human GRK 5 (C-20) antibody from Santa Cruz Biotechnology (sc-565) diluted 1:500 in PBST (final antibody concentration 3920.00ng/mL). For detection of actin, membrane segment *B* (spanning 34-50kDa) was placed in rabbit α-human actin antibody from Sigma-Aldrich (A2066) diluted to 1:2000 in PBSTM 1% (final antibody concentration 349.83ng/mL). The membrane segments were incubated in their respective primary antibody solutions on a tilt rocker (Bellco Biotechnology) at a speed of 25rpm overnight (approximately 16 hours) at 4^{o}C (or alternatively, for 2 hours at room temperature). Following primary antibody incubation, the membrane segments were rinsed in PBST followed by three 15 minute washes (also in PBST) before being transferred to the appropriate secondary antibody solution.

3.2.7.3 Secondary antibody incubation

For detection of GRK5, membrane segment *A* (50-95kDa) was transferred to a solution of donkey α-rabbit IgG HRP-conjugated secondary antibody from GE Amersham (NA934)

diluted to 1:1000 in PBSTM 1% (final antibody concentration 159.84ng/mL). For detection of actin, membrane segment *B* (34-50kDa) was transferred to a solution of goat α-rabbit IgG HRP-conjugated secondary antibody from Sigma-Aldrich (A0545), diluted to 1:30,000 in PBSTM 2% (final antibody concentration 349.99ng/mL).

The membrane segments were incubated in their respective secondary antibody solutions for 2 hours at room temperature on a tilt rocker (Heidolph DUOMAX 1030) at 25rpm. Following secondary antibody incubation, the membrane segments were rinsed with PBST followed by three 15 minute washes in PBST to remove unbound antibodies. A final rinse and 5 minute wash with PBS removed traces of Tween-20 from the membrane. This was necessary as Tween-20 can interfere with the HRP-catalysed production of chemiluminescence.

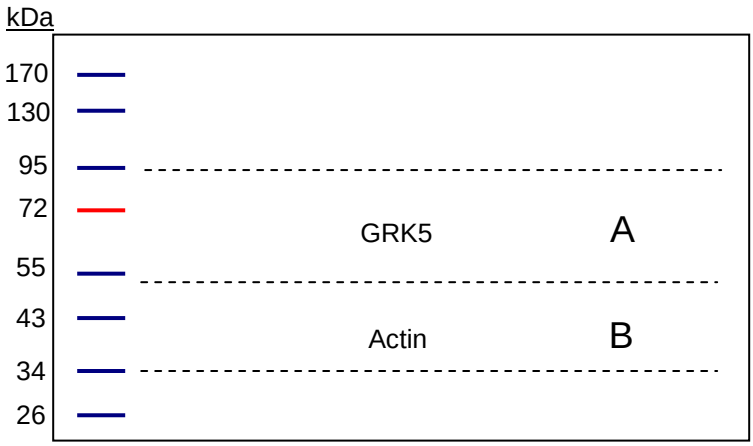

Fig 3.4 Membrane strips used for immunoblotting. The membrane was cut into strips prior to immunoblotting to allow the detection of actin and GRK5 to be performed simultaneously.

3.2.8 Analysis

3.2.8.1 Image Capture

The SuperSignal West Pico Chemiluminescence Reagent (ThermoScientific) was used for detection of antibody labelled bands. The working reagent was prepared by mixing Reagent A

and Reagent B at a 1:1 ratio in a foil-covered microtube. The working reagent was applied, and the membrane tilted gently to ensure full and even coverage (approximately 0.1mL of working reagent per cm^2 of membrane) and incubated in the dark for 5 minutes. The membrane pieces were then shaken gently to remove excess working reagent, sandwiched between two sheets of clear overhead projector plastic and photographed using a Syngene Chemigenius 2 CCD camera. The target protein is visualised via the following mechanism: the working reagent is processed by the secondary antibody-conjugated HRP enzyme into a chemiluminescent product. The resulting photons are detected by the CCD sensor pixel wells, giving each well an electron charge that is directly proportional to the amount of fluorescence detected. At the end of the exposure, the accumulated electron charges are converted to a digital signal. This signal is displayed as a digital image that can be analysed to quantitate differences in the intensity between bands (SYNGENE, 2009). The camera settings used were: 'No Filter', 'No Light', 'and Medium Sensitivity'. Exposure times were 5 minutes for actin detection and 10 minutes for GRK5 detection.

3.2.8.2 Band quantification

The intensity of each band was detected by analysis of the collected digital images with GeneTools software from Syngene. The 'Manual Spot Blot Analysis' program set to 'Fluorescence' was used. Each band to be analysed was fitted tightly with a sampling box. The digital signal contained within the sampling box was classified as the 'band intensity'. The placement of the sample boxes was finalised prior to conversion of the signal to numerical form, in an effort to prevent operator bias. The automatic background setting was used to generate a value for the background intensity of each box, and this value was subtracted from the measured intensity of the bands.

3.2.8.3 Analysis of GRK5 expression

3.2.8.3.1 Normalisation to internal control

The background-corrected data were used for normalisation. The intensity of the 45kDa actin band detected in each sample was determined as described above, and examined for variation.

These values were used to adjust the values measured for the GRK5 bands to account for errors in loading. To normalise the measured intensity of the GRK5 bands for variability in the internal controls, the intensity of the GRK5 band for each lane was divided by the intensity of its actin band, as shown in Equation 3.2, where χ is the normalised band intensity.

Equation 3.2 χ = GRK5 intensity / Actin intensity

3.2.8.3.2 Measuring changes in GRK5 expression

To quantify RNAi-induced changes in the expression of GRK5, the χ values for GRK5-targeted siRNA treated samples were expressed relative to the χ values for "medium-only" controls, as shown in Equation 3.3.

Equation 3.3

$$\text{GRK5 band intensity relative to control} = (\chi^{\text{GRK5-siRNA treated}} / \chi^{\text{Medium Control}})$$

The effect of treatment with GRK5-targeted siRNA was examined for all bands detected.

3.3 OPTIMISATION OF WESTERN BLOTTING

3.3.1 Important parameters for optimisation of Western blotting protocols

The aim of optimising a Western blotting protocol is to deliver a method that i) is specific to its target protein, ii) is sensitive iii) is reliable and reproducible, iv) allows relative antigen expression to be quantitated, and v) is economical. These parameters are discussed below.

3.3.1.1 Specificity

The specificity of an ideal Western blotting protocol would allow the detection of a single target antigen within a population of non-target antigens. Assay specificity is dependent on i) the specificity of the primary and secondary antibodies for their antigens, and ii) the reaction conditions used. The interaction between an antibody and its antigen is based on shape- or 'lock and key'-complementarity between the interacting surfaces of the antigen and the antigen-binding site of the antibody (Kumagai & Tsumoto, 2010). The bonds formed between the antibody and its antigen are generally non-covalent hydrophobic interactions, such as electrostatic interactions (e.g. hydrogen bonds), van der Waals interactions and salt bridges (Kumagai & Tsumoto, 2010; Ramos-Vara, 2005). Induced fit, a phenomenon observed between enzyme active sites and bound substrates, also appears to occur between the antibody and its antigen. These conformational changes to the antigen-binding site upon antigen binding may be necessary to achieve an interaction that has high specificity and affinity (Kumagai & Tsumoto, 2010).

Specificity of the secondary antibody for its antigen (the primary antibody) can be tested by determining the binding pattern it produces in the absence of the primary antibody. If the secondary antibody is specific, no bands will be produced under these conditions. Specificity of the primary antibody however is more difficult to confirm. A commonly used test is preabsorption of the primary antibody with its immunising antigen. This treatment should result in a marked decrease or even elimination of its ability to interact with membrane-bound antigen. However, this control does not distinguish between the 'selective' and 'specific' binding of the primary antibody. For example, a primary antibody may bind 'selectively' to the epitope of its immunizing antigen, yet bind to non-target antigens present in the protein sample being probed, meaning it is not 'specific' to its target protein. An advantage of Western blotting is that the molecular weight of the detected protein band can be determined. Whether or not the molecular weight of the bands detected conform to that predicted for the target protein can also be used as indication of primary antibody specificity. This is not possible in more 'quantitative' immunoassays such as ELISA which measure total chemiluminescence. The availability of antibodies of appropriate quality is a primary limiting factor in producing a specific Western blotting assay.

In addition to the intrinsic specificity of the antibodies, the reaction conditions can also affect the specificity of antibody binding. Increasing the stringency of the reaction decreases the probability of off-target antibody interactions happening by chance, as only interactions of high affinity/avidity would be able to form. The stringency can be increased by decreasing the antibody concentrations, increasing the duration of blocking, and/or increasing the amount of protein in the blocking solution and antibody diluents. Furthermore, the characteristics of the antigen and antigen-binding sites involved in their interaction, e.g. shape and size, may be altered under different conditions. As such, the formation of interacting epitopes may be 'conditional' (Willingham, 1999). An example of a conditional epitope was described by Josephsen, Smith and Nanci (1999), who noted during immunocytochemical screening of rat incisor odontoblasts that crosslinking of enamel proteins by glyceraldehyde fixation generated an epitope that was recognised with high selectivity by an antibody raised against the protein vimentin. The conditionality of the epitope is an important factor for consideration when selecting antibodies and Western blotting protocol details, with regard to the use of reducing or native conditions, and buffer selection.

3.3.1.2 Sensitivity

The sensitivity of an assay is determined by a combination of numerous factors, such as antigen concentration, the affinity and/or avidity of the antibodies for their antigens, antibody concentration, signal production, and signal detection, and may be defined as the ability of the assay to detect the target protein. The more sensitive the assay, the lower the minimum amount of antigen required to produce a signal. In Western blots where the expression level of the target protein is too low to easily detect, high antibody concentrations, or overloading the wells with protein can increase the detection of the antigen, but can also produce a reciprocal decrease in assay specificity. Similarly, decreasing the stringency of the assay conditions can increase its sensitivity, but may result in lower specificity. For an optimised assay, it is important to strike a balance between sensitivity and specificity.

The sensitivity of an assay can also be affected by the use of chemicals which interfere with production of a signal. For example, sodium azide —commonly used in buffers as a

preservative— is not appropriate when HRP-conjugated secondary antibodies are used. While sodium azide extends the life of antibody solutions it has been shown to irreversibly inhibit HRP enzyme activity (Ortiz de Montellano *et al.*, 1988; Richardson *et al.*, 1983).

3.3.1.3 Consistency and error identification.

Assessing the consistency of Western blot is an important step in its validation. Due to constraints relating to the number of wells in a gel and the potential for large inter-gel variation, samples are generally assessed in singlet. As technical replication is not a practical option, it is crucial to assess the consistancy of the assay, and to monitor the progress of the Western blot carefully to identify potential sources of artefacts. Frequently in Western blotting, a second protein is detected as an internal control. Commonly, structural proteins such as actin or β-tubulin are used for this purpose. The expression of the test protein, in this case GRK5, is then assessed by normalising its expression to that of the internal control protein. This allows artefacts caused by processing and loading errors, and uneven transfer to be corrected for. The expression of the internal control should not be altered by the experimental treatment. The consistency of the assay can be assessed by calculating the coefficient of variation for each Western blot. The effect of the experimental treatment on the internal control can be determined by checking for treatment-based changes in the CV values produced (Liu & Xu, 2006).

3.3.1.4 Quantifiability

Western blotting is at best, a semi-quantitative technique, better suited to determining the relative expression of the target protein across samples than quantifying the amount of antigen in each sample. Use of Western blotting for the semi-quantitative determination of relative expression requires the use of an internal control against which the target gene can be normalised. Furthermore it is important to determine the dynamic range of the assay, i.e. the range of relative concentrations over which the target protein can be detected, and changes can be measured. The dynamic range can be determined by serial dilution of a sample, and is shown graphically in Figure 3.5 The lower end of the dynamic range is limited by the amount of antigen present and the sensitivity of the assay or detection system. At the higher end (where

the lanes are overloaded with protein) the signal is saturated, preventing different quantities of antigen from being distinguishable from each other. The dynamic range is the middle section of the curve, at which the realationship between the increase in antigen and the increase in intensity is approximately liner.

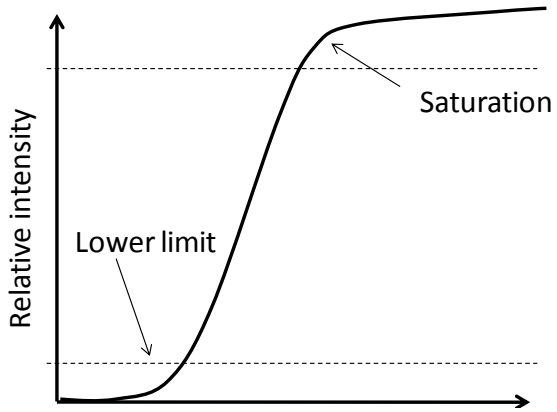

Figure 3.4 Graphical representation of the dynamic range of a Western blotting assay, in which the signal is saturated by overloading with protein, and limited by insufficient antigen, sensitivity and/or the detection limit of the imaging system.

3.3.2 Western Blot Optimisation: Additional protocols

Large volumes of homogenous whole cell lysate were prepared, and used for optimisation of the Western blotting protocol. This was done to prevent the introduction of unnecessary variables when trialling different Western blotting conditions. No significant differences in quality or relative GRK5 expression were seen between preparations. Cells grown for bulk preparations were not allowed to become over-confluent, as GRK5 expression may be up-regulated under these conditions (Gatehouse, 2008). Unless otherwise stated, steps were performed on ice.

3.3.2.1. Plating and culture

For each bulk protein preparation, HEK293 cells were plated into ten 35mm-diameter sterile culture dishes (Becton Dickinson Biosciences) at a density of 20,000 cells/cm^2 (2 x 10^5 cells/dish). A plating volume of 2.5mL was used. The medium was removed 24 hours after

plating by vacuum aspiration and replaced with 2.5mL of fresh MEM+. The cells were cultured for 3 days until 80-90% confluent.

3.3.2.2 Lysis and protein measurement

The protocol for lysis described in Section 3.2.3 was followed with the following exceptions:
i) the culture medium from up to three dishes was removed to each 15mL centrifuge tube, ii) following sonication the cell lysates were pooled and repipetted to produce a single large sample. The bulk sample was aliquoted into 100µL volumes and stored at -20^{o}C until used. The protein concentration of each preparation was determined via BCA assay as described in Section 3.2.4. Protein concentrations for these bulk preparations ranged from 2.2-3.5µg/µL.

3.3.3 Western blotting optimisation: GRK5

The optimisation and validation of a protocol for GRK5 detection via Western blotting occurred in two parts. The first set of experiments was largely unsuccessful and is described briefly in Section 3.3.3.1. The second set, described in Section 3.3.3.2, constituted the majority of the optimisation of the protocol described in Section 3.2, and is therefore described in more detail. Only elements of the Western blotting protocol altered during optimisation of GRK5 detection are described below. For unspecified details refer to the optimised protocol (Section 3.2).

3.3.3.1 Western blotting for GRK5 detection protocol optimisation: Part One

This section describes experiments that were unsuccessful in producing a protocol suitable for measuring the relative expression of GRK5 by Western blotting.

3.3.3.1.1 Antibodies

Initial attempts to produce an optimised protocol for GRK5 detection via immunoblotting were made using a polyclonal rabbit anti-human GRK5 (C-20) affinity purified antibody from Santa Cruz Biotechnology (Product Number: sc-565, Batch Number: D0208), in combination with a

goat anti-rabbit IgG (whole molecule) horseradish-peroxidase conjugate from Sigma-Aldrich (Product Number: A0545, Lot Number 078K4844).

3.3.3.1.2 Variables tested

Multiple experimental conditions were varied. Their effect on the intensity of the GRK5 signal is described below.

3.3.3.1.2.1 Antigen quantity

Initially, 40µg of whole cell protein was loaded per lane for GRK5 Western blotting protocol optimization, and resulted in GRK5 bands of low intensity. Increasing the amount of protein loaded to 60µg of protein per lane resulted in modest increases in signal intensity. Based on the increased intensity of the bands detected, loading 60µg per lane was used for the initial experiments.

3.3.3.1.2.2 Transfer duration

The effect of the duration of the electrophoretic transfer of proteins from the gel to the membrane was also examined. Transfer times of 90, 120 and 150 minutes were trailed. As the maximum capacity of the transfer system was two cassettes, the 90 minute and 150 minutes transfers were separately compared to the 120 minute transfer. A symmetrically loaded gel was cut in two vertically following SDS-PAGE. Two separate transfer cassettes were set up as described in Section 3.2.6.1, but with two layers of nitrocellulose membrane between the gel and filter paper. The cassettes were transferred concurrently. When the shorter transfer time had elapsed (i.e. 90 minutes or 120 minutes), the transfer was halted and a single cassette removed. Transfer of the remaining cassette was then completed, and the transfer evaluated as described in Section 3.2.6.2. This technique was used to ensure that transfer conditions were keep as consistent as possible between cassettes. Inclusion of a second layer of membrane in the transfer cassettes allowed capture of any GRK5 passing though the first membrane, which would indicate that the transfer duration was too long. Both sets of membrane were then immunologically probed for GRK5, using the primary antibody at a dilution of 1:500 in

PBSTM 0.5%, and the secondary antibody at a dilution of 1:1000 in PBSTM 0.5%. When a transfer time of 90 minutes was used, no GRK5 was detected on the second membrane. This indicated that significant quantities of GRK5 had not passed through the first membrane during transfer. However, the GRK5 signal detected on the first membrane was less intense than that seen after a 120 minute transfer. No GRK5 was detected on the second membrane following transfer for 120 minutes. Transfer for 150 minutes resulted in GRK5 bands on the first membrane that were equal intensity to those seen after 120 minutes, but GRK5 bands also were clearly detected on the second membrane. Heating of the transfer unit is increased by longer transfer times, and can affect the quality of the transfer. For this reason the shorter transfer time of 120 minutes was selected for future experiments.

3.3.3.1.2.3 Blocking buffers

Differences in the blocking efficiencies of milk proteins and BSA were examined. Milk powder is often used as a blocking agent as it is inexpensive and readily available. The ability of PBST with 2% (wt/vole) milk powder to prevent non-specific binding of antibodies in various diluents was compared with that of PBST with 2% (wt/vole) BSA (PBSTBSA 2%). In all cases, membranes blocked with PBSTM 2% showed fewer instances of non-specific binding than membranes blocked in PBSTBSA 2%. PBST with milk at 2% was shown to be preferable to both PBSTM 1% and 5% as it produced an acceptable compromise between band specificity and band intensity (sensitivity).

3.3.3.1.2.4 Antibody diluents

Both the primary and secondary antibodies (see Section 3.3.3.1.1 for details) were found to be sensitive to changes in the type and concentration of protein in their diluent. The presence of as little as 0.1% protein in the GRK5 primary antibody diluent resulted in dramatic decreases in the intensity of GRK5-specific banding. PBST with no protein was therefore used as the diluent for the anti-GRK5 primary antibody. Dilution of the secondary antibody with PBST containing 2% FBS or BSA, or PBSTM of less than 2% resulted in an increase in non-specific banding. PBSTM 2% was chosen as the most appropriate diluent for the anti-rabbit IgG HRP-conjugated secondary antibody.

3.3.3.1.2.5 Antibody dilutions

Both the primary and secondary antibodies were tested over a range of dilutions. GRK5-specific banding was seen with combinations of primary antibody diluted 1:100 with secondary antibody diluted 1:1000-1:10,000, and primary antibody diluted 1:200 with secondary antibody diluted 1:1000. The strongest GRK5 signal was detected with primary antibody diluted 1:100 in PBST with secondary antibody diluted 1:1000 in PBSTM 2%. However, even at such high concentrations of antibody, the assay was extremely variable, and GRK5 could not be consistently detected. This combination produced primary antibody-dependant bands within the membrane section probed (see Section 3.2.7) at ~55, ~68, and ~90kDa. The predicted molecular weight of GRK5 is 68kDa. The significance of the additional bands is discussed in Section 3.3.3.2.7.1.

3.3.3.1.2.6 Image capture

Serial image capture, in which the signal derived from each exposure is added to that of previous exposures, was used to track the development of the GRK5 signal over time. For example, in a six image series, image two would contain the digital signal captured in both exposures one and two, while image six would contain the digital signal captured during all six exposures. Multiples of 10 minute exposures were used. An exposure time of 90 minutes was set as the longest feasible exposure time. For all conditions trialled (see above) a set of nine 10 minute exposures produced the best images, which were used for analysis

3.3.3.1.3 Evaluation

The best conditions found for visualising GRK5 with the antibody combination described in Section 3.3.2.1.1 were as follows: loading of 60μg protein per lane, electrophoretic transfer for 2 hours, blocking of the membrane with PBSTM 2%, dilution of the primary anti-GRK5 antibody to 1:100 in PBST, dilution of the secondary HRP-conjugated antibody to 1:1000 in PBSTM2%, and an exposure time of 1.5 hours for image capture. This protocol was not considered to be fit for purpose as i) it lacked reproducibility - with large run-to-run variability seen under the same conditions, ii) the primary antibody concentration required was very high compared to those reported in the literature for the same antibody, and iii) the long exposure

times required were impractical. While the complete details of Western blotting protocols were not routinely included in published articles, multiple papers were found which reported the use of the sc-565 antibody at a 1:500 dilution for detection of GRK5 (Bezard *et al.*, 2005; Bychkov *et al.*, 2008; Iyer & Canty Jr, 2005; Metaye *et al.*, 2002; Voigt *et al.*, 2004). In addition to use of this lower concentration, some of the above groups also reported the use of more stringent binding conditions (Voigt *et al.*, 2004), substantially lower secondary antibody concentrations (Bychkov *et al.*, 2008), and lower antigen levels (Iyer & Canty Jr, 2005) than obtained with the protocol described above.

The discrepancy between the literature and our experience suggested that there might be an issue with the quality of the particular lot of sc-565 antibody we were using. This was supported by a statement made in a recent paper by members of Dr Robert Lefkowitz's research group (Zidar *et al.*, 2009), that the "GRK5 expression could not be assessed reliably by using available antibodies". As the Lefkowitz group had previously published papers using the sc-565 antibody for analysis of GRK5 expression (Kim *et al.*, 2005; Ren *et al.*, 2005; Violin *et al.*, 2008; Violin *et al.*, 2006), we considered that this statement might be relevant to our problems with reliable GRK5 detection. In response to our enquires, Dr S. Ahn of the Lefkowitz group reported that they had found substantial variability in the performance of different batches of the sc-565 antibody, including the number of bands produced. Dr Ahn went on to say that they did not currently have a batch with which they could produce Western blots of acceptable quality. In light of this feedback, a second batch of the sc-565 antibody (Lot Number: B1610) was obtained from Santa Cruz and its performance compared to our original batch (Lot Number: D0208) in the hope that it would produce better results.

3.3.3.1.4 Conclusion

While these trials were unsuccessful in producing a suitable protocol, they were useful in illustrating the effects of each part of the protocol on the signal outcome, and informed the successful optimisation of the final protocol as described below.

3.3.3.2 Western blotting for GRK5 detection protocol optimisation: Part two

This section describes experiments which directly led to the production of the optimised protocols described in Section 3.2

3.3.3.2.1 Primary antibody selection

As discussed in Section 3.3.3.1.3, a second batch (Lot Number: B1610) of the sc-565 anti-GRK5 primary antibody was obtained after initial attempts to establish a protocol for Western blotting of GRK5 (Section 3.3.3.1) were unsuccessful. Information supplied by the Lefkowitz group suggested that the quality of the original batch (Lot Number: D0208) might be the cause of this failure, and that substitution with an alternative batch (B1610) of sc-565 batch might improve the results.

Both batches were trialled using the protocol described in Section 3.3.3.1.3. Substantial differences were seen between the banding patterns produced by batch D0208 and batch B1610. Both batches resulted in visible bands at ~55, ~68, ~80, ~95, ~110, ~115, ~130, and ~170kDa. However the relative intensities of the bands differed greatly (Figure 3.6). The most intense bands produced by batch B1610 were (in descending order) at ~170, ~130, and ~95kDa. The brightest band produced by batch D0208 was at ~68kDa followed closely by that at ~55kDa. As the bands seen with D0208 corresponded better to both the predicted molecular weight of GRK5, and the molecular weight of bands identified in the literature as GRK5 (Jones *et al.*, 2002), batch D0208 was selected for subsequent use. However, this did not solve the lack of reproducibility and the requirement for very high primary antibody concentrations associated with this batch of sc-565

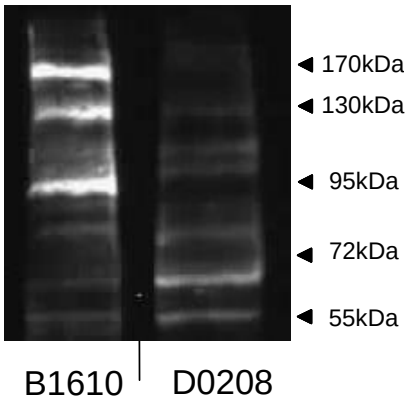

Figure 3.6 Comparison of banding pattern produced by alternate batches of the sc-565 anti-GRK5 primary antibody from Santa Cruz. On the left, batch B1610 produced multiple bands in addition to the predicted band at ~65kDa. On the right, batch D0208 produced a similar banding pattern; however the relative intensity of the bands at each molecular weight differed between batches

3.3.3.2.2 Examination of the affinity of the Sigma-Aldrich Secondary antibody for the anti-GRK5 sc-565 primary antibody

Western blotting is a form of indirect immunoblotting, requiring strong specific interactions to occur between both primary and secondary antibodies and their antigens. The possibility that GRK5 detection was being limited by a poor interaction between the secondary antibody and its antigen, the rabbit anti-GRK5 sc-565 primary antibody, was investigated by comparing the intensity of its banding with that produced by two alternative secondary antibodies when used in combination with sc-565.

The three anti-rabbit IgG HRP-conjugated secondary antibodies tested were diluted to 1:1000 in PBSTM 1% and used in combination with batch D0208 of sc-565 rabbit anti-GRK5 primary antibody. The secondary antibodies were i) a goat anti-rabbit IgG (whole molecule) HRP-conjugate from Sigma (Product Number: A0545, Batch Number: 078K4844), ii) a goat polyclonal anti-rabbit IgG HRP-conjugate from Novus Biologicals (Product Number: NB730-H, Lot number P30), and iii) a donkey anti-rabbit IgG (whole molecule) HRP-conjugate from Amersham (Product Number: NA934, Batch Number: 384359). Both the Amersham (Figure 3.8) and Novus biological (Figure 3.7, A&B) secondary antibodies produced bands at ~68kDa and ~55kDa that were substantially brighter than those produced by the Sigma-Aldrich secondary antibody used in the initial optimisation experiments (Section 3.3.3.1). This suggested that the Amersham and Novus Biologicals secondary antibodies were able to interact

with the anti-GRK5 primary antibody with higher affinity and/or avidity than the Sigma-Aldrich secondary antibody, and supports the hypothesis that the previous inability to reliably detect GRK5 was due to a poor interaction between the primary antibody and Sigma-Aldrich secondary antibody. The performance of the Amersham and Novus Biologicals secondary antibodies was examined further. This analysis is found in Section 3.3.3.2.3, and was used to inform the selection of the secondary antibody to be used for detection of GRK5.

3.3.3.2.3 Secondary antibody selection: Evaluation of the Amersham and Novus Biological secondary antibodies.

The banding produced by the Novus Biologicals and Amersham secondary antibodies was examined over a range of concentrations and diluents, and in the absence of primary antibody.

3.3.3.2.3.1 Novus Biologicals secondary antibody

The Novus Biologicals secondary antibody was trialled at 1:1000, 1:2000, and 1:3000 (in PBSTM 2%) with anti-GRK5 sc-565 primary antibody at dilutions of 1:400, 1:500 and 1:600 (in PBST). (Figure 3.7, C). All combinations trialled produced bright bands at ~68kDa and ~55kDa. However, they also produced an additional smeared band from ~72-95kDa.

Antibodies are known to form non-specific interactions when the stringency of the binding conditions is too low. Increasing the stringency should preferentially reduce non-specific interactions due to the lower affinities/avidities of the participants for each other. Attempts were made to remove the 72-95kDa band produced by the Novus Biologicals secondary antibody by increasing the stringency of the assay. This was done by i) decreasing the concentration of the secondary antibody, and ii) increasing the concentration of milk protein in the secondary antibody diluent. The effect of antibody dilution on assay specificity was examined as follows. The Novus Biologicals secondary antibody was diluted in PBSTM 2% to 1:1000, 1:2000, 1:5000, and 1:10,000 and used in combination with the primary antibody at 1:500 in PBST. Decreasing the secondary antibody concentration did decrease the ~72-95kDa band, but only to the same extent that it decreased the ~68kDa and ~55kDa bands.

The effect of increasing the concentration of milk protein in the secondary antibody diluent to 3.5% and 5% (primary antibody 1:500 in PBST, secondary antibody 1:1000) was also examined. This resulted in a small decrease in the intensity of the 71-95kDa band. However in all instances above, the ~55kDa band was more intense than the ~68kDa band.

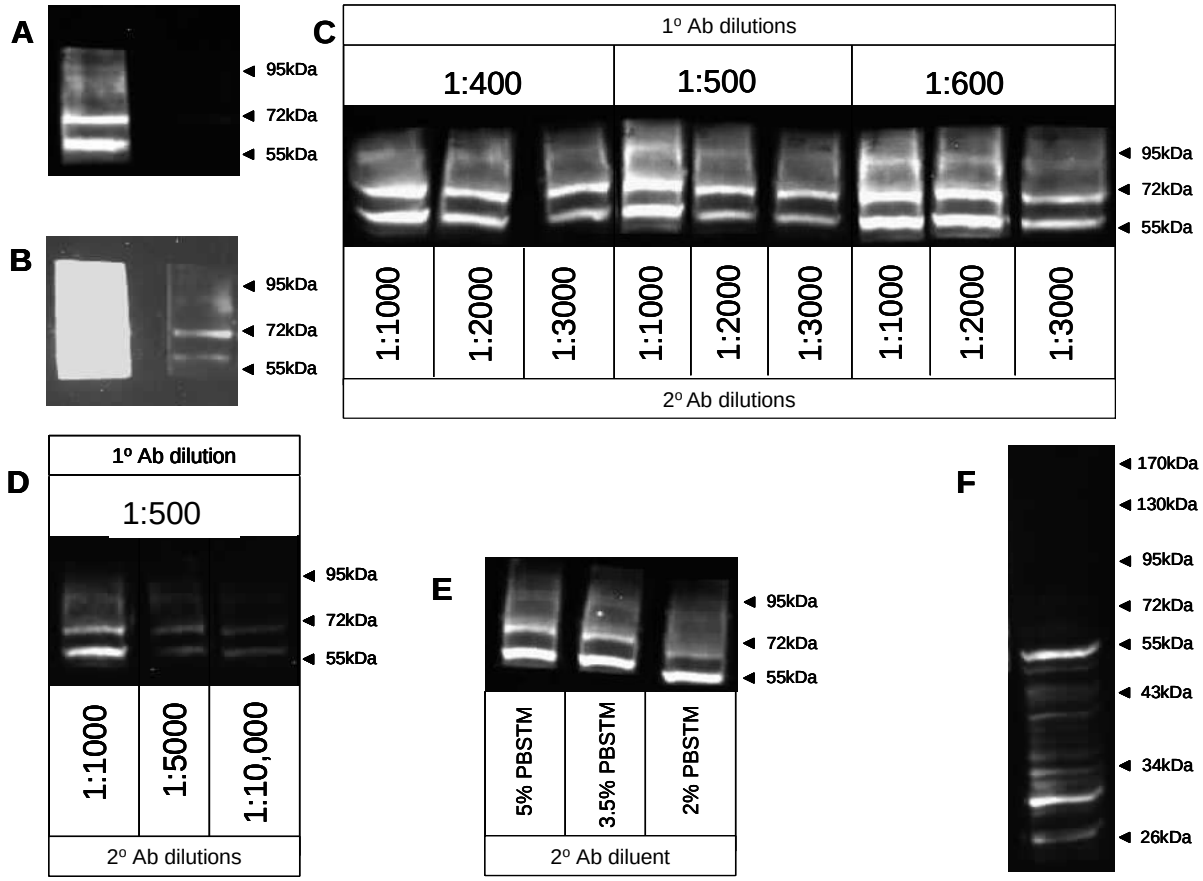

Figure 3.7 Evaluation of Novus Biological secondary antibody. A) Comparison of Novus antibody (left lane) to signal produced by the Sigma-Aldrich secondary antibody (right lane) under identical conditions, B) with contrast adjusted so Sigma-Aldrich antibody-produced bands are visible, C) banding patterns produced by multiple combinations of different primary antibody dilutions with different dilutions of Novus Biological secondary antibody, D) effect of diluting secondary antibody on the specificity of antibody binding, E) the effect of concentration of milk protein in secondary antibody diluent of specificity of antibody binding, and F) the banding pattern produced by the Novus Biological antibody in the absence of primary antibody.

The primary antibody-dependency of the bands produced by the Novus Biologicals secondary antibody was determined by immunoblotting the full length of the membrane with secondary antibody only, diluted to 1:1000 in PBSTM 2% (see Figure 3.7, F). In the absence of primary antibody the Novus biological secondary antibody produced multiple bands, representing substantial off-target binding. The majority of these bands fell below ~50kDa and so would not interfere with the detection of GRK5. However, the brightest of the off-target bands was found at ~55kDa, and two faint bands at ~68kDa and ~72kDa were also detected.

3.3.2.2.3.2 Amersham secondary antibody

The Amersham secondary antibody was trialled at 1:1000 and 1:2000 (in PBSTM 2%) with the primary antibody at 1:500 (in PBST). Both concentrations produced bands at ~68kDa and ~55kDa (Figure 3.8, B). The bands produced by the more concentrated secondary antibody solution were preferable. To determine if the bands detected by the Amersham secondary antibody were primary antibody-dependent, a full length strip of membrane was incubated in secondary antibody only, diluted to 1:1000 in PBSTM 2%. In the absence of primary antibody, the Amersham secondary antibody did not produce any bands (Figure 3.8, A), indicating that the ~55kDa and ~68kDa bands seen earlier represented proteins to which the primary antibody had bound.

The intensities of the bands, while brighter than those seen with the Sigma-Aldrich secondary antibody, were substantially less than those of the bands produced with the Novus Biologicals secondary antibody (Figure 3.8, B).

As illustrated in Section 3.3.3.1.2 the conditions of antibody incubation, such as the quantity of protein in the antibody diluent, has an impact on its ability to bind to its antigen. As no non-specific binding of the Amersham secondary antibody was detected, the milk protein content of its diluent was decreased in an attempt to increase the intensity of the bands. The Amersham antibody was diluted to 1:1000 in PBST, PBSTM 2% and PBSTM 1%, and used in combination with sc-565 α-GRK5 primary antibody. Decreasing the protein in the secondary antibody diluent from 2% to 1% resulted in a modest increase in the intensity of both the ~55kDa and ~68kDa bands and the appearance of a faint band at 72kDa (Figure 3.8, D). In the absence of protein in the diluent however, the Amersham secondary antibody produced bands

at ~55, ~68, and ~72kDa that were comparable in intensity to those seen with the Novus Biological secondary antibody (Figure 3.8, C).

As decreasing the protein content of the Amersham secondary antibody diluent from 1% to 0% had such a marked effect, a range of concentrations between these two values were trialled in an attempt to establish a milk protein concentration at which the band intensity was increased

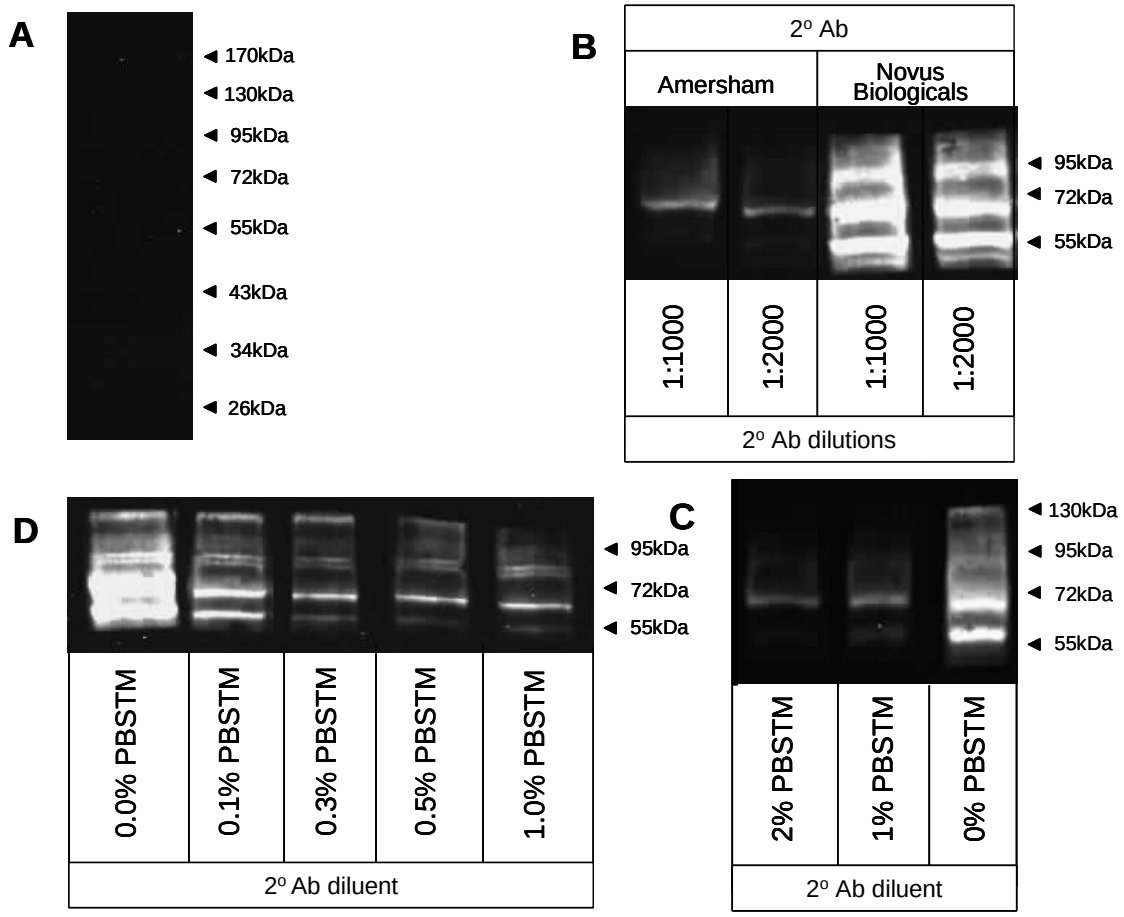

Figure 3.8 Evaluation of the Amersham secondary antibody. *(A)* The banding pattern produced in the absence of primary antibody, *(B)* comparison of band intensity when used at 1:1000 and 1:2000 compared with the Novus Biologicals secondary antibody at the same dilutions, *(C and D)* the effect of decreasing the protein content of the secondary antibody diluent on band intensity. For the evaluation of the Amersham secondary antibody, the primary antibody was used at 1:500 in PBST, except in *(A)* where no primary antibody was used. The Amersham antibody was used at 1:1000 in PBSTM (2%) unless indicated in otherwise.

PBSTM 1, 0.5, 0.3, 0.1 and 0% (Figure 3.8, D). No significant difference was seen in the intensity of the bands produced when PBSTM 0.3, 0.5, and 1% was used as the diluent. All produced a clear bright band at ~68kDa. A faint band was also seen at ~55kDa, as well as additional bands between 72kDa and 95kDa. The intensities of all bands were comparatively increased when PBSTM 0.1% was used as the secondary antibody diluent.

3.3.3.2.4 Secondary antibody selection

The Novus Biological secondary antibody produced substantially brighter bands than those seen with the Amersham antibody. However, unlike the Amersham secondary antibody it also produced primary antibody-independent bands (Figure 3.7 F). Furthermore, in blots produced with the Amersham antibody, the ~68kDa band was brighter than the ~55kDa band (Figure 3.8 D, and Figure 3.9). This relationship was reversed with Novus biological antibody (Figure 3.7 E, and Figure 3.9). As the predicted molecular weight of GRK5 is 68kDa and the identity of the additional bands, including that at ~55kDa, is undetermined, the banding pattern produced by the Amersham antibody was preferable. The Amersham antibody was selected for use.

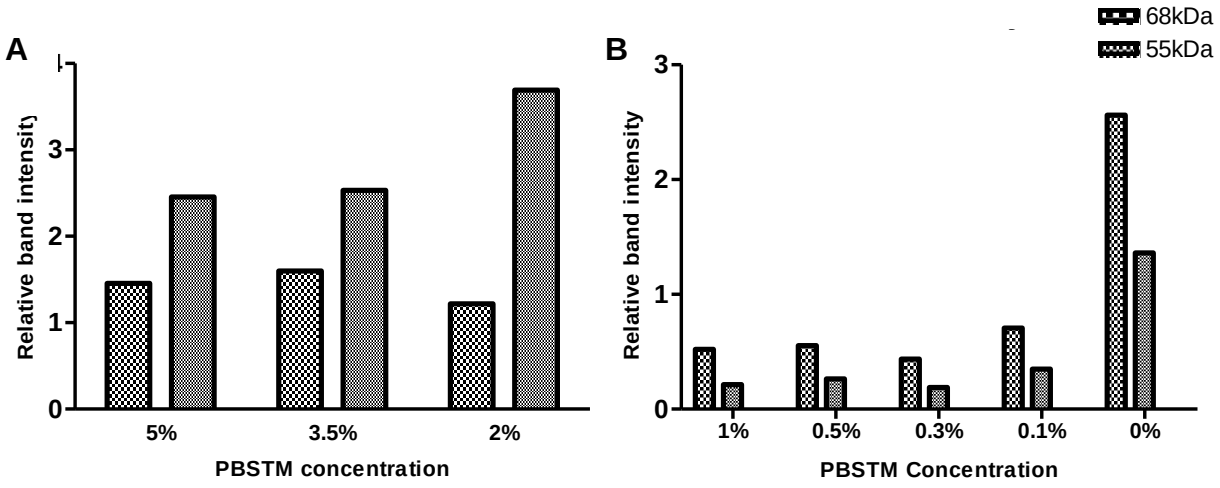

Figure 3.9 Effect of PBSTM concentration on the band intensities produced by a combination of the anti-GRK5 primary antibody and (A*)* the Novus Biologicals secondary antibody, or (*B*) the Amersham secondary antibody, also showing the relationship between the intensity of the 68kDa and 55kDa band for both antibody combinations

3.3.3.2.5 Selection of antibody concentrations

3.3.3.2.5.1 Primary antibody concentration

Due to the relative faintness of the bands produced in the experiments described above, primary antibody dilutions greater than 1:500 were not trialled with the Amersham secondary antibody. A primary antibody dilution of 1:500 was found to produce bands that were strong enough to allow decreases in GRK5 expression to be quantified. Furthermore, this dilution was more consistent with the use of the sc-565 α-GRK5 antibody reported in the literature (Bezard *et al.*, 2005; Bychkov *et al.*, 2008; Iyer & Canty Jr, 2005; Metaye *et al.*, 2002; Voigt *et al.*, 2004). As such, a dilution of 1:500 was selected for use of the anti-GRK5 antibody in combination with the Amersham secondary antibody.

3.3.3.2.5.2 Secondary antibody concentration

The Amersham secondary antibody was trialled at dilutions of 1:1000 and 1:2000 in combination with primary antibody at a 1:500 dilutions (Figure 3.8, B). A secondary antibody dilution of 1:1000 was chosen as it resulted in more intense banding.

3.3.3.2.6 Selection of Antibody diluents

3.3.3.2.6.1 Primary antibody diluent

Experiments performed in Part 1 of the GRK5 Western blotting protocol optimisation (Section 3.3.3.1.2.4) illustrated the sensitivity of primary antibody to the presence of very small concentrations of milk protein in the primary antibody diluent. Addition of as little as 0.1% (wt/vol) milk powder resulted in substantial decreases in the intensity of the primary antibody dependant bands. As such, PBST without protein was used as the primary antibody diluent.

3.3.3.2.6.2 Secondary antibody diluent

The effect of secondary antibody diluent on band intensity is described in Section 3.3.3.2.3.2. Decreasing the protein content of the diluent resulted in increased band intensity. However, this effect was not specific to the ~68kDa band which corresponds to the GRK5, and resulted in a proportionately large increase in the intensity of additional bands, in particular the ~55kDa band. Dilution of the secondary antibody to 1:1000 in PBSTM 1% produced an acceptable compromise between band intensity and specificity. PBSTM 1% was selected as the secondary antibody diluent for detection of GRK5.

3.3.3.2.7 Assessment of protocol

3.3.3.2.7.1 Assessment of assay specificity

As described in Section 3.3.3.2.3.2 the primary antibody-dependency of the bands detected for GRK5 was assessed by incubating a piece of membrane in the Amersham secondary antibody without primary antibody. No bands were present in the absence of the primary antibody (Figure 3.8, A).

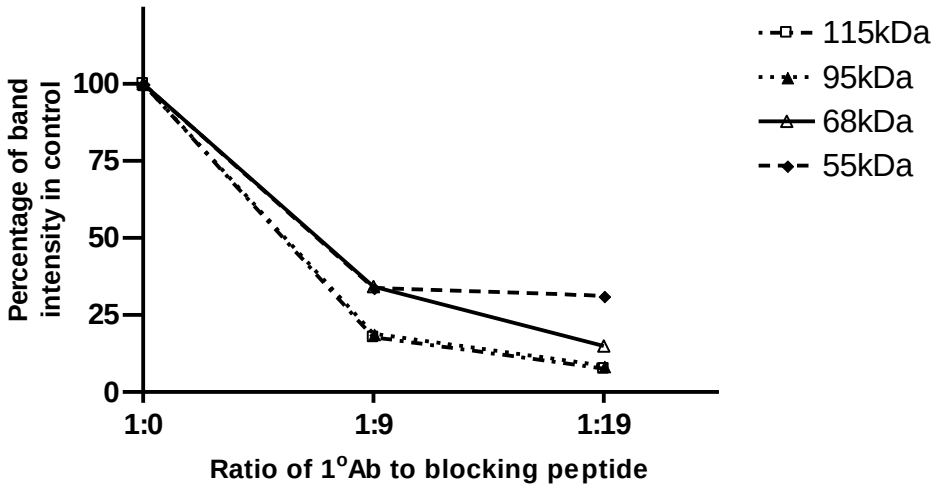

Figure 3.10 Effect on band intensity of preabsorbing the α-GRK5 primary antibody with increasing concentrations of blocking peptide. The intensity of the bands detected at 115kDa, 95kDa, 68kDa, and 55kD treated with preabsorbed antibodies were compared with the intensity of equivalent bands in the control (1:0, i.e. no blocking peptide)

The specificity of the primary antibody for its antigen was also examined. The immunizing antigen used to produce sc-565 was a short peptide which corresponds to the 20 C-terminal amino acids of the human GRK5 polypeptide. This was purchased from Santa Cruz Biotechnologies (sc-565-P, Lot #E172) and used to pre-absorb the primary antibody prior to immunoblotting. This was done by mixing the primary antibody and immunizing antigen at a ratio of 1:9 (Yi *et al.*, 2005) or 1:19, and incubating the mixture at room temperature for 1 hour, followed by incubation overnight at 4^{o}C. It was then centrifuged at maximum speed for 5 minutes. A control was prepared is the same manner as the pre-absorbed treatment, but without the immunizing antigen.

Anti-GRK5 primary antibody-dependent bands were routinely detected at 55, 68, 95, and 115kDa bands. All bands detected with the sc-565 were seen to decrease in the presence of the immunizing antigen. Increasing the relative concentration of the immunizing antigen resulted in further decreases in band intensity (Figure 3.10)

There are multiple possible explanations for the presence of unexpected bands in a Western blot.

Additional bands are often seen when the assay stringency is too low. As described above, the stringency of the assay was increased by increasing the amount of milk protein in the antibody diluent. However, these changes did not result in a drop-off in the intensity of additional bands relative to the 68kDa band, as would be expected if they were caused by random opportunistic binding of the antibodies. Furthermore, preabsorption of the antibody with its immunizing antigen reduced the intensity of all the bands detected. As shown in Figure 3.10, the relative decrease in band intensity of both the 95 and 115kDa bands was greater than that seen for the ~68kDa band. This suggests that the antibody is binding selectively, though perhaps not specifically to GRK5 (Pradidarcheep *et al.*, 2008).

The anti-GRK5 antibody (sc-565) was raised against an oligopeptide corresponding to the 20 C-terminal amino acids of GRK5. This sequence was presumably chosen due to the extensive homology between the remainder of the GRK5 polypeptide and the other members of the GRK4 family (GRKs 4 and 6) (Penela *et al.*, 2003). If this sequence is present in other proteins, it would be unsuitable for use as a GRK5 antigen. An advantage of using synthetic

peptides as an immunizing agent is that the amino acid sequence is known. This allows a degree of selection to avoid cross-reactivity between isoforms of the target protein, or other proteins containing a similar sequences (Ramos-Vara, 2005). Basic Local Alignment Search Tool (BLAST) searches for sequences with homology to the GRK5 C-20 oligopeptide antigen, and/or the whole GRK5 amino acid sequence were performed, and confirmed the specificity of this peptide sequence to GRK5.

The selective binding of the primary antibody below the expected molecular weight could also be due to protein degradation. However, these bands are more likely to be smeared than discrete as seen here. To minimise degradation, protease inhibitors were included in the lysis buffer, and the samples kept on ice at all times. As no evidence of protein degradation was seen in the internal control actin, it is unlikely that protein degradation is the cause of the additional bands detected here. Furthermore, protein degradation would not explain the presence of bands above the expected weight.

An alternative explanation for the presence of additional bands is the detection of multiple GRK5 isoforms. Alternative splicing of the GRK5 pre-mRNA could result in bands of different molecular weights. While no GRK5 splice-variants have currently been positively identified by biochemical techniques, a number of published GRK5 Western blots show multiple bands, though these are generally unaccompanied by molecular weight ladders or an explanation (Bychkov *et al.*, 2008; Horie & Insel, 2000; Martini *et al.*, 2008; Matkovich *et al.*, 2006; Ren *et al.*, 2005). Splice variants of other members of the GRK family, including the closely related GRK4 and GRK6, have, however, been documented (Premont *et al.*, 1999).

Post-translational modification involving the addition of molecules, such as phosphate groups, would increase the molecular weight of the peptide, and could alter the running characteristics; resulting in band at alternative molecular weights. As discussed in Chapter1, phosphorylation of GRK5 is a crucial aspect in regulating both its activity and localisation within the cell. GRK5 is known to be phosphorylated at multiple sites, most of which fall outside the C-terminal twenty amino acids used as the immunizing antigen for the primary anti-GRK5 antibody used in this research. As such, it would be possible for the Western blotting protocol described in Section 3.2 to detect GRK5 in multiple different phosphorylation states. In their

2002 paper, Jones, Baker, and Greenhaff detected bands at approximately 59, and 68kDa, and identified both as GRK5. These authors reported that the ratio of the intensities of the two bands differed between tissues, and suggested that they represented alternative phosphorylation states.

Recently, the crystal structure of GRK6 was determined by Lodowski et al (2006). At the high concentrations of protein required for crystallisation, GRK6 was seen to form a homodimer by interaction of its regulator of G protein signalling homology domains. This region is highly conserved between GRKs, suggesting that dimerisation may be possible for other GRK isoforms such as GRK5. While it is unclear if GRK dimerisation is physiologically relevant, dimerisation of extracted GRKs in cell lysates may result in the appearance of unexpected bands on a Western blot. A ~130kDa band was consistently detected when α-GRK5 antibodies were used. This corresponds with the molecular weight expected from a GRK5 dimer (~136kDa), based on the molecular weight of the monomer (~68kDa).

3.3.3.2.7.2 Assessment of assay consistancy

The reproducibility of the assay was tested by loading the same amount of protein from the same sample into multiple wells (the intensity of the bands produced should be consistant across these lanes), and calculating the coefficient of variation (CV) for the intensity of the bands detected. The CV is a statistical measure of the variation within a data set, and is the ratio of the standard deviation of the mean. CV values are expressed as a percentage, and can be used to compare the amount of variation between data sets in which the means are very different. CV values are calculated as follows;

Equation 3.4 **CV = (standard deviation / mean) * 100**

The CV of the GRK5 assay was determined by loading 40μg of the same sample into 4-6 lanes of an SDS-PAGE gel, and immunoblotting using the protocol described in Section ???. This was repeated 3 times. The Mean CV calculated for the GRK assay was 20.6% ± SEM 6.0%.

3.3.3.2.7.3 Assessment of assay sensitivity and dynamic range

The purpose of the Western blotting assay for GRK5 detection described above is to detect RNAi-induced changes in GRK5 expression. To test the sensitivity of the assay, and determine the range over which it is capable of detecting changes in GRK5 quantity between samples, serial dilutions between 40 and 4µg of a single protein sample were separated by SDS-PAGE, transferred to a NC membrane and immunoblotted as described in Section 3.2. The band intensities with the background subtracted were quantitated as described in Sections 3.2.8, and plotted against the amount of whole protein loaded in each lane.

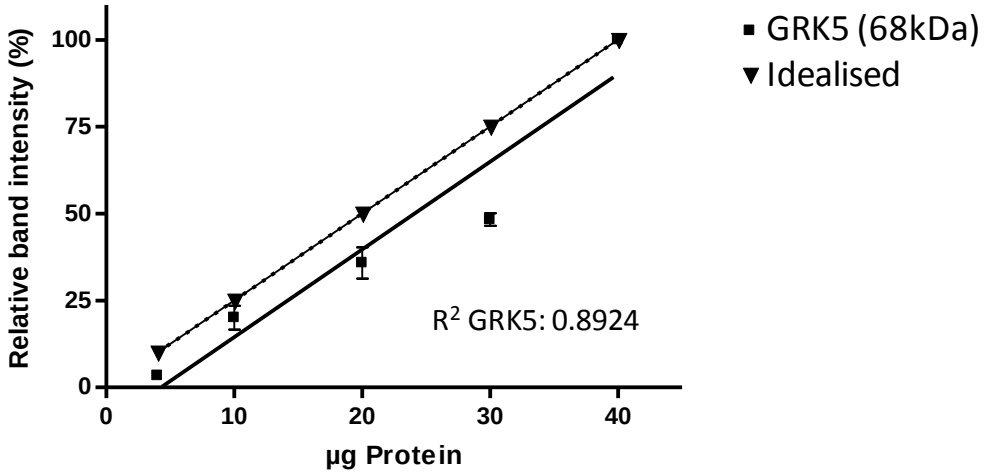

Figure 3.11 Assessment of GRK5 Western blot assay, showing assay sensitivity, range and relationship between the amount of protein loaded and the relative intensity detected. The idealised data points represent a hypothetical data set with the ideal relationship between the intensity of the band produced and the amount of antigen present. For the GRK5 data set, n= 4 for '40', '20', '10', n=3 for '30', and n=1 for '4'µg protein. SEM are shown. A liner regression was used to plot the lines of best fit. The slope of the measured (solid line) and idealised (broken line) trends were not significantly different (two-tailed p value =0.9559).

As shown in Figure 3.11, the GRK5 assay was able to detect a measurable signal when as little as 4µg of whole cell lysate was loaded. This suggests that the described protocol is sufficiently sensitive to detect GRK5 in cells in which GRK5 expression has been reduced by up to 90%.
To determine the dynamic range of the assay, the data was analysed with GraphPad Prism 4.00 using a linear regression to plot the line of best fit. A linear relationship was detected between

the intensity of the signal measured and the amount of antigen present (R^2= 0.8924), indicating that the assay could be used to detect changes in relative GRK5 expression between samples. The slope of the line of best fit for the measured intensity data was compared to that generated from an idealised data set (in which loading 25% less protein would result in a band 25% less intense) using a two-tailed t test. No significant difference was seen between the measured and idealised slopes (two-tailed p value = 0.9559). All points of the serial dilution use appear to be within the dynamic range of the assay, and loss of signal was not seen at the lowest quantity of protein loaded (4μg), and saturation was not seen at the highest quantity used (40μg).

3.3.3.2.8 Conclusions

The optimisation described in part II produced a protocol for detecting GRK5 which was sensitive, and could detect changes in the amount of GRK5 present. The consistency of the assay however was less than ideal, with a CV value of 20.6% ± 4.5% (mean ± SEM). Changing from the Sigma-Aldrich secondary antibody to the Amersham secondary antibody resulted in a marked increase in both the intensity of the bands, and the reproducibility of the assay. The Amersham secondary antibody was shown to bind specifically to the primary antibody, based on the absence of bands when the secondary antibody was used without the primary antibody. The specificity of the primary anti-GRK5 antibody is less certain, as multiple additional bands were detected, the intensity of which was not decreased relative to the 68kDa band by increasing the stringency of the assay. The final protocol employed primary anti-GRK5 antibody (batch D0208) diluted 1:500 in PBST, with Amersham secondary antibody diluted 1:1000 in PBSTM 1%. This protocol was deemed to be appropriate for be used to evaluate protein knockdown following GRK5-targeted siRNA treatment.

3.3.4 Western blotting optimisation: Actin, for use as an internal control

To ensure observed changes in the intensity of the GRK5 bands are due to changes in GRK5 expression rather than uneven loading or transfer, it is recommended that a second protein is detected to act as an internal control. The expression of this protein should not be altered by the test treatment (in this case siRNA-induced knockdown of GRK5 expression), and so should be constant between the control and test samples. Variation in the intensity of bands

corresponding to this protein would then act as an indicator that unequal amounts of test and control samples were loaded onto the gel. Actin is commonly reported in the literature as the internal control (Ren *et al.*, 2005) and was evaluated for use in this thesis.

Elements of the Western blotting protocol altered during optimisation of actin detection are described in Section 3.3.4.2. For unspecified details refer to the optimised protocols (Section 3.2).

3.3.4.1 Antibodies for actin detection

For immunodetection of actin, a rabbit anti-human actin affinity-isolated antibody from Sigma-Aldrich (Product Number A2066, Lot Number 048K4861) was used as the primary antibody. The goat α-rabbit IgG (whole molecule) horseradish-peroxidase conjugate also from Sigma-Aldrich (Product Number A0545, Lot Number 078K4844) was used as the secondary antibody. Use of this Sigma-Aldrich secondary antibody in combination with the α-GRK5 primary antibody (Section 3.3.3.1) resulted in poor GRK5 detection, however based on the intensity of the actin bands it interacts with the anti-actin primary antibody with high affinity.

3.3.4.2 Variables tested during optimisation

3.3.4.2.1 Antigen quantity

Loading 80, 60, 40, 30, and 20µg of whole protein per lane was trialled. All quantities produced strong clear bands. Loading of 20µg of protein was selected as sufficient for detection of actin in knockdown experiments. Due to problems encountered during the initial attempts to optimise the detection of GRK5 (described in Section 3.3.3.1) 60µg of protein was used during some parts of the optimisation described below. For clarity, the quantity of protein loaded at each stage is specified.

3.3.4.2.2 Blocking

The intensity of actin bands on immunoblots blocked in PBSTM containing 1% and 2% milk were compared (60µg protein loaded). No difference was seen in band intensity between the two conditions and both appeared to provide sufficient blocking, as shown by the lack of non-specific bands in either condition (Figure 3.12, A). Blocking with BSA 2% (wt/vol) was also trialled, and resulted in an increase in non-specific banding (not shown). PBSTM 2% was selected for blocking membranes for actin-detection in all subsequent immunoblots.

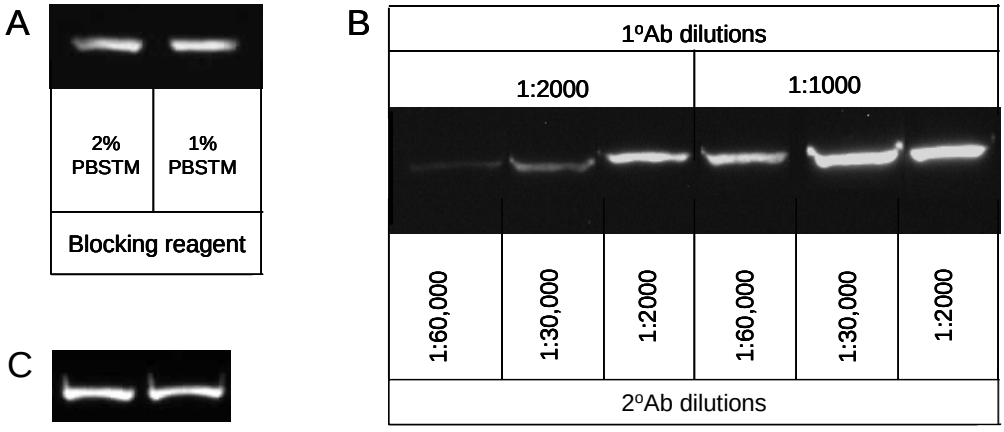

Figure 3.12 Optimisation of Western blotting protocol for actin. *(A)* The effect of protein concentration in blocking reagent on band intensity and specificity, *(B)* the band intensity produced by various combinations of primary and secondary antibody concentrations, and *(C)* the bands produced in a typical assay (using 1:2000 primary antibody in PBSTM1% and 1:30,000 secondary antibody in PBST2%).

3.3.4.2.3 Antibody concentrations

In selecting antibody concentrations a balance must be struck between signal specificity, signal intensity, and signal durability. For example, lowering the antibody concentration reduces the signal intensity, but improves signal specificity. To identify appropriate antibody concentrations for actin detection, six different combinations of primary and secondary antibody dilutions (Figure 3.12, B) were trialled. Both antibodies were diluted in PBSTM 2%, and the membrane was imaged for approximately 12 minutes. All six combinations produced a single band at approximately ~42 kDa, the predicted molecular weight for actin. This suggests that in all combinations both antibodies are interacting with their intended antigens in a specific manner. The band intensities produced by the primary antibody diluted to 1:2000 were sufficient for actin detection, and preferable to a dilution of 1:1000 as they were i) more cost

effective, ii) potentially more specific, and iii) less prone to over-saturation which can impair the accuracy of signal quantification. A combination of primary antibody at 1:2000 and secondary antibody at 1:30,000 was selected for use. This combination typically produced a band stronger than that shown in Figure 3.12, B. As such, bands representative of those typically produced are shown in Figure 3.12, C.

3.3.4.2.4 Antibody Diluents

The effect of reducing the amount of milk powder present in the primary and secondary antibody diluents was examined. Decreasing the amount of milk protein in the primary antibody diluent to less than 1% resulted in an increase in off-target interactions, as shown by the appearance of additional bands. For this reason PBSTM 1% was selected as the diluent for the anti-actin primary antibody. Reduction of the amount of milk protein in the secondary antibody diluent to less than 2% caused a reduction in the specificity of the assay. This was shown by an increase in the occurrence of off-target bands. Multiple immunoblots using primary antibody diluted 1:2000 in PBSTM 1% with secondary antibody diluted 1:30,000 in PBSTM 2% confirmed that this combination could be used to specifically and reproducibly detect actin (Figure 3.12).

3.3.4.3 Assessment of protocol

3.3.4.3.1 Assessment of assay specificity

A single band of expected weight of ~42kDa was detected using the α-actin primary antibody, suggesting that this antibody was binding specifically to its target antigen. The specificity of the secondary antibody under the immunoblotting conditions used was evaluated by incubating a piece of membrane corresponding to a single lane of protein with secondary antibody only, and comparing it to lanes incubated in both primary and secondary antibody (Figure . No signal was detected in the absence of the primary antibody.

3.3.4.3.2 Assessment of assay consistency

The consistency of the assay was assessed as described in Section 3.3.3.2.7.2. The CV of the actin was calculated for four assays in which 40µg of untreated protein was run in 4-6 lanes of the same gel, and immunoblotted as described in Section 3.2.7, producing a mean CV of 8.8 ± SEM 4.5%

3.3.4.3.3 Assessment of assay sensitivity

The sensitivy and dynamic range of the Western blotting assay for actin was tested as described in Section 3.3.3.2.7.3, by running serial dilutions of protein ranging from 40 to 4µg on a gel and immunoblotting as described in Section 3.2.

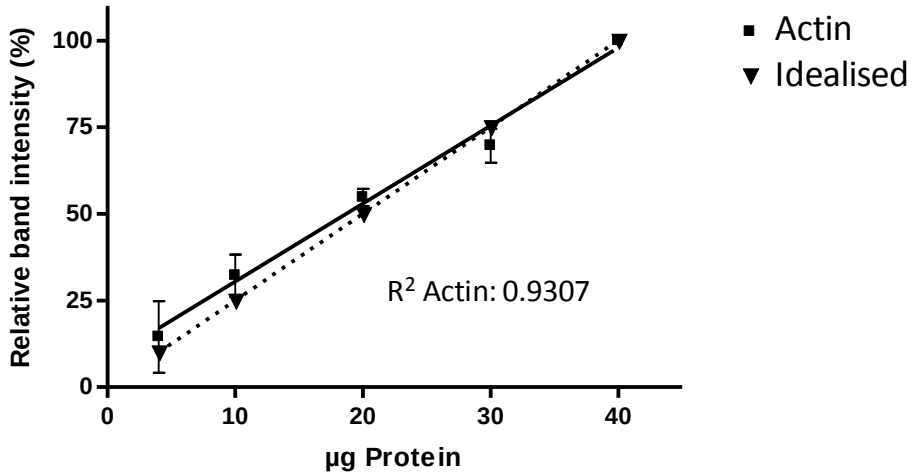

Figure 3.13 Assessment of Actin Western blot assay, showing assay sensitivity, range and relationship between the amount of protein loaded and the relative intensity detected. The expected data points represent the hypothetical ideal relationship between the intensity of the band produced and the amount of antigen present. For the Actin data set, n= 4 for '40', '20', '10', n=3 for '30', and n=2 for '4'µg protein. SEM are shown. The slopes of the measured (solid line) and ideal (broken line) lines were not significantly different (two-tailed p value =0.409)

As shown in Figure 3.13, the actin assay was able to detect a measurable signal when as little as 4µg of whole cell lysate was loaded. The data generated from serial dilution of protein was analysed with GraphPad Prism 4.00 using a linear regression to plot the line of best fit. A strong linear relationship was detected between the intensity of the signal measured and the amount of antigen present (R^2= 0.9307), indicating that the assay could be used to accurately detect changes in relative actin expression between samples. The slope of the line of best fit for

the measured intensity data was compared to that generated from an idealised data set (in which loading 25% less protein would result in a band 25% less intense) using a two-tailed t test. No significant difference was seen between the measured and idealised slopes (two-tailed p value = 0.409). As with the GRK5 assay, all points of the serial dilution used appear to be within the dynamic range of the assay, as loss of signal was not seen at the lowest quantity of protein loaded (4µg), and saturation was not seen at the highest quantity used (40µg).

3.3.4.4 Conclusions

The final protocol for the detection of actin via Western blotting involved the loading of 40µg of protein, blocking of the membrane in PBSTM 2%, and use of the Sigma-Aldrich anti-actin primary antibody diluted 1:1000 in PBSTM 1% in combination with the Sigma-Aldrich secondary antibody diluted to 1:30,000 in PBSTM 2%. This protocol was able to reproducibly detect actin and was sensitive to changes in the amount of actin present over a large dynamic range, and was consistent (as assessed by CV analysis).

4

DEVELOPMENT OF A QUANTITAVE REVERSE TRANSCRIPTASE PCR PROTOCOL FOR ASSESSING HUMAN GRK5 mRNA EXPRESSION IN HEK293 CELLS

4.1 INTRODUCTION

To confirm the siRNA-mediated knock down of GRK5 during RNA interference experiments (Chapters 5 & 6), it was necessary to compare the level of GRK5 mRNA present in control and treated cells. Qualitative real-time PCR (qPCR) is a form of polymerase chain reaction (PCR) in which the formation of PCR products is measured at the end of each amplification cycle. This information is then used to calculate the quantity of the gene of interest in the template. Quantitative reverse transcriptase PCR (qRT-PCR) is a variant of qPCR in which the template is produced by the reverse transcriptase (RT)-catalysed conversion of RNA to complementary DNA (cDNA) (Nolan *et al.*, 2006). qRT-PCR is the favoured method for quantifying steady-state mRNA expression as it is fast, accurate, reproducible, and highly sensitive (Bustin, 2002; Radonic *et al.*, 2004). qRT-PCR is commonly used in assessing the effect of RNA interference on the mRNA expression of the target gene.

In the qRT-PCR protocol described below, the generation of PCR products could be tracked due to the inclusion of SYBR green in the reaction mix. SYBR green is a reporter dye that fluoresces when bound to double-stranded DNA. The interaction between SYBR green and DNA is not sequence specific, meaning that any DNA present in the reaction tube will contribute to the level of fluorescence detected. For this reason, SYBR green is only suitable for ‘single-plexing’ reactions, in which a single target is detected per well.

The fluorescence generated by SYBR green binding to DNA is measured at the end of every amplification cycle, giving real-time updates on product accumulation. The point at which the measured fluorescence rises above the background fluorescence level is termed the threshold cycle (C_t) and is used to calculate the gene expression. The C_t value has an inverse relationship with the quantity of the target transcript in the starting template, i.e. the more target transcript present, the lower the C_t value, as it requires less amplification cycles to reach a detectable level (Radonic *et al.*, 2004).

In the qRT-PCR protocol described in this chapter, the reverse transcriptase (RT) reaction and the qPCR are performed separately. The qRT-PCR methods used to assess the expression of human GRK5 mRNA in HEK293 cells are given in Section 4.2. The purpose of the work presented in Section 4.3 of this chapter was the set up and validation of these methods.

4.2 qRT-PCR PROTOCOLS AND MATERIALS

4.2.1 Materials

For details of materials referred to in this section see Appendix A.

4.2.2 Solutions and Media

For details of solutions and media referred to in this section see Appendix B.

4.2.3 Maintaining RNase-free Conditions

To avoid contaminating the samples and solutions with ribonuclease enzymes (RNases) which degrade RNA, all techniques described in this chapter were performed using dedicated equipment, reagents and consumables. Glass sheets were used as work surfaces, and were prepared before each experiment by treating with RNase-Away (Invitrogen) as per the manufacturer's instructions. Gloves were worn and changed frequently during experiments.

Glassware, plastic ware, spatulas and magnetic stirring bars were baked at 150^{o}C for 2 hours before being used to prepare RNase-free solutions. Nuclease-free, low-retention, filtered pipette tips from Axygen and MPbio were used to avoid contamination of the pipettes by aerosols, which could lead to the contamination of later samples.

4.2.4 Isolation of RNA from Cells

4.2.4.1 RNA Extraction

Total RNA was extracted from HEK293 cells using a TRIzol®Plus RNA Purification Kit (Invitrogen). The medium was removed from each well using a Gilson P1000 pipette and replaced with 200µL of TRIzol® per well. Samples were then either processed immediately, or the plate was taped closed and stored at -80^{o}C until a later date. After the addition of TRIzol® (and thawing if necessary), each well was thoroughly scraped with a Gilson P1000 pipette tip, and its contents vigorously repipetted 6 times to draw cells into suspension and wash the surface of the well. The cell suspension was transferred into a labelled 1.7 mL centrifuge tube. Duplicate wells were pooled at this point. The cells were homogenized by vigorously repipetting the cell suspension twenty times with a Gilson P1000 pipette set to 95% of the total volume, then incubated at room temperature for 5 minutes. Next, 20µL of bromo-chloropropane (BCP) per 200µL TRIzol® was added to each tube, and the tubes were shaken vigorously by hand for twenty seconds. Samples were then incubated at room temperature for 5 minutes. The tubes were spun at 12,000 x g for 15 minutes at 4^{o}C (Eppendorf centrifuge 5417), and the resulting aqueous phase removed and combined with an equal volume of 70% ethanol to give a final ethanol concentration of 35%. Following mixing, each sample was loaded onto a TRIzol®Plus Purification Kit Spin Cartridge with collection tube and spun at 12,000 x g for 15 seconds at room temperature. The column was washed once with 700µL of Wash Buffer I, and once 500µL of Wash Buffer II, spun at 12,000 x g for 15 seconds at room temperature after each addition. The flow through discarded each time. The Spin Cartridge was then transferred to a new collection tube and washed a second time with 500µl of Wash Buffer II, spinning as above and the flow through discarded. The membrane was then dried by centrifuging the Spin Cartridge at room temperature for 1 minute at 12,000 x g. The Spin Cartridge was transferred

to a 1.5mL elution tube and 30µl of RNase-free water was applied directly to the membrane. This was incubated at room temperature for 1 minute. The Spin Cartridge was then centrifuged for 2 minutes at 12,000 x g (also at room temperature), to elute the RNA with the water.

4.2.4.2 Analysis of RNA

The concentration and purity of the eluted RNA in each sample was determined using a ND1000 NanoDrop spectrophotometer (ThermoScientific). RNase-free NPH_2O was used both to clean the spectrophotometer platform before use, and as a blank to zero the spectrophotometer before sample analysis. The RNA concentration (ng/µL) of each sample was determined by the NanoDrop software based on its absorbance at 260nm. The purity of each sample was shown by the 260/280 and 260/230 absorbance ratios.

4.2.5 Reverse Transcriptase reaction

The SuperScript III First-Strand Synthesis System for RT-PCR (Invitrogen) was used as per the manufacturer's instructions to convert the extracted RNA to complementary DNA (cDNA), using an RNA-dependant DNA polymerase enzyme called reverse transcriptase (RT). An Eppendorf Mastercycler® gradient or *ep* gradient *S* PCR machine was used for the heating steps, during which the lid was headed to 105^{o}C to avoid evaporation.

Each RT reaction was set us as shown in Table 4.1 *A*. This RNA mixture was denatured by incubation at 65^{o}C for 5 minutes. The mix was then placed on ice for at least 1 minute to allow the oligo$(dT)_{20}$ primers to anneal. Ten microlitres of cDNA synthesis mix, shown in Table 4.1 *B*, was added to the RNA mix, and the 2 solutions mixed by gently tapping the reaction tube. The combined solution was collected by brief centrifugation and incubated at 50^{o}C for 50 minutes, during which cDNA synthesis occurred. The RT reaction was terminated by heating the solution to 85^{o}C for 5 minutes. The quantity of cDNA produced by the RT reaction is indeterminable, so it was assumed to be equal to the quantity of RNA used as a template, i.e. 400ng (20ng/µL). The cDNA was stored at -80^{o}C.

A

400ng RNA
1µL 50µM oligo$(dT)_{20}$ primers
1µL 10mM dNTP mix
NPH_2O to make volume up to 10µL

B

2µL 10X RT buffer
4µL 25mM $MgCl_2$
2µL 0.1M DTT
1µL 40U/µL RNaseOUT
1µL 200U/µL SuperScript III RT enzyme

Table 4.1 Master mixes for RT reaction. A) Components of the RNA RT reaction mixture, B) components of the cDNA synthesis mix.

4.2.6 qPCR Assay

The qPCR segment of the qRT-PCR protocol, in which selected transcripts in the template were amplified and quantified, was performed using a Stratagene Mx3005P™ real time qPCR machine. cDNA was used as a template (see Section 4.2.5 for synthesis details).

4.2.6.1. Experimental Design

SYBRGreenER qPCR SuperMix Universal from Invitrogen was used according to the manufacturer's instructions. This mix contains *Taq* polymerase, SYBR green, and other components required for qPCR. The *Taq* polymerase present in this mix is of the 'hot-start' variety i.e. it has been chemically modified to make it inactive at ambient temperatures. This increases the specificity of the assay as it prevents amplification being primed by non-specific interactions which can occur during set up (Bustin, 2002). The polymerase activity was restored by 10 minute incubation at 95^{o}C at the start of PCR cycling.

The expression level of GRK5, tyrosine 3-monooxygenase/tryptophan 5-monooxygenase activation protein-zeta polypeptide (YWHAZ) and tata box binding protein (TBP) was measured for each template, and all reactions were run in duplicate. Each 20µL reaction was set us as described in Table 4.2. The templates were diluted 1/37.5 before use to minimise the concentration of RT reaction components in the qPCR reaction mix. This resulted in template solutions with a cDNA concentration of 0.533ng/µL. Non-template controls (NTC) were run for each primer set (see Table 4.2)

	Gene			
Reagent	**GRK5**	**YWHAZ**	**TBP**	**NTC**
SYBRGreenER SuperMix Universal	10µL	10µL	10µL	10µL
cDNA template (3ng)	5.63uL	5.63µL	5.63µL	0µL (0ng)
NPH_2O	3.57µL	3.57µL	3.17µL	8.8 µL or 9.2µL
10µM F primer	0.4µL	0.4µL	0.6µL	0.4 µL or 0.6µL
10µM R primer	0.4µL	0.4µL	0.6µL	0.4 µL or 0.6µL
TOTAL VOLUME	**20µL**	**20µL**	**20µL**	**20µL**

Table 4.2 Volumes of each component for test and non-template control qPCR reactions

The final F and R primer concentrations were 200nM for reactions measuring GRK5 or YWHAZ expression, and 300nM for TBP reactions. Master mixes were used where possible to reduce the potential for pipetting errors.

The following 2 step thermal profile was used: 50^{o}C for 2 minutes, 95^{o}C for 10 minutes to activate the *Taq* polymerase, followed by 40 cycles of denaturation at 95^{o}C for 15 seconds, and annealing and extension at 60^{o}C for 60 seconds. Nucleic acids of different lengths melt at different temperatures. The dissociation curves of a reaction in which a single product was amplified will show a single clean peak. If additional products or primer-dimers are formed, the curve will contain multiple peaks. Dissociation curve analysis with a thermal profile of 1 minute at 95^{o}C, 30 seconds at 55^{o}C, and 30 seconds at 95^{o}C was performed at the end of PCR thermocycling.

4.2.6.2 Analysis

Normalisation of target gene expression to endogenous controls is advantageous as the reference genes and target genes are exposed to identical preparation conditions. This accounts for differences in template amount and quality between samples caused by differences in RNA

extraction, RT reaction efficiency (Radonic *et al.*, 2004) cell number, and experimental treatment (Schmittgen & Zakrajsek, 2000). Though many papers have been published using a single reference gene, the use of multiple reference genes for each assay is preferable (Bustin, 2002; Radonic *et al.*, 2004). Ideally reference genes are expressed at similar levels to the target gene, and are not influenced by the experimental treatment. YWHAZ and TBP were used as reference genes for assays measuring changes in GRK5 expression.

The baseline fluorescence, C_t values, and dissociation curves for each reaction were automatically determined by the Stratagene Mx3005P qRT-PCR software. The C_t values were used to determine the expression levels of GRK5, TBP, and YWHAZ in each sample. The dissociation curves were examined for the presence of additional products and primer dimers.

REST© 2009 software (Pfaffl *et al.*, 2002) was used to calculate the relative expression level of GRK5 across samples, using the expression of TBP and YWHAZ as endogenous controls. The C_t values of both the target gene and reference genes were adjusted using the calculated efficiencies of their primer sets, as determined from their standard curves (Section 4.3.2.5.2). Statistical analysis of the calculated changes in gene expression was also performed as part of the REST© 2009 software analysis. The statistical significance of detected changes in the expression of each gene between the control and test samples was determined using a hypothesis test, and expressed as a *p* value.

4.3 DEVELOPMENT OF QRT-PCR PROTOCOL

4.3.1 Materials and solutions

For the sources of all materials used in this chapter, refer to Appendix A. For the details of all solutions used in this chapter, refer to Appendix B.

4.3.2 Methods

4.3.2.1 Template generation

To prevent unnecessary template variability during qPCR protocol development, RNA and cDNA were produced in large quantities for use in primer analysis experiments.

4.3.2.1.1 RNA Extraction for qPCR protocol optimisation

The standard RNA extraction protocol described in Section 4.2.4 was followed, with the following exceptions:
i) HEK293 cells were plated at 60,000 cells/well in 9 wells of a 24-well culture plate, ii) RNA was harvested when the cells had reached 80-100% confluence, iii) following resuspension of the cells in TRIzol®, the contents of three wells were pooled into a single 1.7mL microfuge tube, iv) the aqueous phase from each of the 3 tubes was individually combined with an equal volume of 70% alcohol, and the resulting mixtures were loaded onto a single Spin Cartridge, and eluted in 30µL of NPH_2O. The RNA yield from two such preparations ranged from 0.557 to 1.0576 µg/µL.

4.3.2.1.2 Reverse Transcriptase Reaction for qPCR development

The standard RT protocol found in Section 4.2.5 was followed with the following exceptions: i) 3µg RNA (RNA extraction described in Section 4.3.2.1.1) was used as the template for the RT reaction, and ii) after reaction termination, the sample was collected by brief centrifugation and 130µL of RNase-free water was added, giving a total volume of 150µL and a concentration of 20ng cDNA per µL (based on RNA input).

4.3.2.2 Selection of candidate primer sets

DNA polymerases require an existing 3’ end to synthesise DNA (Watson *et al.*, 2004). PCR techniques make use of synthetic primers to ‘prime’ polymerisation and select the section of template to be amplified. Primers are short (~20bp) stretches of single stranded DNA which hybridise by Watson-Crick base pairing to their target within the template cDNA in a sequence-dependant manner. This provides the 3’ ends required for DNA polymerase-mediated

DNA synthesis (van Pelt-Verkuli *et al.*, 2008). The primers are effectively consumed by the PCR as they are extended into the PCR products.

4.3.2.2.1 Primer sets for amplification of GRK5

Numerous primers pairs for GRK5 have been published in the literature for use in both end-product and quantitative PCR. Nine published primer pairs for GRK5 taken from the literature were screened for complementarity to the human GRK5 mRNA sequence using the NCBI BLAST nucleotide alignment engine (http://blast.ncbi.nlm.nih.gov/Blast.cg). Of these, three pairs (designated here as GRK5 RTP, GRK5 ZhC, and GRK5 Vgt) were shown to have sequence complementarity, and were selected for further assessment, along with 3 sets of PCR primer pairs for human GRK5 previously designed in this laboratory (designated GRK5 MG, MG1 &MG2) by Michelle Gatehouse (Gatehouse, 2008), and 3 primer pairs (designated GRK5 PB1-3) from the Harvard Primerbank (http://pga.mgh.harvard.edu/cgi-bin/primerbank/search.cgi) (Spandidos *et al.*, 2010). Details for each GRK5 primer set tested are shown in Table 4.3. The alignment of the selected primer sets with the GRK5 cDNA sequence is shown in Appendix C.

4.3.2.2.2 Primer sets for amplification of reference genes

Primer pairs for 11 reference genes were selected for *in silico* assessment, upon recommendation from Dr Aaron Jeffs (Department of Pathology, University of Otago). The primer pairs tested were for; β-Actin (ACTB) (Metaye *et al.*, 2002), TBP (Dallol *et al.*, 2002), glyceraldehyde-3-phosphate dehydrogenase (GAPDH), hydroxymethylbilane synthase (HMBS), hypoxanthine-guanine phosphoribosyltransferase 1 (HPRT1), 60S ribosomal protein LI3a (RPLI3A), succinate dehyrogenase complex (subunit A, SDHA), ubiquitin C (UBC) and YWHAZ (Vandesompele *et al.*, 2002), guanine nucleotide-binding protein subunit beta-2-like-1 (GNB2L1) (Jeffs *et al.*, 2009), and peptidyl isomerase B (PPIB) (Prof. M. Eccles, Department of Pathology, University of Otago: unpublished). Primer details for candidate reference genes are shown in Table 4.4

Primer name	Direction	Sequence	Product size (nt)	Source	Species
GRK5 (MG)	F	5'-AAA GAG GAA AGG GGA GTC CA-3'	221	Michelle Gatehouse (2008)	Human
	R	5'-AGA GGA TCT CTG CCG CAT AA-3'			
GRK5 (MG1)	F	5'-CTG CTC ACG AAA GAT GCG AA-3'	360	Michelle Gatehouse (2008)	Human
	R	5'-CGG AGG GTG GTT TCT GTT CA-3'			
GRK5 (MG2)	F	5'-AAC CAC CAC ATA AAC TCA AAC CA-3'	290	Michelle Gatehouse (2008)	Human
	R	5'-AAT GTT CAC CAA AGA CAA ATC CA-3'			
GRK5 (PB1)	F	5'-CAA CAC GGT CTT GCT GAA AGC-3'	104	Harvard Primerbank (ID: 4885349a1)	Human
	R	5'-CAC ACT GGC TAA TGT GAG GGA-3'			
GRK5 (PB2)	F	5'-TGG GCT GGA GTG TTA CAT TCA-3'	111	Harvard Primerbank (ID: 4885349a2)	Human
	R	5'-GGG GTG AGG TAC TTG GTC ATA AT-3'			
GRK5 (PB3)	F	5'-CCC AAA GTC CCC TGT TTT CAT-3'	138	Harvard Primerbank (ID: 4885349a3)	Human
	R	5'-GGTTCTCCCCTCAGGTACTCG-3'			
GRK5 (RTP)	F	5'-GAC CAC ACA GAC GAC GAC TTC-3'	103	Pattyn et al (2003), Metaye et al (2002), Liu et al (2010)	Human
	R	5'-CGT TCA GCT CCT TAA AGC ATT C-3'			
GRK5 (ZhC)	F	5'-ACC TGA GGG GAG AAC CAT TC-3'	233	Zhou et al (2009), Cohn et al (2009)	Human
	R	5'-TGG ACT CCC CTT TCC TCT TT-3'			
GRK5 (Vgt)	F	5'-CGA CTG TCA ATG GAG CTG GA-3'	1789	Voigt et al 2004	Human
	R	5'-GCC GAA ACT AGC TGC TTC CG-3'			
Gprk (FM)	F	5'-AAT GGA GCT GGA AAA CAT CG-3'	NA	Fan & Malik et al (2003)	Mouse
	R	5'-GGT TGT CTT TCT AAC CAT TT-3'			
GRK5 (Hat)	F	5'-GAA GGT TAA GCG GGA AGA GG-3'	NA	Hata et al (2006)	Human
	R	5'-TCC AGG CGC TTA AAG TTC AT-3'			
GRK5 (Li)	F	5'-CAA GTG TGA GGT AGG GTA CAG AAT-3'	NA	Li et al (2008)	Mouse
	R	5'-CTA TCC ATT CAC CTC CAT GCT CCC-3'			
GRK5 (Key)	F	5'-GAA GGT TAA GCG GGA AGA GG-3'	NA	Keys et al (2005)	Mouse
	R	5'-TCC AGG CGC TTA AAG TTC AT-3'			
GRK5 (Pre)	F	5'-ACC TAT GCC TCC CTT TCT ATT CTC-3'	NA	Premont et al (1999)	Mouse
	R	5'-TTA CAA CTT CTC CCA TCC CAG TGT-3'			
GRK5 (Zub)	F	5'-CTG GCT TTG AGG AAG AAC GA-3'	NA	Zubare-Samuelov et al (2005)	Rat
	R	5'-GTT TTG ATG CTG ACG CCT GA-3'			

Table 4.3 Details for candidate GRK5 primer sets for use in qRT-PCR. Primer sets which were found to not align with the human GRK5 cDNA sequence are show in grey

Primer name	Direction	Sequence	NCBI mRNA assession number	Product size (nt)	Source
ACTB	F	5'-TCC CTG GAG AAG AGC TAC G-3'	NM_001101	131	Metaye et al. (2002)
	R	5'-GTA GTT TCG TGG ATG CCA CA-3'			
GADPH	F	5'-TGC ACC ACC AAC TGC TTA GC-3'	NM_002046	87	Vandesompele et al. (2002)
	R	5'-GGC ATG GAC TGT GGT CAT GAG-3'			
GNB2L1	F	5'-CAC AAC GGG CAC CAC CAC-3'	NM_006098	138	Jeffs et al. (2009)
	R	5'-CAC ACA CCC AGG GTA TTC CAT-3'			
HMBS	F	5'-GGC AAT GCG GCT GCA A-3'	NM_000190	523	Vandesompele et al. (2002)
	R	5'-GGG TAC CCA CGC GAA TCA C-3'			
HPRT1	F	5'-TGA CAC TGG CAA AAC AAT GCA-3'	NM_000194	94	Vandesompele et al. (2002)
	R	5'-GGT CCT TTT CAC CAG CAA GCT-3'			
PPIB	F	5'-ATG ATC CAG GGC GGA GAC TT-3'	NM_000942.4	106	Prof. M Eccles, Department of Pathology University of Otago: Unpublished
	R	5'-CAG GCC CGT AGT GCT TCA G-3'			
RPL13A	F	5'-CCT GGA GGA GAA GAG GAA AGA GA-3'	NM_012423	127	Vandesompele et al. (2002)
	R	5'-TTG AGG ACC TCT GTG TAT TTG TCA A-3'			
SDHA	F	5'-TGG GAA CAA GAG GGC ATC TG-3'	NM_004168	86	Vandesompele et al. (2002)
	R	5'-CCA CCA CTG CAT CAA ATT CAT G-3'			
TBP	F	5'-TGC ACA GGA GCC AAG AGT GAA-3'	NM_003194	132	Dallol et al. (2002)
	R	5'-CAC ATC ACA GCT CCC CAC CA-3'			
UBC	F	5'-ATT TGG GTC GCG GTT CTT G-3'	NM_021009	133	Vandesompele et al. (2002)
	R	5'-TGC CTT GAC ATT CTC GAT GGT-3'			
YWHAZ	F	5'-ACT TTT GGT ACA TTG TGG CTT CAA-3'	NM_001135699	94	Vandesompele et al. (2002)
	R	5'-CCG CCA GGA CAA ACC AGT AT-3'			

Table 4.4 Details of candidate reference gene primers sets for use in qRT-PCR

4.3.2.3 *In silico* assessment of candidate primer sets

The mRNA sequences for GRK5, ACTB, GAPDH, HMBS, HPRT1, PPIB, RPL13A, SDHA, TBP, UBC, and YWHAZ were retrieved from the Genebank data base (www.ncbi.nlm.nih.gov). Reference gene NCBI accession numbers are shown in Table 4.4. The NCBI accession number for GRK5 is NM_005308.2.

4.3.2.3.1 Primer specificity

The use of specific primer sets is important for accurate quantitative PCR. If primers have poor specificity, i.e. the sequence targeted by the primer is not unique to the target gene, they may also prime the amplification of off-target sequences. To determine the specificity of each primer pair for its target sequence, the BLAST search engine (http://blast.ncbi.nlm.nih.gov/Blast.cgi) was used to predict off-target interactions, by searching each pair against the mRNA sequence of their template gene and the NCBI human transcript reference sequence database (organism limited to *Homo sapiens*). Expect (E) values were generated by the BLAST search engine, and indicated the likelihood of interactions occurring simply by chance. The larger the E value, the lower the likelihood that the interaction will occur. Primers with off-target reactions with E values <1 were eliminated.

4.3.2.3.2 Secondary structure prediction

Sequence complementarity within a primer, such as an inverse repeat, can lead to the formation of hairpins and homo-dimers, while sequence complementarity between F and R primers means there is potential for hetero-dimer formation. Secondary structures caused by strong interactions can impair the PCR amplification efficiency of the target transcript by i) sequestering reagents and primers from the available pool by out-competing the template for amplification (amplification of short-primer dimers is easier than amplification of the longer target sequences and therefore more favourable) (van Pelt-Verkuli *et al.*, 2008), ii) causing inefficient hybridisation to the target sequence within the template (Nolan *et al.*, 2006), and iii) producing a potentially significant contribution to the measured fluorescence by binding SYBR

green. Involvement of a primer's 3' terminus in a secondary structure increases the potential of the structure to interfere with specific amplification of the target sequence.

Beacon Designer Free Edition software from Premier Biosoft International (http://www.premierbiosoft.com/index.html) was used to predict the propensity of each primer to form hairpins, and to homo- and hetero-dimerise. The calculated Gibbs free energy (ΔG) of a predicted secondary structure gives an indication of how likely it is to interfere with correct primer hybridisation during PCR, with low energies being less likely to interfere. Technical notes provided on the Premier Biosoft website (http://www.premierbiosoft.com/tech_notes/PCR_Primer_Design.html) were used to guide analysis of *in silico* results. For vetting the candidate primer sets, secondary structures with ΔG values greater than those listed below were considered to be likely to interfere with the PCR reaction.; -3 kcal/mol for internal hairpins, -2kcal/mol for 3' hairpins, -6kcal/mol internal homo-and hetero-dimers, and -5kcal/mol for dimers involving the 3' end. Full details of secondary structures predicted for each primer pair can be found in Appendix F.

4.3.2.3.3 Primer and product characteristic prediction

Ideal qPCR primers are typically approximately 20 base pairs in length and bind only to their target sequence. The presence of at least one guanine (G) or cytosine (C) residue at the 5' termini is known as a G/C clamp and is favourable for specific primer binding. Ideal primer sets have similar melting temperatures, and the annealing temperature for each primer should be within 5^{o}C of its partner. Furthermore, primer pairs should have similar G/C contents, ideally between 40% and 60%.

The melting temperature and GC content of each primer and the size of the product produced by each primer set was calculated using Primer-BLAST (http://www.ncbi.nlm.nih.gov/tools/primer-blast/index.cgi?LINK_LOC=BlastHome). 5' G/C clamps were identified manually.

Due to inter-run variation, reference gene analysis for each qPCR reaction must be done on the same plate as the target gene analysis. As such, primer sets for reference genes must be

compatible with the reaction conditions required by the target gene primer sets, namely the melt temperatures, annealing temperature and elongation times. Increasing the elongation time increases the likelihood of off-target amplification. Primer sets for reference genes were therefore also vetted on the basis of melting and annealing temperature, and product size compatibility to the GRK5 targeting primer sets.

Primer pairs for reference genes which produced a product more than 35bp shorter or longer than the predicted product produced by the selected GRK5 primers (see Section 4.3.4.3) were deemed to be incompatible with the GRK5 primers. Reference gene primer pairs with melt temperatures more than 5^{o}C higher or lower that the selected GRK5 primers were also excluded. The compatibility of reference gene annealing temperatures with the selected GRK5 primer sets was assessed experimentally in Section 4.3.2.4. Predicted characteristics for each pair of candidate primers and their products can be found in Appendix F.

4.3.2.3.4 Results of in silico assessment

In silico assessment of GRK5 primer pairs identified six sets that fulfilled the selection criteria. These were GRK5 MG1, GRK5 MG2, GRK5 PB1, GRK5 PB2, GRK5 RTP, GRK5 Vgt. Of these, two were selected for further assessment based on the similarity of their product lengths, as they could be used with the same contingent of reference gene primers. The selected sets were; GRK5 RTP (product length 103bp) and GRK5 PB2 (product length 111bp).

In silico assessment of the reference gene primer pairs identified six sets suitable for further analysis. They were; GADPH (product length 87bp), GNB2L1 (product length 138bp), HPRT1 (product length 94bp), PPIB (product length 106bp), SDHA (product length 86bp), and YWHAZ (product length 94bp). A seventh reference gene, TBP (product length 132bp), did not quite meet selection criteria due to the predicted formation of a 3' homo-dimer with a calculated ΔG of -5.3 kcal/mol, which was 0.3 kcal/mol higher than the cut off point used for vetting. Due to the slimness of this margin, and the unknown effect of reaction conditions on the formation of secondary structures, TBP was also selected for experimental testing.

4.3.2.4 PCR-based Primer Testing

PCR assessment of the primers was undertaken as it is a simple and cost-effective way to gain information about the way primers perform under reaction conditions. To assess the performance of each primer set, its products were examined by electrophoretic separation. Separation of products from primer sets which bound specifically to their target sequence, and did not form significant secondary structures would produce gels containing a single band at the expected molecular weight. The presence of additional bands would be evidence for the occurrence of off-target binding and secondary structure formation. PCR assessment was also used to gain an understanding of the approximate expression levels of GRK5 and the reference genes, as for accurate qPCR it is preferable for the expression levels of the reference and target genes to be similar so that the resulting CV values are similar. The annealing temperature used for PCR can affect the specificity of the amplification. Higher annealing temperatures result in more specific amplification, as only primers with high sequence homology with the template (and thus the maximum number of Watson-Crick hydrogen bonds) can anneal. As such, an annealing temperature gradient was performed for all primer sets, to indicate the specificity of their amplification over a range of temperatures.

The performance of the primer pairs was examined over a range of annealing temperatures, to a) determine the minimum appropriate annealing temperature for GRK5 primer sets, and b) identify reference gene primers that were compatible with these conditions.

4.3.2.4.1 PCR methods

PCR reactions were performed using KAPATaq Ready Mix DNA Polymerase from KapaBiosystems, and an Eppendorf Mastercycler e*p* gradient *S* PCR machine. The 20µL reactions were performed in singlet, the details of which are shown in Table 4.5. ‘Water’ and ‘no-template’ controls were run for each primer set. The ‘water’ controls were included to detect potential nucleic acid contamination of the PCR buffer and nuclease-free ddH_2O, while the ‘no-template’ controls controlled for the presence of primer-dimers as their formation is more favourable in the absence of template.

	Reaction Type		
Reagent	**Test**	**Water control**	**No template control**
2X KAPATaq Ready Mix DNA Polymerase	10µL	10µL	10µL
cDNA (20ng/µL)	1µL	0µL	0µL
Forward primer	0.5µL	0µL	0.5µL
Reverse primer	0.5µL	0µL	0.5µL
Nuclease-free ddH_2O	8µL	10µL	9µL

Table 4.5 Reaction components and volumes for PCR assessment of candidate primer sets

The final concentrations of KAPATaq Ready Mix DNA Polymerase components for all reactions were; 0.025 U/µL Taq, 1X buffer, and 0.2mM dNTPs. The final concentrations both the forward and reverse primers in the 'test' and 'No template control' reactions was 250nM.

The following thermal profile was used for PCR. An initial denaturation at 95^{o}C for 2 minutes was followed by 30 cycles of; denaturation at 95^{o}C for 30 seconds, annealing for 30 seconds, and extension at 72^{o}C for 15 seconds. A final extension of 1 minute was performed at 72^{o}C. The annealing temperature was varied across the heat plate. Test wells for each primer set were run at 48^{o}C, 50.7^{o}C, 53^{o}C, 54.8^{o}C and 55.8^{o}C. As the annealing temperature decreases, the potential for primers to anneal non-specifically increases. For this reason, the annealing temperature used for the 'Water' and 'No-Template' controls was 47.3^{o}C. The lid was heated to 105^{o}C to avoid sample evaporation.

The PCR products from the 'test' and 'control' reactions were separated on 1.5% agarose gels containing 0.01% SYBRsafe dye (Invitrogen), at 250 volts for approximately 25 minutes. DNA bands were visualised by UV transillumination using the ChemiGenius^2 CCD Imaging System (Syngene), and photographed using GeneSnap software (Syngene).

4.3.2.4.2 Results

The results for all primer sets are shown in Figure 4.1.

4.3.2.4.2.1 Secondary structure formation

The presence of bands in the 'no-template' controls at <100bp indicates the formation of primer dimers or other secondary structures. These bands were also present at varying intensities in the 'test' PCR products from some primer sets, indicating that primer secondary structure was occurring (Figure 4.1). A band indicative of secondary structure was seen for the following primer pairs; SDHA, GAPDH, GRK5 (RTP), HPRT1, PPIB and GNB2L1. The intensity of this band differed between primer sets. A dark band was seen with GADPH, SDHA and PPIB, suggesting extensive secondary structure formation. In comparison, the <100bp bands for GRK5 (RTP), HPRT1 and GNB2L1 were faint. The 'no-template' control was important for informed analysis as the bands seen in these controls would otherwise be indistinguishable from off-target products.

4.3.2.4.2.2 Specificity

In the lanes in which the 'test' products were run, the presence of additional bands that were not also found in the 'no-template' control would indicate the presence of additional products, likely caused by off-target binding. However, a single product of the expected size was seen for all primer sets over all annealing temperatures assayed. The 'water' controls did not contain any bands, indicating that cross-contamination of reagents had not occurred during set up (Figure 4.1).

4.3.2.4.2.3 Band intensity

The intensity of the bands produced was used to give an approximate indication of the relative expression levels for the target gene of each primer set. The range of band intensities detected was large, with the following order; GADPH > GNB2L1 > PPIB > SDHA > HPRT1 > TBP > GRK5 (PB2) > GRK5 (RTP).

Several primer sets showed an increase in band intensity with an increase in annealing temperature. This may be due to increased activity of the thermophillic polymerase, and suggests that there is the potential for using higher annealing temperatures to increase product formation.

4.3.2.4.3 Primer selection for qPCR assessment

Based on assessment of their PCR products, both sets of primers for GRK5 amplification (GRK5 RTP, and GRK5 PB2) were chosen for qPCR analysis, as they i) showed no evidence of off-target binding, and ii) showed minimal or no evidence of secondary structure formation.

Primer sets for four reference genes were also selected for qPCR-based analysis. They were: GNB2L1, HPRT1, TBP, and YWHAZ. They were selected as their expression levels were the most similar to that of GRK5, they showed no evidence of off-target binding, and they showed the lowest levels of primer-dimer formation.

The low levels of primer secondary structure formation seen when the GRK5 (RTP), HPRT1 and GNB2L1 primer sets were used was not considered grounds for exclusion as the composition of the reaction buffer—such as Mg^{2+} concentration—can affect secondary structure formation.

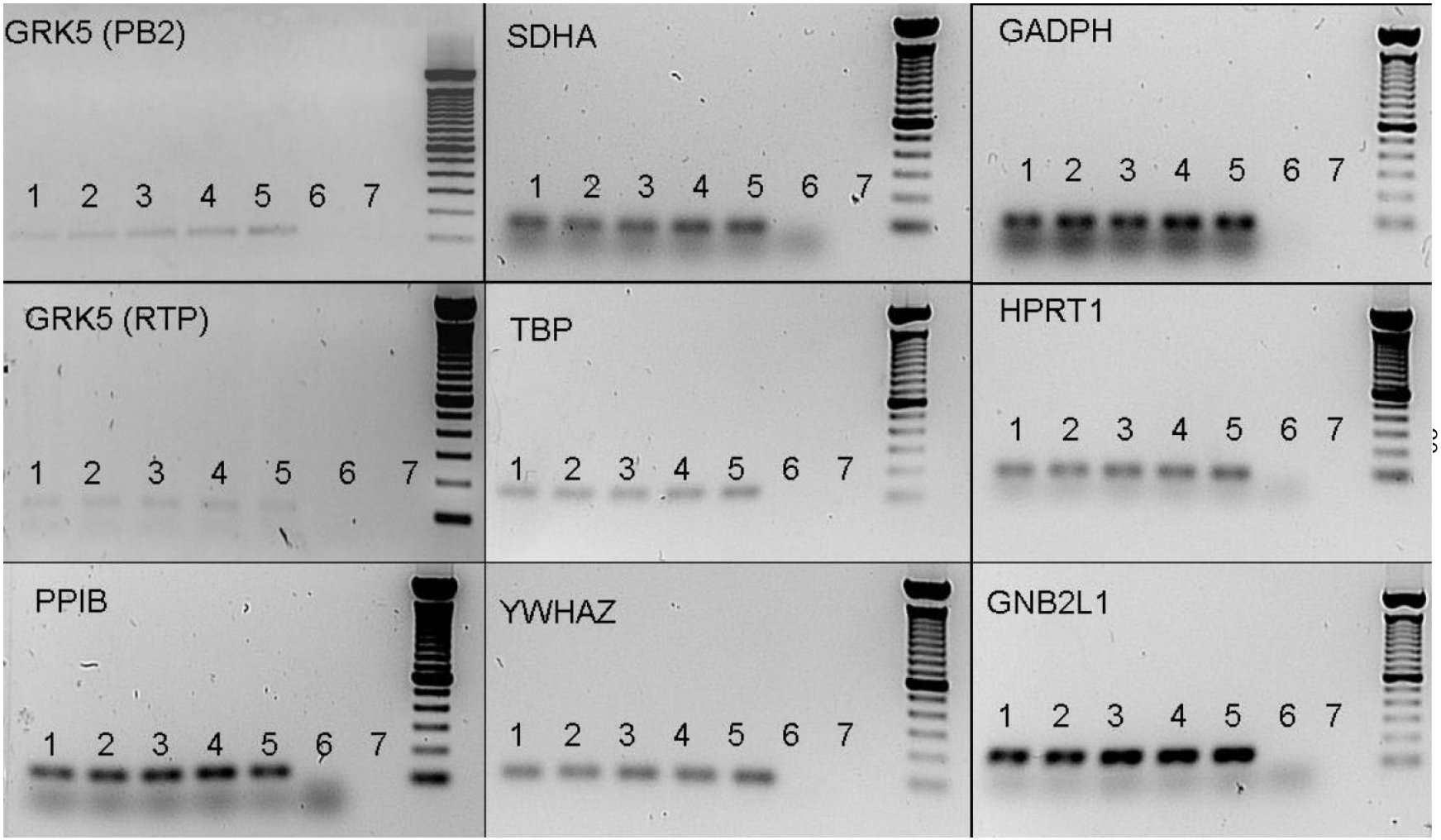

Figure 4.1 PCR products from annealing temperature gradient. The performance of the primer sets was tested over the following range of temperatures; lane 1: 48^{o}C, lane 2: 50.7^{o}C, lane 3: 53^{o}C, lane 4: 54.8^{o}C, lane 5: 55.8^{o}C, lanes 6 and 7: 47.3^{o}C. Lanes 1-4 show the products of the amplification reactions. Non template and water controls are shown in lane 6 and 7 respectively

4.3.2.5 qPCR assessment

The template used for qPCR assessment was generated using the protocol described in Section 4.3.2.1. All qPCR reactions were performed using SYBR® GreenER qPCR SuperMix Universal from Invitrogen, and a Stratagene Mx3005P qPCR machine.

4.3.2.5.1 Primer Test and Selection of Assay Details

4.3.2.5.1.1 qPCR assay details

The compatibility of the primers with the standard qPCR protocol provided by Invitrogen for use with the SYBR® GreenER qPCR SuperMix Universal reagent (http://tools.invitrogen.com/content/sfs/manuals/sybrgreener_supermix_uni_man.pdf) was tested prior to commencement of protocol optimisation. For this trial, each primer set was tested in singlet, with a reaction volume of 20µL. Each reaction contained: 10µL SYBR® GreenER qPCR SuperMix Universal, 200nM of both the F and R primers, 5ng of template cDNA, and sufficient NPH_2O to bring the volume to 20µL.

qPCR was performed using the PCR thermal profile and melt curve described in the standard methods (Section 4.2.6). The melt curve analysis was used to determine if primer-based secondary structures were being formed. These structures are generally seen as peaks around 75^{o}C.

4.3.2.5.1.2 Results

Amplification and dissociation curves for all primers tested are shown in Figure 4.2. As evidenced by the dissociation curves, each primer pair produced a single peak indicating a single product. Primer-dimers were not detected for any primer sets. The amplification curve for both GRK5 primers, and the primers for reference genes GNB2L1, TBP, and YWHAZ, have the classical curved shape typical of qPCR reactions (Bustin, 2004). The amplification curve for HPRT1 however does not conform to this shape, showing a slow and almost linear

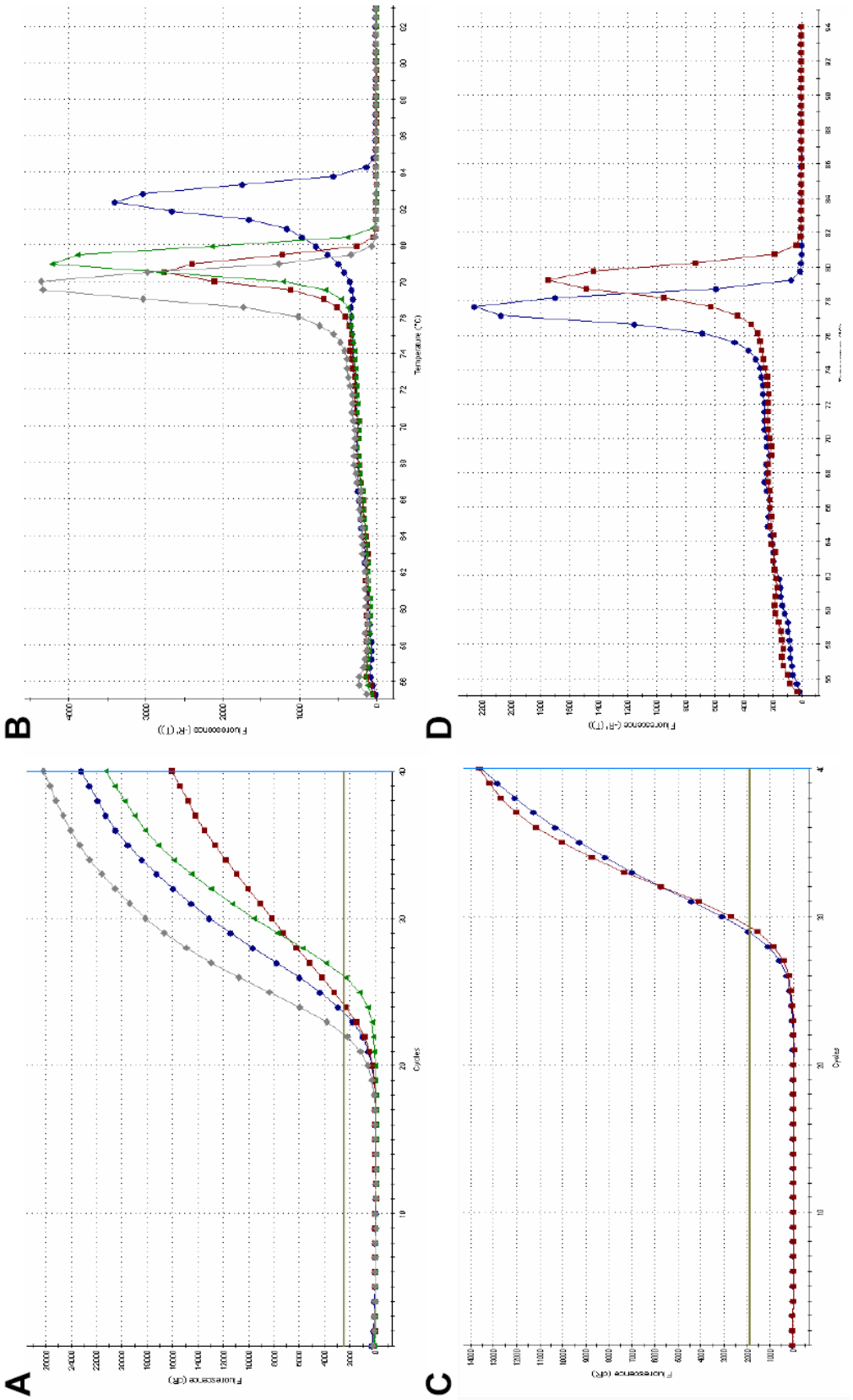

Figure 4.5. qPCR test amplification dissociation curves. The performance of using GNB2L1 (blue), HPRT1 (red), TBP (green) and YWHAZ (grey) are shown in A and B. The performance of the RTP (red) and PB2 (blue) primers for GRK5 are shown in C and D. All primers were present at a concentration of 200nM, and the test reactions completed in singlet

increase in fluorescence between cycles 23.6 and 40. This atypical amplification curve indicates the PCR reaction is proceeding with poor efficiency. The primers for HPRT1 were

not analysed further. The remaining primers appeared to be compatible with the thermal profile of the standard assay, and as such, the profile was not altered.

The intensity of the bands seen during PCR assessment of the primers (Section 4.3.2.4) suggested that the primer sets may be compatible with annealing temperatures higher than the 55.8^{o}C, which was the highest temperature used for that assessment. This was confirmed by the successful priming seen during qPCR assessment, when 60^{o}C was used as the annealing temperature.

The C_t values produced by both GRK5 primers were extremely similar. This is the expected results, as they are measuring the expression of the same gene. The difference in the T_m of their respective products is indicative of their different amplicons.

4.3.2.5.2 Determination of primer set amplification efficiencies

As PCR is an exponential reaction, small differences in primer set amplification efficiencies can result in C_t values that are not truly representative of the relative concentrations of their targets in the template. If the amplification efficiency for each primer set is determined, the C_t values can be mathematically adjusted to compensate for this, allowing more accurate interpretation of the results. The amplification efficiency of a qPCR reaction can be determined by diluting the template to produce a standard curve. The relationship between the C_t value intervals and the dilution factor is shown by the slope of the standard curve, and is used to determine the efficiency of amplification.

4.3.2.5.2.1 Standard curve generation

The amplification efficiencies of the remaining primer sets (GRK5 RTP, GRK5 PB2, TBP, YWHAZ and GNB2L1) were determined by analysis of qPCR performed over five dilutions of the template. The template cDNA was diluted in nuclease-free NPH_2O to the following amounts per reaction: 20ng, 10ng, 4ng, 2ng, and 0.4ng. Primers for GRK5 and YWHAZ were used at a concentration of 200nM, while primers for TBP were used at a concentration of 300nM. All reactions were performed in duplicate. The qPCR and melt curve thermal profiles

described in Section 4.2.6 were used. Standard curves were generated automatically by the Stratagene MxP3005™ software, by plotting the C_t values against the initial template quantity.

4.3.2.5.2.2 Determination of amplification efficiencies

Data points which showed reaction inhibition or the production of unwanted products/secondary structures were excluded from generation of the standard curve as these occurrences would impair the amplification efficiency, and would not be considered acceptable in qPCR assay data.

The amplification efficiency of each primer set was determined from the slope of standard curve by the Mx3005P™ software. The following equation was used:

Equation 4.1 **Amplification efficiency = $[10^{(1-slope)}]-1$**

A reaction with 100% efficiency correlates to a slope of -3.322. The 'goodness-of-fit' of the standard curve to the data is indicated by the R squared (R^2) value. A value of 1 indicates a perfect fit.

4.3.2.5.2.3 Results

Examination of the amplification curves for GRK5 (RTP), GRK5 (PB2), GN2BL1, and YWHAZ showed that the curves were deviating from the ideal shape in reactions containing 20ng and 10ng of template (see Appendix D). This deviation was likely due to inhibition of the PCR reaction by something present in the template solution, possibly carried over from RNA extraction or the RT reaction (Nolan *et al.*, 2006). Exclusion of these points from the standard curves altered the calculated efficiencies of the primer curves. The three remaining points were considered to be sufficient to generate the standard curves. The resulting standard curves, and their calculated efficiencies and R^2 values are shown in Figure 4.3. Lower concentrations of template were not trialled, as the C_t values produced by the GRK5 primer set were already high. Ideally, C_t values fall between 10 and 30 cycles.

The standard curve for TBP was generated at a later date, and as such a different template was used. Examination of the amplification curves showed evidence of inhibition in reactions containing 20ng of template, and as such these data were excluded (See Appendix D). One of the reactions containing 0.4ng template had an unusual amplification curve. Examination of the dissociation curve for this reaction showed the presence of a second product (see Appendix D). This reaction was excluded, but since its replicate was unaffected it was used. The remaining data points were used to generate the standard curve. As above, the standard curve, amplification efficiency, and R^2 value for TBP are shown in Figure 4.3.

Ideally, primer sets should have an amplification efficiency between 90% and 110%. At 87.2% the primer efficiency for YWHAZ is slightly outside this range. However, as the calculations used to analyse the qPCR data (see Section 4.2.6.2) correct for the amplification efficiencies of both the target and reference gene, it was considered to be acceptable.

For the calculated amplification efficiencies of each primer set to be used accurately, the qPCR assay reactions need to contain a template concentration that is within the range used to generate the standard curves, i.e. between 0.4-4μg for YWHAZ and GRK5, and between 0.4-10μg for TBP. For this reason, 3μg of template was selected as an appropriate starting template quantity for use in qPCR assays.

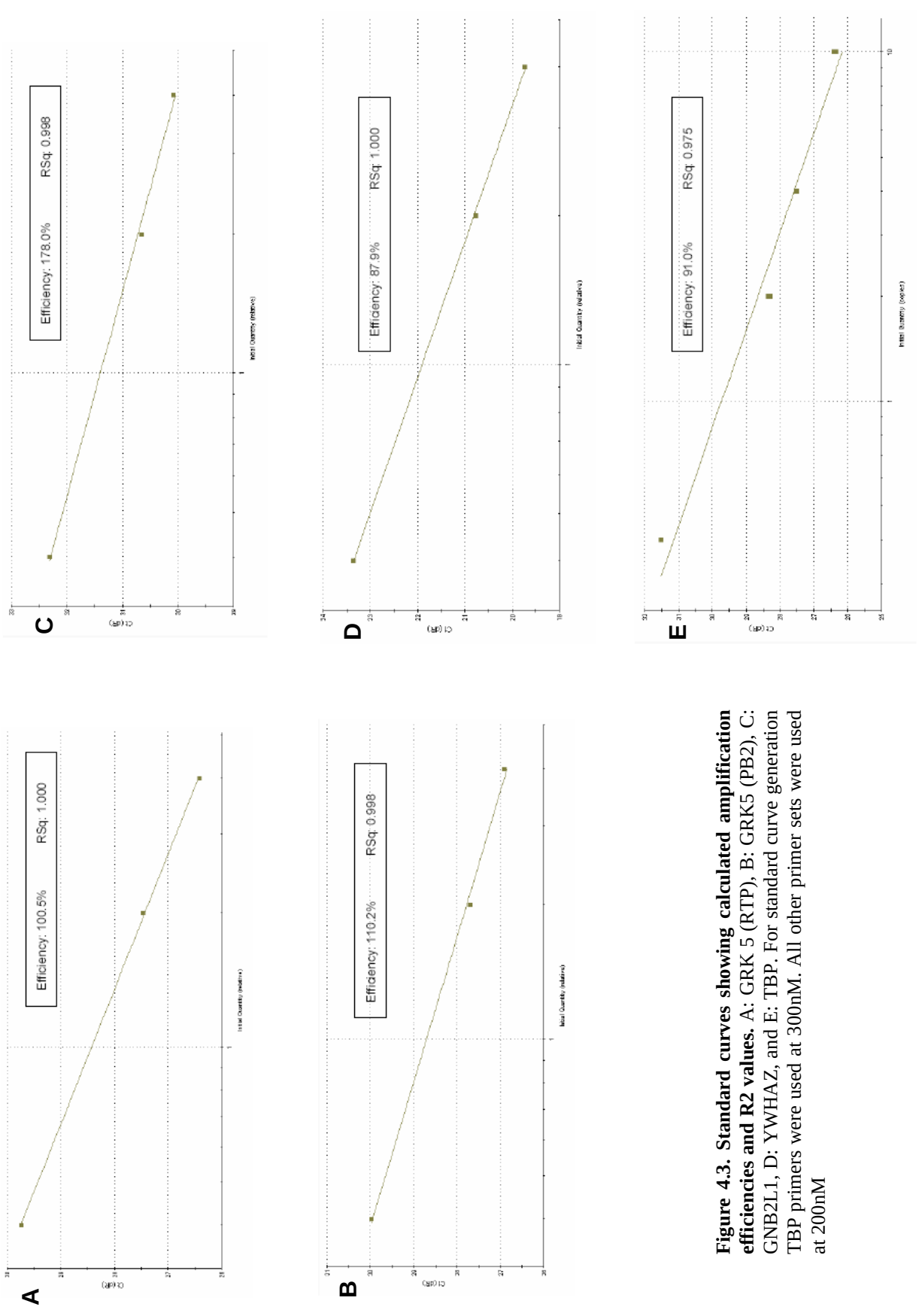

Figure 4.3. Standard curves showing calculated amplification efficiencies and R2 values. A: GRK 5 (RTP), B: GRK5 (PB2), C: GNB2L1, D: YWHAZ, and E: TBP. For standard curve generation TBP primers were used at 300nM. All other primer sets were used at 200nM

4.3.2.6 Final primer selection and cloning

The qPCR products generated by the GRK5 (RTP), TBP and YWHAZ primer sets were sequenced to confirm the identity of their amplicons. Due to their short length (~100bp), the PCR products had to be legated into an expression vector and cloned to facilitate sequencing. This process exploits the fact that *Taq* polymerase adds an additional adenosine to the 3' end of both strands of its products. This allows the products to be easily inserted into vectors with T overhangs, such as the poem®-T Vector system used below. Primer sequencing can then be performed, using M13 primers which bind to the plasmid sequence on either side of the insert.

4.3.2.6.1 Preparation of qPCR products for ligation

Initial attempts to legate the qPCR products into the pGEM®-T Vector were unsuccessful. It was thought that the carryover of reagents from previous applications, such as qPCR, may have been inhibiting the ligation reaction. Typically products are cleaned and concentrated on column-based systems prior to ligation. However, such systems generally do not retain nucleic acids less than ~200bp long, making them incompatible with the qPCR products generated by the TBP (132bp), YWHAZ (94bp) and GRK5 (103bp) primer sets. Instead, the qPCR products were used as a template for a PCR reaction containing no dye, and the products of this reaction were used for ligation. This limited the carryover of SYBR green from the qPCR reaction.

4.3.2.6.1.1 PCR protocol

Each 50µL reaction was performed in singlet, details of which are provided in Table 4.7.
The following thermoprofile was used for amplification: 95^{o}C for 2 minutes, followed by 30 cycles of 95^{o}C for 30 seconds, 60^{o}C for 30 seconds, and 72^{o}C for 15 seconds. A final extension of 1 minute was performed at 72^{o}C.

After PCR amplification, 10µL of each reaction was run on a 2% agarose gel containing 0.01% SYBR safe (Invitrogen), at 80V for 40 minutes to confirm successful amplification. The remainder of each sample was used for ligation.

	Gene			
Reagent	**GRK5**	**YWHAZ**	**TBP**	**NTC**
Biotaq DNA polymerase (Bioline, 5U/µL)	0.5µL	0.5µL	0.5µL	0.5µL
50mM $MgCl_2$ (Bioline)	3µL	3µL	3µL	3µL
dNTPs	3µL	3µL	3µL	3µL
10 X NH_4 Reaction Buffer (Bioline)	5µL	5µL	5µL	5µL
Appropriate qPCR product	1µL	1µL	1µL	0µL
Forward primer	0.9µL	0.9µL	1.5µL	0.9-1.5µL
Reverse primer	0.9µL	0.9µL	1.5µL	0.9-1.5µL
Nuclease-free NPH_2O	35.7µL	35.7µL	34.5µL	35.5-36.7µL

Table 4.6 Reaction components for pre-ligation PCR of qRT-PCR products for sequencing

4.3.2.6.1.2 PCR Results

Agarose gel separation of an aliquot of the PCR products resulted in a band of the expected size for each primer set (Figure 4.4). A faint band <100bp was also seen for TBP and YWHAZ.

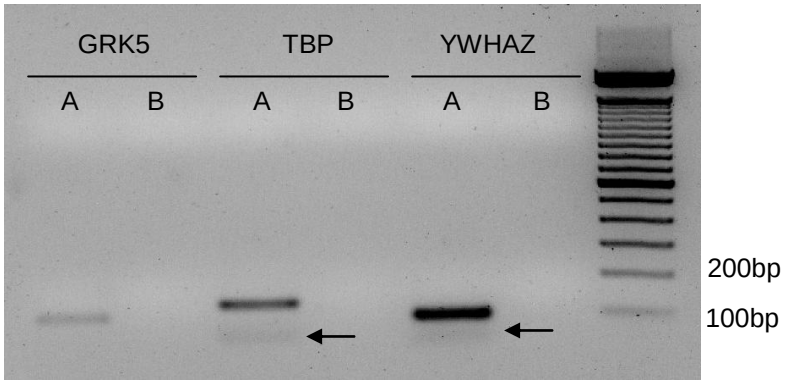

Figure 4.4 Products from "clean up' PCR separated on a 2% agarose gel containing 0.01% SYBR safe. A= template, B= no template control. All produced products of the expected size. For GRK5 (left) a single clean band was seen, while TBP (middle) and YWHAZ (right) produced a second band <100bp in size which represent primer dimers

4.3.2.6.2 TA Ligation

The following reagents were used to ligate the PCR products into a vector for cloning: the pGEM®-T Vector System (Promega, vector sequence available at www.promega.com/vectors), T4 DNA Ligase (Fermentas), and the 10X T4 DNA Ligase Buffer (Fermentas). The pGEM®-T Vector is an expression vector containing the *lacZ* gene and an ampicillin resistance gene. A multiple cloning site (MCS), at which foreign DNA such as qPCR products are inserted during ligation, is located within the *lacZ* gene. Transcription of the *lacZ* gene results in the production of the LacZ protein, also known as β-galactosidase, whose normal activity is to catalyse the conversion of lactose into galactose and sugar. Ligation of foreign DNA, such as a PCR product, into the vector results in the disruption of the *lacZ* gene, and thus inhibition of β-galactosidase production.

A ligation reaction was set up for each primer pair. Ten microlitre reactions were used. The relative volumes of the ligation mixture components are shown in Table 4.7. The mixtures were incubated at 4°C overnight.

Reagent	Volume (µL)
PCR product	3.5
pGEM®-T Vector System	0.5
T4 DNA Ligase (1000CEU/µL)	1
Ligation Buffer	5

Table 4.7 Ligation reaction components and their volumes

4.3.2.6.3 Transformation of competent cells with ligated vector

The ligated pGEM®-T vectors generated in Section 4.3.2.6.2 were used to transform competent DH5α *E. Coli* cells. This step results in the amplification of the vector, and allows the vectors containing an insert to be identified via blue/white colony selection.

4.3.2.6.3.1 Transformation

The DH5α cells were thawed on ice before use. Five microlitres of each ligated vector was added to a 1.7ml microtube containing 50µL of competent cells (one tube per vector). The cell/ligate mixtures were 'heat shocked' using the following thermoprofile; 10 minutes on ice, followed by 1.5 minutes at 37^{o}C, and 2 minutes on ice. Two-hundred microlitres of Luria broth was then added to each tube, and the contents mixed by gentle tapping. The tubes were incubated for 30 minutes at 37^{o}C before plating.

4.3.2.6.3.2 Plating

Immediately prior to plating, 100mm Luria plates (+10% ampicillin) were prepared by adding 10µL of isopropyl-[β]-D-thiogalactopyranoside (IPTG) (Fermentas) and 50µL of X-Gal (5-bromo-4-chloro-3-indolyl-[β]-D-galactopyranoside) (Zymo Research) to the surface of the media. The DH5α cells/ligation mix was then added to the plate, and the solutions spread with a flamed glass rod. The plates were sealed and incubated overnight at 37^{o}C.

4.3.2.6.4 Blue/white colony selection, generation of stab plates, and insert screening

The presence of ampicillin in the growth medium selected for DH5α cells which had been transformed, and thus gained the gene for ampicillin-resistance carried on the vector. Inclusion of IPTG, the activator for *lacZ* gene transcription, in the culture allowed DH5α cells transformed with the pGEM®-T Vector to express β-galactosidase. Blue/white colony selection was used to identify cells transformed with the pGEM®-T+PCR product vectors. Cells transformed with pGEM®-T vectors lacking a PCR product insert produce functional β-galactosidase which converts the colourless modified galactose sugar known as X-GAL into a bright blue product, resulting in blue colonies. In cells transformed by pGEM®-T+PCR product vectors, the expression of functional β-galactosidase was prevented by the insertion of the PCR product, resulting in white colonies.

Due to the small size of the PCR product inserts, in practise the phenotype expressed by pGEM®-T+PCR product vector transformed cells ranged from pale blue to white. The size of the insert for each selected colony was screened via PCR, using M13 F/R primers to amplify the inserts and vector sequences on either side.

Pale blue/white colonies were picked from the plate using a yellow pipette tip and 'stabbed' on to a 100mm Luria plate (+10% ampicillin) marked with a numbered grid. The pipette tip was then used to introduce the sequence into a 0.2mL PCR tube containing 10µL 2x KAPA Taq Readymix, 0.5µL of M13 F/R primer mix, and 9.5µL of ddH_2O. Four pale blue/white colonies were picked for each vector, resulting in the following colonies on the stab plate; T1-4, Y1-4, and G1-4. The PCR was run using the following thermoprofile: 2 minutes at 94°C, followed by 25 cycles of; 2 minutes at 94°C, 30 seconds at 52°C, and 30 seconds at 72°C. This was followed by a final 1 minute and 30 seconds at 72°C. The PCR products were run on a 2% agarose gel containing 0.1% SYBR Safe for ~30minutes at 80V (Figure 4.5).

Figure 4.5 M13 PCR screen showing the insert present in each culture. GRK5 colonies G1-4 produced a bad of the same size., however both TBP and YWHAZ colonies contained inserts of two different sizes. One of each size was selected for sequencing (T2 and T3, Y3 and Y4), along with G1 and G2.

All four clones generated using the GRK5 PCR product-ligated vector (G1-4) produced insert bands of the same size (Figure 4.5). Both the TBP and YWHAZ clones produced inserts of two different sizes. A clone representing each insert size for TBP (T2 and T3) and YWHAZ (Y3 And Y4) was selected for sequencing, along with two GRK5 PCR product-ligated vector transformed clones (G1 and G2). The clones were prepared for sequencing as described below.

4.3.2.6.5 Plasmid preparations

Plasmid preparations were generated for the clones selected based on the PCR insert screen. The stab-plate colonies were used. The colonies corresponding to T2, T3, Y3, Y4, G1 and G2 were 'picked' using a yellow pipette tip and each was used to seed ~5mL of Luria broth (with 0.1% ampicillin) in a labelled McCartney bottle. The bottles were incubated at 37°C overnight with agitation.

4.3.2.6.6 DNA extraction

The DNA was extracted for sequencing using an 'Isolate Plasmid Mini Kit' from Bioline (Cat # BIO-52027). For each sample, 2mL of plasmid preparation was transferred to two 2mL centrifuge tubes (total of 4mL plasmid prep). The tubes were spun at the maximum centrifuge speed for 2 minutes. The supernatant was discarded from both tubes. To resuspend the pellets, 250µL of resuspension buffer was added to one tube, and the tube tapped until the pellet was fully resuspended. The cell suspension was then transferred to the second tube, and the tube tapped until the pellet was resuspended. The first tube was discarded. Two hundred and fifty microlitres of Lysis Buffer P was added to the cell suspension, and the two solutions mixed by inverting the tube 5 times. This was followed by the addition of 350µL of Neutralisation buffer. The contents of the tube were mixed by inverting the tube 5 times. The tube was then spun at maximum centrifuge speed for 10 minutes to pellet the cellular debris. The supernatant was transferred to a labelled Spin Column P placed in a collection tube. The column was spun at 10,000 x g for 1 minute, and the filtrate discarded. The column was washed with 500µL of Wash Buffer AP and 700µL of Wash buffer BP, spinning the column at 10,000 x g for 1 minute and discarding the filtrate after each addition. The column was then spun at maximum centrifuge speed for 2 minutes to remove all traces of the wash buffered. The Spin column was transferred to a labelled elution tube, while the collection tube and filtrate were discarded. Fifty microlitres of elution buffer was added directly to the column matrix and incubated at room temperature for 2 minutes. The column was then spun at 10,000 x g for 1 minute to elute the DNA. The DNA concentration of the samples was then determined using a ND1000 NanoDrop spectrophotometer, using Elution buffer as a blank. Concentrations ranged from 130.7 to 256.9ng DNA per µL.

4.3.2.6.7 Sequencing

The inserts were sequenced by Macrogen Inc. (http://dna.macrogen.com/eng/) using ABI3730*xl* DNA Analyzer (Applied Biosciences) sequencing machines. The resulting sequences were supplied as FASTA files and were searched against the NCBI human transcript reference database (limited to *Homo sapiens*) using the BLAST search engine. The TBP,

YWHAZ and GRK5 (RTP) primer sets were aligned with their products using MEGA 5.0 software.

4.3.2.6.7.1 Results

The sequence of each insert (with primers aligned) is shown in Appendix E.

Both inserts generated from the GRK5 (RTP) primer qPCR products (G1 and G2) were of the expected size (103bp) and had a sequence identical to that of the predicted product.

The sequences for the 'T2' and 'T3' inserts generated from the TBP primer qPCR products were not identical. The 'T3' insert was consistent in size (132bp) and sequence with the predicted product. The 'T2' insert however, was only 52bp long, and its sequence consisted of a combination of the forward and reverse primer sequences, identifying the insert as a primer-dimer. Similarly the inserts generated from the YWHAZ primer qPCR products contained two different products. One, the 'Y3' insert was consistent in sequence and length (94bp) with the expected product. The 'Y4' insert however was short (43bp) and represented the hetero-dimerisation of the forward and reverse primer.

4.3.2.6.7.2 Interpretation of sequencing results

As both the sequenced inserts generated from the GRK5 (RTP) products were identical in sequence to the target amplicon, the GRK5 (RTP) primer set was deemed to be fit for use.
Both YWHAZ and TBP products produced one insert that corresponded to the target amplicon, and a second insert that corresponded to a primer-dimer. This suggests that these primers are not suitable for use with the reaction conditions described in Section 4.2. However, due to the 'clean up' PCR reaction run to prepare the qPCR products for ligation, it is unclear whether the primer-dimers sequenced for YWHAZ and TBP were present in the qPCR products, or if they were introduced during the PCR. Examination of the gel run after the PCR (Figure 4.4) and the melt curves produced by the qPCR products (Figure 4.6) suggested that the primer-dimers were introduced during the PCR step, as there is no evidence of primer-dimer formation of the qPCR product melt curves.

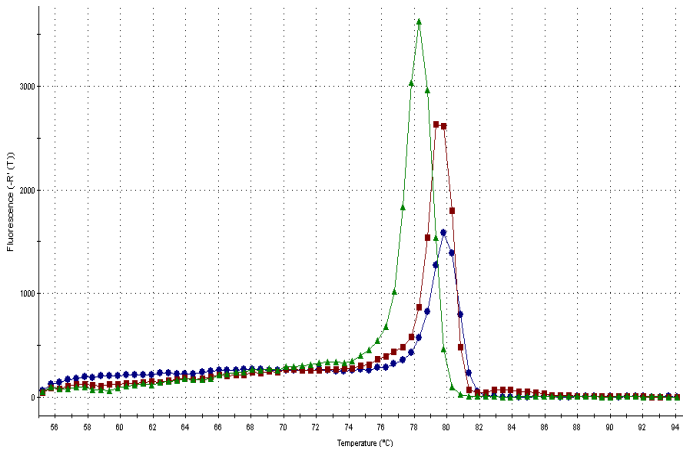

Figure 4.6 Melt curves for the YWHAZ (green), TBP (red) and GRK RTP (blue) qRT-PCR products used as a template for sequencing.

4.3.3 Conclusions and future work

The sequencing results identified the presence of primer-dimers in the TBP and YWHAZ qPCR/PCR products used for the ligation. As an additional PCR step using the primers was required to prepare the qPCR products for sequencing, it is unclear whether these primer-dimers are products from the qPCR or if they were introduced by the PCR step used to remove the fluorescent dye. While no evidence of primer dimers was seen in the melt curves associated with the qPCR products, further optimisation of the qPCR protocol described in Section 4.2 may be necessary to ensure that the qPCR results are accurate.

Increasing the annealing temperature from 60 to 61^{o}C should represent an increase in reaction stringency sufficient to eliminate potential primer-dimer formation. This proposed increase in stringency should be reflected in the resulting melt curves, in particular, as a decrease in the width of the recorded peak when compared with that recorded using an annealing temperature of 60^{o}C. As qPCR assays for GRK5 need to be run on the same plate as the reference genes, the GRK5 primer set will also need to be tested for complimentarity with the increased annealing temperature. The amplification efficiency for all three primer sets would then need to be re-calculated; using standard curves generated using the more stringent thermoprofile.

Unfortunately, the Stratagene qPCR machine used in this study was damaged in the magnitude 6.3 earthquake which occurred in Canterbury on the 22 of February 2011. The machine was not available for use for the remainder of the project. This prevented the final optimisation steps from being completed. qPCR data generated before sequencing of the qPCR products was considered to be indicative of the relative gene expression, and is presented in Chapter 5. However, these data will need to be confirmed by reanalysis of the cDNA using a qPCR protocol which incorporates the proposed changes.

5

DEVELOPMENT OF A PROTOCOL FOR RNA INTERFERENCE-INDUCED KNOCKDOWN OF GRK5 EXPRESSION IN HEK293 CELLS

5.1 INTRODUCTION

The original aim of this research was examine the role of GRK5 in desensitisation of the V1bR to AVP, having first established the methods to achieve this. Over-expression studies have previously been used to investigate the role of GRKs in cell signalling (for example Gaudreau *et al.*, 2002; Menard *et al.*, 1996). This involves transfecting intact cells with homologous cDNA to induce the expression of the protein of interest at a level dramatically higher than seen endogenously. However over-expression of a protein can result in artefactual protein-protein interactions that do not occur when the target protein is expressed at endogenous levels. This is particularly problematic when dealing with proteins such as GRKs which have a degree of functional redundancy, and as a consequence can act in a compensatory manner under such conditions (Violin *et al.*, 2006). Furthermore the presence of both endogenously expressed and transfected GRKs can complicate the interpretation of results. A more physiologically relevant approach is to determine the effect of removing the target protein from the system. There are a number of experimental approaches that can be used to selectively induce a loss-of-function effect, by a) reducing the activity of the target protein, or b) reducing its expression (Nature Cell Biology Editorial, 2003).

Previous research in the Mason laboratory used pharmacological agents to investigate the role of various proteins and cellular processes in V1bR desensitisation, by measuring the effect on receptor responsiveness of altering their levels of activity (Hassan & Mason, 2005).

Historically heparin, Zn^{2+}, and mastoparan have been used to inhibit GRK function. However all three have off-target effects which may affect GPCR signalling (Hasbi *et al.*, 1998; Higashijima *et al.*, 1988; Kobayashi *et al.*, 1989). Recently, a new generation of GRK-targeted pharmacological inhibitors have been identified. Some are reported to be specific for GRK2 (Hull *et al.*, 2010; Iino *et al.*, 2002; Thal *et al.*, 2011), though the specificity testing performed has been largely limited to computer modelling and inhibitory tests against PKA. Short peptide GRK-inhibitors have also been developed (Winstel *et al.*, 2005), and are highly selective for GRKs compared with PKA and PKC. They showed no inhibitory effect on the activity of these kinases when used at concentrations that were 100-fold higher than their K_m values for GRKs. However these peptides were shown to have only modest selectivity between GRK isoforms (Winstel *et al.*, 2005). As there are currently no GRK5-specific inhibitors available, an alternative approach was required for this research.

There are a number of methods available with which protein knockdown, (i.e. reduced expression) or knockout (i.e. no expression) can be induced (Dykxhoorn & Lieberman, 2005). GRK5-knockout animals (generated using recombination techniques) have been used by others to investigate the role of GRK5 *in vivo*, by examining the behaviour, physiology, and/or tissues of GRK5-knockout animals compared with wild type animals (Fong *et al.*, 2002; Gainetdinov *et al.*, 1999; Li *et al.*, 2009; Suo *et al.*, 2007; Tarrant *et al.*, 2008). Primary cell cultures can also be prepared from knockout animals, and compared to equivalent cultures from wild type animals, allowing the role of the protein in the signalling of a particular cell type to be examined (Tanoue *et al.*, 2004). However, knockout mutants are time consuming and expensive to produce, and represent a complex system in which the knockdown of the target protein occurs in all tissues.

Knockdown of GRKs has previously been achieved using specific antibodies (Dhami *et al.*, 2002), antisense oligonucleotides (Nagayama *et al.*, 1996), and RNAi (Ren *et al.*, 2005). RNAi is the preferred methodology for loss-of-function experiments as the development of the specific and effective interfering agent is relatively efficient (Nature Cell Biology Editorial, 2003). RNAi is a homology-dependant silencing system found in all eukaryotes (Agrawal *et al.*, 2003) that can be exploited to induce post-transcriptional silencing of specific genes (Fire *et al.*, 1998). The introduction or expression of small double stranded interfering RNAs

(siRNAs) homologous to the target gene mRNA sequence results in knockdown of the expression of that gene at the protein level, by guiding the destruction of its mRNA before translation occurs (Cullen, 2006).

As RNAi-mediated knockdown is based on homology between nucleic acids, it can be targeted against a sequence unique to the target protein therefore giving it the potential to be more specific than pharmacological inhibitors. Furthermore, RNAi can be used in a simple system (such as an immortal cell line) with relative ease compared to the preparation of knockout animals (Agrawal *et al.*, 2003). However, RNAi has its drawbacks with the potential for off-target effects (Jackson *et al.*, 2003), toxic phenotypes (Fedorov *et al.*, 2006) and induction of the interferon-response (Bridge *et al.*, 2003). Proper validation of the knockdown protocol can minimise these undesirable effects and is discussed in Section 5.3.

Since its inception as a research tool, RNAi has been used extensively to investigate the function of GRKs and other components of GPCR-related signalling pathways (for example: Ahn *et al.*, 2003; Chen *et al.*, 2009; Kim *et al.*, 2005; Premont *et al.*, 1996; Rajagopal *et al.*, 2006; Ren *et al.*, 2005; Shenoy *et al.*, 2009; Violin *et al.*, 2008; Zidar *et al.*, 2009).

5.1.1 Mechanism of RNA interference

RNAi is thought to be an ancient antiviral immune response present in all known eukaryotes. The eukaryotic genome consists of double stranded DNA (dsDNA), of which one strand is transcribed to single stranded RNA and translated to protein. The partner strand acts as a ‘back up’ copy, allowing the accurate repair of damage to the active strand (Wadhwa *et al.*, 2004). Most RNA viruses induce the production of long dsRNA by a cell as part of their replication cycle. In the event of such a viral challenge, the production of long dsRNA triggers RNAi-mediated degradation of RNA with sequence homology to the infecting duplex, resulting in the silencing of genes that may be harmful to the host organism (Cullen, 2006). In mammals it appears that RNAi has been replaced as the primary anti-viral defence mechanism by the interferon response, in which long dsRNA (among other stimuli) induce non-specific RNA degradation, global inhibition of translation, and finally apoptosis (Cullen, 2006; Dykxhoorn *et*

al., 2003). As such, experimental activation of the RNAi pathway with dsRNA longer than 30 nucleotides (used with high efficiency in plants and invertebrates) has limited applicability for work in mammalian cells (Cullen, 2006; Dykxhoorn *et al.*, 2003). Investigations into the mechanism of RNAi in *Caenorhabditis elegans* (Grishok *et al.*, 2000) and *Drosophila melanogaster* (Elbashir *et al.*, 2001; Hammond *et al.*, 2000; Parrish *et al.*, 2000; Yang *et al.*, 2000; Zamore *et al.*, 2000) have demonstrated that enzymatic-cleavage of the long dsRNA into 5' phosphorylated short interfering dsRNAs (siRNAs) by the RNase Dicer is required for homologous silencing, indicating that siRNA are the molecules which induce target knockdown.

While there are several methods of RNAi delivery available (reviewed in Shim & Kwon, 2010), transient transfection with synthetic siRNAs is the preferred method for inducing transient RNAi-mediated knockdown in mammalian cells, as siRNAs are less likely to induce the interferon response and they immediately initiate efficient and potent silencing (Dykxhoorn *et al.*, 2003). For these reasons, transient transfection with synthetic siRNAs was the chosen method for this research. The mechanism of RNAi-mediated silencing induced by transfection of cells with synthetic siRNA is shown schematically in Figure 5.1 and described below.

The short synthetic siRNAs are transfected into the cell with the aid of a liposomal carrier molecule. siRNAs initiate silencing of a gene via the 'classical' mechanism of RNA as follows; once in the cytoplasm, the siRNA interacts with the RNA-induced silencing complex (RISC). This activates RISC which proceeds to unwind the sense and antisense strands of the siRNA. The sense strand dissociates, leaving the antisense strand bound to RISC. Here it acts as a guide, using base pairing to target RISC to mRNA with which it has sequence homology. RISC interacts directly with the mRNA, resulting in mRNA cleavage.

The protocol used in this research to induce RNAi-mediated knockdown of GRK5 expression is provided in Section 5.2. The development and validation of this protocol is described in Section 5.3.

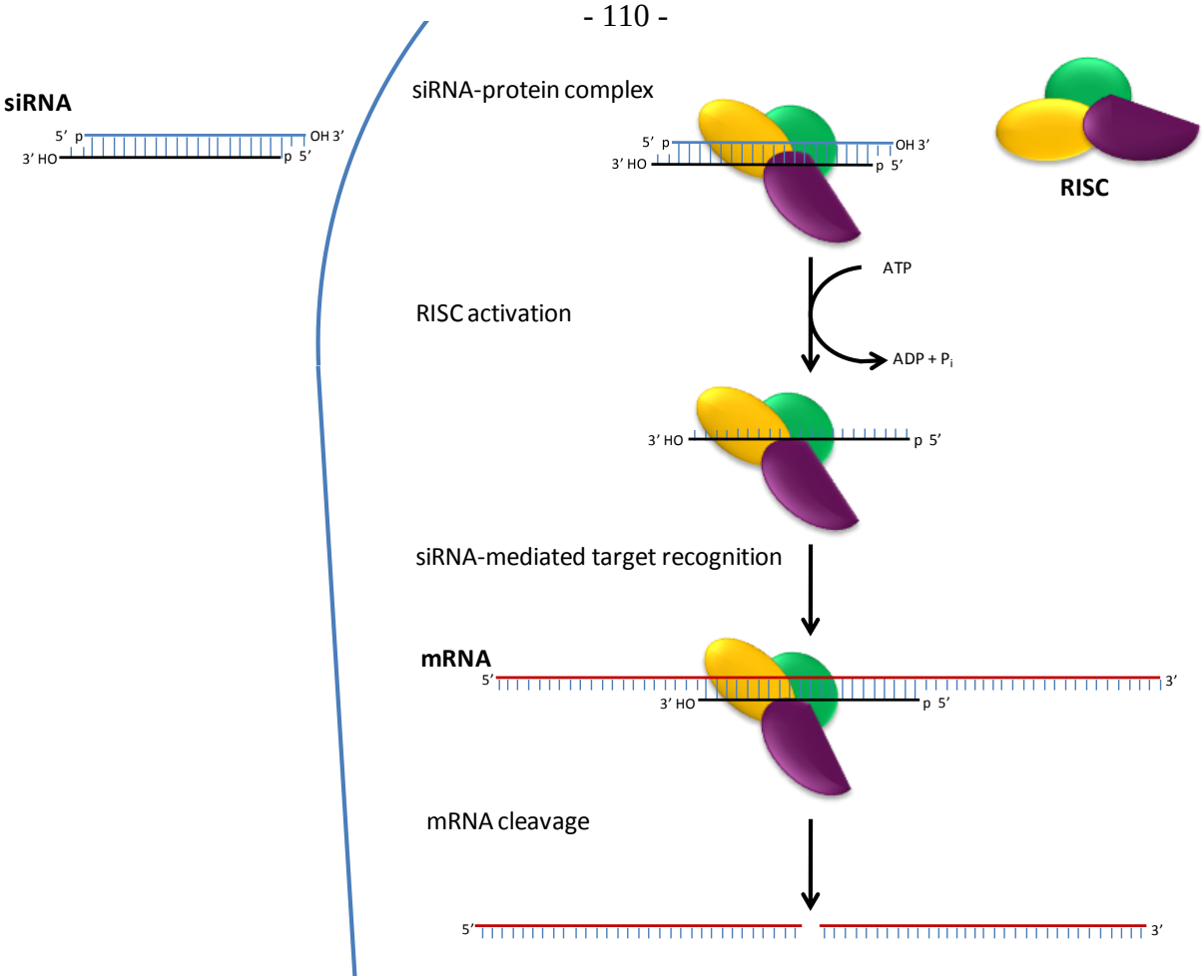

Figure 5.1 Mechanism of RNAi-induced degradation of target mRNA. Synthetic siRNAs are transfected into the cytoplasm leading to RISC assembly. RISC unwinds the siRNA duplex exposing the antisense sequence. This sequence then targets RISC to mRNA with which it has sequence homology, resulting in RISC-catalysed mRNA cleavage.

5.2 METHODS AND MATERIALS

5.2.1 Materials

For source information regarding materials referred to in this Chapter, refer to Appendix A.

5.2.2 Solutions and media

For details of the solutions and media referred to in this Chapter, refer to Appendix B.

5.2.3 Handling of siRNA

As nucleic acids, siRNA duplexes are susceptible to degradation by nucleases. To maintain nuclease-free conditions, the measures described in Section 4.2.3 were also taken when handling siRNA. The duplexes were used to transfect HEK293 cell cultures. For this reason all handling of the siRNA duplexes and associated buffers and media was performed in a Laminar flowhood or Biohazard containment hood, with sterile RNase-free consumables to ensure that sterility was maintained.

5.2.4 siRNA details

All siRNA were obtained from Dharmacon, and provided as 2'hydroxyl, annealed, and desalted duplexes (see Table 5.1 for sequence and details). The sequence for the GRK5-targeted siRNA was obtained from Ren et al, (2005) and custom manufactured.

	GRK5-Targeted siRNA
Sequence	5'-GCCGUGCAAAGAACUCUUU-3'
Length	21bp
Molecular Weight	13,300.2 g/mol
Extinction coefficient	361,162 L/mol·com

Table 5.1 GRK5-targeted siRNA duplex details

5.2.5 Resuspension of siRNA

Resuspension of the siRNA duplexes was performed according to the manufacturer's instructions. The duplexes were resuspended to give a 20µM stock solution using the following procedure. The tube containing the siRNA was spun briefly to collect the duplexes. 5X siRNA buffer (Dharmacon) was diluted 1X and the appropriate volume was added to the tube. The solution mixed by repipetting gently five times with a Gilson P1000 pipette. Care was taken not to introduce bubbles into the solution. The siRNA/buffer mix was incubated at room temperature for 30 minutes on an orbital shaker, set to 80+ rotations per minute. The tube was then spun briefly to collect the solution and a small aliquot taken to determine its concentration

using Nanodrop UV spectroscopy with 1X siRNA buffer was used as a blank. The A260nm was recorded and used to calculate the actual concentration of the duplex solution using the following equation;

Equation 5.1

$$[(A260nm \times 40) / MW] \times 1000 = \mu M$$

The solution was then aliquoted into 0.6mL microtubes, to avoid repeated freeze/thaws (which can damage the siRNA) and stored at -80^{o}C.

5.2.6 Plating and reverse transfection of HEK293 cells with siRNA duplexes

Reverse transfection of HEK293 cells with GRK-targeted was performed at the time of plating. The transfection complex was prepared as a master mix (allowing for an additional 10% in volume), and was added to each well/plate immediately before addition of the cells.

Cells destined for qRT-PCR analysis were plated into 24-well NUNC culture plates, with an n value of 2 wells per treatment at a density of 15,000 cells per cm^2. Cells destined for Western blotting analysis were plated into 35mm-diameter culture dishes, with an n value of 1 dish per treatment at a density of 15,000 cells per cm^2. The plating volumes used were 500µL per well of a 24-well plate, and 2.5mL per 35mm-diameter dish. Medium controls, consisting of MEM-, were run in all experiments.
The relative timing of each part of the protocol is shown in Figure 5.2

5.2.6.1 Preparation of medium controls, and dilution of siRNA

This section of the protocol was performed immediately prior to passaging the cells.

Medium controls were aliquoted as appropriate into the culture plates in the following volumes; 100µL per well of a 24-well plate, and 500µL per 35mm-diameter dish. GRK5-

targeted siRNA was diluted with MEM in 1.7mL microtubes to a concentration of 10nM, and kept at room temperature until use.

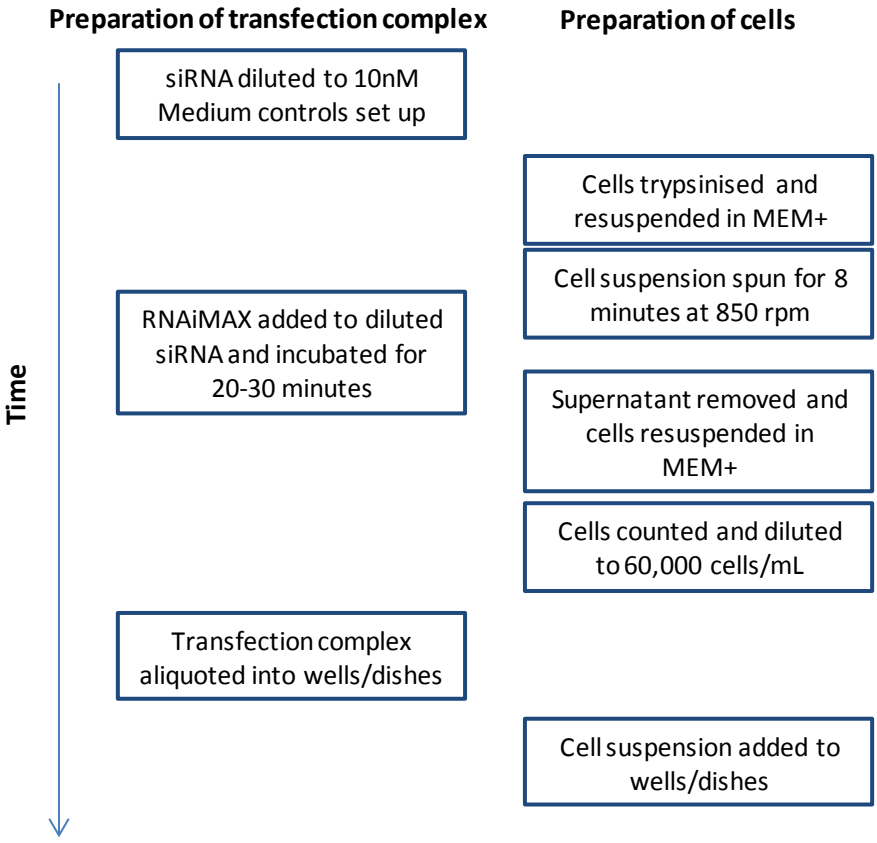

Figure 5.2 Flow-diagram showing the relative timing of steps in the transfection of HEK293 cells with siRNA.

5.2.6.2 Preparation of the transfection complex and cells, and reverse transfection

Preparation of the transfection complex and HEK293 cells was performed simultaneously. Cell passaging was performed as described in Section 2.4.1.2, unless otherwise specified. Relative volumes for transfection complex components are given in Table 5.2.

	Reagent quantity	
Reagent	**per well of 24 well plate**	**per 35mm-diameter dish**
10nM siRNA (diluted in MEM)	100µL	500µL
Lipofectamine™ RNAiMAX	0.5µL	2.5µL

Table 5.2 Relative volumes of RNAi transfection complex components.

The cells were trypsinised and the resulting cell suspension transferred to a 50mL centrifuge tube, which was spun at 850rpm for 8 minutes to pellet the cells. Towards the end of the spin, the transfection reagent Lipofectamine™ RNAiMAX (RNAiMAX) was added to the diluted siRNA at a ratio of 0.5µL RNAiMAX per 100µL. RNAi MAX is a liposomal carrier molecule which enables the siRNA to enter the cell. The solutions were mixed by tapping the tube and then incubated at room temperature for 20-30 minutes. On completion of the cell pelleting spin, the medium was carefully removed from the cell pellet via vacuum aspiration, and the tube tapped vigorously to spread the pellet up the side. The cells were then resuspended in 3mL of MEM+, and a 50µL aliquot taken for counting. The cell suspension was then diluted to give an appropriate volume at 60,000 cells per mL. The transfection complexes were then added to the wells/dishes (100µL per well of a 24-well plate, 500µL per 35mm-diameter dish) followed by the appropriate volume of cell suspension, which was added to the centre of each well/dish (500µL per well of a 24-well plate, 2.5mL per 35mm-diameter dish). The cells were incubated at 37^{o}C in a CO_2 incubator.

5.2.7 Analysis of GRK5 expression

Extraction of whole cell protein was performed 60-96 hours after siRNA transfection. Cells were 60-100% confluent at this time point. The protein was extracted and the expression of GRK5 protein analysed using the Western blotting protocols described in Section 3.2. Extraction of RNA was performed 24-72 hours after siRNA transfection. Cells were ~40-90% confluent at this time point. RNA was extracted and GRK5 mRNA expression levels analysed using the qRT-PCR protocols described in Section 4.2.

5.3 DEVELOPMENT OF AN RNA INTERFERENCE PROTOCOL FOR THE KNOCKDOWN OF GRK5 EXPRESSION IN HEK293 CELLS

It is becoming increasingly clear that the mechanisms responsible for siRNA-mediated homologous silencing are complex and incompletely defined. As such, careful experimental design, the use of appropriate controls and protocol validation are crucial for accurate use of RNAi. In 2003, Nature Cell Biology published an editorial outlining the basic methodological requirements and recommendations for publishing the results of experiments using RNAi (Nature Cell Biology Editorial, 2003). These requirements and other important methodological considerations are described below.

5.3.1 Important methodological considerations for RNA interference experiments

5.3.1.1 Ensuring specificity: minimizing off-target and non-specific effects

Careful siRNA design is essential for accurate use of RNAi. There is potential for siRNA to induce both off-target, and non-specific effects. Off-target effects, in which the siRNA interact with non-target miRNAs based on sequence homology, can be minimised by careful selection of the siRNA sequence to ensure it is unique to the target gene. This can be assessed by using BLAST to search the sequence against the appropriate NCBI databases. siRNA have also been shown to be capable of inducing a variety of non-specific effects, such as cytotoxic phenotypes (Fedorov *et al.*, 2006) and the interferon response (Sledz *et al.*, 2003). Titration of the siRNA is recommended to minimise the potential for the induction of non-specific effects (Nature Cell Biology Editorial, 2003). In their 2003 paper documenting induction of interferon stimulated genes by siRNAs, Sledz and colleagues noted that for some interferon stimulated genes, this effect was concentration dependant (Sledz *et al.*, 2003). The ability of many siRNAs to induce effective knockdown at very low concentrations, coupled with the fact that the RISC assembly is saturable under some conditions (Cuccato *et al.*, 2011), makes titration prudent for both experimental and economic reasons.

5.3.1.2 Assessing knockdown

siRNA have been shown to be capable of acting as micro RNA (miRNA) by binding imperfectly to mRNA (Doench *et al.*, 2003). Unlike classical siRNA-mediated silencing in which mRNA is degraded, miRNA-mediated silencing produces gene silencing by inhibiting translation of the mRNA to protein (Dykxhoorn & Lieberman, 2005). To ensure that the siRNA are acting via the classical pathway, it is recommended that the effect of siRNA-transfection on expression is assessed by measuring both the protein and mRNA (Nature Cell Biology Editorial, 2003).

5.3.1.3 Use of appropriate siRNA controls

Further confidence that the phenotype produced by a siRNA is caused by selective silencing of the target gene can be gained by use of a 'multiplicity' control, i.e. a second siRNA targeting a different section of the same mRNA (Nature Cell Biology Editorial, 2003). While siRNAs for the same gene can have very different efficiencies, this control is useful to confirm results. Non-targeting (NT) siRNA are sometimes used as a control. However, these are thought by some to be an uninformative control as they are often too different from the targeting siRNA (Nature Cell Biology Editorial, 2003). Demonstration that the 'rescue' of expression of the target gene by plasmid mediated-expression of the siRNA-targeted mRNA results in the reversal of the knockdown phenotype is considered to be the best control currently available (Nature Cell Biology Editorial, 2003). However as this is a considerable undertaking in itself, it is not considered to be essential for publication, provided that the siRNA has been titrated and the mechanism of knockdown confirmed as classical siRNA-mediated RNAi (Nature Cell Biology Editorial, 2003)

5.3.2 Development of a protocol for inducing siRNA mediated GRK5 knockdown

5.3.2.1 Selection of GRK5-targetd siRNA

An siRNA duplex used successfully by Ren et al. (2005) to achieve a high level of protein knockdown (>95%) was selected for use as the GRK5-targeting duplex for this research (details in Table 5.1). To confirm specificity of the duplex sequence for GRK5, BLAST was used to search the siRNA sequence against the NCBI Transcript Reference database (organism limited to *Homo sapiens*). The siRNA was found to have 100% homology to the human GRK5 mRNA transcript (NM_005308.2), and an E value for this interaction of 0.002. The most likely off-target interaction had a homology of 73%, and an E value of 1.6. This indicates that the GRK5-siRNA target sequence is unlikely to interact with other mRNA sequences. However, as the sequence had partial homology to other genes, it is possible that it may induce silencing via miRNA-mediated effects.

5.3.2.2 Titration of GRK5-targeted siRNA concentration

As described in Section 5.3.1.1, it is recommended that the lowest possible concentration of siRNA be used to minimise the potential for off-target effects. To determine the lowest concentration of siRNA which could be used without compromising maximum knockdown, a titration experiment was done. To determine if the measured knockdown was occurring via the classical mechanism of RNAi, the GRK5 mRNA levels were measured by qRT-PCR.

5.3.2.2.1 Generation of a titration curve for GRK5-targeted siRNA

Knockdown was induced as described in Section 5.2.6, with the following exceptions: the GRK siRNA was diluted to 1, 5, 10 and 50nM in MEM. Two wells of a 24 well plate were transfected per solution. A medium control, or ‘0nM siRNA’, consisting of 100µL of MEM-

was also run. Wells were supplemented by the addition of 500µL of MEM+ per well 24 hours after plating. RNA was extracted 48 hours after transfection for qPCR-based analysis (as described in Section 4.2.). The expression data from each concentration was compared to that of cells which received the control treatment (0nM).

5.3.2.2.2 Results

qRT-PCR analysis indicated that the GRK5 siRNA-targeted duplex produced GRK5 mRNA-degradation in a dose-dependant manner, as shown in Figure 5.3. Concentrations as low as 1nM were seen to cause a measurable decrease in GRK5 mRNA levels (56.8% knockdown). Increasing the siRNA concentration resulted in an increase in knockdown, up to a concentration of 5nM (72.7% knockdown). No difference was seen in knockdown produced by the use of concentrations from 5nM to 50nM siRNA. No difference in cell confluence or morphology was seen between treatments. The siRNA-dependant decrease in GRK5 mRNA also indicates that the knockdown is occurring via the classical siRNA-mediated pathway, rather than the miRNA-mediated inhibition of translation. To ensure that this trend was also seen in the expression of GRK5 protein 35mm-diameter dishes were then transfected with 0, 5,

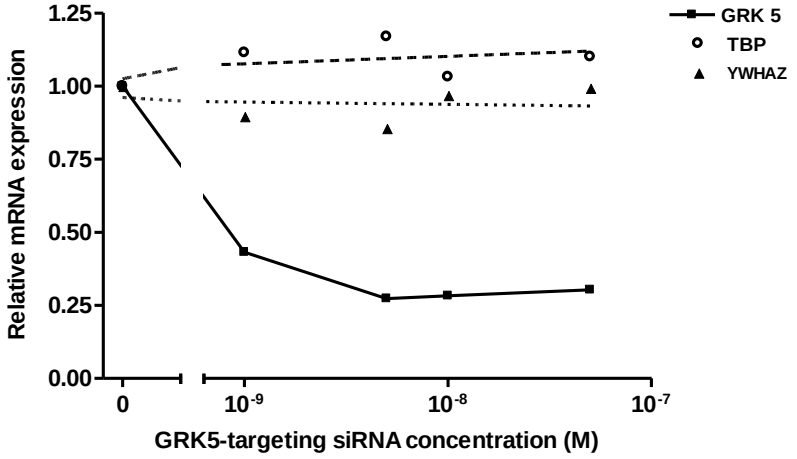

Figure 5.3 Titration curve showing the effect of increasing the GRK5-targeting siRNA concentration on the expression of GRK5. HEK293 cells were transfected with increasing concentrations of GRK5-targeted siRNA duplexes, and the resulting knockdown quantified using qRT-PCR and expressed relative to TBP and YWHAZ (n=1).

or 10nM GRK5-targeting siRNA and the relative expression of GRK5 assessed using Western blotting. This showed that 10nM siRNA was inducing measurably greater knockdown than 5nM siRNA (~50% vs. ~25%) at the protein level (data not shown).

5.3.2.2.3 Conclusion

The titration curve suggested that 5nM siRNA is the optimal concentration for KD of GRK5 using the current GRK5 targeted duplex, as it was the lowest concentration seen to produce the maximal response. However, comparison of the effect of 10nM and 5nM on GRK5 protein expression indicated that 10nM was inducing greater knockdown. As such, a siRNA concentration of 10nM was used for subsequent experiments.

5.3.2.3 Selection of a time point for assay for the effect of GRK5 knockdown on desensitisation: Time course of protein knockdown

To select a time point suitable for performing the desensitisation assay (i.e. at which the protein was maximally knockdown), it was necessary to determine the time course of GRK5 protein knockdown. This was done was transfecting multiple dishes of cells and staggering the time of cell lysis.

5.3.2.3.1 Generation of time course

Four 35mm-diameter dishes were plated with HEK293 cells and reverse transfected with the GRK5-targeted siRNA diluted to 10nM, and as described in Section 5.2.6. In addition, a medium control was also plated and lysed at 72 hours. The transfected cells were lysed via the standard protocol in Section 3.2.3 at the following time points: 60, 72, 84 and 96 hours following transfection. Cells to be lysed at 84 and 96 hours were passaged at 72 hours to prevent them from becoming over-confluent. For passaging, the medium was removed from the dish by vacuum aspiration and replaced with 800µL of T/E. The plates were tilted to ensure that the cells were covered with T/E, and the excess T/E aspirated. The dishes were placed on the microscope stage for 8 minutes, at which time the cells could be seen to have dissociated

from each other and the surface of the dish. The cells in each dish were then resuspended by the addition of 1mL of pre-warmed MEM+, and the cell suspension was repipetted 4 times, flushing the dish with each ejection. The cell suspension from each dish was transferred to a 50mL falcon containing 3mL pre-warmed MEM+. The base of each dish was then washed a second time with another 1mL aliquot of pre-warmed MEM+. This was then pooled with the first aliquot from that dish. Each cell suspension was swirled to mix and was split between two new 35mm-diameter dishes which were incubated at 37^{o}C until lysis. Following lysis the samples were analysed using the Western blotting protocol described in Section 3.2.

5.3.2.3.2 Results

The expression of GRK5 protein was substantially decreased at all time points tested (Figure 5.4). The difference between each time point however was small. The least knockdown appeared to be occurring at 60 hours, while, 72 hours produced slightly greater knockdown than the other time points. No difference in expression was seen between 84 and 96 hours. Both the expected 68kDa band, and the additional 55kDa detected with the anti-GRK5 antibody used were seen to be knocked down at all time points. This suggests that the 55kDa

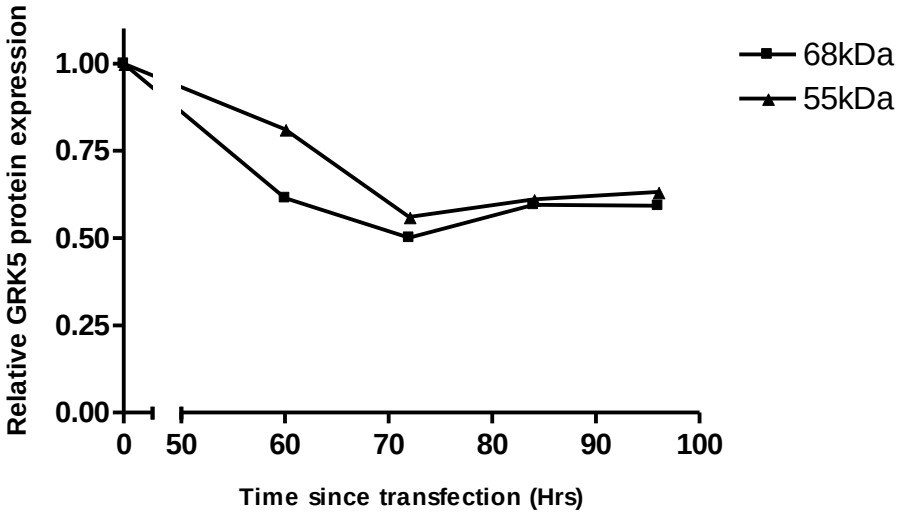

Figure 5.4 Time course showing the progression of GRK5 protein knockdown as detected using Western blotting. The intensity of bands detected at 68kDa (GRK5) and 55kDa (a potential GRK5 isoform) is plotted. Representative data is shown.

band may represent an alternative isoform of GRK5 (as proposed in Section 3.3.3.2.7.1).

5.3.2.3.3 Conclusions

From this it appears that 72 hours after transfection with GRK5-targeted siRNA is the optimal time point for the desensitisation assay to be performed. However, any time point between 72 and 96 hours could be used to similar effect, depending on the timing required by other aspects of the desensitisation protocol (see Chapter 6).

5.3.2.4 Validation of detection methods for use with knockdown protocol

Both qRT-PCR and Western blotting make use of internal controls or reference genes, relative to which GRK5 expression is normalised. As such, it is essential that in both instances the expression of the reference genes is not altered by the test treatment.

5.3.2.4.1 Validation of TBP and YWHAZ as appropriate reference genes for qRT-PCR analysis of GRK5-knockdown experiments

The effect of increasing concentrations of GRK5-targeted siRNA on the concentration of YWHAZ and TBP was assessed in the experiment described in Section 5.3.2.2.2. Linear regressions were fitted to the data to determine if reference gene expression was affected as the siRNA concentration increased. There was no evidence from this data that the test treatment alters the expression of TBP and YWHAZ. Small variation seen between concentrations was likely due to differences in sample processing (the reason for which GRK5-mRNA measurement is normalised to the reference genes), however no overall trend was seen. YWHAZ and TBP were therefore deemed to be suitable for use as reference genes during analysis of GRK5-directed RNAi experiments.

5.3.2.4.2 Validation of actin as an appropriate internal control for Western blotting analysis of GRK5-knockdown experiments

The affect of a test treatment on the expression of the internal control can be assessed by comparing the CV values from a Western blot in which both control and test protein is run with that of the a Western blot in which only untreated protein is run (Liu & Xu, 2006). If the test treatment is affecting the expression of the internal control protein, the CV from the test

Western blot will be greater than that of the control Western blot. To assess the effect of the RNAi protocol described in Section ??? on the expression of actin, the CV value was calculated for actin bands from protein treated with 0, 5 and 10nM of GRK5-targeted siRNA, and compare to the control actin CV of 8.8 ± 6.0% (mean, SEM) as calculated in Section ???. The actin CV value of the test Western blot was 6.0%. As such, there is no evidence to suggest that actin expression is being affected by siRNA treatments.

5.3.2.5 Conclusions

The RNAi protocol described in Section 5.2.6 can be successfully used to induce a knockdown in the expression of GRK5 protein. qRT-PCR analysis of GRK5-targeting siRNA-treated cells confirmed that this knockdown was proceeding via the classical siRNA-mediated degradation of GRK mRNA. Titration of the siRNA concentration determined that the optimal siRNA concentration was 10nM, as it produced maximal knockdown (~50%) of GRK5 mRNA and protein, and did not induce a cytotoxic phenotype. The extent of the protein knockdown achieved was less than that reported in the literature (Ren *et al.*, 2005), however it should be sufficient to produce a change in the magnitude of GRK5-dependent processes.

5.3.3 Selection of a non-targeting control siRNA duplex

5.3.3.1 Non-targeting siRNA details

Two non-targeting (NT) siRNA were obtained from Dharmacon and resuspended as described in Section 5.2.5. They were NT siRNA #3 (D-001210-03), and NT siRNA #1 (D-001210-01) (details in Table 5.3). The molecular weight of the non-targeting duplexes was not provided by the manufacturers. For resuspension calculations, duplex molecular weight was assumed to be 13,300g/mol (that of the average siRNA according to the Dharmacon website).

	Non-Targeting siRNA #3 (NT#3)	Non-Targeting siRNA #1 (NT#1)
Sequence	5'-AUGUAUUGGCCUGUAUUAG-3'	5'-UAGCGACUAAACACAUCAA-3'
Length	19bp	19bp
MW	~13,300 g/mol*	~13,000 g/mol*

Table 5.3 Non-targeting siRNA details * assumed weight.

5.3.3.2 *In silico* assessment of non-targeting siRNA sequences

Both non-targeting duplexes were searched against the NBCI Transcript Reference database (organism limited to *Homo sapiens*) using BLAST. For NT#1, the maximum measured homology was 68%, with an E value for this interaction of 146.0. For NT#3, the maximum measured homology was 68%, with an E value of 6.0.

5.3.3.3 Experimental assessment of non-targeting siRNA sequences

5.3.3.3.1 Protocol of experimental assessment

Non-targeting siRNA are typically used under identical conditions (of siRNA amount and transfection reagent) as the targeting-siRNA, and act as a type of control. As the GRK5-targeting siRNA was used at a concentration of 10nM, both non-targeting duplexes were trialled at this concentration. For generation of non-targeting duplex transfection complexes the RNAi protocol described in Section 5.2.6 was used, with the non-targeting duplexes substituted for GRK5-targeting siRNA. HEK293 cells were plated in to 35mm-diameter dishes and cultured for 84 hours prior to lysis.

5.3.3.3.2 Results

Use of either the NT#3 or NT#1 duplexes at 10nM resulted in a cytotoxic phenotype in ~50% of the transfections carried out (shown in Figure 5.5), leading to a marked difference in the confluence of the cells over time. Both duplexes also appeared to produce subtle changes to the morphology of the cells, making them slightly more angular (Figure 5.5). These effects were not seen in cells transfected with the GRK5-targeted siRNA at equivalent (Figure 5.5) or even higher concentrations (data not shown).

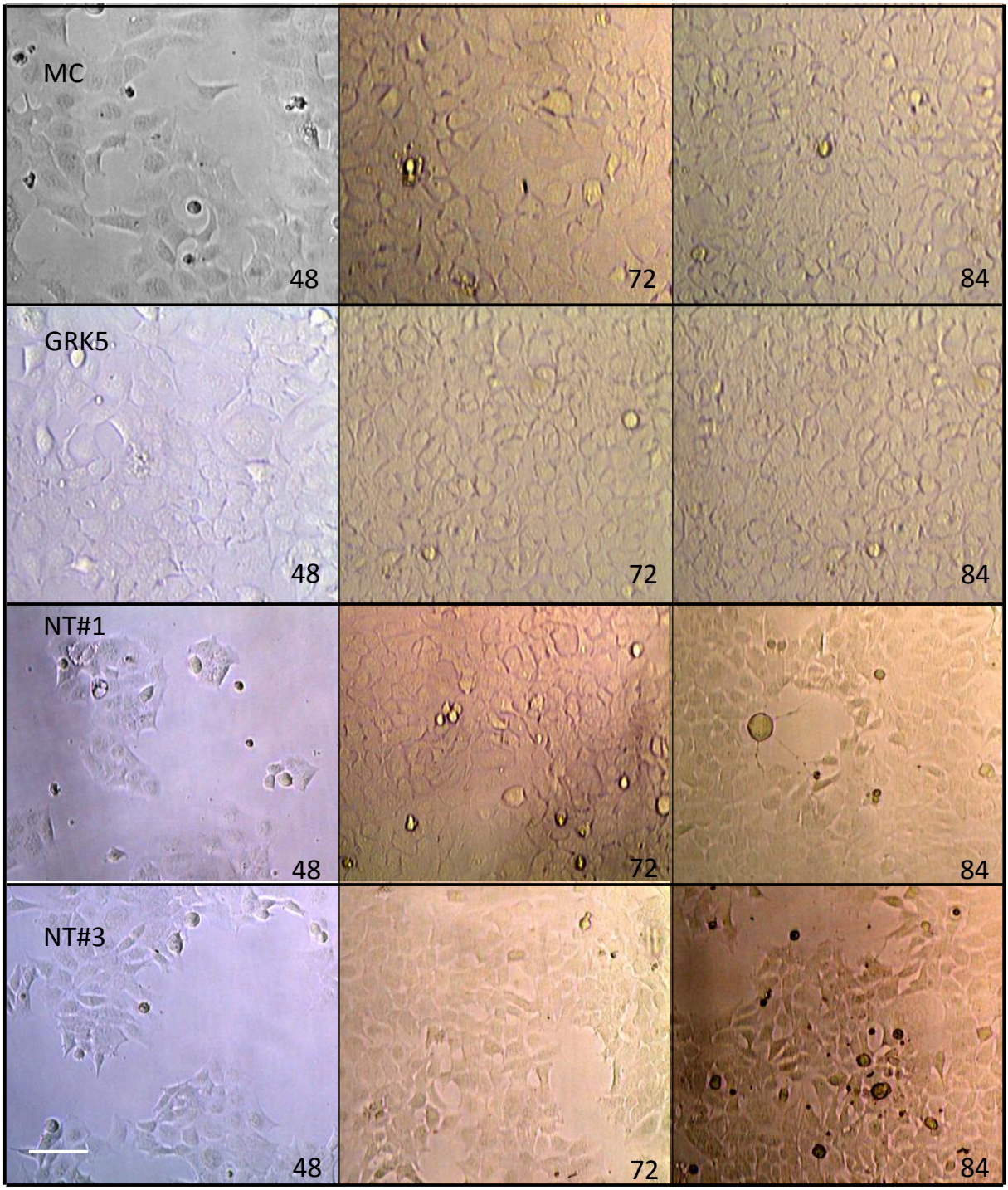
MC
48
72
84
GRK5
48
72
84
NT#1
48
72
84
NT#3
48
72
84

The effect of the non-targeting siRNA on GRK5 protein expression was also tested. Due to the inconsistency of the cytotoxic phenotype shown in Figure 5.5, the transfection complex for each non-targeting duplex was prepared in duplicate. These (along with 10nM GRK5-targeting siRNA and medium controls) were used to transfect cells from the same batch, and the protein harvested at 84 hours. Both non-targeting siRNA produced a measurable knockdown in GRK5 expression, the extent of which was not consistently replicated between transfections (Figure 5.6). This decrease is likely due to induction of non-specific mRNA degradation and/or translational inhibition rather than a specific silencing of GRK5.

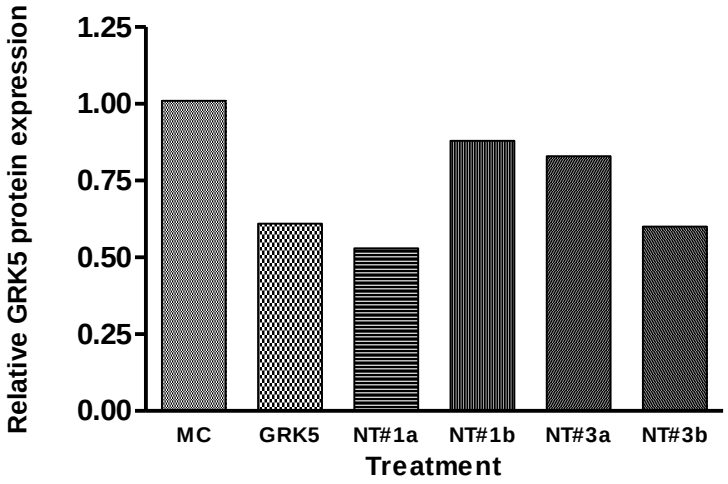

Figure 5.6 Effect of siRNA treatment on GRK5 protein expression. Due to the inconsistent effects produced by NT#1and NT#3 duplexes, two separate transfection complexes (resulting in NT#1a & b, and NT#3 a & b) were prepared identically for each duplex and used to transfect cells from the same passage.

5.3.3.4 Conclusions

Due to their induction of cytotoxic effects and possibility non-specific GRK5 protein knockdown, neither non-targeting duplex was considered to be suitable for use as a siRNA control.

6

EFFECT OF GRK5 EXPRESSION ON THE DESENSITISATION OF THE VASOPRESSIN V1b RECEPTOR: DESGIN AND VALIDATION OF AN EXPERIMENTAL PROTOCOL

6.1 INTRODUCTION

As discussed in Chapter 1, GRK5 has been linked to AVP-mediated desensitisation of the V1bR receptor. The aim of this thesis was to determine whether GRK5 is involved in desensitisation of the V1bR in response to AVP stimulation, by measuring the effect of RNAi-mediated GRK5 knockdown on the magnitude of the desensitisation achieved. The various protocols required for this experiment have already been described in detail. They are i) the generation of a model cell system by transient transfection of HEK293 cells to express the rV1bR (Chapter 2), ii) the RNAi-mediated knockdown of GRK5 mRNA and protein (Chapter 5), iii) stimulation/desensitisation of the V1b receptor (Chapter 2), iv) measurement of receptor activity by IP assay (Chapter 2), and v) confirmation of RNAi-mediated knockdown of GRK5 mRNA (Chapter 4) and protein (Chapter 3).

The purpose of this chapter is to describe an experimental design which would coordinate the use of all the protocols developed and/or described in Chapters 2, 3, 4, and 5. The compatibility of overlapping protocols was assessed (described in Section 6.3) to ensure that the functionality of each step was not compromised. In the experimental protocol described below, chronic stimulation of HEK293-rV1bR cells is used to induce desensitisation, and their response to AVP measured by IP assay. Sampling of cells after AVP stimulation for 0, 5, 15, 30 and 60 minutes allows the progression of desensitisation to be monitored. Similar

desensitisation assays have been previously reported for protease-activated receptor 1 and 2 (Paing *et al.*, 2002; Ricks & Trejo, 2009). Finally, the GRK5-targeted siRNA-mediated knockdown of GRK5 mRNA and protein in cells treated identically to those used for the desensitisation experiment is assessed using qRT-PCR and Western blotting.

6.2 MATERIALS, MEDIA AND SOLUTIONS

Details of all materials referred to in this chapter can be found in Appendix A. Details of all solutions and media referred to in this chapter can be found in Appendix B.

6.3 EXPERIMENTAL PROTOCOL FOR DETERMINATION OF THE EFFECT OF GRK5 KNOCKDOWN ON DESENSITISATION OF THE RESPONSE TO AVP

6.3.1 Overview

The proposed experimental protocol is designed to take place over six days, with a suggested 'time zero' (the time at which the plated/ siRNA-treated cells are placed in the incubator) of 10pm on day 1. This allows for at least 3 hours of preparation time before the start of the IP assay on day 5. The relative timing of each section of the experiment is shown in Figure 6.1.

6.3.2 Plating and treatment with RNAi

6.3.2.1 Plating of HEK293 cells for the desensitisation assay, qRT-PCR and Western blotting

Cells for all purposes are plated at a density of 15,000 cells per cm^2, with a plating volume of 250µL per cm^2. This equates to 30,000 cells in 500µL per well of a 24-well plate, and 150,000

cells in 2.5mL per 35mm-diameter dish. The suggested plating plan for this experiment is shown schematically in Figure 6.2 and described in detail below.

Cells to be used for the desensitisation assay and subsequent analysis by IP assay will be plated into two 24-well Primeria™ MultiWell™ culture plates (See Figure 6.2, *A*). These plates were chosen as they have been treated to promote cell adhesion. This helps to minimise cell loss during the washes and medium changes that occur during labelling and the desensitisation assay (Cummings, 2011). A total of forty wells are plated for this purpose. At the time of plating, 20 of these wells are reverse transfected with 10nM GRK-targeted siRNA, and the remaining 20 wells act as the medium control (See Section 6.3.2.2 and Figure 6.2, *A*).

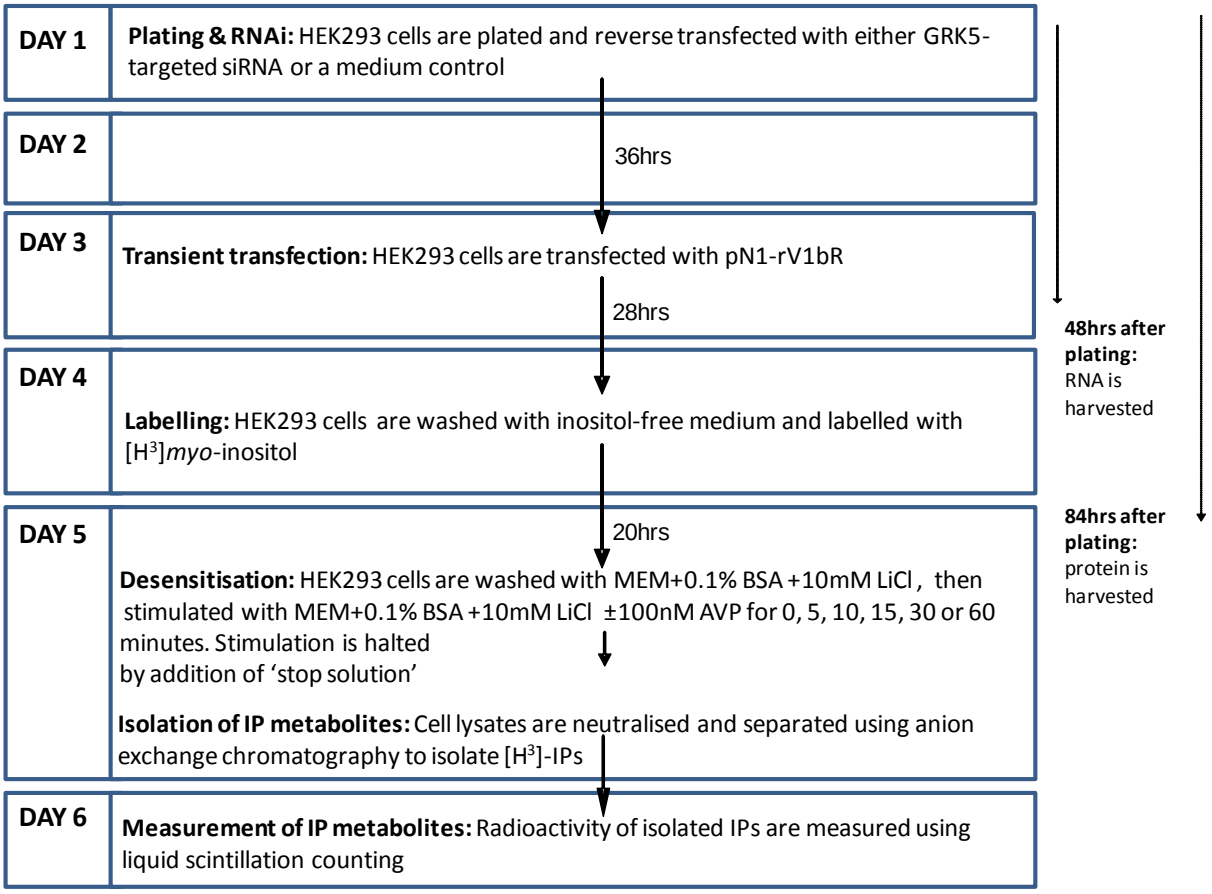

Figure 6.1 Relative timing of steps in the experimental protocol for determining the role of GRK5 in desensitisation of the V1bR

Cells used to monitor GRK5 mRNA expression are plated into standard cell culture 24-well plates (NUNC). Six wells are plated for each RNAi-treatment (see Figure 6.2, *B*). At the time of harvest, two wells are pooled per replicate, giving a final replicate number of three for each RNAi treatment. Cells to be used for Western blot analysis of GRK5 protein expression are plated into 35mm-diameter dishes (BD Falcon). Three dishes are plated for each RNAi treatment, resulting in a replicate number of three (see Figure 6.2, *C*).

6.3.2.2 RNAi treatments

RNAi-treatments are applied by reverse transfection at the time of plating. This protocol is described in detail in Section 5.2.6. Briefly, the cells receive one of two treatments; i) a medium control (shown in orange in Figure 6.2), or ii) transfection with 10nM of the GRK5-targeting siRNA duplex (shown in green in Figure 6.2). The transfection complex or medium alone is aliquoted into the appropriate wells/dishes immediately prior to addition of the cells, at a volume of 100µL per well of a 24-well plate, and 500µL per 35mm-diameter culture dish.

6.3.2.3 Confirmation of GRK5 knockdown

To confirm the siRNA-mediated knockdown of GRK5 mRNA and protein, the cells plated for this purpose are harvested. RNA is extracted from the designated cells 48 hours after plating, and changes in GRK5 mRNA levels are measured using the qRT-PCR protocols described in Section 4.2. Protein is harvested from the designated cells at 84 hours (immediately before the desensitisation assay), and changes in GRK5 protein levels are detected using the Western blotting protocols described in Section 3.2.

6.3.2.4 Transient transfection of HEK293 cells to express V1bR

The HEK293 cells destined for use in the desensitisation assay are transiently transfected with the pN1-rV1bR plasmid 36 hours after plating and reverse transfection with siRNA or medium alone. This step results in the expression of the rV1bR, allowing the HEK293 cells to acts as a model system for investigating the desensitisation of the V1b receptor. The transfection protocol is described in detail in Section 2.4.2.2. Briefly, the transfection complex is made by

mixing the pN1-rV1bR plasmid with MEM and FuGENE® 6. One hundred micolitres of the transfection complex is then be added to each well
of the 24-well Primeria™ MultiWell™ culture plates (Figure 6.2, *A*).

6.3.2.5 Labelling of the HEK293 cells with [^{3}H]-*myo*-inositol

The labelling protocol is described in detail in Section 2.4.3.1. For these experiments, the HEK293 cells are incubated in inositol-free medium spiked with [^{3}H]-*myo*-inositol for 20 hours before the desensitisation assay is performed. The radiolabelled inositol is incorporated into the IP metabolic pathway, allowing the activity of the rV1BR to be monitored by measuring the amount of [^{3}H]-IPs produced following stimulation of the cells with AVP (or exposure to the basal medium i.e. 0nM AVP. Briefly, the culture medium is removed by vacuum aspiration and replaced with 500µL of DMEM+ containing [^{3}H]-*myo*-inositol (0.25µL/mL). The cells are then returned to the incubator, and cultured for 20 hours.

6.3.2.6 Desensitisation assay

To examine the effect of reducing GRK5 expression on the progression and extent of V1bR desensitisation, cells will be stimulated with 0nM (basal) or 100nM AVP for a variety of durations, as described below (see Figure 6.2, *A*).

Following labelling, the cells are washed once with 500µL of pre-warmed MEM (containing 0.1% BSA + 10mM LiCl) to remove traces of unincorporated *myo*-[^{3}H]-inositol phosphate. Five hundred microlitres of MEM (0.1% BSA + 10mM LiCl) ±100mM AVP is then added to each well, as indicated in Figure 6.2 (*A*). The cells are incubated at 37^{o}C for the duration of the stimulation, i.e. for 0, 5, 15, 30 or 60 minutes. The desensitisation treatment is halted by the addition of 500µL of ice cold ‘stop’ solution to each well (as described in Section 2.4.3.2). The presence of LiCl in the wash and treatment solutions prevents inositol monophosphatase-mediated-degradation of IP_1 to free inositol, resulting in the accumulation of [^{3}H]-IPs produced in response to AVP stimulation.

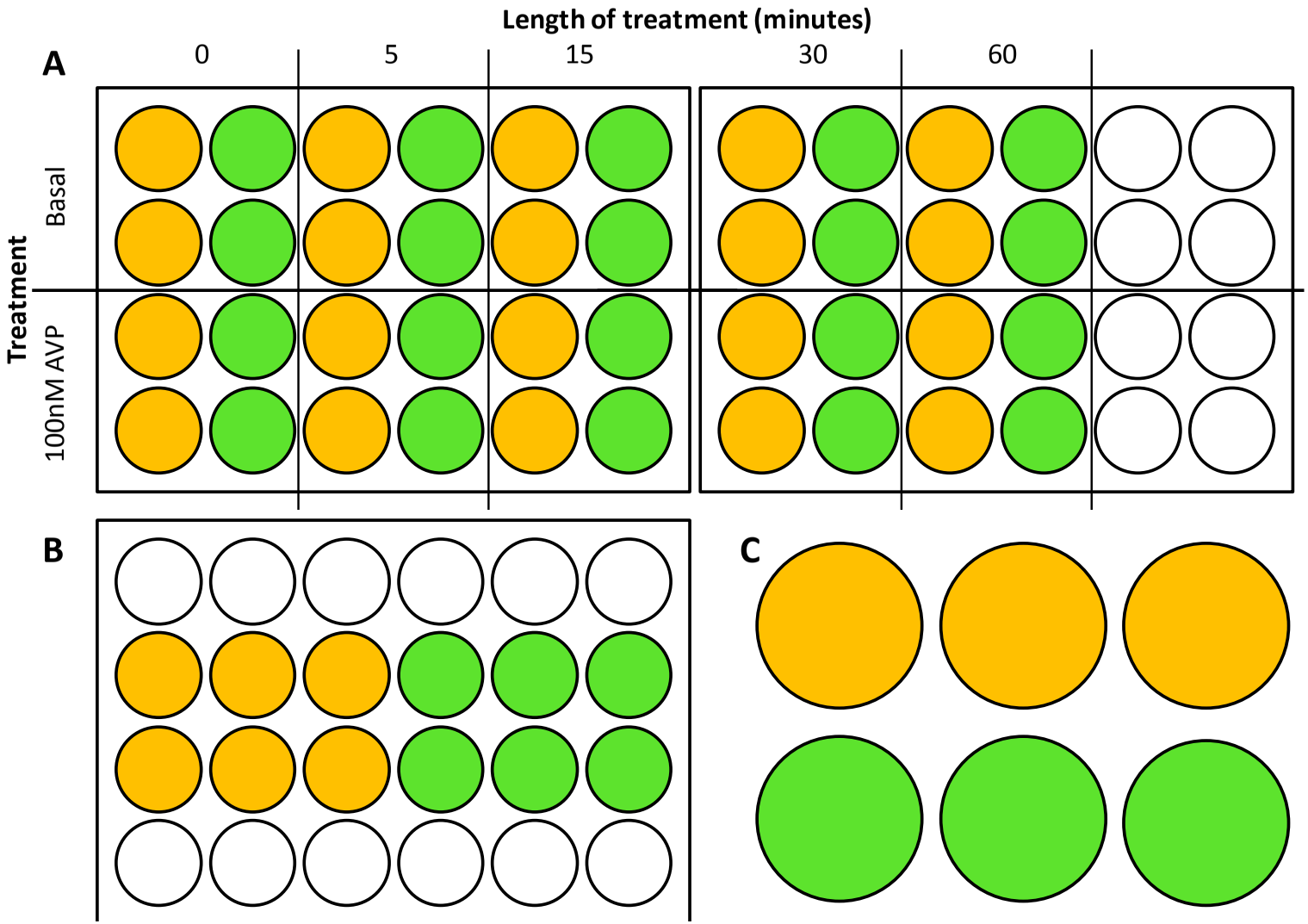

Figure 6.2 Proposed plating plan for Experimental protocol for determination of the effect of GRK5 knockdown on desensitisation of the response to AVP. Medium control treated wells are shown in orange., and wells transfected with 10nM GRK5-targeted siRNA are shown in green. *A*) plating plan for cells destined for desensitisation assay, showing the division of the wells into RNAi-treatments, basal (0nM) AVP or stimulated (100nM AVP), and duration of stimulation. *B*) Plating plan for cells destined for RNA extraction and analysis of GRK5 mRNA expression using qRT-PCR. *C*) Plating plan for cells destined for Western blotting analysis of GRK5 protein expression.

6.3.2.7 IP assay: Isolation and quantitation of the [^{3}H]-IPs by anion-exchange chromatography and liquid scintillation counting

The [^{3}H]-IPs are isolated using anion-exchange chromatography. This protocol is described in detail in Section 2.4.3.3. Briefly, 40 Bio-Rad AG1-X8-resin (formate form) columns are poured, with a bed depth of ~2cm. The cell lysates are returned to pH 7.0 by the addition of neutralisation solution, homogenised by vigorous scraping and repipetting, and loaded carefully onto a column (one sample per column). The columns are washed with 10mL of NPH_2O and 8mL of elution buffer II to elute free inositol and glycerophosphoinositides. The [^{3}H]-IPs are then eluted by washing the columns with 3mL of elution buffer VI.

To allow the amount of [^{3}H]-IPs in each elution to be measure, 1mL of each elution is mixed with 10mL of OPTIPHASE 'HISAFE' 3 scintillation cocktail (Perkin-Elmer), and left in the dark overnight. The following day, the radioactivity of the samples is determined by liquid scintillation counting (as described in Section 2.4.3.4) and expressed as CPM.

6.3.2.8 Analysis and expected results

6.3.2.8.1 Effect of GRK5-knockdown on desensitisation of the rV1bR

GraphPad Prism 4.0 is used to calculate the mean and SEM for all replicates. The mean CPM from wells stimulated with 100nM AVP will then be expressed as a percentage of the CPM of the control cells (0nM AVP; basal treatment) which is treated for the same duration (i.e. 5 minutes stimulated vs. 5 minutes basally treated). This allows the AVP-stimulated-increase in [^{3}H]-IP levels at each time point. This data can then be graphed to show the relationship between time and IP accumulation in response to AVP for the medium control (i.e. no siRNA treatment) and GRK5-targeting siRNA-treated cells.

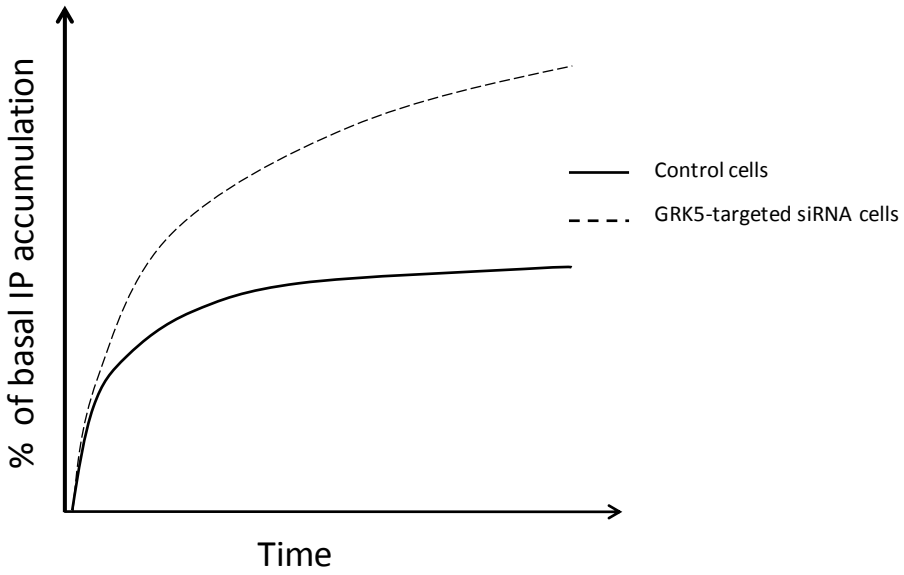

Figure 6.3 Graphical representation of the expected change in the IP accumulation profile following treatment with GRK5-targeted siRNA if GRK5 is involved in desensitisation of the V1bR. The solid line shows the predicted accumulation of [^{3}H]-IPs over time for control cells. As the receptors undergo desensitisation, they cannot activate their signalling pathway. This results in a plateau if the receptors have been completely desensitised, as no new [^{3}H]-IPs can be produced. The broken line represents the change in the IP accumulation profile predicted in GRK5-targeted siRNA-treated cells if GRK5 is involved in V1bR desensitisation. As receptor desensitisation is reduced due to reduction in GRK5 expression, receptors continue to activate the intracellular signalling pathway, resulting in the continued production of [^{3}H]-IPs.

In cells which have not been subjected to siRNA treatment (i.e. the medium only controls) stimulation with 100nM AVP is expected to cause a rapid initial increase in [^{3}H]-IP accumulation. This will occur while the rV1bR is able to respond to AVP stimulation, but once

receptor desensitisation begins, the increase in [^{3}H]-IPs is expected to taper-off, possibly reaching a plateau if rV1bR are completely desensitised.

This is depicted graphically in Figure 6.3. If V1bR desensitisation involves phosphorylation of the receptor by GRK5, the ability of the rV1bR to undergo desensitisation should be impaired in GRK5-targeted siRNA-treated cells. This would be seen as a continued increase in [^{3}H]-IP levels overtime, as the activated receptors continue to activate the PLCβ-mediated intracellular signalling pathway in response to AVP stimulation.

6.4 DEVELOPMENT OF THE EXPERIMENTAL PROTOCOL FOR DETERMINATION OF THE EFFECT OF GRK5 KNOCKDOWN ON DESENSITISATION OF THE RESPONSE TO AVP

Measures were taken to ensure that when the protocols described in Section 6.3 were used concurrently they did not affect each other in a manner that would compromise the efficiency of the individual protocols. In the experimental protocol, the HEK293 cells used for the desensitisation assay are transfected twice, the first, a reverse transfection at the time of plating with siRNA and RNAiMAX, and the second, 36 hours after plating with the pN1-rV1bR and FuGENE® 6.

The compatibility of the siRNA and pN1-rV1bR transfections was tested as follows (Sections 6.4.1-3) to ensure that:

1) The time required for siRNA-mediated knockdown of GRK5 protein was compatible with the time required after pN1-rV1bR transfection for HEK293 cells to express functional rV1bR at the cell membrane (Section 6.4.1).
2) That the presence of RNAiMAX from the siRNA-transfection does not affect the efficiency of pN1-rV1bR transfection (which would be detected as a reduction is responsiveness to AVP stimulation, and would compromise the desensitisation results) (Section 6.4.2), and
3) The transfection of GRK5-targeted siRNA-treated cells with the pN1-rV1bR/ FuGENE® 6 transfection complex did not affect the extent of GRK5 protein knockdown achieved (Section 6.4.3).

The duration of stimulation with 100nM AVP required to produce rV1bR desensitisation was also assessed, and is described in Section 6.4.4.

6.4.1 The temporal compatibility of rV1bR desensitisation with the knockdown of GRK5 protein

The time course of siRNA-mediated knockdown of GRK5 protein expression was previously determined in Section 5.3.2.3 (Figure 5.4). Knockdown was seen to be greatest at 72 hours after transfection. This margin was small however, with <10% difference seen between GRK5 expression at 72, 84 and 96 hours. It was therefore determined that any time point between 72 and 96 hours could be used for the desensitisation assay with approximately equal effect.

In the protocol for transient transfection of HEK293 cells previously used in the Mason Laboratory, the cells were plated at a density of 30,000 cells/cm^2 and transiently transfected 24 hours later, at which time their confluence ranged from 50-80%. The cells were then cultured for at least 48 hours to allow expression of the rV1bR (Cummings, 2011). The plating density used in this protocol is twice that used for the RNAi experiments (15,000 cells/cm^2). The lower plating density is necessary for the RNAi experiments as the cells need to be cultured for 72-96 hours after plating and reverse transfection, to ensure maximal knockdown of the GRK5 protein is achieved. To combine the siRNA and pN1-rV1bR transfection protocols, it was necessary to increase the time between plating and transfection with the pN1-rV1bR plasmid to 36 hours. This allowed the cells to become sufficiently confluent for V1bR-transfection (>50%) and aligned the optimal time for receptor assay (48 hours after transfection) with an acceptable time for GRK5 knockdown (84 hours after plating and reverse transfection with GRK5-targeted siRNA).

The suitability of the timing of this protocol was tested by measuring the AVP-stimulated increase in [^{3}H]-IP production over basal [^{3}H]-IP levels. The cells were plated and incubated for 36 hrs before transfection with the pN1-rV1bR. The cells were incubated for a further 28 hours, and then labelled with [^{3}H]-*myo*-inositol. Twenty hours later (84 hours after plating) the cells were stimulated with 100nM AVP for 15 minutes, and the resulting increase in [^{3}H]-IP production measured. This protocol produced a 481.5% ± 37.5% (n=2) increase in [^{3}H]-IP levels above the basal level, indicating that proposed timing of the experiment was compatible with expression of functional rV1bR.

6.4.2 The effect of RNAiMAX on the efficiency of the pN1-V1bR transfection

It was unknown how the presence of both RNAiMAX and FuGENE®6 would affect the transfection of the pN1-rV1bR. To determine if the presence of RNAiMAX impaired the transfection efficiency, the [^{3}H]-IP response above basal was compared between cells which received one of two treatments at the time of plating: either 100µL of MEM (control), or 100µL of MEM + 0.5µL RNAiMAX (RNAi 1 and 2, 'mock siRNA-transfection') (Figure 6.4). During previous use of the pN1-rV1bR the cells were plated in 500µL of MEM+. However in RNAi experiments, the 500µL of cell suspension is added to a well already containing 100µL of transfection complex or medium control, resulting in a total volume of 600µL of solution per well at the time of subsequent transient transfection with the receptor. To determine if the additional volume was affecting the efficiency of the pN1-rV1bR transfection, and if returning the volume to 500µL would improve transfection efficiency, 100µL was removed from four wells 'mock transfected' with RNAiMAX (RNAi 2).

As shown in Figure 6.4, no significant difference was detected between the [^{3}H]-IP response above basal in cells that received the medium control and cells that were 'mock transfected' with RNAiMAX. Furthermore, the difference in the volume of medium in the wells at the time

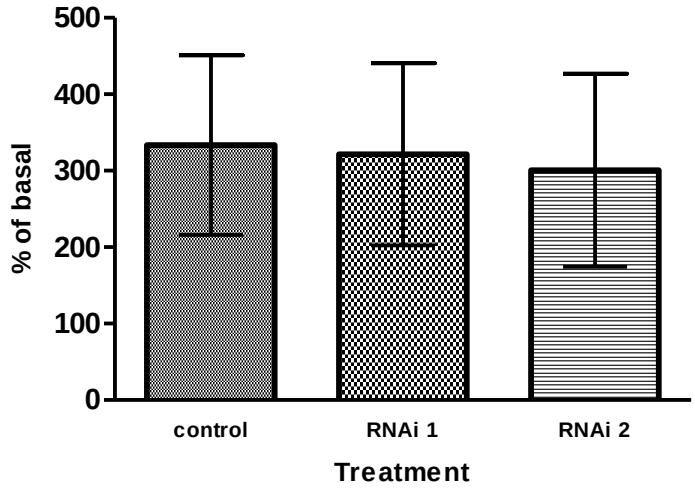

Figure 6.4 The effect of RNAiMAX and the volume of medium-per-well on the efficiency of transfection with the pN1-rv1bR plasmid. RNAi 1-treated cells were 'mock transfected' with RNAiMAX at the time of plating. There was 600µL of solution in each well at the time of transfection with the pN1-rv1bR plasmid. RNAi 2-treated cells were also 'mock transfected' with RNAiMAX. In addition, 100µL of solution was removed from the wells prior to transfection, returning the volume to that previously used. No significant difference was seen between any of the conditions trialled.

of transfection with the pN1-rV1bR plasmid did not appear to have a significant effect on transfection efficiency (Figure 6.4). This indicates that the double transfection proposed in Section 6.3 does not affect the performance of transient transfection of the HEK293 cells with the pN1-rV1bR plasmid.

6.4.3 The effect of pN1-rV1bR transfection on the extent of siRNA-mediated GRK5 protein knockdown

To determine if the subsequent transfection of GRK5-targeted siRNA-treated HEK293 cells with the pN1-rV1bR plasmid affected the extent of GRK5 protein knockdown, Western blotting was used to compare GRK5 expression under the following conditions: i) medium control (MC) (i.e. not transfected with either siRNA or pN1-rV1bR), ii) knockdown control (KC) (i.e. transfected with siRNA, but not with pN1-rV1bR), iii) RNAi 1 (i.e. transfected with GRK5 and pN1-V1bR), and iv) RNA 2 (i.e. transfected with GRK5 and 100μL of medium removed prior to transfection with pN1-V1bR) (See Figure 6.5).

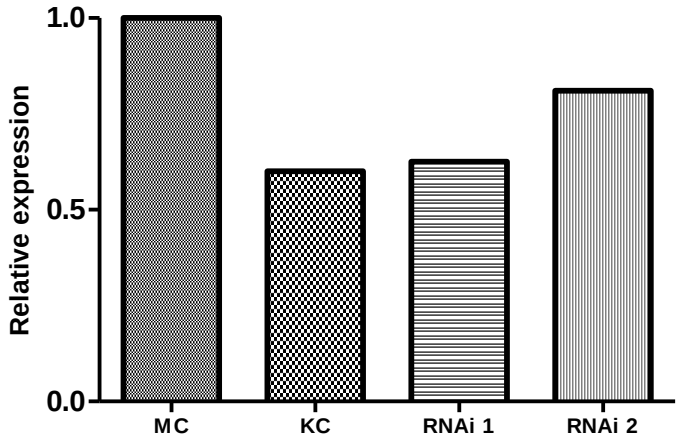

Figure 6.5 The effect of transfection conditions on the siRNA-mediated knockdown of GRK5 protein expression. Transfection of HEK293 cells with 10nM GRK5-targeted siRNA results in a significant decrease in GRK protein expression (KC) compared to its expression in medium control (MC) treated cells. Subsequent transfection of siRNA-treated cells with the pN1-rV1bR plasmid did not appear to affect the extent of GRK5 knockdown (RNAi 1), though removal of 100μL of medium from the well prior to pN1-rV1bR transfection resulted in large loss of GRK5 knockdown (RNAi 2).

A large decrease was seen in GRK5 protein expression in KC-treated cells compared to MC-treated cells. The extent of this knockdown was not affected by transfection of the cells with

pN1-rV1bR (Figure 6.5, RNAi 1). However, removal of 100µL of medium prior to pN1-rV1bR transfection resulted in a dramatic decrease (~20%) in the extent of GRK5 knockdown (Figure 6.5, RNAi 2).

This indicated that transient transfection with the pN1-rV1bR did not affect the siRNA-mediated knockdown of GRK5 protein, provided that no medium was removed from the well.

6.2.4 Time course of desensitisation: determining the duration of chronic stimulation with 100nM AVP required to achieve desensitisation

Previous studies using HEK293 cells transiently transfected with the rV1bR induced receptor desensitisation using a 5 minute pre treatment with 5nM AVP (Gatehouse, 2008). This was sufficient to reduce the responsiveness of the receptor to a subsequent 15 minute stimulation with 100nM AVP to 68.5 ± 7.9% that of cells that did not receive the pre-treatment (Gatehouse, 2008). For this research, desensitisation caused by chronic stimulation with 100nM AVP was used, as it allowed the progression of rV1bR desensitisation to be tracked over time, giving the best chance of detecting GRK-targeted siRNA-mediated effects on rV1bR responsiveness.

On two separate occasions, the time course of rV1bR desensitisation was measured by stimulating cells with 100nM AVP for 0 to 60 minutes (Figure 6.6). In both time courses performed, a rapid initial increase in [^{3}H]-IP levels was detected after 5 minutes of stimulation with 100nM AVP. No increase in [^{3}H]-IP levels were seen between 30 and 60 minutes, indicating that desensitisation was complete after 30 minutes (Figure 6.6). In both experiments, the level of measured [^{3}H]-IP levels displayed a temporary decrease between 5 and 10-20 minutes, after which the [^{3}H]-IP levels resumed accumulating. The appearance of this unexpected profile may be coincidental, caused by variation is transfection efficiency and/or cell loss during washes. However, it is possible that the decrease between 5 and 10-20 minutes was caused by incomplete inhibition of inositol monophosphatase (the enzyme which degrades IP_1 to free inositol), i.e. activation of the receptor by AVP stimulation produces an initial increase in [^{3}H]-IPs (seen as an increase between 0 and 5 minutes). The remaining active inositol monophosphatase processes [^{3}H]-IP_1 to free inositol (which is not retained by the

anion exchange system used). This results in the decrease in [^{3}H]-IPs levels seen between 5 minutes and 10 minutes. In this scenario, LiCl-mediate inhibition of inositol monophosphatase is complete after 10-20 minutes, allowing any [^{3}H]-IP produced to accumulate, resulting in the additional increase seen between 10-20 and 60 minutes. However, this scenario is contrary to evidence from previous use of IP assay in the Mason laboratory which suggested that a 2 minute exposure to LiCl during the washes was sufficient to block the breakdown of [^{3}H]-IP_1.

The following durations were chosen for AVP-stimulation treatments for the experimental protocol described in Section 6.3. They were 0, 5, 15, 30 and 60 minutes. The high frequency of time points during the initial stages of receptor activation will allow the [^{3}H]-IP accumulation to be tracked. Furthermore, these time points will serve to confirm the decrease in [3H]-IP between 5 and ~20 minutes as a biologically relevant event, or discount it as an experimental artefact. Although receptor desensitisation was seen to be complete after 30 minutes of stimulation with 100nM AVP, 60 minutes was selected as the longest duration. This was to enhance the ability of the assay to detect any differences between the desensitisation profile of controls cells, and that seen in GRK5-targeted siRNA-treated cells. If desensitisation is impaired by siRNA treatment, these cells will accumulate [3H]-IP for ~30 minutes longer that the control cells. This should insure that any change in the ability of the receptor to undergo desensitisation can be detected.

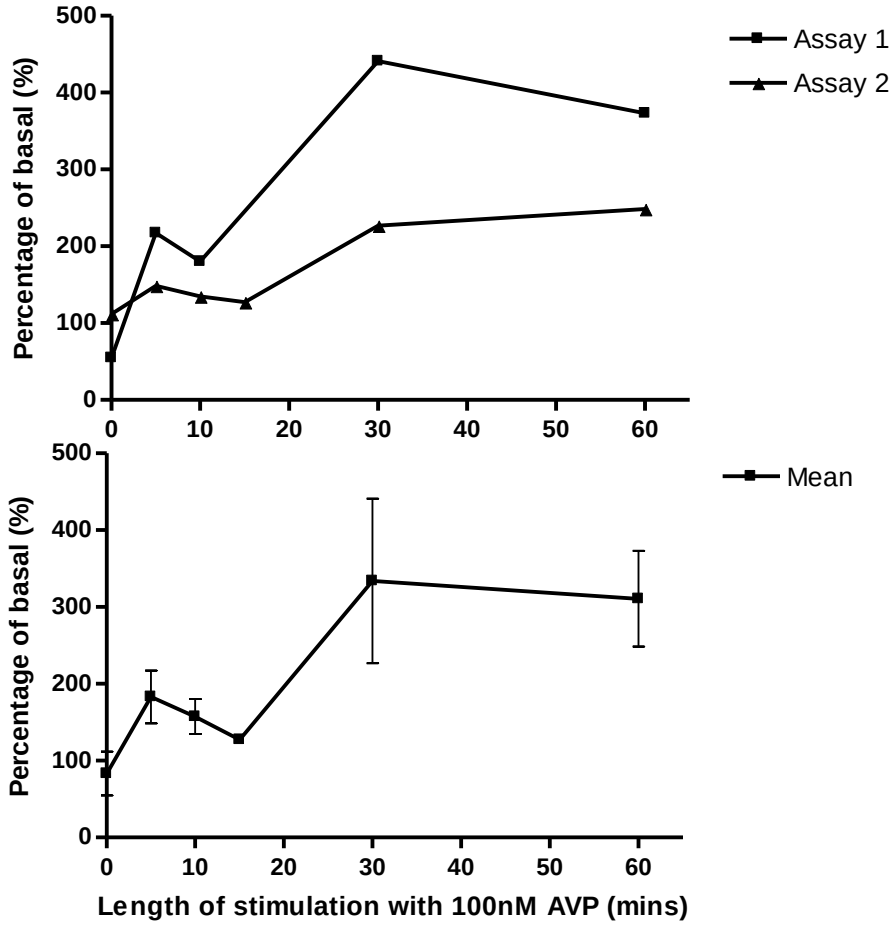

Figure 6.6 The increase in 100nM AVP-increased [^{3}H]-IP levels overtime. The desensitisation profiles produced by stimulation with 100nM AVP for 0 to 60 minutes A) plotted individually, and B) the mean (and SEM) of the two assays.

7

DISCUSSION

7.1 SUMMARY

Desensitisation of the V1bR *in vitro* may involve phosphorylation (probably of the receptor) by an unidentified kinase (Hassan & Mason, 2005). The involvement of other kinases that commonly phosphorylate GPCRs which activate the phosphoinositide pathway (PKC and CKα1) have been discounted, suggesting that GRK-mediated phosphorylation may be responsible. Previously, tentative evidence of a physical association between the V1bR and GRK5 has been reported (Berrada *et al.*, 2000), making GRK5 an isoform of particular interest. The lack of isoform specific pharmacological inhibitors for GRKs necessitated a change in methodology from that previously used by the Mason laboratory to investigate the involvement of various protein and cellular processes in V1bR desensitisation (Hassan & Mason, 2005). As such, one aim of this research was to generate and validate the methods required to determine if GRK5-mediated phosphorylation is involved in desensitisation of the V1bR to AVP stimulation.

A protocol for RNAi-mediated knockdown of GRK5 was established, to allow the effect of reduced expression of GRK5 protein to be determined in HEK293 cells transfected to transiently express the rV1bR. In this system rV1bR activity was determined by measuring the AVP-induced production of IPs. GRK5 knockdown was monitored using qRT-PCR to measure GRK5 mRNA levels, and Western blotting was used to measure GRK5 protein levels. The methodologies for both detection techniques were established as part of this research. qRT-PCR analysis of RNA extracted from cells 48 hours after treatment, showed that transfection with 10nM GRK5-targeted siRNA reduced GRK5 mRNA levels to 28.7% ± 1.9% (n=3,

$p<0.001$) of that seen in untransfected control cells. TBP and YWHAZ were used as reference genes in the qRT-PCR, and they were shown to be unaffected by the GRK5 siRNA treatment. Western blotting analysis of protein harvested 84 hours after treatment showed that the relative GRK5 protein expression in GRK5-siRNA treated cells was reduced to 53.4% ± 3.4% ($n=5$, $p<0.0005$) of that seen in untransfected control cells. Actin was used as an internal control and was shown to be unaffected by the GRK5 siRNA treatment. Finally, an experiment was designed, and partially tested, to coordinate the protocols needed to induced and measure GRK5 knockdown (siRNA transfection, qRT-PCR, and Western blotting) with the protocols required to use a model cell system (HEK293 cells transiently transfected with the pN1-rV1bR plasmid) to determine the effect of knockdown on IP-accumulation following AVP-stimulation of the V1bR system (by measuring the production of [^{3}H]-IPs in [^{3}H]-*myo*-inositol labelled cells). This protocol can be used in future to determine if GRK5 is involved in the desensitisation of rV1bR to stimulation with AVP.

7.2 COMMENTS ON METHODS USED AND OPTIMISED IN THIS RESEARCH

7.2.1 Use of HEK293 cells transiently transfected to express the rV1bR as a model cell system

The use of a model cell system, rather than the primary pituitary cell cultures used previously (Hassan *et al.*, 2003; Hassan & Mason, 2005), was necessary to allow the use of RNAi-mediated knockdown of GRK5 expression. HEK293 cells were selected as they are relatively easy to transfect (Shaw *et al.*, 2002b), and represent a homogenous cell population. Use of a cell line derived from human tissue was advantageous due the availability of siRNA duplexes and primary antibodies targeted against human GRKs. Furthermore, the availability of human genome/transcriptome information was useful during optimisation of the qRT-PCR protocol.

As with all model systems, departures from endogenous conditions can affect the ability to extrapolate data obtained using the model system to the *in vivo* situation. In investigating

GPCR signalling, it is important to remember that to some extent, the mechanisms by which the receptors signal and are regulated dependant on the cell-type and expression-level of key proteins in the pathway (Violin *et al.*, 2006). However, model cell systems enable the use of techniques (such as RNAi) which are difficult, if not impossible to use in primary cell cultures, and which provide useful insights into signalling pathways.

To generate the model system used for this research HEK293 cells were transiently transfected with the rat V1bR. The rV1bR displays high sequence homology to the human V1bR [reference] and has previously been used in the Mason laboratory. While there is potential for inter-species differences in pharmacological properties (Ventura *et al.*, 1999), rV1bR expressed both transiently (Gatehouse, 2008) and stably (Cummings, 2011) has been shown to successfully activate the human PLCβ-mediated intracellular signalling pathway. This was demonstrated by an increase in IP production in AVP-stimulated HEK293 cells transiently transfected with the rV1bR. Crucially, this increase was shown to be dependent on the expression of the rV1bR, as it did not occur in untransfected HEK293 cells (Gatehouse, 2008). rV1bR expressed in HEK293 cells was also able to interact with components of the desensitisation machinery as the responsiveness of the rV1bR to stimulation with AVP was impaired by both repeated and chronic AVP stimulation. As such, this model system fulfils the requirements needed for this research.

The use of transient transfection for inducing the expression of a protein comes with the potential for variability between transfection events. When receptors are being expressed, radioligand binding assays can be performed to assess variation in transfection efficiency, though this is a time consuming and costly process. Multiple repetitions of the experiment proposed in Chapter 6 will be required to ensure the measured effects are real.

7.2.2 Establishing, validating and optimising a Western blotting protocol for measuring the relative expression of GRK5 protein

A Western blotting protocol was established as part of this research to allow changes in the expression of GRK5 to be monitored. A protocol of immunodetection of actin was also optimised, and actin expression used as an internal control against which GRK5 expression was normalised. The Western blotting conditions were optimised by systematically altering the transfer time, blocking solution, antibody concentrations and antibody diluents. The optimised assays for GRK5 and actin were tested for sensitivity, accuracy and reproducibility. The optimised assay for actin performed well (see Section 3.3.4.3). A strong linear relationship was detected between the amount of protein present and the intensity of the actin band, as determined by linear regression of band intensity produced by serial dilution of protein (R^2= 0.9307) (Figure 3.13). Furthermore, the slope of the line detected for actin was not significantly different to that of an idealised data set (two-tailed p value = 0.409) (i.e. in which 25% less protein loaded resulting in a band 25% less intense). The actin assay was able to detect a signal when as little as 4μg of whole protein was loaded, making it very sensitive. The reproducibility of the assay was assessed by running the same amount of protein in multiple lanes, and calculating the CV (see Section 3.3.4.3.2). This was repeated 4 times, with a mean CV of 8.8 ± 4.5% (mean, SEM). This value is very similar to those previously published for β-arrestin (6.5% ± 0.9%) and β-tubulin (7.6 ± 1.4%) (Liu & Xu, 2006)

The optimised GRK5 assay was not as accurate as the actin assay (see Section 3.3.3.2.7). A linear relationship was detected between the amount of protein present and the intensity of the band measured. The R^2 value for the 'line of best fit' for the serially diluted protein was 0.8924, indicating that 89.24% of the variation seen was due to the amount of protein loaded. The p value for this slope was <0.0001, indicating there is a significant correlation between the amount of protein loaded and the intensity of the band produced (Figure 3.11). The measured slope was compared to the slope produced by the idealised data set, and as with actin, no significant difference was seen between the two slopes (two-tailed p value = 0.9559). As above, the reproducibility of the assay was assessed by calculating the CV for multiple lanes loaded with the same amount of protein (Section 3.3.3.2.7.2). In contrast to the low value obtained for actin, and the published CV values shown above, the mean CV for GRK5 was 20.6 ± 6.0% (mean, SEM, n=3).

Use of the optimised GRK5 protocol described in Section 3.2 routinely resulted in the detection of multiple additional bands. Possible explanations for the identity of these bands are discussed in detail in Section 3.3.3.2.7.1. One explanation proposed was that some of the bands seen in addition to the 68kDa one that is consistent with the putative GRK5 band, represent alternative isoforms or phosphorylation states of GRK5. Though no GRK5 isoforms have yet been positively identified in the literature, multiple isoforms of GRK4 and 6 (to which GRK5 is closely related) have been found. Furthermore, unexplained additional bands are often shown in published immunoblots against GRK5. One such band, located at ~55kDa has been proposed to be an alternative isoform of GRK5 (Jones *et al.*, 2002) This is supported by the results from the research reported here, which demonstrated a GRK5-targeted siRNA mediated decrease in both the expected 68kDa band, and the unidentified 55kDa band. However it is likely that the remaining additional bands detected are due to off-target binding of the primary GRK5 antibody.

One of the difficulties of Western blotting is that its accuracy and reliability are reliant on the use of good antibodies. The Santa Cruz primary anti-GRK5 antibody used for this research was shown to vary considerably between batches, and for this reason its use has been abandoned by some researchers when batches are of inferior quality. While the reaction conditions used in the protocol developed for this research were thoroughly optimised, the quality of the Western blotting protocol produced was limited by the quality of the primary anti-GRK5 antibody. As Western blots allow the molecular weight of the detected proteins to be measured, this protocol it is still considered to be useful for indicating the relative expression of the GRK5 68kDa band between samples, and was used successfully in the optimisation of the RNAi protocol to assess the effects of different conditions trialled. A more accurate value for relative expression could be determined via use of a standard curve of purified protein. However, practical constraints (such as gel size and inter-gel variability) make use of a standard curve difficult. Furthermore, Western blotting is a best a semi-quantitative technique, and in many cases (such as this) it is sufficient to simply show a relative decrease in target protein expression.

7.2.3 Establishing, validating and optimising a qRT-PCR protocol for measuring the relative levels of GRK5 mRNA between samples.

Primer sets for qRT-PCR were subjected to three levels of testing prior to selection. The first level, '*in silico* analysis', was used to predict both the specificity of a primer set for its target (using BLAST searches) and its potential to form secondary structures (using Beacon designer software). A second level of analysis, using PCR, was done for primer sets with low potential for undesired interactions (as determined by *in silico* analysis). PCR analysis was used to indicate how the primer sets behaved over a range of annealing temperatures. All of the primer sets tested showed high specificity, as indicated by the lack of additional bands seen when the PCR products were electrophoretically separated. Primer sets which showed little to no production of secondary structure (e.g. primer dimers), and bands of a similar intensity to those produced by the GRK5 primer sets were then selected for analysis under qRT-PCR conditions. Examination of the amplification and melt curves identified some primer sets that displayed unusual amplification characteristics and or producing secondary structures. These primer sets were discarded. Standard curves were then produced by the remaining primer sets and used to calculate the amplification efficiency for each primer set, and select a primer set for GRK5 (GRK5 RTP, efficiency= 100.5%) and primer sets for two reference gene (YWHAZ, efficiency= 87.9%, and TBP, efficiency= 91.0%)

The specificity of the primer sets was checked by comparing the actual sequence of their qRT-PCR products with the predicted sequence. The GRK5-targeted primer set (GRK5 RTP) amplified a single product identical to the predicted sequence, indicating that the primer set was appropriate for use with the current protocol. However, both of the reference gene-targeted primers sets (TBP and YWHAZ) amplified two products, one corresponding to the predicted sequence and a second short product resulting from primer-dimer formation. This result was unexpected, as careful analysis of the melt curves (which show the melting points of any amplified products) suggested the presence of only one product. It is possible that the primer-dimers were introduced during an additional PCR step used to prepare the products for ligation and cloning (by effectively diluting the concentration of qRT-PCR reagents which can interfere in downstream reactions). As suggested in Chapter 4, the specificity of the primer-template interaction (and thus, confidence in the results) could be ensured by increasing the annealing temperature used by 1^{o}C, and rerunning the standard curve protocol described in Section 4.3.2.5.2 at this annealing temperature. This is suggested for future use of the protocol, once the qRT-PCR machine is again available.

7.2.4 Establishing, validating and optimising an RNAi protocol for knockdown of GRK5 expression

An RNAi protocol for knockdown of GRK5 was developed as part of this research (Chapter 5). Use of 10nM GRK5-targeted siRNA reduced GRK5 mRNA levels (as measured by qRT-PCR) to ~25% of that seen in untransfected cells, while GRK5 protein levels (as measured by Western blotting) were reduced to ~50% that measured in untransfected cells. Titration of the GRK5-targeted siRNA indicated that no further increase in GRK5 knockdown was induced with siRNA concentrations higher than 10nM. No cytotoxic phenotype was observed at any concentration trialled (0 – 50nM). Two siRNA duplexes were obtained from Dharmacon (NT#1 and NT#3) and trialled for use as a non-targeting control. However both produced cytotoxic phenotypes when used with the GRK5-targeted siRNA transfection protocol (as would be required for their use as a control), and as such neither was deemed to be appropriate for use as a non-targeting control. Non-targeting controls are thought by some to be of limited use as they can be too different from the targeting duplex to be truly informative (Nature Cell Biology Editorial, 2003). Instead, for future validation of the results obtained with the current GRK5-targeted siRNA, it would be preferable to replicate GRK5 knockdown with a second GRK5-targeted siRNA duplexes. This could be advantageous in three ways: i) it would confirm that any functional phenotype obtained using the current duplex was indeed due to knockdown of GRK5 expression, ii) as different siRNA for the same mRNA can have very different knockdown efficiencies, it may induce GRK5 knockdown greater than that achieved with the current duplex, and, iii) the transfection protocol used for the second duplex (including siRNA concentration) could be optimised to reduce the chance of off-target effects such as cytotoxic phenotypes (which is not valid for non-targeting controls). In this thesis, HEK293 confluence and morphology was monitored during the RNAi experiments to assess the effect of the treatment on cell viability. This could in future be assessed more quantitatively using a cell viability assay such as a MTT cell proliferation assay. The ability to assess some aspects of the RNAi protocol described in Chapter 5 was prevented by the lack of availability of the Stratagene qRT-PCR machine used for this research after the February 22nd earthquake. This prevented the GRK5-targeted siRNA titration experiment from being repeated. qRT-PCR was the favoured protocol for this as it allows more accurate quantitation than Western blotting. Additionally, HEK293 cells were plated, transfected and the RNA harvested at 24, 48

and 72 hours after transfection with the intention of using this time course to select the best time point for RNA harvesting, but this experiment was unable to be completed.

The sequence of the GRK5-targeted siRNA duplex used in this research was taken from a paper by Ren et al. (2005). They reported achieving >95% knockdown of GRK5 protein with this duplex. The effect of siRNA transfection of mRNA was not examined. The extent of the reported knockdown was greater than that obtained in this research (~50%). This may be due to differences in experimental design. For example, Ren et al. (2005) plated their HEK293 cells in 100-mm dishes, and simultaneously transfected with 20ng siRNA and a receptor plasmid (using GeneSilencer from Gene Therapy Systems as a transfection reagent) when the cells reached 30-40% confluence. The cells were passaged after 48 hours and split into plates for various different assays, which were performed at least 3 days after transfection. Ren et al.(2005) assessed knockdown exclusively by Western blotting analysis. They also used the Santa Cruz antibody used in this research for immunoblotting of GRK5; however they subsequently stopped using the antibody as later batches did not produce acceptable results (correspondence with co-author Dr S. Ahn). No other details on the immunoblotting protocol used (e.g. amount of protein loaded, diluents, and antibody concentrations) for Western blotting detection of GRK5 were published.

As stated above, the level of GRK5 mRNA and protein knockdown measured following transfection with GRK5-targered siRNA differed by ~25%. This is potentially due to difference in the accuracy of the two detection methods used (i.e. qRT-PCR and Western blotting). However, as the relationship between mRNA and protein levels is complex, depending on the rates of transcription, translation and degradation of the protein, the mRNA levels are not always predictive of subsequent protein levels (Chen *et al.*, 2002). This emphasises the need to measure the expression of the target protein at the time of the functional assay.

7.3 COORDINATION OF ALL METHODOLOGIES TO DESIGN AN EXPERIMENTAL PROTOCOL FOR DETERMINING THE EFFECT OF

GRK5 KNOCKDOWN ON DESENSITISATION OF THE IP RESPONSE TO AVP

A protocol was designed that would allow the effect of GRK5 knockdown on desensitisation of the rV1bR-dependant response to AVP to be determined. It coordinated the transfection of HEK293 cells with GRK5-targeted siRNA (to knockdown GRK expression) with transfection with the pN1-rV1bR plasmid (to induce V1bR expression), and a desensitisation assay. The expression of GRK5 protein and mRNA are measured by Western blotting and qRT-PCR, respectively, while the responsiveness of the receptor is determined by measuring the AVP stimulated IP production. The proposed desensitisation assay involves stimulating HEK293 cells expressing the rV1bR with 0 or 100nM AVP for 0, 5, 15, 30 or 60 minutes, and measuring the IP accumulation over time. An increase in the IP accumulation with time in cells previously transfected with GRK5-targeting siRNA would suggest that GRK5 is involved in V1bR desensitisation. The compatibility of the two transfections was tested, by examining i) the effect of pN1-rV1bR transfection on siRNA-mediated knockdown, and ii) the effect of a mock siRNA transfection on the responsiveness of pN1-rV1bR-transfected cells to AVP. The double transfection did not appear to negatively impact the individual success of either transfection, making the combined protocol suitable for use.

The experimental design outlined in Chapter 6 only allows for duplicates of each treatment in the desensitisation assay. While replicates of three or more would be preferable, the size of the experiment is limited by the time-dependency of several of the steps. This is particularly problematic at steps which involve multiple medium changes For example; the cells are labelled 64 hours after plating and then incubated for 20 hours before the functional assay. For this the cells are washed once, and then medium spiked with [3H]-*myo*-inositol is added. The HEK293 cells grow in a monolayer, which has the tendency to lift during medium changes, even when grown on special plates which promote adhesion. This results in loss of cells from the wells. This cell loss can be minimised by taking extreme care when adding medium to the wells. This is, however, very time consuming, and can introduce variability into the experiment as there can be a large difference in time (hours) between the first and last well receiving the

treatment. As such, the use of a larger number of replicates is not practicable. Instead, it is recommended that the whole experiment is repeated numerous times to confirm the results.

7.4 SUGGESTIONS FOR FUTURE RESEARCH

This study has provided the methods required to determine the effect of GRK5 knockdown on desensitisation of the rV1bR to AVP. The experimental protocol designed as part of this thesis to coordinate these methods can now be used to examine the role of GRK5. Introduction of a second GRK5-targeted siRNA will confirm that the phenotype induced by the current siRNA is caused by knockdown of GRK. Furthermore, once the Stratagene qPCR is available, increasing the annealing temperature used during qRT-PCR analysis will ensure that the primer sets for the reference genes TBP and YWHAZ are not able to form primer dimers.

Once the involvement of GRK5 in V1bR desensitisation has been assessed, it will be necessary to look at other GRKs such as GRKs 2, 3 and 6, to establish which kinase is responsible for the probable phosphorylation of the V1bR during desensitisation. Furthermore, as internalisation has been shown to play a role in V1bR desensitisation to AVP, knockdown experiments investigating the role of would also be informative. The protocols for Western blotting and qRT-PCR could be adapted for this purpose, as the Western blotting conditions for actin detection have already been optimised, and reference genes (TBP and YWHAZ) selected for qRT-PCR.

ACKNOWLDEGEMENTS

I would like to sincerely thank my supervisor, Dr. Drusilla Mason, for her encouragement and support during what has been an eventful and often frustrating project. I am very grateful for her guidance and assistance which have been invaluable. Many thanks are also due to my associate supervisor Dr. Arvind Varsani for his advice regarding qRT-PCR work, and the use of his lab for parts of the project. Thanks to my other associated supervisors Dr. Maxine Bryant and Associate Professor Steven Gieseg for their ideas and suggestions. I would also like to thank the technical staff from the School of Biological Sciences, in particular Linda Morris, Maggie Tichs, Jackie Healy, Gavin Robinson and Alan Woods for their technical support.

Many thanks to Dr. John Lewis and the Steroid & Immunobiochemistry Laboratory of Canterbury Health Laboratories for letting me use their liquid scintillation counter after the University of Canterbury counter was broken in the February 22nd Earthquake. Thanks are also due to Dr. Aaron Jeffs (University of Otago) for his advice regarding qRT-PCR and RNA interference experiments, and his gift of reference gene primer sets. I would like to thank Dr. Seungkirl Ahn of the Lefkowitz research group for their generous and timely advice regarding GRK5 antibodies. I would also like to thank Davon Callander for her excellent advice on all things qPCR, and members of the University of Otago Christchurch Free Radical Research Group for their advice on Western blots.

I acknowledge receipt of the New Zealand Federation of Graduate Woman (Inc.) Sadie Balkind Award for financial support during part of this research.

Thanks are due to Jacqui Lee, Anne van Bysterveldt, Clare van Bysterveldt and Jessica Southern for assistance with consistency and proof-reading, and their invaluable suggestions during the writing of this thesis. Many thanks also to Lachlan van Bysterveldt for the loan of his laptop when mine stumbled at the post.

I am very grateful to my fellow post-graduate students from the School of Biological Sciences, in particular Siobhan Cummings, Jacqui Lee, Tejraj Janmale, Anastasia Shchepkina, Daisy Stainton, Simona Kraberger, Ryan Catchpole and James Hadfield for their help friendship, support, commiseration and many, many laughs. Thanks also to my other truly excellent friends, in particular Christopher Bradley, David Jackson, and Jessica Southern for their support and midnight trips into Uni.

Finally, I would like to thank my family for their love and unwavering support. I could not have done it without you.

REFERENCES

Abou-Samra, A.-B., Harwood, J. P., Manganiello, V. C., Catt, K. C. & Aguilera, G. (1987). Phorbol 12-Myristate 13-Acetate and Vasopressin Potentiate the Effect of Corticotropin-releasing Factor on Cyclic AM P Production in Rat Anterior Pituitary Cells MECHANISMS OF ACTION. *The Journal of Biological Chemistry* **262**, 1129-1136.

Agrawal, N., Dasaradhi, P. V. N., Mohmmed, A., Malhotra, P., K., B. R. & Mukherjee, S. K. (2003). RNA Interference: Biology, Mechanism, and Applications. *Microbiology and Molecular Biology Reviews,* **67**, 657-685.

Aguilera, G. (1994). Regulation of Pituitary ACTH Secretion during Chronic Stress. *Frontiers in Neuroendocrinology* **15**, 321-350.

Ahn, S., Maudsley, S., Luttrell, L. M., Lefkowitz, R. J. & Daaka, Y. (1999). Src-mediated Tyrosine Phosphorylation of Dynamin Is Required for β_2-Adrenergic Receptor Internalisation and Mitogen-activated Protein Kinase Signaling. *Journal of Biological Chemistry* **274**, 1185-1188.

Ahn, S., Nelson, C. D., Garrison, T. R., Miller, W. E. & Lefkowitz, R. J. (2003). Desensitization, internalization, and signaling functions of β-arrestins demonstrated by RNA interference. *Proceedings of the National Academy of Science* **100**, 1740-1744.

Albizu, L., Moreno, J. L., Gonzalez-Maeso, J. & Sealfon, S. C. (2010). Heteromerization of G Protein-coupled Receptors: Relevance to Neurological Disorders and Neurotherapeutics. *CNS & Neurological Disorders - Drug Targets* **9**, 636-650.

Anderson, L., Alexander, C. L., Faccenda, E. & Eidne, K. A. (1995). Rapid desensitization of the thyrotropin-releasing hormone receptor expresed in single human embryonal kidney 293 cells. *Biochemical Journal* **311**, 385-392.

Antoni, F. A. (1993). Vasopressinergic Control of Pituitary Adrenocorticotropin Secretion Comes of Age. *Frontiers in Neuroendocrinology* **14**, 76-122.

Ashwell, J. D., Lu, F. W. M. & Vacchio, M. S. (2000). Glucocorticoids in T Cell Development and Function. *Annual Review of Immunology* **18**, 309-345.

Atwood, B., Lopez, J., Wager-Miller, J., Mackie, K. & Straiker, A. (2011). Expressin of G protein-coupled receptors and related proteins in HEK293, AtT20, BV2, and N18 cell lines as revealed by microarray analysis. *BMC Genomics* **12**, 14.

Barberis, C., Mouillac, B. & Durroux, T. (1998). Structural bases of vasopressin/oxytocin receptor function. *Journal of Endocrinology* **156**, 223-229.

Barki-Harrington, L. & Rockman, H. A. (2008). β-Arrestins: Multifunctional Cellular Mediators. *Physiology* **23**, 17-22.

Berrada, K., Plesnicher, C. L., Luo, X. & Thibonnier, M. (2000). Dynamic Interaction of Human Vasopressin/Oxytocin Receptor Subtypes with G Protein-coupled Receptor Kinases and Protein Kinase C after Agonist Stimulation. *The Journal of Biological Chemistry* **275**, 27229-27237.

Berridge, M. J. (1985). The Molecular Basis of Communication within the Cell. *Scientific American* **253**, 142-152.

Berridge, M. J. & Irvine, R. F. (1984). Inositol trisphosphate, a novel second messenger in cellular signal transduction. *Nature* **312**, 315-321.

Bezard, E., Gross, C. E., Qin, L., Gurevich, V. V., Benovic, J. L. & Gurevich, E. V. (2005). L-DOPA reverses the MPTP-induced elevation of the arrestin2 and GRK6 expression and enhanced ERK activation in monkey brain. *Neurobiology of Disease* **18**, 323-335.

Bilezikjian, L. M. & Vale, W. W. (1987). Regulation of ACTH Secretion from Corticotrophs: The Interaction of Vasopressin and CRF. *Annals of the New York Academy of Science* **512**, 85-95.

Bio-Rad (2000). AG® 1, AG MP-1 and AG 2 Strong Anion Exchange Resin Instructional Manual. Hercules, California: Bio-Rad Laboritories.

Birnbaumer, M. (2000). Vasopressin Receptors. *Trends in Endocrinology and Metabolism* **11**, 406-410.

Böhm, S., Grady, E. F. & Bunnett, N. W. (1997). Regulatory mechanisms that modulate signalling by G-protein-coupled receptors. *Biochemical Journal* **322**, 1-18.

Bouvier, M., Collins, S., O'Dowd, B. F., Campbell, P. T., de Blasi, A., Kobilka, B. K., MacGregor, C., Irons, G. P., Caron, M. G. & Lefkowitz, R. J. (1989). Two Distinct Pathways for cAMP-mediated Down-regulation of the β_2-Adrenergic Receptor: Phosphorylation of the Receptor and Regulation of its mRNA Level. *Journal of Biological Chemistry* **264**, 16786-16792.

Bridge, A. J., Pebernard, S., Ducraux, A., Nicoulaz, A.-L. & Iggo, R. (2003). Induction of an interferon response by RNAi vectors in mammalian cells. *Nature Genetics* **34**, 263-264.

Buckingham, J. C., Gilllies, G. E. & Cowell, A.-M. (1997). *Stress, Stress Hormones and the Immune System*. Chichester: John Wiley & Sons Ltd.

Budd, D. C., McDonald, J. E. & Tobin, A. B. (2000). Phosphorylation and Regulation of a $G_{q/11}$-coupled Receptor by Casein Kinase 1α. *The Journal of Biological Chemistry* **275**, 19667-19675.

Burnette, W. N. (1981). "Western Blotting": Electrophoretic transfer of proteins from sodium dodecyl sulfate-polyacrylamide gels to unmodified nitrocellulose and radiographic detection with antibody and radioiodinated protein A. *Analytical Biochemistry* **112**, 195-203.

Bustin, S. A. (2002). Quantification of mRNA using real-time reverse transcription PCR (RT-PCR): trends and problems. *J Mol Endocrinol* **29**, 23-39.

Bustin, S. A. (2004). *A-Z of Quantitative PCR*. La Jolla: International University Line.

Bychkov, E. R., Gurevich, V. V., Joyce, J. N., Benovic, J. L. & Gurevich, E. V. (2008). Arrestins and two receptor kinases are upregulated in Parkinson's disease with dementia. *Neurobiology of Aging* **29**, 379-396.

Caraty, A., Grino, M., Locatelli, A., Guillaume, V., Boudouresque, F., Conte-Devolx, B. & Oliver, C. (1990). Insulin-induced Hypoglycemia Stimulates Corticotropin-releasing Factor and Arginine Vasopressin Secretion into Hypophysial Portal Blood of Conscious, Unrestained Rams. *Journal of Clinical Investigation* **85**, 1716-1721.

Caraty, A., Grino, M., Locatelli, A. & Oliver, C. (1988). Secretion of corticotropin releasing factor (CRF) and vasopressin into the hypophysial portal blood or conscious, unrestrained rams. *Biochemical and Biophysical Research Communications* **155**, 841-849.

Chang, L., Sundaresh, S., Elliott, J., Anton, P. A., Baldi, P., Licudine, A., Mayer, M., Vuong, T., Hirano, M., Naliboff, B. D., Ameen, V. Z. & Mayer, E. A. (2009). Dysregulation of the hypothalamic-pituitary-adrenal (HPA) axis in irritable bowel syndrome. *Neurogastroenterology and motility* **21**, 149-159.

Chen, G., Gharib, T. G., Huang, C.-C., Taylor, J. M. G., Misek, D. E., Kardia, S. L. R., Giordano, T. J., Iannettoni, M. D., Orringer, M. B., Hanash, S. M. & Beer, D. G. (2002). Discordant Protein and mRNA Expression in Lung Adenocarcinomas. *Molecular and Cellular Proteomics* **1**, 303-313.

Chen, M., Philipp, M., Wang, J., Premont, R. T., Garrison, T. R., Caron, M. G., Lefkowitz, R. J. & Chen, W. (2009). G Protein-coupled Receptor Kinases Phosphorylate LRP6 in the Wnt Pathway. *The Journal of Biological Chemistry* **284**, 35040–35048.

Chini, B. & Manning, M. (2007). Agonist selectivity in the oxytocin/vasopressin receptor family: new insights and challenges. *Biochemical Society Transactions* **35**, 737-741.

Cottet, M., Albizu, L., Perkovska, S., Jean-Alphonse, F., Rahmeh, R., Orcel, H., Mejean, C., Granier, S., Mendre, C., Mouillac, B. & Durroux, T. (2010). Past, present and future of vasopressin and oxytocin receptor oligomers, prototypical GPCR models to study dimerization processes. *Current Opinion in Pharmacology* **10**, 59-66.

Cuccato, G., Polynikis, A., Siciliano, V., Graziano, M. & di Bernardo, M. (2011). Modeling RNA interference in mammalian cells. *BMC Systems Biology* **5**, 19.

Cullen, B. R. (2006). Is RNA interference involved in intrinsic antiviral immunity in mammals? *Nature Immunology* **7**, 563-567.

Cummings, S. (2011). Desensitisation of the Pituitary Vasopressin Receptor: Development and Use of a Stably-transfected Model Cell System to Assess the Role of G Protein-coupled Receptor Kinases. In *School of Biological Sciences*. Christchurch: University of Canterbury.

Daaka, Y., Luttrell, L. M. & Lefkowitz, R. J. (1997). Switching of the coupling of the beta2-adrenergic receptor to different G proteins by protein kinase A. *Nature* **390**, 88-91.

Daikoku, R., Kunitake, T., Kato, K., Tanoue, A., Tsujimoto, G. & Kannan, H. (2007). Body water balance and body temperature in vasopressin V1b receptor knockout mice. *Autonomic Neuroscience: Basic and Clinical* **136**, 58-62

Dale, L. B., Bhattacharya, M., Anborgh, P. H., Murdoch, B., Bhatia, M., Nakanish, S. & Ferguson, S. S. G. (2000). G Protein-coupled Receptor Kinase-mediated Desensitization of Metabotropic Glutamate Receptor 1A Protects against Cell Death. *The Journal of Biological Chemistry* **275**, 38213-38220.

Dallol, A., Fernades Da Silva, N., Viacava, P., Minna, J. D., Bieche, I., Maher, E. R. & Latif, F. (2002). SLIT2, a Human Homologue of the Drosophila Slit2 Gene, Has Tumor Suppressor Activity and Is Frequently Inactivated in Lung and Breast Cancers. *Cancer Research* **62**, 5874-5880.

Dautzenberg, F. M., Higelin, J. & Teichert, U. (2000). Functional characterization of the corticotropin-releasing factor type 1 receptor endogenously expressed in human embryonic kidney 293 cells. *European Journal of Pharmacology* **390**, 51-59.

de Keyzer, Y., Auzan, C., Lenne, F., Beldjord, C., Thibonnier, M., Bertagna, X. & Clauser, E. (1994). Cloning and characterization of the human V3 pituitary vasopressin receptor. *FEBS Letters* **356**, 215-220.

Dhami, K., Anborgh, P. H., Dale, L. B., Sterne-Marr, R. & Ferguson, S. S. G. (2002). Phosphorylation-independent regulation of metabotrophic glutamate receptor signaling by G protein-coupled receptor kinase 2. *Journal of Biological Chemistry* **277**, 25266-25272.

Doench, J. G., Petersen, C. P. & Sharp, P. S. (2003). siRNAs can function as miRNAs. *Genes & Development* **17**, 438-442.

Dressler, F., Whalen, J. A., Reinhardt, B. N. & Steere, A. C. (1993). Western Blotting in the Serodiagnosis of Lyme Disease. *The Journal of Infectious Diseases* **167**, 392-400.

Drouin, J., Trifiro, M. A., Plante, R. K., Nemer, M., Eriksson, P. & Wrange, O. (1989). Glucocorticoid Receptor Binding to a Specific DNA Sequence Is Required for Hormone-Dependent Repressin of Pro-Opiomelanocortin Gene Transcription. *Molecular and Cellular Biology* **9**, 5305-5314.

Dykxhoorn, D. M. & Lieberman, J. (2005). THE SILENT REVOLUTION: RNA Interference as Basic Biology, Research Tool, and Therapeutic. *Annual Review of Medicine* **56**, 401-423.

Dykxhoorn, D. M., Novina, C. D. & Sharp, P. A. (2003). Killing the Messenger: Short RNAs that Silence Gene Expression. *Nature Reviews: Molecular Cell Biology* **4**, 457-467.

Egashira, N., Tanoue, A., Higashihara, F., Fuchigami, H., Sano, K., Mishima, K., Fukue, Y., Nagai, H., Takano, Y., Tsujimoto, G., Stemmelin, J., Griebel, G., Iwasaki, K., Ikeda, T., Nishimura, R. & Fujiwara, M. (2005). Disruption of the Prepulse Inhibition of the Startle Reflex in Vasopressin V1b Receptor Knockout Mice: Reversal by Antipsychotic Drugs. *Neuropsychopharmacology* **30**, 1996-2005.

Elbashir, S. M., Lendeckel, W. & Tuschl, T. (2001). RNA interference is mediated by 21- and 22- nucleotide RNAs. *Genes & Development* **15**, 188-200.

Elemkov, I. J. & Chrousos, G. P. (1999). Stress Hormones, Th1/Th2 patterns, Pro/Anti-inflammatory Cytokines and Susceptibility to Disease. *Trends in Endocrinology and Metabolism* **10**, 359-368.

Evans, M. J., Marshall, A. G., Kitson, N. E., Summers, K. & Donald, R. A. (1993). Factors affecting ACTH release from perifused equine anterior pituitary cells. *Journal of Endocrinology* **137**, 391-401.

Evans, M. J., Mulligan, R. S., Livesey, J. H. & Donald, R. A. (1996). The integrative control of adrenocorticotropin secretion : a critical role for corticotrophin-releasing hormone. *Journal of Endocrinology* **148**, 475-483.

Fedorov, Y., Anderson, E. M., Birmingham, A., Reynolds, A., Karpilow, J., Robinson, K., Leake, D., Marshall, W. S. & Khvorova, A. (2006). Off-target effects by siRNA can induce toxic phenotype. *RNA* **12**, 1188-1196.

Ferguson, S. S. G. (2001). Evolving Concepts in G Protein-Coupled Receptor Endocytosis: The Role in Receptor Desensitization and Signaling. *Pharacological Reviews* **53**, 1-24.

Fire, A., Xu, S., Montgomery, M. K., Kostas, S. A., Driver, S. E. & Mello, C. C. (1998). Potent and specific genetic interference by double-stranded RNA in *Caenorhabditis elegans*. *Nature* **391**, 806-811.

Flint, M. S., Baum, A., Chambers, W. H. & Jenkins, F. J. (2007). Induction of DNA damage, alteration of DNA repair and transcriptional activation by stress hormones. *Psychoneuroendocrinology* **2007**, 470-479.

Fong, A. M., Premont, R. T., Richardson, R. M., Yu, Y.-R. A., Lefkowitz, R. J. & Patel, D. D. (2002). Defective lymphocyte chemotaxis in beta-arrestin2- and GRK6-deficient mice. *Proceedings of the National Academy of Science* **99**, 7478-7483.

Frank, E. & Landgraf, R. (2008). The vasopressin system - From antidiuresis to psychopathology. *European Journal of Pharmacology* **583**, 226-242.

Fujiwara, Y., Hiroyama, M., Sanbe, A., Aoyagi, T., Birumachi, J.-I., Yamauchi, J., Tsujimoto, G. & Tanoue, A. (2007a). Insulin hypersensitivity in mice lacking the V1b vasopressin receptor. *Journal of Physiology* **584**, 235-244.

Fujiwara, Y., Hiroyama, M., Sanbe, A., Yamauchi, J., Tsujimoto, G. & Tanoue, A. (2007b). Mutual regulation of vasopressin- and oxytocin-induced glucagon secretion in V1b vasopressin receptor knockout mice. *Journal of Endocrinology* **192**, 361-369.

Gainetdinov, R. R., Bohn, L. M., Walker, J. K. L., Laporte, S. A., Macrae, A. D., Caron, M. G., Leftkowitz, R. J. & Premont, R. T. (1999). Muscarinic Supersensitivity and Impaired Receptor Desensitization in G Protein–Coupled Receptor Kinase 5–Deficient Mice. *Neuron* **24**, 1029-1036.

Garrett, R. H. & Grisham, C. M. (2005). *Biochemistry*. Belmont,Ca (USA): Thomson Brooks/Cole.

Gatehouse, M. (2008). Desensitisation of the pituitary vasopressin receptor: development of a model system to assess involvement of G protein-coupled receptor kinase In *School of Biological Sciences*. Christchurch: University of Canterbury.

Gaudreau, R., Gouill, C. L., Venne, M.-H. & Stankova, J. (2002). Threonine 308 within a putative casein kinase 2 site of the cytoplasmic tail of the leukotriene b4 receptor (BLT1) desensitisation. *The Journal of Biological Chemistry* **277**, 31567-31578.

Gilllies, G. E., Linton, E. A. & Lowry, P. J. (1982). Corticotropin releasing activity of the new CRF is potentiated several times by vasopressin. *Nature* **299**, 355-357.

Gold, S. M., Raji, A., Huitinga, I., Wiedemann, K., Schulz, K.-H. & Heesen, C. (2005). Hypothalamo-pituitary-adrenal axis activity predicts disease progression in multiple sclerosis. *Journal of Neuroimmunology* **165**, 186-191.

Graham, F. L., Smiley, J., Russell, W. C. & Nairn, R. (1977). Characteristics of a Human Cell Line Transformed by DNA from Human Adenovirus Type 5. *Journal of GeneralVirology* **35**, 59-72.

Grishok, A., Tabara, H. & Mello, C. C. (2000). Genetic Requirements for Inheritance of RNAi in *C. elegans*. *Science* **287**, 2494-2497.

Hadcock, J. R. & Malbon, C. C. (1993). Agonist Regulation of Gene Expression of Adrenergic Receptors and G Proteins. *Journal of Neurochemistry* **60**, 1-9.

Hammen, C. (2005). Stress and Depression. *Annual Review of Clinical Psychology* **1**, 293-319.

Hammond, S. M., Bernsteink, E., Beach, D. & Hannon, G. J. (2000). An RNA-directed nuclease mediates post-transcriptional gene silencing in *Drosophila* cells. *Nature* **404**, 293-296.

Han, M., Gurevich, V. V., Vishnivetskiy, S. A., Sigler, P. B. & Schubert, C. (2001). Crystal Structure of β-Arrestin at 1.9 Å: Possible Mechanism of Receptor Binding and Membrane Translocation. *Structure* **9**, 869-880.

Hasbi, A., Polastron, J., Allouche, S., Stanasila, L., Massoute, D. & Jauzac, P. (1998). Desensitisation of the delta-opiod receptor correlates with it's phosphorylation in SK-N-BE cells: involvement of a G protein-coupled receptor kinase. *Journal of Neurochemistry* **70**, 2129-2138.

Hassan, A., Chacko, S. & Mason, D. (2003). Desensitization of the adrenocorticotropin responses to arginine vasopressin and corticotropin-releasing hormone in ovine anterior pituitary cells. *Journal of Endocrinology* **178**, 491-501.

Hassan, A. & Mason, D. (2005). Mechanisms of desensitization of the adrenocorticotropin response to arginine vasopressin in ovine anterior pituitary cells. *Journal of Endocrinology* **184**, 29-40.

Hawtin, S. R., Wesley, V. J., Simms, J., Argent, C. C. H., Latif, K. & Wheatley, M. (2005). The N-Terminal Juxtamembrane Segment of the V1a Vasopressin Receptor Provides Two Independent Epitopes Required for High-Affinity Agonist Binding and Signaling. *Molecular Endocrinology* **19**, 2871-2881.

He, B. & Soderlund, D. M. (2010). Human embryonic kidney (293) cells express endogenous voltage-gated sodium currents and Na v 1.7 sodium channels. *Neuroscience letters* **469**, 268-272.

Higashijima, T., Uzu, S., Nakajima, T. & Ross, E. M. (1988). Mastoparan, a peptide toxin from wasp venom, mimics receptors by activating GTP-binding regulatory proteins (G proteins). *Journal of Biological Chemistry* **263**, 6491-6494.

Holmes, C. L., Landry, D. W. & Granton, J. T. (2003). Science Review: Vasopressin and the cardiovascular system part 1 -receptor physiology. *Critical Care* **7**, 427-434.

Horie, K. & Insel, P. (2000). Retrovirally Mediated Transfer of a G Protein-coupled Receptor Kinase (GRK) Dominant-negative Mutant Enhances Endogenous Calcitonin Receptor Signaling in Chinese Hamster Ovary Cells: GRK INHIBITION ENHANCES EXPRESSION OF RECEPTORS AND RECEPTOR mRNA. *The Journal of Biological Chemistry* **275**, 29433-29440.

Hull, L. C., Llorente, J., Gabra, B. H., Smith, F. L., Kelly, E., bailey, C., Henderson, G. & Dewey, W. L. (2010). The Effect of Protein Kinase C and G Protein-Coupled Receptor Kinase Inhibition on Tolerance Induced by μ-Opioid Agonists of Different Efficacy. *The Journal of Pharamcology and Experimental Therapeutics* **332**, 1127-1135.

Iino, M., Furugori, T., Mori, T., Moriyama, S., Fukuzawa, A. & Shibano, T. (2002). Rational design and evaluation of new lead compound structures for selective βARK1 inhibitors. *Journal of Medicinal Chemistry* **45**, 2150-2159.

Itoh, S., Yamada, S., Mori, T., Miwa, T., Tottori, K., Uwahodo, Y., Yamamura, Y., Fukuda, M., Yamamoto, K., Tanoue, A. & Tsujimoto, G. (2006). Attenuated stress-induced catecholamine release in mice lacking the vasopressin V1b receptor. *American Journal of Physiology - Endocrinology and Metabolism* **291**, E147-E151.

Iwata, K., Luo, J., Penn, R. B. & Benovic, J. L. (2005). Bimodal Regulation of the Human H1 Histamine Receptor by G Protein-coupled Receptor Kinase 2. *The Journal of Biological Chemistry* **280**, 2197-2204.

Iyer, V. S. & Canty Jr, J. M. (2005). Regional Desensitization of β-Adrenergic Receptor Signaling in Swine With Chronic Hibernating Myocardium. *Circulation Research* **97**, 789-795.

Jackson, A. L., Bartz, S. R., Schelter, J., Kobayashi, S. V., Burchard, J., Mao, M., B., L., Cavet, G. & Linsley, P. S. (2003). Expression profiling reveals off-target gene regulation by RNAi. *Nature Biotechnology* **21**, 635-635.

Jard, S., Gaillard, R. C., Guillon, G., Marie, J., Schoenenberg, P., Muller, A. F., Manning, M. & Sawyer, W. H. (1986). Vasopressin Antagonists Allow Demonstration of a Novel Type of Vasopressin Receptor in the Rat Adenohypophysis. *Molecular Pharmacology* **30**, 171-177.

Jeffs, A. R., Glover, A. C., J., S. L., Wang, L., He, S., Hazlett, J. A., Awasthi, A., Woolley, A. G., Marshall, E. S., Joseph, W. R., Print, C. G., Baguley, B. C. & Eccles, M. R. (2009). A Gene Expression Signature of Invasive Potential in Metastatic Melanoma Cells. *PLoS ONE* **4**, e8461.

Joergensen, A., Broedbaek, K., Weimann, A., Semba, R. D., Ferrucci, L., Joergensen, M. B. & Poulsen, H. E. (2011). Association between Urinary Excretion of Cortisol and Markers of Oxidatively Damaged DNA and RNA in Humans. *PLoS ONE* **6**, e20795.

Jones, S. W., Baker, D. J. & Greenhaff, P. L. (2002). G protein-coupled receptor kinases 2 and 5 are differentially expressed in rat skeletal muscle and remain unchanged following b2-agonist administration. *Experimental Physiology* **88**, 277-284.

Josephsen, K., Smith, C. E. & Nanci, A. (1999). Selective but Nonspecific Immunolabeling of Enamel Protein-associated Compartments by a Monoclonal Antibody Against Vimentin. *The Journal of Histochemistry & Cytochemistry* **47**, 1237-1245.

Kelly, E., Bailey, C. P. & Henderson, G. (2008). Agonist-selective mechanisms of GPCR densensitization. *British Journal of Pharmacology* **153**, s379-s388.

Kim, J., Ahn, S., Ren, X.-R., Whalen, E. J., Reiter, E., Wei, H. & Lefkowitz, R. J. (2005). Functional antagonism of different G protein-coupled receptor kinases for β-arrestin-mediated angiotensin II receptor signaling. *Proceedings of the National Academy of Science* **102**, 1442-1447.

Kobayashi, S., Kitzawa, T., Somlyo, A. V. & Somlyo, A. P. (1989). Cytosolic heparin inhibits muscarinic and alpha-adrenergic Ca^{2+} release in smooth muscle. Physiological role of inositol 1,4,5-triphosphate in pharmomechanical coupling. *Journal of Biological Chemistry* **264**, 17997-18004.

Kobilka, B. K. (2007). G protein coupled receptor structure and activation. *Biochimica et Biophysica Acta* **1768**, 794-807.

Krupnick, J. G. & Benovic, J. L. (1998). The Role of Receptor Kinases and Arrestins in G Protein-coupled Receptor Regulation. *Annual Review of Pharmacology and Toxicology* **38**, 289-319.

Kumagai, I. & Tsumoto, K. (2010). Antigen-Antibody Binding. In *Encyclopedia of Life Sciences*: John Wiley & Sons Ltd, Chichester. http://www.els.net

Labrie, F., Giguere, V., Proulx, L. & Lefevre, G. (1984). Interactions Between CRF, Epinephrine, Vasopressin and Glucocorticoids in The Control of ACTH Secretion. *Journal of Steroid Biochemistry* **20**, 153-160.

Laemmli, U. K. (1970). Cleavage of structural Proteins during the Assembly of the Head of Bacteriophage T4. *Nature* **227**, 680-685.

Li, L., Rasul, I., Liu, J., Zhao, B., Tang, R. & Premont, R. T. (2009). Augmented axonal defects and synaptic degenerative changes in female GRK5 deficient mice. *Brain Research Bulletin* **78**, 145-151.

Liu, J.-P., Robinson, P. J., Funder, J. W. & Englers, D. (1990). The Biosynthesis and Secretion of Adrenocorticotropin by the Ovine Anterior Pituitary Is Predominantly Regulated by Arginine Vasopressin (AVP) EVIDENCE THAT PROTEIN KINASE C MEDIATES THE ACTION OF AVP. *Journal of Biological Chemistry* **265**, 14136-14142.

Liu, N.-K. & Xu, X.-M. (2006). β-Tubublin Is a More Suitable Internal Control than β-Actin in Western Blot Analysis of Spinal Cord Tissues after Traumatic Injury. *Journal of Neurotrauma* **23**, 1794-1801.

Lodowski, D. T., Tesmer, V. M., Benovic, J. L. & Tesmer, J. J. G. (2006). The Structure of G Protein-coupled Receptor Kinase (GRK)-6 Defines a Second Lineage of GRKs. *The Journal of Biological Chemistry* **281**, 16785-16793.

Lohse, M. J. (1993). Molecular mechanisms of membrane receptor desensitization. *Biochimica et Biophysica Acta* **1179**, 171-188.

Lohse, M. J., Benovic, J. L., Caron, M. G. & Lefkowitz, R. J. (1990). Multiple Pathways of Rapid β2-Adrenergic Receptor Desensitization: Delineation With Specific Inhibitors. *The Journal of Biological Chemistry* **265**, 3202-3209.

Lolait, S., Stewart, L. Q., Jessop, D. S., Young III, W. S. & O'Carroll, A. M. (2007a). The Hypothalamic-Pituitary-Adrenal Axis Response to Stress in Mice Lacking Functional Vasopressin V1b Receptors. *Endocrinology* **148**, 849-856.

Lolait, S., Stewart, L. Q., Roper, J. A., Harrison, G., Jessop, D. S., Young III, W. S. & O'Carroll, A. M. (2007b). Attenuated Stress Response to Acute Lipopolysaccharide Challenge and Ethanol Administration in Vasopressin V1b Receptor Knockout MIce. *Journal of Neuroendocrinology* **19**, 543-551.

Lolait, S. J., O'Carroll, A. M., Mahan, L. C., Felder, C. C., Button, D. C., Young, W. S., Mezey, E. & Brownstein, M. J. (1995). Extrapituitary expression of the rat V1b vasopressin receptor gene. *Proceedings of the National Academy of Sciences of the United States of America* **92**, 6783-6787.

Martini, J. S., Raake, P., Vinge, L. E., DeGeorge Jr, B. R., Chuprun, J. K., Harris, D. M., Gao, E., Eckhart, A. D., Pitcher, J. A. & Koch, W. J. (2008). Uncovering G protein-coupled receptor kinase-5 as a histone deacetylase kinase in the nucleus of cardiomyocytes. *Proceedings of the National Academy of Science* **105**, 12457-12462.

Martini, L. & Morpurgo, C. (1955). Neurohumoral Control of the Release of Adrenocorticotropic Hormone. *Nature* **175**, 1127-1128.

Mason, D., Hassan, A., Chacko, S. & Thompson, P. (2002). Acute and Chronic Regulation of Pituitary Receptors for Vasopressin and Corticotropin Releasing Hormone. *Archives of Physiology and Biochemistry* **110**, 74-89.

Matkovich, S. J., Diwan, A., Klanke, J. L., Hammer, D., Marreez, Y., Odley, A. M., Brunskill, E. W., Koch, W. J., Schwartz, R. J. & Dorn II, G. W. (2006). Cardiac-Specific Ablation of G-Protein Receptor Kinase 2 Redefines Its Roles in Heart Development and Beta-Adrenergic Signaling. *Circulation Research* **99**, 996-1003.

Maybauer, M. O., Maybauer, D. M., Enkhbaatar, P. & Traber, D. L. (2008). Physiology of the vasopressin receptors. *Best Practise & Research Clinical Anaesthesiology* **22**, 253-263.

McFarlane, A. R., Coghlan, J., Tresham, J. & M., W. E. (1995). Corticotropin-releasing factor alone, but not arginine vasopressin alone, stimulates the release of adrenocorticotropin in the conscious intact sheep. *Endocrinology* **136**, 1821-1827.

Menard, L., Ferguson, S. S. G., Barak, L. S., Bertrand, L., Premont, R. T., Colapietro, A.-M., Lefkowitz, R. J. & Caron, M. G. (1996). Members of the G Protein-Coupled Receptor Kinase Family That Phosphorylate the β2-Adrenergic Receptor Facilitate Sequesteration. *Biochemistry* **35**, 4155-4160.

Metaye, T., Menet, E., Guilhot, J. & Kraimps, J.-L. (2002). Expression and Activity of G Protein-Coupled Receptor Kinases in Differentiated Thyroid Carcinoma. *J Clin Endocrinol Metab* **87**, 3279-3286.

Milano, S. K., Pace, H. C., Kim, Y.-M., Brenner, C. & Benovic, J. L. (2002). Scaffolding Functions of Arrestin-2 Revealed by Crystal Structure and Mutagenesis. *Biochemistry* **41**, 3321-3328.

Milligan, G. & Kostenis, E. (2006). Heterotrimeric G-proteins: a short history. *British Journal of Pharmacology* **147**, s46-s55.

Morand, E. F. & Leech, M. (2001). Hypothalamic-pituitary-adrenal axis regulation of inflammation in rheumatoid arthritis. *Immunology and Cell Biology* **79**, 395-399.

Nagayama, Y., Tanaka, K., Hara, T., Namba, H., Yamashita, S., Taniyama, K. & Niwa, M. (1996). Involvement of G protein-coupled receptor kinase 5 in homologous desensitisation of the thyrotropin receptor. *Journal of Biological Chemistry* **271**, 10143-10148.

Nagy, V. & Watzele, M. (2006). FuGENE® 6 Transfection Reagent: minimizing reagent-dependent side effects as analyzed by gene-expression profiling and cytotoxicity assays. In *Nature Methods*, pp. iii-v. Edited by R. Diagnositics.

Nature Cell Biology Editorial (2003). Whither RNAi? *Nature Cell Biology* **5**, 489-490.

Nolan, T., Hands, R. E. & Bustin, S. A. (2006). Quantification of mRNA using real-time RT-PCR. *Nature Protocols* **1**, 1559-1582.

Oldham, W. M., Eps, N. V., Preininger, A. M., Hubbell, W. L. & Hamm, H. E. (2006). Mechanism of the receptor-catalyzed activation of heterotrimeric G proteins. *Nature Structural & Molecular Biology* **13**, 772-777.

Orcel, H., Albizu, L., Perkovska, S., Durroux, T., Mendre, C., Ansanay, H., Mouillac, B. & Rabie, A. (2009). Differential Coupling of the Vaspressin V_{1b} Receptor through Compartmentalization within the Plasma Membrane. *Molecular Pharmacology* **75**, 637-647.

Ortiz de Montellano, P. R., David, S. K., Ator, M. A. & Tew, D. (1988). Mechanism-based inactivation of horseradish peroxidase by sodium azide. Formation of meso-azidoprotoporphyrin IX. *Biochemistry* **27**, 5470-5476.

Paing, M. M., Stutts, A. B., Kohout, T. A., Lefkowitz, R. J. & Trejo, J. (2002). Beta-Arrestins Regulate Protease-activated Receptor-1 Desensitization but Not Internalization or Down-regulation. *Journal of Biological Chemistry* **277**, 1292-1300.

Park, P. S.-H. & Palczewski, K. (2005). Diversifying the repertoire of G protein-coupled receptors through oligomerization. *Proceedings of the National Academy of Science* **102**, 8793-8794.

Parrish, S., Fleenor, J., Xi, S., Mello, C. & Fire, A. (2000). Functional Anatomy of a dsRNA Trigger: Differential Requirement for the Two Trigger Strands in RNA Interference. *Molecular Cell* **6**, 1077-1087.

Penela, P., Ribas, C. & Mayor, J. F. (2003). Mechansims of regulation of the expression and function of G protein-coupled receptor kinases. *Cellular Signalling* **15**, 973-981.

Penn, R. B., Pronin, A. N. & Benovic, J. L. (2000). Regulation of G Protein-Coupled Receptor Kinases. *Trends in Cardiovascular Medicine* **10**, 81-89.

Perrin, M. H. & Vale, W. W. (1999). Corticotropin Releasign Factor Receptors and Their Ligand Family. *Annals of the New York Academy of Science* **885**, 312-328.

Pfaffl, M. W., Horgan, G. W. & Dempfle, L. (2002). Relative expression software tool (REST©) for group-wise comparison and statistical analysis of relative expression results in real-time PCR. *Nucleic Acid Research* **30**, e36.

Pitcher, J. A., Freedman, N. J. & Lefkowitz, R. J. (1998). G PROTEIN-COUPLED RECEPTOR KINASES. *Annual Review of Biochemistry* **67**, 653-692.

Pradidarcheep, W., Labruyere, W. T., Dabhoiwala, N. F. & Lamers, W. H. (2008). Lack of Specificity of Commercially Available Antisera: Better Specifications Needed. *J Histochem Cytochem* **56**, 1099-1111.

Premont, R. T., Macrae, A. D., Aparicio, S. A. J. R., Kendall, H. E., Welch, J. E. & Lefkowitz, R. J. (1999). The GRK4 Subfamily of G Protein-coupled Receptor Kinases: Alternative Splicing, Gene Organisation, and Sequence Conservation. *The Journal of Biological Chemistry* **274**, 29381-29389.

Premont, R. T., Macrae, A. D., Stoffel, R. H., Chung, N., Pitcher, J. A., Ambrose, C., Inglese, J., MacDonald, M. E. & Lefkowitz, R. J. (1996). Characterization of the G Protein-coupled Receptor Kinase GRK4 IDENTIFICATION OF FOUR SPLICE VARIANTS. *The Journal of Biological Chemistry* **271**, 6403–6410.

Price, R. R., Morris, D. P., Biswas, G., Smith, M. P. & Schwinn, D. A. (2002). Acute Agonist-mediated Desensitization of the Human α1a-Adrenergic Receptor Is Primarily Independent of Carboxyl Terminus Regulation. *Journal of Biological Chemistry* **277**, 9570-9579.

Radonic, A., Thulke, S., Mackay, I. M., Landt, O., Siegert, W. & Nitsche, A. (2004). Guideline to reference gene selection for quantitative real-time PCR. *Biochemical and Biophysical Research Communications* **313**, 856-862.

Raggenbass, M. (2008). Overview of cellular electrophysiological actions of vasopressin *European Journal of Pharmacology* **583**, 243-254.

Rajagopal, K., Whalen, E. J., Violin, J. D., Stiber, J. A., Rosenberg, P. B., Premont, R. T., Coffman, T. M., Rockman, H. A. & Lefkowitz, R. J. (2006). Beta-Arrestin2-mediated inotropic effects of the angiotensin II type 1A receptor in isolated cardiac myocytes. *Proceedings of the National Academy of Science* **103**, 16284–16289.

Ramos-Vara, J. A. (2005). Technical Aspects of Immunohistochemistry. *Veterinary Pathology* **42**, 405-426.

Regard, J. B., Sato, I. T. & Coughlin, S. R. (2008). Anatomical Profiling of G Protein-Coupled Receptor Expression. *Cell* **135**, 561-571.

Ren, X.-R., Reiter, E., Ahn, S., Kim, J., Chen, W. & Lefkowitz, R. J. (2005). Different G protein-coupled receptor kinases govern G protein and β-arrestin-mediated signaling of V2 vasopressin receptor. *Proceedings of the National Academy of Science* **102**, 1448-1453.

Renart, J., Reiser, J. & Stark, G. R. (1979). Transfer of proteins from gels to diazobenzyloxymethyl-paper and detection with antisera: a method for studying antibody specificity and antigen structure. *Proceedings of the National Academy of Sciences of the United States of America* **76**, 3116-3120.

Richardson, T. C., Chapman, D. & Heyderman, E. (1983). Immunoperoxidase techniques: the deletarious effect of sodium azide on the activity of peroxidase conjugates. *Journal of Clinical Pathology* **36**, 411-414

Ricks, T. K. & Trejo, J. (2009). Phosphorylation of Protease-activated Receptor-2 Differentially Regulates Desensitization and Internalization. *Journal of Biological Chemistry* **284**, 34444-34457.

Rivier, C. & Vale, W. (1983). Interaction of corticotropin-releasing factor and arginine vasopressin on adrenocorticotropin secretion in vivo. *Endocrinology* **113**, 939-942.

Roche (2006). FuGene® 6 Transfection Reagent: Roche Diagnostics.

Roper, J. A., O'Carroll, A. M., Young III, W. S. & Lolait, S. (2011). The vasopressin Avpr1b receptor: Molecular and pharmacological studies. *Stress* **14**, 98-115.

Rosmond, R. & Björntorp, P. (2000). The hypothalamic-pituitary-adrenal axis activity as a predictor of cardiovascular disease, type 2 diabetes and stroke. *Journal of Internal Medicine* **247**, 188-197.

Rousseau-Merck, M. F., Rene, P., Derre, J., Bienvenu, T., Berger, R. & De Keyzer, Y. (1995). Chromosomal localisation of the human V3 pituitary vasopressin receptor (AVPR3) to 1q32. *Genomics* **30**, 405-406.

Sambrook, J., Fritsch, E. F. & Maniatis, T. (1989). *Molecular Cloning: A Laboratory Manual*: Cold Spring Harbour Laboratory Press.

Schachter, J. B., Sromek, S. M., Nicholas, R. A. & Harden, T. K. (1997). HEK293 human embryonic kidney cells endogenously express the P2Y1 and P2Y2 receptors. *Neuropharmacology* **36**, 1181-1187.

Schaller, O., Fatzer, R., Stack, M., Clark, J., Cooley, W., Biffiger, K., Egli, S., Doherr, M., Vandevelde, M., Heim, D., Oesch, B. & Moser, M. (1999). Validation of a Western immunoblotting procedure for bovine PrP^{Sc} detection and its use as a rapid surveillance method for the diagnosis of bovine spongiform encephalopathy (BSE). *Acta Neuropathologica* **98**, 437-443.

Schmittgen, T. D. & Zakrajsek, B. A. (2000). Effect of experimental treatment on housekeeping gene expression: validation by real-time, quantitative RT-PCR. *Journal of Biochemical and Biophysical Methods* **46**, 69-81.

Schneppenheim, R. & Rautenberg, P. (1987). A Luminescence Western blot with enhanced sensitivity for antibodies to human immunodeficiency virus. *European Journal of Clinical Microbiology & Infectious Diseases* **6**, 49-51.

Shaw, G., Morse, S., Ararah, M. & Graham, F. L. (2002a). Preferential transformation of human neuronal cells by human adenoviruses and the origin of HEK 293 cells *FASEB Journal Express* **April 10**.

Shaw, G., Morse, S., Ararah, M. & Graham, F. L. (2002b). Preferential transformation of human neuronal cells by human adenoviruses and the origin of HEK 293 cells *FASEB Journal* **16**, 869-871.

Shenoy, S. K., Modi, A. S., Shukla, A. K., Xiao, K., Berthouze, M., Ahn, S., Wilkinson, K. D., Miller, W. E. & Lefkowitz, R. J. (2009). Î²-Arrestin-dependent signaling and trafficking of 7-transmembrane receptors is reciprocally regulated by the deubiquitinase USP33 and the E3 ligase Mdm2. *Proceedings of the National Academy of Sciences* **106**, 6650-6655.

Sherwood, L., Klandorf, H. & Yancey, P. (2005). *Animal Physiology: From Genes to Organisms*. Belmont, CA: Thomson Brooks/Cole.

Shim, M. S. & Kwon, Y. J. (2010). Efficient and targeted delivery of siRNA *in vivo*. *FEBS Journal* **277**, 4814-4827.

Sledz, C. A., Holko, M., de Veer, M. J., Silverman, R. H. & Williams, B. R. G. (2003). Activation of the interferon system by short-interfering RNAs. *Nature Cell Biology* **5**, 834-839.

Smith, P. K., Krohn, R. I., Hermanson, G. T., Mallia, A. K., Gartner, F. H., Provenzano, M. D., Fujimoto, E. K., Goeke, N. M., Olson, B. J. & Klenk, D. C. (1985). Measurement of Protein Using Bicinchoninic Acid. *Analytical Biochemisty* **150**, 76-85.

Spandidos, A., Wang, X., Wang, H. & Seed, B. (2010). PrimerBank: a resource of human and mouse PCR primer pairs for gene expression detection and quantification. *Nucleic Acid Research* **38**, D792-D799.

Steele, J. C. H. & Nielsen, T. B. (1978). Evaluation of Cross-Linked Polyperptides in SDS Gel Electrophoresis. *Analytical Biochemistry* **84**, 218-224.

Sternberg, E. (2001). Neuroendocrine regulation of autoimmune/inflammatory disease. *Journal of Endocrinology* **169**, 429-435.

Strader, C. D., Fong, T. M., Tota, M. R. & Underwood, D. (1994). Structure and Function of G Protein-coupled Receptors. *Annual Review of Biochemistry* **63**, 101-132.

Sugimoto, T., Saito, M., Mochizuki, S., Watanabe, Y., Hashimoto, S. & Kawashima, H. (1994). Molecular Cloning and Functional Expression of a cDNA Encoding the Human v1b Vasopressin Receptor. *Journal of Biological Chemistry* **269**, 27088-27092.

Suo, Z., Cox, A. A., Bartelli, N., Imtiaz Rasul, I., Festoff, B. W., Premont, R. T. & Arendash, G. W. (2007). GRK5 deficiency leads to early Alzheimer-like pathology and working memory impairment. *Neurobiology of Aging* **28**, 1873-1883.

SYNGENE (2009). Application Note 17 (17.08.09). On chip integration versus image additions in series capture: Which method is best?: www.syngene.com.

Tanoue, A., Ito, S., Honda, K., Oshikawa, S., Kitagawa, Y., Koshimizu, T.-A., Mori, T. & Tsujimoto, G. (2004). The vasopressin V1b receptor critically regulates hypothalamic-pituitary-adrenal axis activity under both stress and resting conditions. *Journal of Clincal Investigations* **113**, 302-309.

Tarrant, T. K., Rampersad, R. R., Esserman, D., R., R. L., Liu, P., T., P. R., Lefkowitz, R. J., Lee, D. M. & Patel, D. D. (2008). Granulocyte chemotaxis and disease expression are differentially regulated by GRK subtype in an acute inflammatory arthritis model (K/BxN). *Clinical Immunology* **129**, 115–122.

Taylor, S. J., Smith, J. A. & Exton, J. H. (1990). Purification from Bovine Liver Membranes of a Guanin Nucleotide-dependent Activator of Phosphoinositide-specific Phospholipase C: Immunological Identification as a Novel G-Protein α Subunit. *The Journal of Biological Chemistry* **265**, 17150-17156.

Terrillon, S. & Bouvier, M. (2004). Roles of G-protein-coupled receptor dimerization: From ontogeny to signalling regulation. *EMBO reports* **5**, 30-34.

Thal, D. M., Yeow, R. Y., Schoenau, C., Huber, J. & Tesmer, J. J. (2011). Molecular Mechanism of Selectivity among G Protein-Coupled Receptor Kinase 2 Inhibitors. *Molecular Pharmacology* **80**, 294-303.

Thibonnier, M., Preston, J. A., Dulin, N., Wilkins, P. L., Berti-Mattera, L. N. & Mattera, R. (1997). The Human V3 Pituitary Vasopressin Receptor: Ligand Binding Profile and Density-Dependent Signaling Pathways. *Endocrinology* **138**, 4109-4122.

Tobin, A. B., Totty, N. F., Sterlin, A. E. & Nahorski, S. R. (1997). Stimulus-dependent Phosphorylation of G-protein-coupled Receptors by Casein Kinase 1Î±. *Journal of Biological Chemistry* **272**, 20844-20849.

Towbin, H., Staehelin, T. & Gordon, J. (1979). Electrophoretic transfer of proteins from polyacrylamide gels to nitrocellulose sheets: procedure and some applications. *Proceedings of the National Academy of Science* **76**, 4350-4354.

Ulloa-Aguirre, A., Stanislaus, D., Janovick, J. A. & Conn, P. M. (1999). Structure-Activity Relationships of G protein-Coupled Receptors. *Achives of Medical Research* **30**, 420-435.

Vale, W., Vaughan, J., Smith, M., Yamamoto, G., Rivier, J. & Rivier, C. (1983). Effects of synthetic ovine corticotropin-releasing factor, glucocorticoids, catecholamines, neurohypophysial peptides, and other substances on cultured corticotroph cells. *Endocrinology* **113**, 1121-1131.

van Koppen, C., Meyer zu Heringdorf, M., Laser, K. T., Zhang, C., Jakobs, K. H., Bunemann, M. & Pott, L. (1996). Activation of a high affinity Gi protein-coupled plasma membrane receptor by sphingosine-1-phosphate. *Journal of Biological Chemistry* **271**, 2082-2087.

van Pelt-Verkuli, E., van Belkum, A. & Hays, J. P. (2008). *Principles and Technical Aspects of PCR Amplification*: Springer Netherlands.

Vandesompele, J., De Preter, K., Pattyn, F., Poppe, B., Van Roy, N., De Paepe, A. & Speleman, F. (2002). Accurate normalization of real-time quantitative RT-PCR data by geometric averaging of multiple internal control genes. *Genome Biology* **3**, 1-12.

Ventura, M. A., Rene, P., de Keyzer, Y., Bertagna, X. & Clauser, E. (1999). Gene and cDNA cloning and characterisation of the mouse V3/V1b pituitary vasopressin receptor. *Journal of Molecular Endocrinology* **22**, 251-260.

Violin, J. D., DiPilato, L. M., Yildirim, N., Elston, T. C., Zhang, J. & Lefkowitz, R. J. (2008). β_2-Adrenergic Receptor Signaling and Desensitization Elucidated by Quantitative Modeling of Real Time cAMP Dynamics. *The Journal of Biological Chemistry* **283**, 2949-2961.

Violin, J. D., Ren, X.-R. & Leftkowitz, R. J. (2006). G-protein-coupled Receptor Kinase Specificity for β-Arrestin Recruitment to the β_2-Adrenergic Receptor Revealed

by Fluorescence Resonance Energy Transfer. *The Journal of Biological Chemistry* **281**, 20577-20588.

Voigt, C., Holzapfel, H.-P., Meyer, S. & Paschke, R. (2004). Increased expression of G-protein-coupled receptor kinases 3 and 4 in hyperfunctioning thyroid nodules. *Journal of Endocrinology* **182**, 173-182.

Wadhwa, R., Kaul, S. C., Miyagishi, M. & Taira, K. (2004). Know-how of RNA interference and its applications in reaseach and therapy. *Mutation Research* **567**, 71-84.

Walker, J. M. (1996). *The Protein Protocols Handbook.* Totowa: Humana Press.

Watson, J. D., Baker, T. A., Bell, S. B., Gann, A., Levine, M. & Losick, R. (2004). *Molecular Biology of the Gene*: Cold Spring Harbor Laboratory Press.

Webb, K. S., Mickey, D. D., Stone, K., R. & Paulson, D. F. (1977). Correlation of Apparent Moleculary Weight and Antigenicity of Viral Proteins: An SDS-PAGE Separation Followed by Acrylamide-Agarose Electrophoresis and Immunoprecipitation. *Journal of Immunological Methods* **14**, 343-353.

Wersinger, S. R., Caldwell, H. K., Christiansen, M. & Young III, W. S. (2007). Disruption of the vasopressin 1b receptor gene impairs the attack component of aggressive behavior in mice. *Genes, Brain and Behavior* **6**, 653-660.

Wersinger, S. R., Ginns, E. I., O'Carroll, A. M., Lolait, S. & Young, W. S. (2002). Vasopressin V1b receptor knockout reduces aggressive behavior in male mice. *Molecular Psychiatry* **7**, 975-984.

Wersinger, S. R., Temple, J. L., Caldwell, H. K. & Young III, W. S. (2008). Inactivation of the Oxytocin and the Vasopressin (Avp) 1b Receptor Genes, But Not the Avp 1a Receptor Gene, Differentially Impairs te Bruce Effect in Laboratory Mice (Mus musculus). *Endocrinology* **149**, 116-121.

Willingham, M. C. (1999). Conditional Epitopes: Is Your Antibody Always Specific? *J Histochem Cytochem* **47**, 1233-1236.

Winstel, R., Ihlenfeldt, H.-G., Jung, G., Krasel, C. & Lohse, M. J. (2005). Peptide inhibitors of G protein-coupled receptor kinases. *Biochemical Pharmacology* **70**, 1001-1008.

Wirtz, P. H., von Känel, R., Emini, L., Ruedisueli, K., Groessbauer, S., Maercker, A. & Ehlert, U. (2007). Evidence for altered hypothalamus-pituitary-adrenal axis functioning in systemic hypertension: Blunted cortisol response to awakening and lower negative feedback sensitivity. *Psychoneuroendocrinology* **32**, 430-436.

Yang, D., Lu, H. & Erickson, J. W. (2000). Evidence that processed small dsRNAs may mediate sequence-specific mRNA degradation during RNAi in *Drosophila* embryos. *Current Biology* **10**, 1191-1200.

Yi, X. P., Zhou, J., Baker, J., Wang, X., Gerdes, A. M. & Li, F. (2005). Myocardial Expression and Redistribution of GRKs in Hypertensive Hypertrophy and Failure. *The Anatomical Record Part A* **282A**, 13-23.

Young, S. F., Griffante, C. & Aguilera, G. (2007). Dimerization Between Vasopressin 1b and Corticotrophin Releasing Hormone Type 1 Receptors. *Cellular and Molecular Neurobiology* **27**, 439-461.

Zamore, P. D., Tuschl, T., Sharp, P. S. & Bartel, D. P. (2000). RNAi: Double-Stranded RNA Directs the ATP-Dependent Cleavage of mRNA at 21 to 23 Nucleotide Intervals. *Cell* **101**, 24-33.

Zhu, G., Zhang, H., Xu, H. & Jiang, C. (1998). Identification of endogenous outward currents in the human embryonic kidney (HEK293) cell line. *Journal of Neuroscience Methods* **81**, 73-83.

Zidar, D. A., Violin, J. D., Whalen, E. J. & Lefkowitz, R. J. (2009). Selective engagement of G protein coupled receptor kinases (GRKs) encodes distinct functions of biased ligands. *Proceedings of the National Academy of Sciences* **106**, 9649-9654.

APPENDIX A

MATERIALS

5 X siRNA buffer	Dharmacon
100bp Ladder	Gibco, Invitrogen Corporation
AG1-X8 anion-exchange resin	Bio-Rad
Agarose	Gibco, Invitrogen Corporation
Acrylamide solution	Bio-Rad
Ammonium Formate	Sigma-Aldrich Company
Ammonium Persulfate	Sigma-Aldrich Company
Arginine Vasopressin (AVP)	Sigma-Aldrich Company
Bromochloropropate (BCP)	Molecular Research Centre, Inc.
BCA protein assay kit	Pierce
Beta-mercaptoethanol	Sigma-Aldrich Company
Bis solution (2%)	Bio-Rad
Bovine Serum Albumin	Gibco, Invitrogen Corporation
Bromophenol blue	Sigma-Aldrich Company
Coomassie Brilliant Blue G	Sigma-Aldrich Company
Donkey anti-rabbit IgG HRP-conjugated IgG	Amersham
Dulbecco's modified Eagle's medium (-inositol)	MP Biomedical
DMSO	Sigma-Aldrich
EDTA disodium salt	Boehringer Mannheim
Ethanol 100%	BDH
Fetal Bovine Serum	Gibco, Invitrogen Corporation
Formic Acid	Sigma-Aldrich Company
Glacial acetic acid	BDH
GlutaMax	Invitrogen
GRK5 (C-20) blocking peptide	Santa Cruz Biotechnology, Inc.
GRK5-targeting siRNA	Dharmacon
Glycine	Sigma-Aldrich Company
High DNA Mass Ladder	Gibco, Invitrogen Corporation
Horse anti-rabbit IgG HRP-conjugated IgG	Sigma-Aldrich Company
Horse anti-rabbit IgG HRP-conjugated IgG	Novus Biologicals
HEK293 cell line	ATCC
Hybond-C-extra Nitrocellulose Membrane	Amersham
Hydrochloric acid (HCl)	BDH
KAPA Taq ReadyMix DNA Polymerase	Kapa Biosystems
Lithium chloride (LiCl)	Sigma-Aldrich Company

Minimum Essential Medium (MEM)	Gibco, Invitrogen Corporation
Methanol	Burdick & Jackson
Milk Powder (0.1 % fat)	pams®
Myo-[^{3}H]-inositol	Amersham Biosciences
Nitrocellulose membranes	Hybond
Mini Protease inhibitor	Roche
Nanopure H_2O	Biology building
Non-Essential Amino Acids	Gibco, Invitrogen Corporation
Non-targeting siRNA #1	Dharmacon
Non-targeting siRNA # 3	Dharmacon
OPTISAFE 'HISAFE' 3 scintillation cocktail	Perkin-Elmer
PageRuler Prestained Protein Ladder	Fermentes Life Sciences
Polyprep® chromatography columns	BioRad
Ponceau S stain	Sigma-Aldrich Company
Potassium chloride (KCl)	BDH
Potassium dihydrogen phosphate (KH_2PO_4)	BDH
PureLink RNA Mini Extraction Kit	Invitrogen
Rabbit anti-GRK 5 (c-20) polyclonal IgG (SC-565)	Santa Cruz Biotechnology
Rabbit anti-actin polyclonal IgG (A2066)	Sigma-Aldrich Company
RNase-Away	Invitrogen
Scintillation cocktail (NMCS104)	Sigma-Aldrich Comparny
Sodium bicarbonate ($NaHCO_{3)}$	BDH
Sodium chloride (NaCl)	BDH limited
Sodium hydrogen phosphate (Na_2HPO_4)	BDH
Sodium dodycel sulfate	Sigma-Aldrich Company
Sodium formate	Sigma-Aldrich Company
Sodium hydroxide	BDH
Sodium pyruvate	Gibco, Invitrogen Corporation
Super Signal West Pico Chemilluminecsence reagent	Thermo Fisher Scientific
Sodium Tertraborate	MP Biomedicals
Sucrose	BDH
SuperScript III First-Strand Synthesis System for RT-PCR	Invitrogen
SYBR GreenER qPCR SuperMix Universal	Invitrogen
SYBRsafe dye	Invitrogen
Tris	Invitrogen
TRIzol Plus RNA Purification Kit	Invitrogen
Trypan blue	BDH
Trypsin/EDTA (TE)	Gibco, Invitrogen Corporation
TEMED	Invitrogen
Tween-20	Sigma-Aldrich Company
Trizma base	Sigma-Aldrich Company
Trizol Plus RNA Purification Kit	Invitrogen
Trypsin-EDTA	Gibco, Invitrogen Corporation
UltaPure Distilled Water	Gibco, Invitrogen Corporation

APPENDIX B

SOLUTIONS, MEDIA & GELS

B.1 CHAPTER 2: MODEL CELL SYSTEM & ASSOCIATED METHODS

B.1.1 Minimum Essential Medium (MEM)

MEM was prepared by dissolving one packet of commercially prepared powdered MEM (Gibco, Cat # 41500-034) in ddH_2O (18.2ΩM). The medium was completed by addition of 1.5g of sodium bicarbonate, and 10ml of sodium pyruvate. The volume was then made up to 1L and pH adjusted to 7.1. The medium was sterilised by negative pressure filtration through a 0.45µm filter, and transferred into sterile Schott bottles. The medium was stored at 4^oC for up to 2 months. A sub of the medium from each bottle was transferred to McCartney bottles, which were incubated at 37$^oC/CO_2$ 5% for 3 days to check the sterility. Prior to use, the medium was supplemented with 10% FBS, and for medium more than 2 weeks old, 1% GlutaMAX.

B.1.2 Phosphate buffered saline (PBS)

The reagents listed below were dissolved in ddH_2O and made up to 200ml for 5 x PBS or 1L for 1 x PBS. The pH was adjusted to 7.4 before use. The solution was stored at room temperature.

Na_2HPO_4 (anhydrous)	1.15 g
NaCl	8.0 g
KCl	0.2 g
KH_2PO_4	0.2 g

B.1.3 Trypan blue: stock solution

A 0.2% stock solution of trypan blue was made and stored at 4^oC until use. 0.02g of Trypan Blue was dissolved in 10ml of ddH_2O and filtered through a 0.2µm filter into a clean glass vial.

B.1.4 Trypan blue: working solution

Trypan blue working solution was made fresh as required for cell counts by diluting trypan blue stock solution (B.1.3) 4/5 with 5 x PBS.

B.1.5 Labelling solution

For each experiment, the labelling solution was made up at a volume that allowed 500µL per well, plus 3mL spare. [^{3}H]-*myo*-inositol (2.5µL/mL) was added to sterile inositol-free DMEM containing 0.1% BSA, and 1% GlutaMax. E.g., for 24 wells, 14.85mL of DMEM- and 0.15mL GlutaMax were combined in a glass beaker. 0.015g of BSA was then added and swirled to dissolve. The media was filter sterilised through a 0.2µm filter into a sterile beaker. 12.5mL was then transferred to a 50mL falcon tube, and incubated at 37^{o}C in a CO_2 incubator for approximately 1 hour before use. Immediately before use, 31.25µL [^{3}H]-*myo*-inositol was added to the tube.

B.1.6 "Stop" solution

The reagents listed below were dissolved in the order listed into approximately 450ml of ddH_2O. The solution was made up to 500ml with dH_2O and stored at 4^{o}C.

B.1.7. "Neutralization" solution

A 7.5% HCl solution was made by adding 37.5mL of 37% hydrochloric acid to 462.5mL of ddH_2O. 5mL of this solution was combined with 5mL of inositol-free culture medium and 5mL of "stop" solution, and the acidity adjusted to pH7. by addition of ddH_2O. The neutral solution was stored at 4^{o}C.

B.1.8. Elution Buffer II

Elution buffer II was made fresh on the day of inositol phosphate separation by dissolving the following reagents 100mL of ddH_2O.

Sodium borate	0.191g
Sodium formate	0.408g

B.1.8. Elution Buffer VI

Elution buffer VI was made fresh on the day of inositol phosphate separation by dissolving the following reagents in 100mL of ddH_2O.

Formic acid	436µL
Ammonium formate	12.612g

B.1.9. Regeneration Solution

The following reagents were dissolved in 100mL ddH_2O. The solution was made fresh as required.

Formic Acid	436µL
Ammonium formate	18.920g

B.2CHAPTER 3: WESTERN BLOTTING & ASSOCIATED METHODS

B.2.1 20% SDS

SDS (10g) was mixed with 50ml nanopure H_2O, and heated to 68^oC until dissolved. The solution was then cooled and stored at room temperature

B.2.2 0.5M Tris Buffer (pH 6.8)

Tris (12.114g, MW 121.1) was dissolved in 150ml nanopure H_2O, the pH adjusted to 6.8 with concentrated HCl (without overshooting). The volume was made up to 200ml with NPH_2O. The solution was stored at room temperature.

B.2.3 0.5M Tris Buffer (pH 6.8)

Tris (12.114g, MW 121.1) was dissolved in 150ml nanopure H_2O, the pH adjusted to 6.8 with concentrated HCl (without overshooting). The volume was made up to 200ml with NPH_2O. The solution was stored at room temperature.

B.2.4 1.5M Tris Buffer (pH 8.8)

Tris (36.342g, MW 121.1) was dissolved in 150ml nanopure H_2O, the pH adjusted to 8.8 with concentrated HCl (without overshooting). The volume was made up to 200ml with NPH_2O. The solution was stored at room temperature.

B.2.5 SDS Lysis Buffer

The following reagents were added to 8mL of NPH_2O, and the solution stirred to dissolve the sucrose.

1M Tris HCl (pH 6.8)	1.25 ml
20% SDS	2 ml
Sucrose (MW 342.30)	1 g

The volume was then adjusted to 15.14ml using NPH_2O. The solution was stored at -20^oC.

B.2.6 BCA assay working Reagent

The BCA assay working reagent was prepared in the day of the assay by mixing reagents A and B at a ratio of 50:1. This reagent could be stored at room temperature for several hours before use.

B 2.7 1X SDS Buffer

The following reagents were added to 8mL of NPH_2O, and the solution stirred to dissolve the sucrose.

1M Tris HCl (pH 6.8)	1.25 ml
20% SDS	2 ml
Sucrose (MW 342.30)	1 g

The volume was then adjusted to 18ml with NPH_2O. The solution was stored at -20^oC.

B.2.81 1% Bromophenol Blue Solution

A 1% (wt/vol) solution of Bromophenol blue was prepared by dissolving 0.1g bromophenol blue powder in 10mL 70% ethanol. This solution was stored at room temperature.

B 2.9 0.1% Bromophenol Blue Solution

10µl of 1% Bromophenol blue solution was added to 90µl of Nanopure H_2O, and the resulting solution stored at room temperature.

B.2.10 'Fresh' 10% Ammonium persulfate (APS)

10% APS solution was prepared fresh for each gel by dissolving APS in Nanopure H_2O (0.1g/ml). The solution was discarded after use.

B.2.11 8% Separating gel

The reagents listed below were added in order and mixed by swirling between additions. The resulting gel solution was transferred into the casting frame, covered in a layer of Nanopure

H_2O and left to set for 45-60 minutes at room temperature. The water was then poured off and the cavity dried in preparation for pouring of the stacking gel.

Nanopure H_2O	2417 µl
40% Acrylamide Solution	1160 µl
2% Bis Solution	800 µl
1.5 M TRIS (pH 8.8)	1500 µl
20% SDS	30 µl
10% ammonium persulfate	60 µl
TEMED	3 µl

B.2.12 Stacking gel

The below reagents were added in order and swirled to mix between additions. 1ml of the resulting solution was added to the top of the separating gel and the comb inserted. The gel was left to set for 30-45 minutes. The gel could be used immediately or stored overnight at 4^{o}C.

Nanopure H_2O	1049 µl
40% Acrylamide solution	242 µl
2% Bis solution	167 µl
0.5 M TRIS (pH 6.8)	500 µl
20% SDS	10 µl
10% Ammonium persulfate	20 µl
TEMED	2.5 µl

B 2.13 10 x Tris Glycine Buffer

The following chemicals were dissolved in 500ml Nanopure H_2O (heating to 68^{o}C if necessary) and made up to 1L with Nanopure H_2O. The solution was stored at room temperature.

Glycine	144 g
Tris (MW. 121.1)	30 g

B.2.14 Running Buffer

The following reagents were mixed and made up to 900ml with Nanopure H_2O. The resulting buffer stored at room temperature.

10 x Tris-Glycine	90 ml
20% SDS	4.5 ml

B.2.15 Transfer Buffer

The following reagents were added in order and mixed between additions. The solution was stored at room temperature and chilled at -20^{o}C for one hour before use;

10 x Tris-Glycine buffer	100 ml
Nanopure H_2O	700 ml
Methanol	100 ml
20% SDS	0.5 ml

B.2.16 Ponceau S Stain

The following reagents were mixed and the resulting solution stored at room temperature;

Ponceau S	0.005 g
Acetic acid	2.5 ml
Nanopure H_2O	47.5 ml

B.2.17 Coomassie Brilliant Blue G Solution

The following reagents were mixed and the resulting solution stored at room temperature;

Coomassie Brilliant Blue R-250	0.25 g
Nanopure H_2O	125 ml
Methanol	100 ml
Acetic acid	25 ml

B.2.18 Coomassie Brilliant Blue Destain Solution

The following reagents were mixed and the resulting solution stored at room temperature;

Methanol	225 ml
Acetic acid	50 ml
Nanopure H_2O	225 ml

B.2.19 PBS with 0.1% Tween 20 (PBST)

0.1ml of Tween 20 was added per 100ml of PBS. The resulting solution was shaken vigorously to mix and stored at room temperature.

B.2.20 PBST with 2% Milk powder (PBSTM 2%)

Milk powder (0.1% fat) was dissolved in PBST (0.2g/10ml)

B.3 CHAPTER 4: QRT-PCR & ASSOCIATED METHODS

B.3.1 0.5M EDTA Solution

93.05g of EDTA disodium salt (FW= 372.2) was mixed dissolved in 400ml of fresh NP water under RNase-free conditions. The pH was adjusted to 8.0 with approximately 10g of NaOH pellets (pH measured with pH paper) in order to get the EDTA into solution. The volume was made up to 500ml with NPH_2O. The solution was stored in an RNase-free Schott bottle at room temperature.

B.3.2 50 x TAE Buffer

242g Tris base (FW=121.14) was dissolved in 750ml of fresh NP water. 57.1ml of glacial acetic acid and 100ml of 0.5M EDTA (pH 8.0) were added and the solution made up to 1L with fresh NPH_2O

B.3.3 1 x TAE Buffer

On the day of use, 1 part 50 x TAE buffer was mixed with 49 parts fresh RNase-free NPH_2O.

B.3.4 1% agarose gel

0.5g agarose was mixed with 500ml 1 x TAE, in a 100ml Schott bottle and micro-waved with regular swirling until a clear solution was obtained. 5ul SYBRsafe was added and the bottle was placed in a dark place until cool enough to touch, then poured into a gel tray, covered in tinfoil and left to set for 20 minutes. Before the gel was poured, the casting frame and comb were sprayed with RNase-OUT and wiped with RNase-free Kim wipes.

B.3.5 1.5% agarose gel

0.15g of agarose per 10ml 1 x TAE were mixed and microwave to dissolve agarose. SYBR Safe was added (0.1ul per ml of agarose gel solution) and the solution allowed cooling to about 50^oC. The gel was then poured into a gel tray and left to set for 30mins prior to use.

B.3.6 2% agarose gel

1g of agarose per 50ml 1 x TAE were mixed and microwave to dissolve agarose. SYBR Safe was added (0.1ul per ml of gel agarose solution) and the solution allowed cooling to about 50^{o}C. The gel was then poured into a gel tray and left to set for 30mins prior to use.

B.4 CHAPTER 5: RNA INTERFERENCE & ASSOCITED METHODS

B.4.1 1 X siRNA buffer

One part 5 X siRNA buffer (Dharmacon, catalogue number B-002000-UB-100) was mixed with four parts RNase-free NPH_2O (Gibco, catalogue number 10977-023).

APPENDIX C

GRK5 cDNA SEQUENCE WITH CANDIDATE PRIMER ALIGNMENT

GRK5 cDNA* sequence with the following GRK5-directed primers aligned: Vgt, ZhC, RTP, PB1, PB2, PB3, MG1, MG2, MG3.

* The GRK5 cDNA sequence was obtained by converting the mRNA sequence using Sequence Editor software available at **http://www.fr33.net/seqedit.php**. The GRK5 mRNA sequence and exon information was retrieved from the NCBI database at **http://www.ncbi.nlm.nih.gov/nucleotide/51896033** .

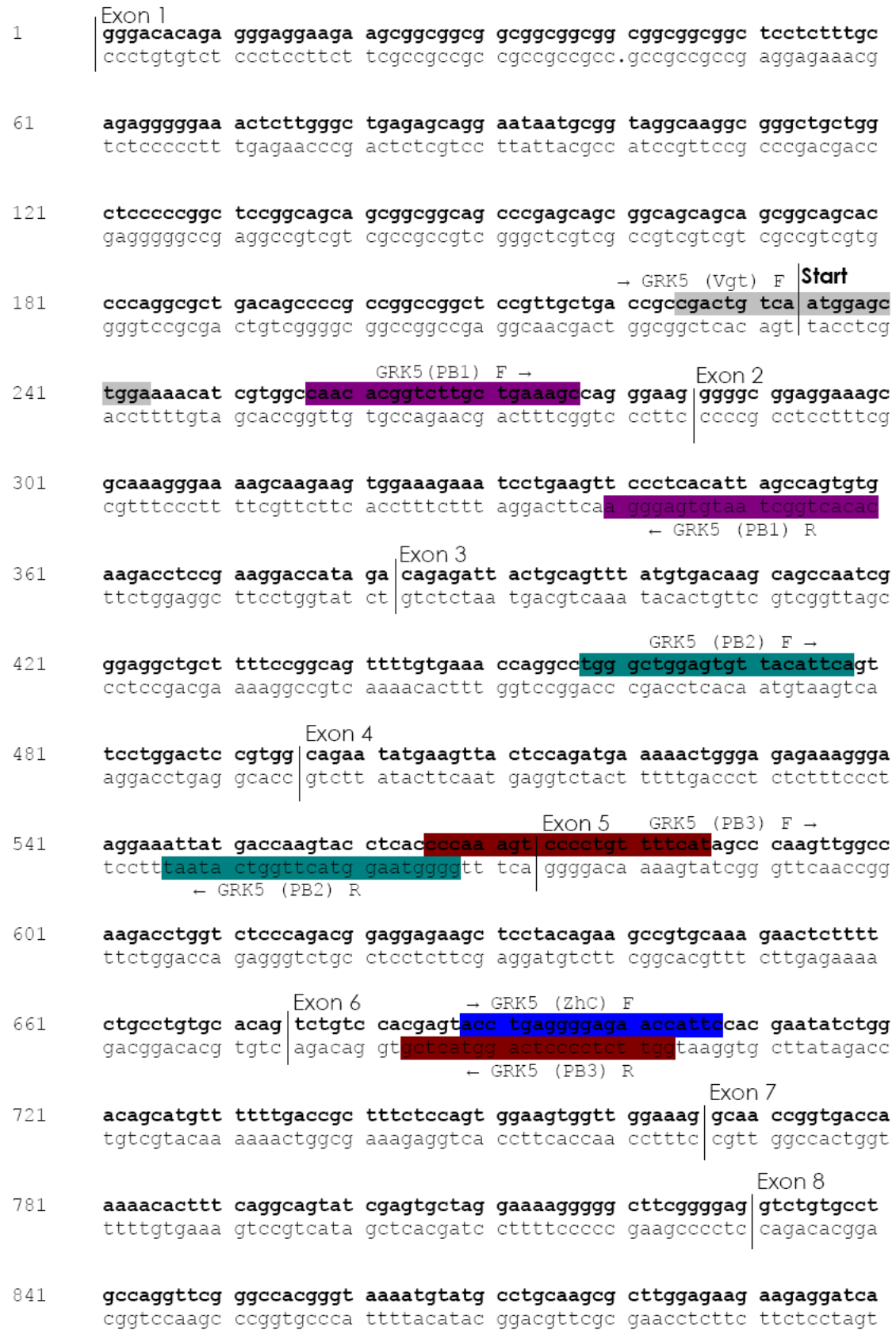
Exon 1
1
gggacacaga gggaggaaga agcggcggcg gcggcggcgg cggcggcggc tcctctttgc
ccctgtgtct ccctccttct tcgccgccgc cgccgccgcc.gccgccgccg aggagaaacg
61
agaggggaa actcttgggc tgagagcagg aataatgcgg taggcaaggc gggctgctgg
tctccccctt tgagaacccg actctcgtcc ttattacgcc atccgttccg cccgacgacc
121
ctcccccggc tccggcagca gcggcggcag cccgagcagc ggcagcagca gcggcagcac
gaggggggccg aggccgtcgt cgccgccgtc gggctcgtcg ccgtcgtcgt cgccgtcgtg
→ GRK5 (Vgt) F
Start
181
cccaggcgct gacagccccg ccggccggct ccgttgctga ccgccgactg tca atggagc
gggtccgcga ctgtcggggc ggccggccga ggcaacgact ggcggctcac agt tacctcg
GRK5(PB1) F →
Exon 2
241
tggaaaacat cgtggccaac acggtcttgc tgaaagccag ggaag ggggc ggaggaaagc
acctttgta gcaccggttg tgccagaacg actttcggtc ccttc ccccg cctcctttcg
301
gcaaagggaa aagcaagaag tggaaagaaa tcctgaagtt ccctcacatt agccagtgtg
cgtttccctt ttcgttcttc acctttcttt aggacttcaa gggagtgtaa tcggtcacac
← GRK5 (PB1) R
Exon 3
361
aagacctccg aaggaccata ga cagagatt actgcagttt atgtgacaag cagccaatcg
ttctggaggc ttcctggtat ct gtctctaa tgacgtcaaa tacactgttc gtcggttagc
GRK5 (PB2) F →
421
ggaggctgct ttccggcag ttttgtgaaa ccaggcctgg gctggagtgt tacattcagt
cctccgacga aaaggccgtc aaaacacttt ggtccggacc cgacctcaca atgtaagtca
Exon 4
481
tcctggactc cgtgg cagaa tatgaagtta ctccagatga aaaactggga gagaaaggga
aggacctgag gcacc gtctt atacttcaat gaggtctact ttttgaccct ctctttccct
Exon 5
GRK5 (PB3) F →
541
aggaaattat gaccaagtac ctcaccccaa agt ccctgt tttcatagcc caagttggcc
tcctttaata ctggttcatg gaatggggtt tca ggggaca aaagtatcgg gttcaaccgg
← GRK5 (PB2) R
601
aagacctggt ctcccagacg gaggagaagc tcctacagaa gccgtgcaaa gaactctttt
ttctggacca gagggtctgc ctcctcttcg aggatgtctt cggcacgttt cttgagaaaa
Exon 6
→ GRK5 (ZhC) F
661
ctgcctgtgc acag tctgtc cacgagtacc tgaggggaga accattccac gaatatctgg
gacggacacg tgtc agacag gtgctcatgg actcccctct tgctaaggtg cttatagacc
← GRK5 (PB3) R
Exon 7
721
acagcatgtt ttttgaccgc tttctccagt ggaagtggtt ggaaag gcaa ccggtgacca
tgtcgtacaa aaaactggcg aaagaggtca ccttcaccaa cctttc cgtt ggccactggt
Exon 8
781
aaaacacttt caggcagtat cgagtgctag gaaaaggggg cttcggggag gtctgtgcct
ttttgtgaaa gtccgtcata gctcacgatc cttttccccc gaagcccctc cagacacgga
841
gccaggttcg ggccacgggt aaaatgtatg cctgcaagcg cttggagaag aagaggatca
cggtccaagc ccggtgccca ttttacatac ggacgttcgc gaacctcttc ttctcctagt


→ GRK5(MG)F
901 aaaagaggaa aggggagtcc atggccctca atgagaagca gatcctcgag aaggtcaaca
ttttctcctt tcccctcagg taccgggagt tactcttcgt ctaggagctc ttccagttgt
← GRK5(ZhC) R
Exon 9
961 gtcagtttgt g|gtcaacctg gcctatgcct acgagaccaa ggatgcactg tgcttggtcc
cagtcaaaca c|cagttggac cggatacgga tgctctggtt cctacgtgac acgaaccagg
1021 tgaccatcat gaatgggggt gacctgaagt tccacatcta caacatgggc aaccctggct
actggtagta cttaccccca ctggacttca aggtgtagat gttgtacccg ttgggaccga
1081 tcgaggagga gcgggccttg ttttatgcgg cagagatcct ctgcggctta gaagacctcc
agctcctcct cgcccggaac aaaatacgcc gtctctagga gacgccgaat cttctggagg
← GRK5 (MG)R
Exon 10
1141 accgtgagaa caccgtctac cg|agatctga aacctgaaaa catcctgtta gatgattatg
tggcactctt gtggcagatg gc|tctagact ttggactttt gtaggacaat ctactaatac
Exon 11
1201 gccacattag gatctcagac ctgggcttgg ctgtgaagat ccccgaggga gacctgatcc
cggtgtaatc ctagagtctg gacccgaacc gacacttcta ggggctccct ctggactagg
Exon 12
1261 gcggccgggt gggcactgtt ggctacatgg|ctccagaggt cctgaacaac cagaggtacg
cgccggccca cccgtgacaa ccgatgtacc|gaggtctcca ggacttgttg gtctccatgc
1321 gcctgagccc cgactactgg ggccttggct gcctcatcta tgagatgatc gagggccagt
cggactcggg gctgatgacc ccggaaccga cggagtagat actctactag ctcccggtca
1381 cgccgttccg cggccgcaag gagaaggtga agcgggagga ggtggaccgc cgggtcctgg
gcggcaaggc gccggcgttc ctcttccact tcgccctcct ccacctggcg gcccaggacc
Exon 13
1441 agacggagga ggtgtactcc cacaagttct ccgaggaggc caagtccatc tgcaagatg|c
tctgcctcct ccacatgagg gtgttcaaga ggctcctccg gttcaggtag acgttctac|g
GRK5 (MG1)→ F
1501 tgctcacgaa agatgcgaag cagaggctgg gctgccagga ggaggggct gcagaggtca
acgagtgctt tctacgcttc gtctccgacc cgacggtcct cctcccccga cgtctccagt
1561 agagacaccc cttcttcagg aacatgaact tcaagcgctt agaagccggg atgttggacc
tctctgtggg gaagaagtcc ttgtacttga agttcgcgaa tcttcggccc tacaacctgg
Exon 14
1621 ctcccttcgt tccagac|ccc cgcgctgtgt actgtaagga cgtgctggac atcgagcagt
gagggaagca aggtctg|ggg gcgcgacaca tgacattcct gcacgacctg tagctcgtca
→ GRK5 (RTP) F
1681 tctccactgt gaagggcgtc aatctggacc acacagacga cgacttctac tccaagttct
agaggtgaca cttcccgcag ttagacctgg tgtgtctgct gctgaagatg aggttcaaga
Exon 15
1741 ccacgggctc tgtgtccatc ccatggcaaa acgag|atgat agaaacagaa tgctttaagg
ggtgcccgag acacaggtag ggtaccgttt tgctc|tacta tctttgtctt acgaaattcc
← GRK5 (RTP) R


1801
agctgaacgt gtttggacct aatggtaccc tcccgccaga tctgaacaga aaccaccctc
tcgacttgca caaacctgga ttaccatggg agggcggtct agacttgtct ttggtgggag
← GRK5 (MG1)R
Exon 16
1861
cggaaccgcc caagaaaggg ctgctccaga gactcttcaa gcggcag|cat cagaacaatt
gccttggcgg gttctttccc gacgaggtct ctgagaagtt cgccgtc|gta gtcttgttaa
GRK5 (MG2)→
1921
ccaagagttc gcccagctcc aagaccagtt ttaaccacca cataaactca aaccatgtca
ggttctcaag cgggtcgagg ttctggtcaa aattggtggt gtatttgagt ttggtacagt
Stop
1981
gctcgaactc caccggaagc agc|tagtttc ggctctggcc tccaagtcca cagtggaacc
cgagcttgag gtggccttcg tcg|atcaaag ccgagaccgg aggttcaggt gtcaccttgg
← GRK5(Vgt) R
2041
agcccagacc cttctcctta gaagtggaag tagtggagcc cctgctctgg tggggctgcc
tcgggtctgg gaagaggaat cttcaccttc atcacctcgg ggacgagacc accccgacgg
2101
aggggagacc ccgggagccg gggaaggagg ccgtccatcc cgtcgacgta gaacctcgag
tcccctctgg ggccctcggc cccttcctcc ggcaggtagg gcagctgcat cttggagctc
2161
gtttctcaaa gaaatttcca ctcaggtctg ttttccgagg cggccccggc cggggtggat
caaagagttt ctttaaaggt gagtccagac aaaaggctcc gccggggccg gccccaccta
2221
tggatttgtc tttggtgaac attgcaatag aaatccaa|tt ggatacgaca acttgcacgt
acctaaacag aaaccacttg taacgttatc tttaggtt|aa cctatgctgt tgaacgtgca
← GRK5 (MG2) R
2281
attttaatag cgtcataact agaactgaat tttgtcttta tgatttttaa agaaaagttt
taaaattatc gcagtattga tcttgactta aaacagaaat actaaaaatt tcttttcaaa
2341
tgtaaatttc tctactgtct cagtttacat tttgtatatt tgtatttaaa tgaaagtgag
acatttaaag agatgacaga gtcaaatgta aaacatataa acataaattt actttcactc
2401
actttgaggg tgtatatttt ctgtgcagcc actgttaagc catgtgttcc aaggcatttt
tgaaactccc acatataaaa gacacgtcgg tgacaattcg gtacacaagg ttccgtaaaa
2461
agcggggagg gggttatcaa aaaaaaaaaa atgtgactca agacttccag agcctcaaat
tcgcccctcc cccaatagtt ttttttttt tacactgagt tctgaaggtc tcggagttta
2521
gagaaaatgt ctttattaaa tgtagaaagt gatccataaa aaaaaaaaaa aaaaa
ctcttttaca gaaataattt acatctttca ctaggtattt ttttttttt ttttt

APPENDIX D

qPCR RAW DATA FROM STANDARD CURVE GENERATION

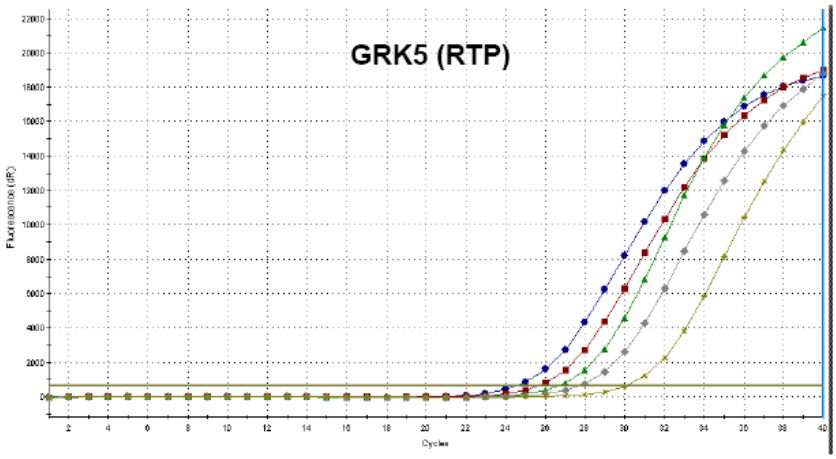
GRK5 (RTP)
Cycles

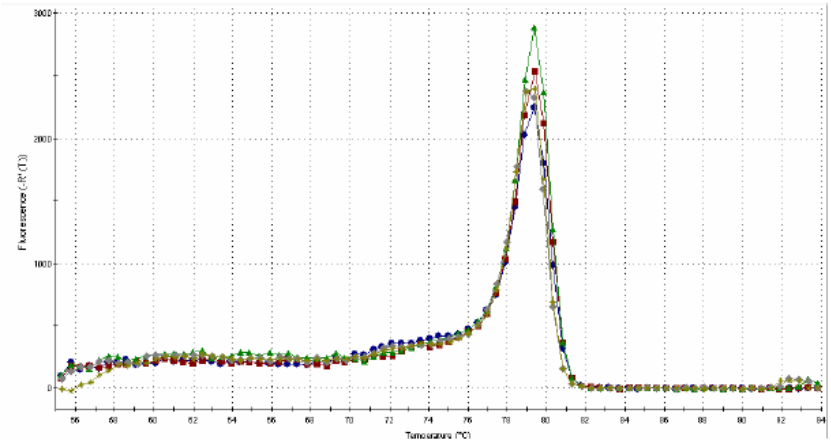
Temperature (°C)

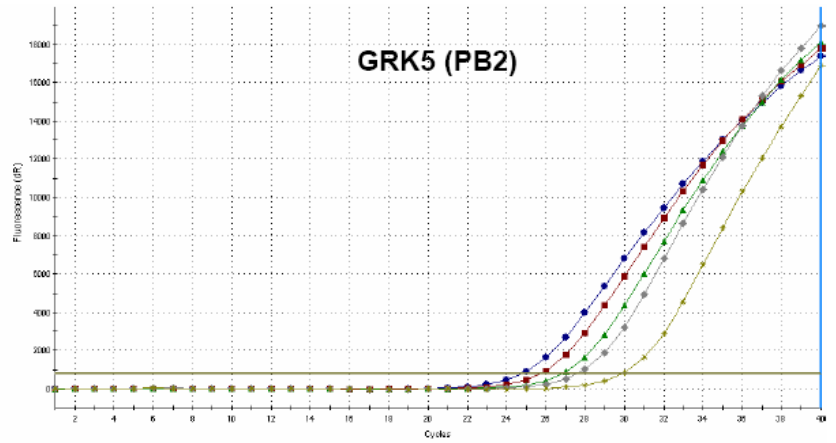
GRK5 (PB2)
Cycles

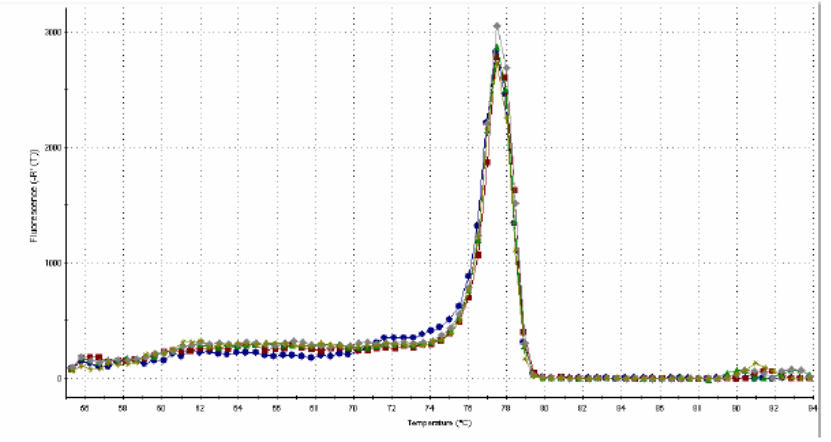
Temperature (°C)

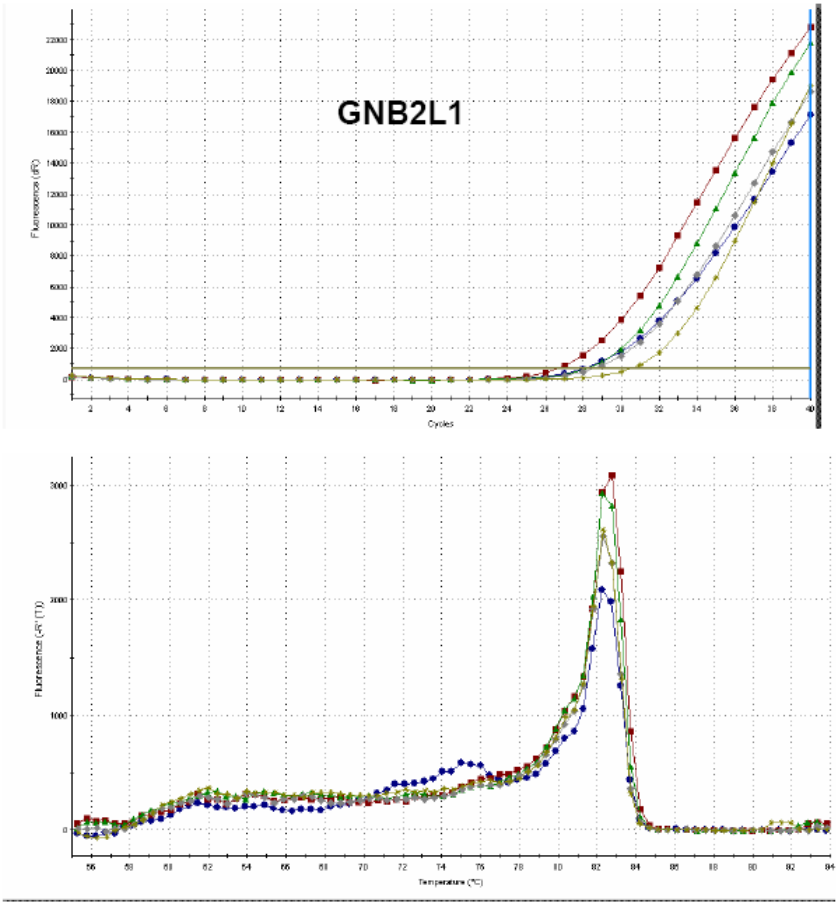
GNB2L1
Fluorescence (dR)
Cycles
Fluorescence (-R' (T))
Temperature (°C)

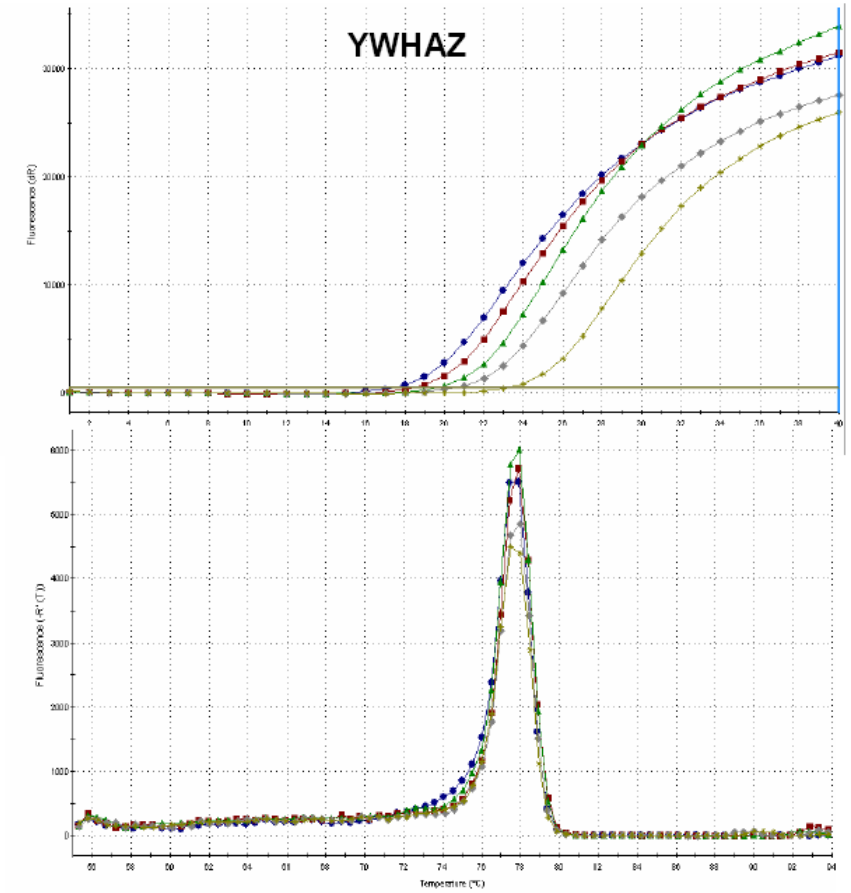
YWHAZ
Fluorescence (dR)
Fluorescence (-R' (T))
Temperature (°C)

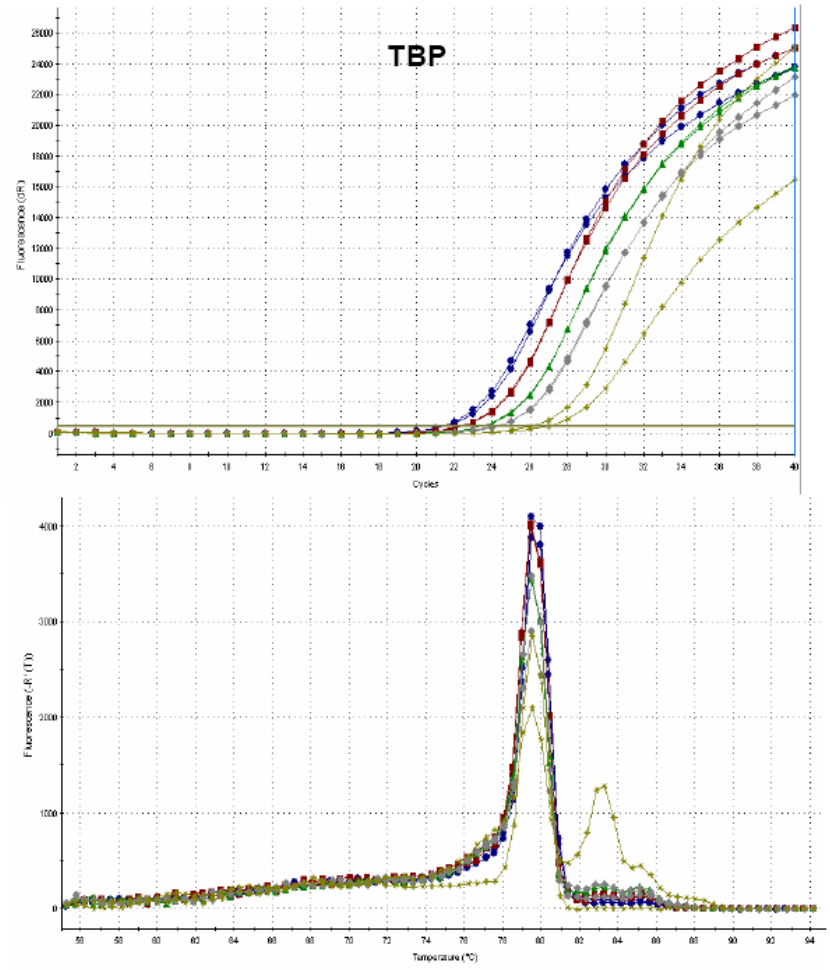
TBP
Fluorescence (dR)
Cycles
Fluorescence (-R' (T))
Temperature (°C)

APPENDIX E

SEQUENCED QRT-PCR PRODUCTS WITH PRIMERS ALIGNED

GRK5

F: GACCACACAGACGACGACTTC
CTGGTGTGTCTGCTGCTGAAG

R: CGTTCAGCTCCTTAAAGCATTC
GCAAGTCGAGGAATTTCGTAAG

>G1
CGTTCAGCTCCTTAAAGCATTCTGTTTCTATCATCTCGTTTTGCCATGGGATGGACACAGAGCCCGTGGAGAACTTGGAGTAGAAGTCGTC
Size: 103bp
>G2
CGTTCAGCTCCTTAAAGCATTCTGTTTCTATCATCTCGTTTTGCCATGGGATGGACACAGAGCCCGTGGAGAACTTGGAGTAGAAGTCGTC
Size: 103bp

TBP

F:TGCACAGGAGCCAAGAGTGAA
ACGTGTCCTCGGTTCTCACTT

R: CACATCACAGCTCCCCACCA
GTGTAGTGTCGAGGGGTGGT

>T2
CACATCACAGCTCCCCACCACCTCCTTCTTGTTCACTCTTGGCTCCTGTGCA Size: 52bp

>T3
TGCACAGGAGCCAAGAGTGAAGAACAGTCCAGACTGGCAGCAAGAAAATATGCTAGAGTTGTACAGAAGTTGGGTTTTCCAGCTAGGTTC
Size:132bp

YWHAZ

F:ACTTTTGGTACATTGTGGCTTCAA
TGAAAACCATGTAACACCGAAGTT

R: CCGCCAGGACAAACCAGTAT
GGCGGTCCTGTTTGGTCATA

>Y3
ACTTTTGGTACATTGTGGCTTCAAAAGGGCCAGTGTAAAACTGCTCCCATGTCTAAGCAAAGAAAACTGCCTACATACTGGTTTGTCCTGG
94bp

>Y4
ACTTTTGGTACATTGTGGCTTCAATACTGGTTTGTCCTGGCGG Size: 43bp

APPENDIX F

PRIMER DETAILS, PREDICTED PRODUCTS AND SECONDARY STRUCTURES

Primer Set Name: ACTB
Source: Metaye et al. (2002)

Details:
Product Length: 131bp

	Forward	Reverse
Sequence	TCCCTGGAGAAGAGCTACG	GTAGTTTCGTGGATGCCACA
Length (bp)	19	20
T_m (^oC)	54.5	55.2
GC content (%)	57.9	50

Predicted Secondary Structures:
Homodimers:

Forward		Reverse	
Configuration	**ΔG**	**Configuration**	**ΔG**
5' TCCCTGGAGAAGAGCTACG 3' |||| 3' GCATCGAGAAGAGGTCCCT 5'	-3.0	5' GTAGTTTCGTGGATGCCACA 3' |||| ¦¦¦¦ 3' ACACCGTAGGTGCTTTGATG 5'	-3.2
5' TCCCTGGAGAAGAGCTACG 3' ||| ¦¦¦ 3' GCATCGAGAAGAGGTCCCT 5'	-1.3		

Heterodimers:

Configuration	ΔG
5' TCCCTGGAGAAGAGCTACG 3' ¦ ¦ ||| 3' ACACCGTAGGTGCTTTGATG 5'	-1.9
5' TCCCTGGAGAAGAGCTACG 3' ¦ ¦ ¦ ¦¦¦¦ 3' ACACCGTAGGTGCTTTGATG 5'	-1.8
5' TCCCTGGAGAAGAGCTACG 3' ||| ¦ ¦ 3' ACACCGTAGGTGCTTTGATG 5'	-1.5
5' TCCCTGGAGAAGAGCTACG 3' ||| ¦ ¦ 3' ACACCGTAGGTGCTTTGATG 5'	-1.3

5' TCCCTGGAGAAGAGCTACG 3' 3' ACACCGTAGGTGCTTTGATG 5'	-0.6

Hairpins/Loops

Forward		Reverse	
Configuration	**-ΔG**	**Configuration**	**-ΔG**
None	NA	/AGGTGCTTTGATG 5' T |||| \GCCACA 3'	-3.2

Primer Set Name: GADPH
Source: Vandesompele et al. (2002)

Details:
Product length: 87 bp

	Forward	Reverse
Sequence	TGCACCACCAACTGCTTAGC	GGCATGGACTGTGGTCATGAG
Length (bp)	20	21
T_m (°C)	58.1	58.2
GC content (%)	55.0	57.1

Predicted Secondary Structures:
Homodimers:

Forward		Reverse	
Configuration	**ΔG**	**Configuration**	**ΔG**
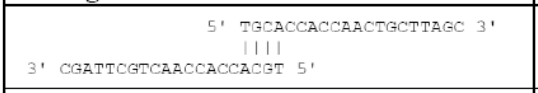	-3.4	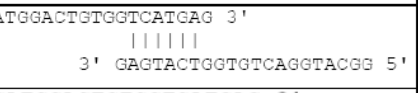	-4.9
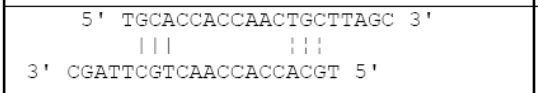	-2.0	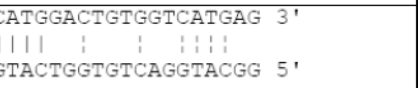	-2.3
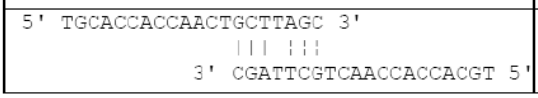	-1.8	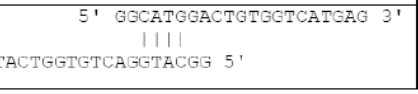	-2.3

Heterodimers:

Configuration	ΔG
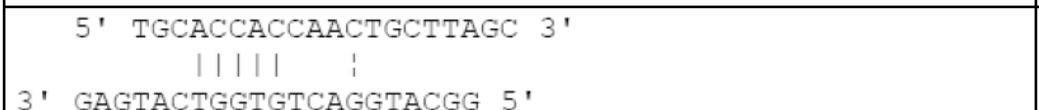	-4.7
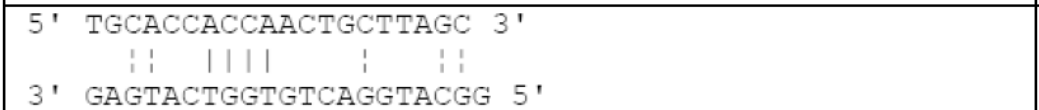	-2.9
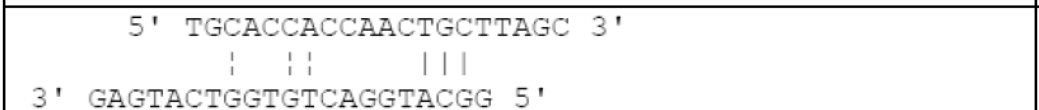	-2.0
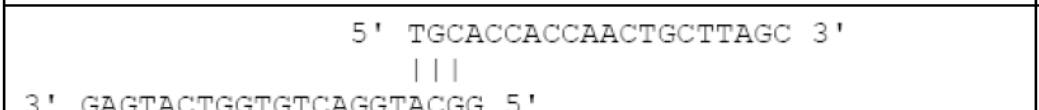	-2.0
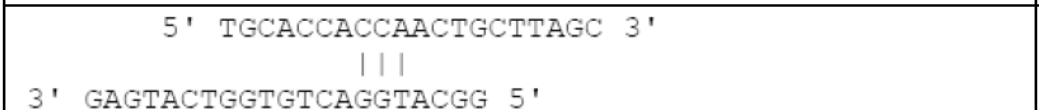	-1.5

5' TGCACCACCAACTGCTTAGC 3' ||| 3' GAGTACTGGTGTCAGGTACGG 5'	-1.5
5' TGCACCACCAACTGCTTAGC 3' ||| ¦ ¦ ¦ 3' GAGTACTGGTGTCAGGTACGG 5'	-1.3

Hairpins/Loops

Forward		**Reverse**	
Configuration	**ΔG**	**Configuration**	**ΔG**
/CACCACGT 5' | ||| \CAACTGCTTAGC 3'	-2.0	/TCAGGTACGG 5' G ¦ |||| \TGGTCATGAG 3'	-2.3
None	NA	/GTCAGGTACGG 5' | ||| \TGGTCATGAG 3'	-1.1

Primer Set Name: GNB2L1
Source:

Details:
Product length: 138 bp

	Forward	Reverse
Sequence	CACAACGGGCACCACCAC	CACACACCCAGGGTATTCCAT
Length (bp)	18	21
T_m (°C)	58.0	56.9
GC content (%)	66.7	52.4

Predicted Secondary Structures:
Homodimers:

Forward		Reverse	
Configuration	**ΔG**	**Configuration**	**ΔG**
		5' CACACACCCAGGGTATTCCAT 3' 3' TACCTTATGGGACCCACACAC 5'	-3.4

Heterodimers:

Configuration	ΔG
5' CACAACGGGCACCACCAC 3' 3' TACCTTATGGGACCCACACAC 5'	-2.0
5' CACAACGGGCACCACCAC 3' 3' TACCTTATGGGACCCACACAC 5'	-1.5
5' CACAACGGGCACCACCAC 3' 3' TACCTTATGGGACCCACACAC 5'	-1.5

Hairpins/Loops

Forward		Reverse	
Configuration	**ΔG**	**Configuration**	**ΔG**
		/CCCACACAC 5' A ||| ¦ \GGGTATTCCAT 3'	-1.5

Primer Set Name: HMBS
Source: Vandesompele et al (2002)

Details:
Product length: 523 bp

	Forward	Reverse
Sequence	GGCAATGCGGCTGCAA	GGGTACCCACGCGAATCAC
Length (bp)	16	19
T_m (°C)	54.7	57.6
GC content (%)	62.5	63.2

Predicted Secondary Structures:
Homodimers:

Forward		Reverse	
Configuration	**ΔG**	**Configuration**	**ΔG**
5' GGCAATGCGGCTGCAA 3' |||| 3' AACGTCGGCGTAACGG 5'	-3.4	5' GGGTACCCACGCGAATCAC 3' |||||||| 3' CACTAAGCGCACCCATGGG 5'	-9.7
5' GGCAATGCGGCTGCAA 3' ||| ||| 3' AACGTCGGCGTAACGG 5'	-2.0	5' GGGTACCCACGCGAATCAC 3' |||| 3' CACTAAGCGCACCCATGGG 5'	-5.2
5' GGCAATGCGGCTGCAA 3' ||| ||| 3' AACGTCGGCGTAACGG 5'	-2.0		
5' GGCAATGCGGCTGCAA 3' ||| || ||| 3' AACGTCGGCGTAACGG 5'	-2.0		

Heterodimers:

Configuration	ΔG
5' GGCAATGCGGCTGCAA 3' | ||| | | 3' CACTAAGCGCACCCATGGG 5'	-2.9

Hairpins/Loops

Forward		Reverse	
Configuration	**ΔG**	**Configuration**	**ΔG**
/GGCGTAACGG 5' | ||| \CTGCAA 3'	-2.0		
/GTAACGG 5' C ||| \GGCTGCAA 3'	-2.0		

Primer Set Name: HPRT1
Source: Vandesompele et al. (2002)

Details:
Product length: 94bp

	Forward	Reverse
Sequence	TGACACTGGCAAAACAATGCA	GGTCCTTTTCACCAGCAAGCT
Length (bp)	21	21
T_m (°C)	56.7	58.3
GC content (%)	42.9	52.4

Predicted Secondary Structures:
Homodimers:

Forward		Reverse	
Configuration	**ΔG**	**Configuration**	**ΔG**
5' TGACACTGGCAAAACAATGCA 3' |||| 3' ACGTAACAAAACGGTCACAGT 5'	-3.4	5' GGTCCTTTTCACCAGCAAGCT 3' |||| 3' TCGAACGACCACTTTTCCTGG 5'	-3.0
5' TGACACTGGCAAAACAATGCA 3' ||| ¦¦¦ 3' ACGTAACAAAACGGTCACAGT 5'	-2.0	5' GGTCCTTTTCACCAGCAAGCT 3' ||| ¦¦¦ 3' TCGAACGACCACTTTTCCTGG 5'	-1.8
		5' GGTCCTTTTCACCAGCAAGCT 3' ||| ¦¦¦ 3' TCGAACGACCACTTTTCCTGG 5'	-1.5
		5' GGTCCTTTTCACCAGCAAGCT 3' ||| ¦¦¦ 3' TCGAACGACCACTTTTCCTGG 5'	-0.5

Heterodimers:

Configuration	ΔG
5' TGACACTGGCAAAACAATGCA 3' |||| ¦¦¦ ¦ 3' TCGAACGACCACTTTTCCTGG 5'	-3.0
5' TGACACTGGCAAAACAATGCA 3' ¦ ||| 3' TCGAACGACCACTTTTCCTGG 5'	-2.0
5' TGACACTGGCAAAACAATGCA 3' ¦ |||| ¦ 3' TCGAACGACCACTTTTCCTGG 5'	-1.3
5' TGACACTGGCAAAACAATGCA 3' ||| 3' TCGAACGACCACTTTTCCTGG 5'	-1.1

5' TGACACTGGCAAAACAATGCA 3' ||| ¦ ¦ ¦ 3' TCGAACGACCACTTTTCCTGG 5'	-0.9
5' TGACACTGGCAAAACAATGCA 3' ¦ ¦ ¦ ||| ¦ 3' TCGAACGACCACTTTTCCTGG 5'	-0.1

Hairpins/Loops

Forward		**Reverse**	
Configuration	**ΔG**	**Configuration**	**ΔG**
/AAAACGGTCACAGT 5' | ||| \CAATGCA 3'	-2.0	/TCCTGG 5' T ||| \TTCACCAGCAAGCT 3'	-1.5
		/ACTTTTCCTGG 5' C ||| \CAGCAAGCT 3'	-0.5

Primer Set Name: PPIB
Source: Unpublished. Eccles Laboratory, University of Otago

Details:
Product length: 106 bp

	Forward	Reverse
Sequence	ATGATCCAGGGCGGAGACTT	CAGGCCCGTAGTGCTTCAG
Length (bp)	20	19
T_m (^oC)	57.6	57.2
GC content (%)	55.0	63.2

Predicted Secondary Structures:
Homodimers:

Forward		Reverse	
Configuration	**ΔG**	**Configuration**	**ΔG**
5' ATGATCCAGGGCGGAGACTT 3' |||| 3' TTCAGAGGCGGGACCTAGTA 5'	-2.0	5' CAGGCCCGTAGTGCTTCAG 3' ¦ |||| ¦ 3' GACTTCGTGATGCCCGGAC 5'	-4.4
5' ATGATCCAGGGCGGAGACTT 3' ¦ ||| ¦¦¦ ¦ 3' TTCAGAGGCGGGACCTAGTA 5'	-1.3		

Heterodimers:

Configuration	ΔG
5' ATGATCCAGGGCGGAGACTT 3' ¦ ¦ |||| 3' GACTTCGTGATGCCCGGAC 5'	-4.4
5' ATGATCCAGGGCGGAGACTT 3' ¦¦¦ ¦¦ ||| 3' GACTTCGTGATGCCCGGAC 5'	-2.4
5' ATGATCCAGGGCGGAGACTT 3' ||| 3' GACTTCGTGATGCCCGGAC 5'	-0.8

Hairpins/Loops

Forward		Reverse	
Configuration	**ΔG**	**Configuration**	**ΔG**
/GACCTAGTA 5' G ||| ¦ \GCGGAGACTT 3'	-1.3		

Primer Set Name: RPL13A
Source: Vandesompele et al. (2002)

Details:
Product length: 127 bp

	Forward	Reverse
Sequence	CCTGGAGGAGAAGAGGAAAGAGA	TTGAGGACCTCTGTGTATTTGTCAA
Length (bp)	23	25
T_m (°C)	58.2	58.2
GC content (%)	52.2	40

Predicted Secondary Structures:
Homodimers:

Forward		Reverse	
Configuration	**ΔG**	**Configuration**	**ΔG**
5' CCTGGAGGAGAAGAGGAAAGAGA 3' 3' AGAGAAAGGAGAAGAGGAGGTCC 5'	-1.3	5' TTGAGGACCTCTGTGTATTTGTCAA 3' 3' AACTGTTTATGTGTCTCCAGGAGTT 5'	-2.9
5' CCTGGAGGAGAAGAGGAAAGAGA 3' ' AGAGAAAGGAGAAGAGGAGGTCC 5'	-1.3	5' TTGAGGACCTCTGTGTATTTGTCAA 3' 3' AACTGTTTATGTGTCTCCAGGAGTT 5'	-2.0
		5' TTGAGGACCTCTGTGTATTTGTCAA 3' 3' AACTGTTTATGTGTCTCCAGGAGTT 5'	-1.1
		' TTGAGGACCTCTGTGTATTTGTCAA 3' 3' AACTGTTTATGTGTCTCCAGGAGTT 5	-0.7

Hairpins/Loops

Forward		Reverse	
Configuration	**ΔG**	**Configuration**	**ΔG**
/GGAGGTCC 5' | ||| \AGAAGAGGAAAGAGA 3'	-1.3	/TCTCCAGGAGTT 5' G ¦ ¦ |||| \TGTATTTGTCAA 3'	-2.0
		/TGTCTCCAGGAGTT 5' | ¦ ||| \GTATTTGTCAA 3'	-1.1
		/GGAGTT 5' A ||| \CCTCTGTGTATTTGTCAA 3'	-1.0

Primer Set Name: SDHA
Source: Vandesompele et al. (2002)

Details:
Product length: 86 bp

	Forward	Reverse
Sequence	TGGGAACAAGAGGGCATCTG	CCACCACTGCATCAAATTCATG
Length (bp)	20	22
T_m (^oC)	56.6	56.0
GC content (%)	55.0	45.5

Predicted Secondary Structures:
Homodimers:

Forward		Reverse	
Configuration	**ΔG**	**Configuration**	**ΔG**
5' TGGGAACAAGAGGGCATCTG 3' 3' GTCTACGGGAGAACAAGGGT 5	-0.7	5' CCACCACTGCATCAAATTCATG 3' 3' GTACTTAAACTACGTCACCACC 5'	-3.4
		5' CCACCACTGCATCAAATTCATG 3' 3' GTACTTAAACTACGTCACCACC 5'	-2.3
		5' CCACCACTGCATCAAATTCATG 3' 3' GTACTTAAACTACGTCACCACC 5'	-1.1
		5' CCACCACTGCATCAAATTCATG 3' 3' GTACTTAAACTACGTCACCACC 5'	-0.5

Heterodimers:

Configuration	ΔG
5' TGGGAACAAGAGGGCATCTG 3' 3' GTACTTAAACTACGTCACCACC 5'	-2.0
5' TGGGAACAAGAGGGCATCTG 3' 3' GTACTTAAACTACGTCACCACC 5'	-1.5
5' TGGGAACAAGAGGGCATCTG 3' 3' GTACTTAAACTACGTCACCACC 5'	-1.5
5' TGGGAACAAGAGGGCATCTG 3' 3' GTACTTAAACTACGTCACCACC 5'	-0.6

5' TGGGAACAAGAGGGCATCTG 3' ||| 3' GTACTTAAACTACGTCACCACC 5'	-0.5

Hairpins/Loops

Forward		Reverse	
Configuration	**ΔG**	**Configuration**	**ΔG**
/GGAGAACAAGGGT 5' G ||| \CATCTG 3'	-0.7	/AACTACGTCACCACC 5' A ¦ ||| \TTCATG 3'	-0.5

Primer Set Name: TBP
Source: Dallol et al., 2002

Details:
Product length: 132 bp

	Forward	Reverse
Sequence	TGCACAGGAGCCAAGAGTGAA	CACATCACAGCTCCCCACCA
Length (bp)	21	20
T_m (^oC)	59.1	59.0
GC content (%)	52.4	60

Predicted Secondary Structures:
Homodimers:

Forward		Reverse	
Configuration	**ΔG**	**Configuration**	**ΔG**
5' TGCACAGGAGCCAAGAGTGAA 3' |||| 3' AAGTGAGAACCGAGGACACGT 5'	-3.4	5' CACATCACAGCTCCCCACCA 3' |||| 3' ACCACCCCTCGACACTACAC 5'	-3.0
5' TGCACAGGAGCCAAGAGTGAA 3' ¦ ||| ¦ ¦ ¦|| ¦ 3' AAGTGAGAACCGAGGACACGT 5'	-1.3		

Heterodimers:

Configuration	ΔG
5' TGCACAGGAGCCAAGAGTGAA 3' ¦¦ ||||| ¦¦ 3' ACCACCCCTCGACACTACAC 5'	-5.3
5' TGCACAGGAGCCAAGAGTGAA 3' ¦ ¦ ¦ |||| 3' ACCACCCCTCGACACTACAC 5'	-2.6
5' TGCACAGGAGCCAAGAGTGAA 3' ||| 3' ACCACCCCTCGACACTACAC 5'	-1.3
5' TGCACAGGAGCCAAGAGTGAA 3' ¦ ¦ ||| 3' ACCACCCCTCGACACTACAC 5'	-1.3
5' TGCACAGGAGCCAAGAGTGAA 3' ¦ ||| 3' ACCACCCCTCGACACTACAC 5'	-1.0

Hairpins/Loops

Forward		Reverse	
Configuration	**ΔG**	**Configuration**	**ΔG**
/GAGGACACGT 5' C ||| ¦ \CAAGAGTGAA 3'	-1.3	None	NA

Primer Set Name: UBC
Source: Vandesompele et al. (2002)

Details:
Product length: 133 bp

	Forward	Reverse
Sequence	ATTTGGGTCGCGGTTCTTG	TGCCTTGACATTCTCGATGGT
Length (bp)	19	21
T_m (°C)	55.5	59.5
GC content (%)	52.6	47.6

Predicted Secondary Structures:
Homodimers:

Forward		Reverse	
Configuration	**ΔG**	**Configuration**	**ΔG**
5' ATTTGGGTCGCGGTTCTTG 3' 3' GTTCTTGGCGCTGGGTTTA 5'	-5.2	5' TGCCTTGACATTCTCGATGGT 3' 3' TGGTAGCTCTTACAGTTCCGT 5	-3.1
		5' TGCCTTGACATTCTCGATGGT 3' 3' TGGTAGCTCTTACAGTTCCGT 5'	-0.5

Heterodimers:

Configuration	ΔG
5' ATTTGGGTCGCGGTTCTTG 3' 3' TGGTAGCTCTTACAGTTCCGT 5'	-1.8
5' ATTTGGGTCGCGGTTCTTG 3' 3' TGGTAGCTCTTACAGTTCCGT 5'	-1.1

Hairpins/Loops

Forward		Reverse	
Configuration	**ΔG**	**Configuration**	**ΔG**
		/CTTACAGTTCCGT 5' T \CGATGGT 3'	-0.5

Primer Set Name: YWHAZ
Source: Vandesompele et al. (2002)

Details:
Product length: 94 bp

	Forward	Reverse
Sequence	ACTTTTGGTACATTGTGGCTTCAA	CCGCCAGGACAAACCAGTAT
Length (bp)	24	20
T_m (^oC)	57.5	57.0
GC content (%)	37.5	55

Predicted Secondary Structures:
Homodimers:

Forward		Reverse	
Configuration	**ΔG**	**Configuration**	**ΔG**
5' ACTTTTGGTACATTGTGGCTTCAA 3' 3' AACTTCGGTGTTACATGGTTTTCA 5'	-2.0		
5' ACTTTTGGTACATTGTGGCTTCAA 3' 3' AACTTCGGTGTTACATGGTTTTCA 5'	-1.0		
5' ACTTTTGGTACATTGTGGCTTCAA 3' 3' AACTTCGGTGTTACATGGTTTTCA 5	-0.7		
5' ACTTTTGGTACATTGTGGCTTCAA 3' 3' AACTTCGGTGTTACATGGTTTTCA 5'	-0.7		

Heterodimers:

Configuration	ΔG
5' ACTTTTGGTACATTGTGGCTTCAA 3' 3' TATGACCAAACAGGACCGCC 5'	-3.9
5' ACTTTTGGTACATTGTGGCTTCAA 3' 3' TATGACCAAACAGGACCGCC 5'	-2.1
5' ACTTTTGGTACATTGTGGCTTCAA 3' 3' TATGACCAAACAGGACCGCC 5'	-1.8

5' ACTTTTGGTACATTGTGGCTTCAA 3' 3' TATGACCAAACAGGACCGCC 5'	-1.5
5' ACTTTTGGTACATTGTGGCTTCAA 3' 3' TATGACCAAACAGGACCGCC 5'	-1.5
5' ACTTTTGGTACATTGTGGCTTCAA 3' 3' TATGACCAAACAGGACCGCC 5'	-0.8
5' ACTTTTGGTACATTGTGGCTTCAA 3' 3' TATGACCAAACAGGACCGCC 5'	-0.3
5' ACTTTTGGTACATTGTGGCTTCAA 3' 3' TATGACCAAACAGGACCGCC 5'	-0.1

Hairpins/Loops

Forward		Reverse	
Configuration	**ΔG**	**Configuration**	**ΔG**
/GGTGTTACATGGTTTTCA 5' \CTTCAA 3'	-0.7		
/TTACATGGTTTTCA 5' \GTGGCTTCAA 3'	-0.7		

Primer Set Name: GRK5 MG1
Source: Michelle Gatehouse Thesis (2008)

Details:
Product length: 221bp

	Forward	Reverse
Sequence	AAAGAGGAAAGGGGAGTCCA	AGAGGATCTCTGCCGCATAA
Length (bp)	20	20
T_m (°C)	54.7	55.2
GC content (%)	50	50

Predicted Secondary Structures:
Homodimers:

Forward		Reverse	
Configuration	**ΔG**	**Configuration**	**ΔG**
5' AAAGAGGAAAGGGGAGTCCA 3' ||| ¦¦¦ 3' ACCTGAGGGGAAAGGAGAAA 5'	-1.3	5' AGAGGATCTCTGCCGCATAA 3 |||| ¦¦¦¦ 3' AATACGCCGTCTCTAGGAGA 5'	-2.2
5' AAAGAGGAAAGGGGAGTCCA 3' ||| ¦¦¦ 3' ACCTGAGGGGAAAGGAGAAA 5'	-1.3	5' AGAGGATCTCTGCCGCATAA 3' |||| 3' AATACGCCGTCTCTAGGAGA 5'	-2.0
		5' AGAGGATCTCTGCCGCATAA 3' ¦ ||| ¦¦¦ ¦ 3' AATACGCCGTCTCTAGGAGA 5'	-2.0
		5' AGAGGATCTCTGCCGCATAA 3' ||| ¦¦¦ 3' AATACGCCGTCTCTAGGAGA 5'	-0.7

Heterodimers:

Configuration	ΔG
5' AAAGAGGAAAGGGGAGTCCA 3' |||| 3' AATACGCCGTCTCTAGGAGA 5'	-2.2
5' AAAGAGGAAAGGGGAGTCCA 3' ¦ ¦ ¦ ||| 3' AATACGCCGTCTCTAGGAGA 5'	-1.3
5' AAAGAGGAAAGGGGAGTCCA 3' ¦ ||| ¦ 3' AATACGCCGTCTCTAGGAGA 5'	-1.0
5' AAAGAGGAAAGGGGAGTCCA 3' ¦ ||| 3' AATACGCCGTCTCTAGGAGA 5'	-0.7

Hairpins/Loops

Forward		Reverse	
Configuration	**ΔG**	**Configuration**	**ΔG**
/GGAAAGGAGAAA 5' | ||| \GGAGTCCA 3'	-1.3	/GGAGA 5' A |||| \TCTCTGCCGCATAA 3'	-2.2
		/GAGA 5' G ||| \ATCTCTGCCGCATAA 3'	-0.7

Primer Set Name: GRK5 MG2
Source: Michelle Gatehouse Thesis (2008)

Details:
Product length: 360bp

	Forward	Reverse
Sequence	CTGCTCACGAAAGATGCGAA	CGGAGGGTGGTTTCTGTTCA
Length (bp)	20	20
T_m (°C)	56.0	56.8
GC content (%)	50	55

Predicted Secondary Structures:

Heterodimers:

Configuration	ΔG
5' CTGCTCACGAAAGATGCGAA 3' |||| 3' ACTTGTCTTTGGTGGGAGGC 5'	-1.7
5' CTGCTCACGAAAGATGCGAA 3' ||| 3' ACTTGTCTTTGGTGGGAGGC 5'	-1.3
5' CTGCTCACGAAAGATGCGAA 3' ||| 3' ACTTGTCTTTGGTGGGAGGC 5'	-1.0
5' CTGCTCACGAAAGATGCGAA 3' ||| 3' ACTTGTCTTTGGTGGGAGGC 5'	-0.7
5' CTGCTCACGAAAGATGCGAA 3' ||| 3' ACTTGTCTTTGGTGGGAGGC 5'	-0.6
5' CTGCTCACGAAAGATGCGAA 3' ||| 3' ACTTGTCTTTGGTGGGAGGC 5'	-0.6
5' CTGCTCACGAAAGATGCGAA 3' ||| 3' ACTTGTCTTTGGTGGGAGGC 5'	-0.6

Primer Set Name: GRK5 MG3
Source: Michelle Gatehouse Thesis (2008)

Details:
Product length: 290 bp

	Forward	Reverse
Sequence	AACCACCACATAAACTCAAACCA	AATGTTCACCAAAGACAAATCCA
Length (bp)	23	23
T_m (°C)	56.4	54.8
GC content (%)	39.1	34.8

Predicted Secondary Structures:
Homodimers:

Forward		Reverse	
Configuration	**ΔG**	**Configuration**	**ΔG**
		5' AATGTTCACCAAAGACAAATCCA 3' ||| ¦¦¦ 3' ACCTAAACAGAAACCACTTGTAA 5'	-1.0

Heterodimers:

Configuration	ΔG
5' AACCACCACATAAACTCAAACCA 3' |||| 3' ACCTAAACAGAAACCACTTGTAA 5'	-2.0
5' AACCACCACATAAACTCAAACCA 3' ¦ ||| 3' ACCTAAACAGAAACCACTTGTAA 5'	-0.7
5' AACCACCACATAAACTCAAACCA 3' ¦ ||| 3' ACCTAAACAGAAACCACTTGTAA 5'	-0.7
5' AACCACCACATAAACTCAAACCA 3' ||| 3' ACCTAAACAGAAACCACTTGTAA 5'	-0.7

Hairpins/Loops

Forward		Reverse	
Configuration	**ΔG**	**Configuration**	**ΔG**
		/CACTTGTAA 5' C ||| \AAAGACAAATCCA 3'	-1.0

Primer Set Name: GRK5 PB1
Source: Harvard Primer Database

Details:
Product length:

	Forward	Reverse
Sequence	CAACACGGTCTTGCTGAAAGC	CACACTGGCTAATGTGAGGGA
Length (bp)	21	21
T_m (°C)	57.9	56.9
GC content (%)	52.4	52.4

Predicted Secondary Structures:
Homodimers:

Forward		Reverse	
Configuration	**ΔG**	**Configuration**	**ΔG**
5' CAACACGGTCTTGCTGAAAGC 3' 3' CGAAAGTCGTTCTGGCACAAC 5'	-1.8	5' CACACTGGCTAATGTGAGGGA 3' 3' AGGGAGTGTAATCGGTCACAC 5'	-2.7
5' CAACACGGTCTTGCTGAAAGC 3' 3' CGAAAGTCGTTCTGGCACAAC 5'	-0.7	5' CACACTGGCTAATGTGAGGGA 3' 3' AGGGAGTGTAATCGGTCACAC 5'	-1.3
5' CAACACGGTCTTGCTGAAAGC 3' 3' CGAAAGTCGTTCTGGCACAAC 5'	-0.5		

Heterodimers:

Configuration	ΔG
5' CAACACGGTCTTGCTGAAAGC 3' 3' AGGGAGTGTAATCGGTCACAC 5'	-1.8
5' CAACACGGTCTTGCTGAAAGC 3' 3' AGGGAGTGTAATCGGTCACAC 5'	-1.3
5' CAACACGGTCTTGCTGAAAGC 3' 3' AGGGAGTGTAATCGGTCACAC 5'	-1.0

Hairpins/Loops

Forward		Reverse	
Configuration	**ΔG**	**Configuration**	**ΔG**
/GTCGTTCTGGCACAAC 5' A ||| \AAGC 3'		/GGTCACAC 5' | ¦ |||| \CTAATGTGAGGGA 3'	-2.7
/CACAAC 5' G ¦ ||| \GTCTTGCTGAAAGC 3'		/CGGTCACAC 5' | ||| ¦ \TAATGTGAGGGA 3'	-1.3
/CGTTCTGGCACAAC 5' T ||| \GAAAGC 3'			

Primer Set Name: GRK5 PB2
Source: Harvard Primer Database

Details:
Product length: 111bp

	Forward	Reverse
Sequence	TGG GCT GGA GTG TTA CAT TCA	GGG GTG AGG TAC TTG GTC ATA AT
Length (bp)	21	23
T_m (^oC)	56.5	57.2
GC content (%)	47.6	47.8

Predicted Secondary Structures:
Homodimers:

Forward		Reverse	
Configuration	**ΔG**	**Configuration**	**ΔG**
5' TGGGCTGGAGTGTTACATTCA 3' 3' ACTTACATTGTGAGGTCGGGT 5'	-1.0	5' GGGGTGAGGTACTTGGTCATAAT 3' 3' TAATACTGGTTCATGGAGTGGGG 5'	-2.0
		5' GGGGTGAGGTACTTGGTCATAAT 3' 3' TAATACTGGTTCATGGAGTGGGG 5'	-0.9

Heterodimers:

Configuration	ΔG
5' TGGGCTGGAGTGTTACATTCA 3' 3' TAATACTGGTTCATGGAGTGGGG 5'	-0.9
5' TGGGCTGGAGTGTTACATTCA 3' 3' TAATACTGGTTCATGGAGTGGGG 5'	-0.8
5' TGGGCTGGAGTGTTACATTCA 3' 3' TAATACTGGTTCATGGAGTGGGG 5'	-0.3
5' TGGGCTGGAGTGTTACATTCA 3' 3' TAATACTGGTTCATGGAGTGGGG 5'	0.0
5' TGGGCTGGAGTGTTACATTCA 3' 3' TAATACTGGTTCATGGAGTGGGG 5'	0.3

Hairpins/Loops

Forward		Reverse	
Configuration	**ΔG**	**Configuration**	**ΔG**
		/ATGGAGTGGGG 5' C ‖‖ \TTGGTCATAAT 3'	-0.9

Primer Set Name: GRK5 PB3
Source: Harvard Primer Database

Details:
Product length: 138bp

	Forward	Reverse
Sequence	CCCAAAGTCCCCTGTTTTCAT	GGTTCTCCCCTCAGGTACTCG
Length (bp)	21	21
T_m (^oC)	55.6	58.5
GC content (%)	47.6	62

Predicted Secondary Structures:
Homodimers:

Forward		Reverse	
Configuration	**ΔG**	**Configuration**	**ΔG**
5' CCCAAAGTCCCCTGTTTTCAT 3' 3' TACTTTTGTCCCCTGAAACCC 5'	-0.1	5' GGTTCTCCCCTCAGGTACTCG 3' 3' GCTCATGGACTCCCCTCTTGG 5'	-2.0
5' CCCAAAGTCCCCTGTTTTCAT 3' 3' TACTTTTGTCCCCTGAAACCC 5'	-0.1	5' GGTTCTCCCCTCAGGTACTCG 3' 3' GCTCATGGACTCCCCTCTTGG 5'	-1.3

Heterodimers:

Configuration	ΔG
5' CCCAAAGTCCCCTGTTTTCAT 3' 3' GCTCATGGACTCCCCTCTTGG 5'	-3.0
5' CCCAAAGTCCCCTGTTTTCAT 3' 3' GCTCATGGACTCCCCTCTTGG 5'	-0.8

Hairpins/Loops

Forward		Reverse	
Configuration	**ΔG**	**Configuration**	**ΔG**
/CCTGAAACCC 5' C \CTGTTTTCAT 3'	-0.1		
/CCTGAAACCC 5' | \CCTGTTTTCAT 3'	-0.1		

Primer Set Name: GRK5 (RTP)
Source: Metayé et al (2002)

Details:
Product length: 103 bp

	Forward	Reverse
Sequence	GACCACACAGACGACGACTTC	CGTTCAGCTCCTTAAAGCATTC
Length (bp)	21	22
T_m (°C)	58.2	55.5
GC content (%)	57.1	45.5

Predicted Secondary Structures:
Homodimers:

Forward		Reverse	
Configuration	**ΔG**	**Configuration**	**ΔG**
		5' CGTTCAGCTCCTTAAAGCATTC 3' |||| 3' CTTACGAAATTCCTCGACTTGC 5'	-3.0
		5' CGTTCAGCTCCTTAAAGCATTC 3' ||| ||| 3' CTTACGAAATTCCTCGACTTGC 5'	-1.8
		5' CGTTCAGCTCCTTAAAGCATTC 3' | | |||| | | 3' CTTACGAAATTCCTCGACTTGC 5'	-0.8
		5' CGTTCAGCTCCTTAAAGCATTC 3' | ||| ||| | 3' CTTACGAAATTCCTCGACTTGC 5'	-0.5

Heterodimers:

Configuration	ΔG
5' GACCACACAGACGACGACTTC 3' | ||| 3' CTTACGAAATTCCTCGACTTGC 5'	-1.9
5' GACCACACAGACGACGACTTC 3' | | ||| 3' CTTACGAAATTCCTCGACTTGC 5'	-1.9
5' GACCACACAGACGACGACTTC 3' || ||| 3' CTTACGAAATTCCTCGACTTGC 5'	-0.5

Hairpins/Loops

Forward		Reverse	
Configuration	**ΔG**	**Configuration**	**ΔG**
		/TCCTCGACTTGC 5' | ||| \TAAAGCATTC 3'	-1.8

Primer Set Name: GRK5 (Vgt)
Source: Voigt et al (2004)

Details:
Product length: 1789 bp

	Forward	Reverse
Sequence	CGACTGTCAATGGAGCTGGA	GCCGAAACTAGCTGCTTCCG
Length (bp)	20	20
T_m (°C)	56.7	58.7
GC content (%)	55	60

Predicted Secondary Structures:
Homodimers:

Forward		Reverse	
Configuration	**ΔG**	**Configuration**	**ΔG**
5' CGACTGTCAATGGAGCTGGA 3' 3' AGGTCGAGGTAACTGTCAGC 5'	-3.0	5' GCCGAAACTAGCTGCTTCCG 3' 3' GCCTTCGTCGATCAAAGCCG 5'	-3.0
5' CGACTGTCAATGGAGCTGGA 3' 3' AGGTCGAGGTAACTGTCAGC 5'	-1.1	5' GCCGAAACTAGCTGCTTCCG 3' 3' GCCTTCGTCGATCAAAGCCG 5'	-1.8
		5' GCCGAAACTAGCTGCTTCCG 3' 3' GCCTTCGTCGATCAAAGCCG 5'	-1.6
		5' GCCGAAACTAGCTGCTTCCG 3' 3' GCCTTCGTCGATCAAAGCCG 5'	-0.6

Heterodimers:

Configuration	ΔG
5' CGACTGTCAATGGAGCTGGA 3' 3' GCCTTCGTCGATCAAAGCCG 5'	-3.0
5' CGACTGTCAATGGAGCTGGA 3' 3' GCCTTCGTCGATCAAAGCCG 5'	-1.8
5' CGACTGTCAATGGAGCTGGA 3' 3' GCCTTCGTCGATCAAAGCCG 5'	-1.6
5' CGACTGTCAATGGAGCTGGA 3' 3' GCCTTCGTCGATCAAAGCCG 5'	-0.6

Hairpins/Loops

Forward		Reverse	
Configuration	**ΔG**	**Configuration**	**ΔG**
		/ATCAAAGCCG 5' G ¦ ||| ¦ \CTGCTTCCG 3'	-0.6

Primer Set Name: GRK5 (ZhC)
Source: Zhou et al (2009), Cohn (2009)

Details:
Product length: 233

	Forward	Reverse
Sequence	ACCTGAGGGGAGAACCATTC	TGGACTCCCCTTTCCTCTTT
Length (bp)	20	20
T_m (°C)	55.6	54.7
GC content (%)	55	50

Predicted Secondary Structures:
Homodimers:

Forward		Reverse	
Configuration	**ΔG**	**Configuration**	**ΔG**
5' ACCTGAGGGGAGAACCATTC 3' 3' CTTACCAAGAGGGGAGTCCA 5'	-1.3	5' TGGACTCCCCTTTCCTCTTT 3' 3' TTTCTCCTTTCCCCTCAGGT 5'	-1.3
5' ACCTGAGGGGAGAACCATTC 3' 3' CTTACCAAGAGGGGAGTCCA 5'	-0.6	5' TGGACTCCCCTTTCCTCTTT 3' 3' TTTCTCCTTTCCCCTCAGGT 5'	-1.3

Heterodimers:

Configuration	ΔG
5' ACCTGAGGGGAGAACCATTC 3' 3' TTTCTCCTTTCCCCTCAGGT 5'	-8.0
5' ACCTGAGGGGAGAACCATTC 3' 3' TTTCTCCTTTCCCCTCAGGT 5'	-2.9
5' ACCTGAGGGGAGAACCATTC 3' 3' TTTCTCCTTTCCCCTCAGGT 5'	-2.0
5' ACCTGAGGGGAGAACCATTC 3' 3' TTTCTCCTTTCCCCTCAGGT 5'	-2.0
5' ACCTGAGGGGAGAACCATTC 3' 3' TTTCTCCTTTCCCCTCAGGT 5'	-1.3

5' ACCTGAGGGGAGAACCATTC 3' ||| ¦ 3' TTTCTCCTTTCCCCTCAGGT 5'	-1.0
5' ACCTGAGGGGAGAACCATTC 3' ¦ ||| ¦ 3' TTTCTCCTTTCCCCTCAGGT 5'	-1.0
5' ACCTGAGGGGAGAACCATTC 3' ||| ¦ 3' TTTCTCCTTTCCCCTCAGGT 5'	-0.7
5' ACCTGAGGGGAGAACCATTC 3' ¦ ¦ ||| 3' TTTCTCCTTTCCCCTCAGGT 5'	-0.6

Hairpins/Loops

Forward		Reverse	
Configuration	**ΔG**	**Configuration**	**ΔG**
/CAAGAGGGGAGTCCA 5' C ||| \ATTC 3'	-0.6	/CCTCAGGT 5' | ||| \CCTTTCCTCTTT 3'	-1.3